The Synthesis and Evaluation of Non-Targeted Near-Infrared Heptamethine Molecular Probes

By

Okoh Adeyi

A thesis submitted in partial fulfilment for the requirements for the degree of Doctor of Philosophy at the University of Central Lancashire

June 2013

Declaration

Concurrent registration for two or more academic awards

I declare that while registered as a candidate for the research degree, I have not been a registered candidate or enrolled student for another award of the University or other academic or professional institution.

Material submitted for another award

I declare that no material contained in the thesis has been used in any other submission for an academic award and is solely my own work except where due reference is made.

Collaboration

Where a candidate's research programme is part of a collaborative project, the thesis must indicate in addition clearly the candidate's individual contribution and the extent of the collaboration. Please state below:

Signature of Candidate

_____

Type of Award   **Doctor of Philosophy**

_____

School   **Forensic and Investigative Sciences**

_____

Commit thy works unto the LORD, and thy thoughts shall be established.

Proverbs 16:3

"Some men see things as they are and say why. I dream things that never were and say why not."

Robert F. Kennedy

Abstract

Detecting and quantifying biomolecules is an important tool in biological research. Ideal dyes have to have a number of characteristics i.e. low toxicity and limited autofluorescence. The properties of near infrared dyes make these ideal for cell and tissue imaging.

The work within this thesis focuses on the development of three families of NIR dyes (linear, rigid and substituted polymethine) and these are actively compared against the clinical standard Indocyanine Green (ICG) and its structural derivative New Indocyanine Green (IR-820). The ultimate aim being to identify dyes which can be used alongside the clinical standards.

The compounds developed within this thesis are structurally based on the NIR heptamethine cyanine (Cy7) dyes. To expand, variations fall into three categories, linear, rigid and polymethine substituted, each being synthesised using either existing methodology or through the development of a novel cascade reaction. The photophysical properties of each dye have been evaluated experimentally, focusing on absorption and emission wavelengths, fluorescence quantum yields and Stokes shifts. It is noted that most dyes synthesised within this thesis, show comparable Stokes shift but increased fluorescence quantum yields when compared against ICG and IR-820. All dyes absorb and emit within the NIR region based on excitation at 785 nm.

The growth inhibition characteristic is an important criterion which determines the practical use of the dyes in living cells. Most of the dyes which showed no growth inhibition were the dyes bearing the sulfonic acid group, suggesting the sulfonic acid limited cellular uptake as a result of decreased membrane permeability. Dyes possessing growth inhibitory characteristics all contain linear *N*-alkyl moieties. It is thus postulated that the increased lipophilicity of these molecules result in increased lipid distortion and subsequent toxicity.

Publications/Patents Related to this Work

UK Patent application 1201641.6
Process for Near-Infrared Dye production – (2012).
Okoh Adeyi Okoh and Robert B. Smith

Promising Near-Infrared Non-Targeted Probes- Benzothiazole Heptamethine Cyanine Dyes.
Journal of Sulfur Chemistry, 2013.
http://dx.doi.org/10.1080/17415993.2013.778258
Okoh Adeyi Okoh, Roger H. Bisby, Clare L. Lawrence, Carole E. Rolph and Robert B. Smith

N-**Alkylated 2,3,3-Trimethylindolenines and 2-Methylbenzothiazoles. Potential Lead Compounds in the Fight against Saccharomyces cerevisiae Infections".**
Submitted to European Journal of Medicinal Chemistry.
doi.org/10.1016/j.ejmech.2013.03.031
Andrew Tyler, Okoh Adeyi Okoh, Clare L. Lawrence, Vicky C. Jones, Colin Moffatt and Robert B. Smith

The Synthesis, Fluorescence and Toxicity Studies of Near-Infrared Heptamethine Cyanine Dyes for use in Oncology Applications.
Submission – Coloration Technology (July 2013).
Manuscript in preparation.
Okoh Adeyi Okoh, *Roger H. Bisby, Clare L. Lawrence and Robert B. Smith*

The Design and Synthesis of Distinct Novel Substituted Near-Infrared Heptamethine Cyanine Probes for Biological Applications.
Submission – New Journal of Chemistry (July 2013).
Manuscript in preparation.
Okoh Adeyi Okoh, *Roger H. Bisby, Clare L. Lawrence and Robert B. Smith*

Oral and Poster Presentations Related to this Work

2012 13th Tetrahedron International Symposium, Amsterdam
Poster Presentation

2012 Peakdale Molecular Symposium, Sheffield
Poster Presentation

2012 Centre for Material Science (UCLan)
Oral Presentation

2011 UCLan Graduate School Research Conference
Oral Presentation

2011 RSC Bioorganic Chemistry Group Meeting, London
Poster Presentation

2010 Peakdale Molecular Symposium, Manchester
Poster Presentation

2010 Brain Tumour North West, Preston.
Oral Presentation

Dedication

In loving memory of my late Mother

Mrs Esther Otuh.

Acknowledgments

First and foremost I would like to thank my God Almighty for giving me the opportunity and strength to complete this research project.

My sincere gratitude and deep appreciation goes to my director of studies Dr Rob Smith for his continuous guidance, support, understanding and encouragement throughout the length of this research project. Words alone cannot express my gratitude, I am deeply indebted to him and it has been my honour to be his student. I am also very thankful to members of my supervisory team. Dr Clare Lawrence for her guidance and valuable support especially, with the biology aspect which have aided this thesis in innumerable ways. My appreciation also goes to Dr Carole Rolph for her support and contribution to this work. A special word of thanks to Professor Roger Bibsy for his generosity in allowing me to use his fluorometer. I will forever be thankful to Dr Stephen Johns for his insightful criticism, support and guidance in the lab.

Special thanks to Andrew Tyler, Shraddha Aptekar, Kate Clarke and Kerry Ann Rostron for their assistance and support at various stages of this research project. Thanks to Dr Helen Godfrey for proofreading this thesis and for her suggestions. Also, I would like to express my appreciation to my lab mates; Vinod, Hajira Faki and Harry for their friendship.

Also, I am grateful to the members of the technical department; Tamar Garcia, Sal Tracey, Jim Donnely, Patrick Cookson, Steven Kirby and staff in the chemistry department for always being so helpful and friendly.

Finally, my appreciation goes to my family members for their support and prayers.

TABLE OF CONTENTS

LIST OF TABLES

X

LIST OF FIGURES

XIII

List of Abbreviations

^{1}H NMR	Proton Nuclear Magnetic Resonance
^{13}C NMR	Carbon Nuclear Magnetic Resonance
AO	Acridine orange
ATT	3-acyl-1,3-thiazolidine-2-thione
BSP	Bromosulfophthalein
CDCA	ChenoDeoxyCholic Acid
CDCl$_3$	Chloroform-d
COSY	Correlation spectroscopy
CuAAC	Copper-Catalyzed Azide-Alkyne Cycloaddition
DA	Dicarbocyclic acid
D$_2$O	Deuterium oxide
DCM	Dichloromethane
DE	Diester
DMSO	Dimethyl sulfoxide
DMF	Dimethylformamide
DNA	Deoxyribonucleic acid
DSSC	Dye-Sensitized Solar Cells
ΔEem	Energy change of emission
ΔEex	Energy change of excitation
EFISH	Electric-Field-Induced-Second-Harmonic
ESIMS	Electron Ionisation Mass Spectrometry
ETG	Electron donor terminal group
EtOH	Ethanol
FDA	Food and Drug Administration
FLT	Fluorescent life time
GPx	Glutathione peroxidase
HCl	Hydrochloric acid
HRMS	High Resolution Mass Spectra
HSA	Human Serum Albumin
ICG	Indocyanine green

ICT	Intramolecular charge transfer
IR	Infra-Red
IR-820	New Indocyanine Green
IWFO	Integrated Waveguide Fluorescence Optodes
Jsc	Short-circuit photocurrent density
λ_{max}	Absorption maxima
MC540	Merocyanine 540
MC	Methine chain
MeCN	Acetonitrile
MeOH	Methanol
ME	Monoester
MHRA	Medicines and Healthcare products Regulatory Agency
MIC	Minimum Inhibitory Concentration
MO	Molecular orbital
MRI	Magnetic Resonance Imaging
NHS	N-hydroxysuccinimidyl
NIR	Near-infrared
OATP	Organic Anion Transporting Peptides
PCE	Photon-to-current conversion efficiency
PDT	Photodynamic Therapy
PET	Photoinduced Electron Transfer
$POCl_3$	Phosphorus oxychloride
PPP	Pariser-Parr-Pole
PSMA	Prostate-Specific Membrane Antigen
QDs	Quantum Dots
ROS	Reactive oxygen species
SAM	Self-Assembled Monolayer
SCN	Isothiocyanate
SHG	Second-Harmonic Generation
S. pombe	*Schizosaccharomyces pombe*
SST	Somatotatin
UV/Vis	Ultra-violet/visible

VH1	Vilsmeier-Haack Intermediate
*V*oc	Open-circuit photovoltage
YE	Yeast Extract

General Introduction: Molecular probes

1.0 Introduction

The work presented in this thesis seeks to develop three different families of Cy7 dyes (linear, rigid and polymethine substituted) and compare their photophysical and growth inhibition characteristics against two classical near infrared (NIR) dyes: Indocyanine Green (ICG) and New Indocyanine Green (IR-820).
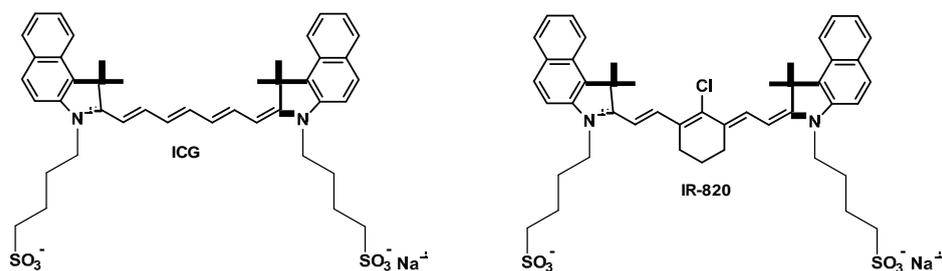
Figure 1.1: Structures of ICG and IR-820

ICG in particular, has been approved by the United States Food and Drug Administration for use in clinical applications, in particular, evaluating blood flow and clearance [1]. ICG derivatives also have the potential as a tool for fluorescence-guided management and treatment of cancer [1]. The impact of this research is timely, as illustrated by a recent article in Nature Methods [appendix] which highlighted the need for novel probes for biological imaging. The thesis focuses on the development of cost-effective molecular probes with enhanced photo-physical and low toxicity characteristics, when compared against the current clinical standard, ICG. The *in situ* cascade reaction also developed in this project provides an

elegant approach to the substituted polymethine linear dyes which can be tailored to develop more structurally sophisticated cyanine dyes.

The research within this thesis is divided into three areas:

1.   The synthesis of the NIR dyes;

2.   The photophysical characterisation of the NIR dyes and

3.   Growth inhibition studies of the NIR dyes.

Figure 1.2 shows the three different structures of the NIR dyes developed during this work with Table 1.1 showing the different array of functionalities attached to these dyes.
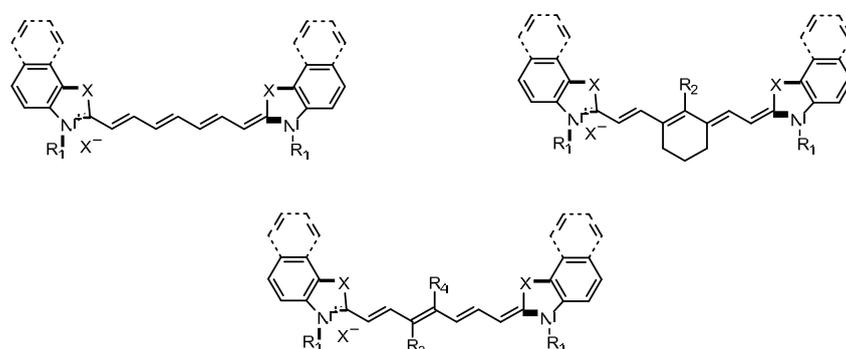
Figure 1.2: Structures of developed NIR dyes.

X	X⁻	R1	R2	R3	R4
S	I⁻	Me	Cl	Br	Ph
(CH$_3$)$_2$	Br⁻	Et	NHPh	Cl	
		n-Pr		Me	
		n-Bu			
		Bn			
		CH$_2$(CH$_2$)$_2$SO$_3^-$			
		CH$_2$(CH$_2$)$_3$SO$_3^-$			

Table 1.1: Structures of developed NIR dyes.

1.1 Molecular Imaging

Molecular imaging, also known as optical imaging is a rapidly developing area of research aimed at enhancing visualisation of cellular and molecular events in a non-invasive manner [1]. These cellular or molecular events could be in the form of simply locating specific population of cells, or an indication of the levels of a given protein receptor on the surface of cells. Molecular imaging allows evaluation and characterisation of gene and protein function, protein-protein interaction, and profiling of signal transduction pathways of human diseases such as cancer in order to gain more understanding into the molecular pathology of such diseases [2]. It also facilitates observation of cellular process at genetic or molecular level *in vivo* [3]. The reasons for observing or monitoring various cellular targets include:

- Characterisation of certain disease processes that might correlate with the concentrations of one or more of the molecular targets. For example, the manifestation of comparatively high levels of somatostatin receptor type 2 (located on cell membranes) in the lungs of a patient or subject may be suggestive of the presence of cancer cells in the lungs. This may in turn help guide and facilitate the medical management of the patient or subject in which such a molecular target is detected [4].

- It also assists in revealing complex underlying biology. For instance, one might be able to investigate the migration of a specific subset of T-lymphocytes (T-cells) into a tumour and subsequent activation of the cells by a T-cell receptor. This enables a better understanding of the details of interaction between the tumour and the immune system [4].

- Another important reason for observation of the cellular targets is to help in the process of drug discovery and validation, as well as in predicting and evaluating response to various types of therapy [4].

Molecular imaging instruments are simpler and less expensive to handle than those required for other imaging technologies such as magnetic resonance imaging (MRI), radiography, hence, facilitating their integration in less specialised medical applications. In order to obtain suitable images, optical contrasts need to be generated by the attachment of unique visualisation labels or contrast agents to the cellular target. Presently, there are three major

types of molecular probes or labels used in imaging applications namely: bioluminescence, fluorescent proteins and fluorescent dyes [5]. Whilst bioluminescence and fluorescent proteins require engineering cell lines or transgenic animals that carry suitable genes, fluorescent dyes do not. This unique feature coupled with its ease of handling and cost effectiveness makes fluorescent dyes a prospective candidate for rapid translation to clinical applications over methods which require genetic engineering [1-5].

Light is produced in molecular imaging by the excitation of a fluorescent molecule with a laser or light source resulting in emitted light of lower energy or longer wavelength that can be employed for imaging applications [6]. Molecular imaging techniques are attractive since they are highly sensitive and capable of detecting picomoles of light-emitting fluorophores in heterogeneous media [5].

1.2 Molecular Imaging Probes

Molecular imaging probes have attracted significant interest in recent years due, in large part, to their important application in clinical and biomedical research for the visualisation of cells and tissues both *in vitro* and *in vivo* [7-12]. The advantages of using molecular imaging probes include:

- High contrast i.e. good signal-to-noise ratio is usually obtained: since only the target and not the background is visible because different wavelengths are used for excitation and recording.
- High sensitivity.
- Several potential imaging modes can be obtained, most of which are unique.
- Easy to use and handle: very similar to classical staining.
- Cost efficient: the computing and optical instrumentation required are quite simple and inexpensive [13].

Most molecular imaging probes exhibit absorption and emission in the ultraviolet-visible (UV/Vis) wavelength region. This makes them difficult for applications relating to investigation of *in vivo* molecular imaging activities, due to the high absorption and autofluorescence of biomolecules in the UV/Vis region [14-16]. Also, light sources within

this wavelength region are easily dispersed and absorbed by biomolecules (e.g. melanin, haemoglobin and oxy-haemoglobin) and hence reduce the efficacy of tissue penetration (Figure 1.3). Furthermore, the autofluorescence from the biomolecules stimulates high background noise which causes a low signal-to-noise ratio [17].

In contrast, molecular imaging probes possessing absorption and emission in the NIR region (700-900 nm) can be efficiently utilised to investigate *in vivo* molecular targets because most tissues generate little NIR fluorescence, deep tissues penetration and minimal photodamage to biological sample [18]. In addition, molecular imaging probes operating in the NIR region result in improved signal-to-noise ratios, since they are spectrally isolated from the autofluorescence of tissue components such as collagen and fluorescence signals arising from other body absorbers [19]. The NIR probes could be used for visualisation and tracking of biomolecules such as melanin and haemoglobin (Figure 1.3) in their intrinsic location and in a non-invasive manner [20].
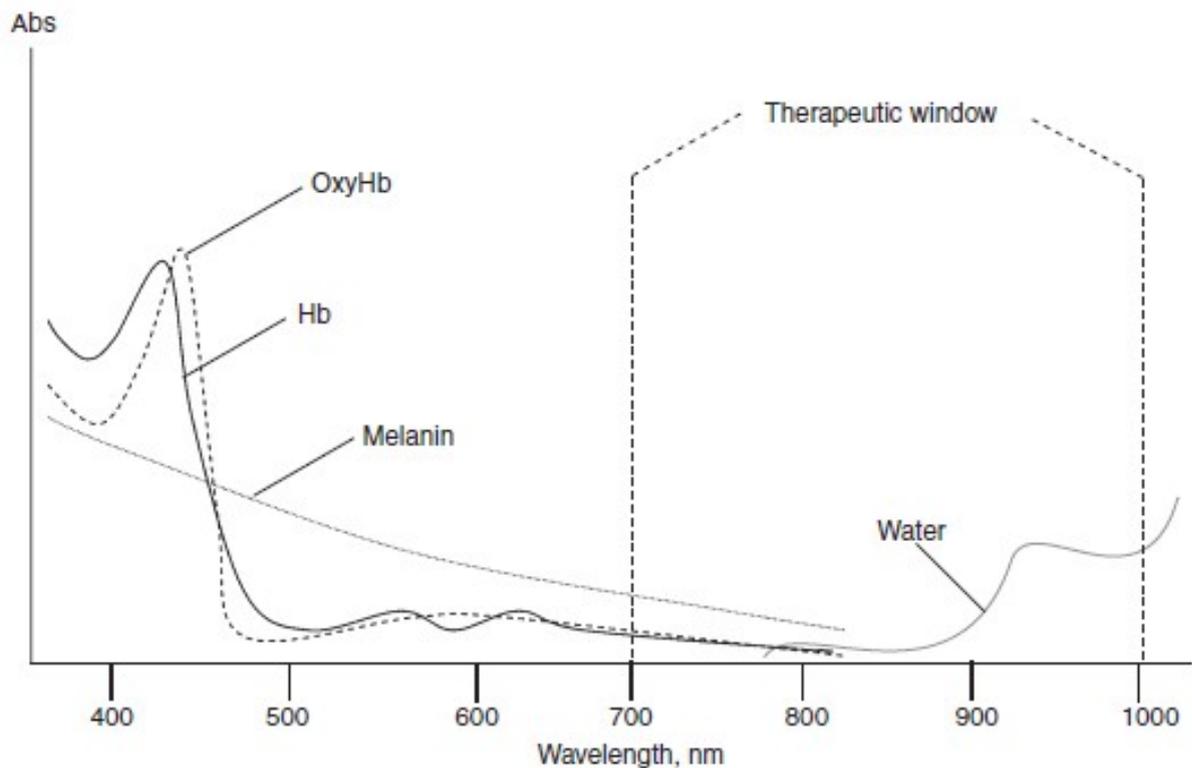
Figure 1.3: Spectra for endogenous visible absorbers [24].

At present, the general paradigm for designing fluorescent imaging probes can be categorised into non-targeting and targeting molecular probes. The non-targeting probes which include a number of NIR fluorescent cyanine dyes such as ICG are currently being used in clinical applications for evaluating blood flow and clearance [21]. A NIR fluorescent dye makes use of the NIR spectrum, facilitating deeper tissue penetration of light. The NIR light can achieve a depth of 5-10 mm, but this usually depends on the tissue type involved [23, 24]. The targeting probes are mostly used for functional imaging of tumour tissues, as cancer cells often overexpress certain surface receptors. This approach involves conjugating the fluorophore to a ligand that binds to a specific molecular target [22]. The targeting probes bind to the target and are retained at the target site, whereas the unbound probes are cleared from the circulation. The targeting probes are further divided into active and activatable probes [22-24].

1.3 Organic Dyes

In order to understand the concept of using non-targeted NIR heptamethine cyanine molecular probes for biomedical applications, it is imperative to grasp the background from which they developed, as this may provide some logical explanation on cell staining and bio-molecular interaction. A significant part of the literature focuses on the synthesis and applications of non-targeting heptamethine cyanine dyes as molecular probes for potential imaging applications. It is widely accepted that many imaging agents e.g. Fluorecein-5-isothiocyanate, Methylene blue etc (Figure 1.4) has been derived from dyes [25].
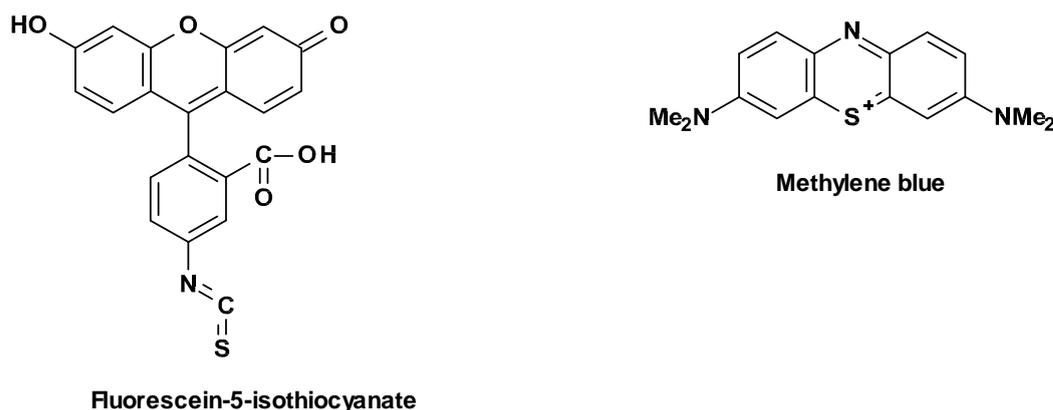
Figure 1.4: Examples of imaging and staining agents derived from dyes.

Dye chemistry has been investigated for over a century [26]. Whilst the developers of modern therapeutics have been inclined to avoid the use of coloured compounds due to their tendency to stain, it is precisely this characteristic which modern biomedicine has come to rely on [27]. There are two major areas of application for dyes in today's medicine, as molecular probes in the field of surgical oncology, and as photosensitizer in Photodynamic Therapy (PDT). Molecular probes are molecules or agents which absorb in the visible or NIR region, enabling them to be used as indicators to visualise and study the *in vivo* molecular properties of certain cells, molecules, enzymes or a biological state of cells [28]. PDT is where the dye is concentrated in a specific site, i.e. a tumour, and the correct wavelength of light is shone on the dye to release reactive oxygen species or redox radicals which are highly toxic to cells. Both these applications are related in that they both require a selective uptake of the dye by the cells [24]. Organic dyes are the most widely developed NIR molecular probes used for *in vivo* imaging investigations. Some of the first organic dyes to receive extensive biomedical application include trimethine cyanine (Cy3), pentamethine cyanine (Cy5) and heptamethine cyanine (Cy7) dyes, which are all based on the polymethine platform [29, 30].

1.4 Polymethine Dyes

Polymethine dyes (trimethine, pentamethine and heptamethine) (Figure 1.5) have been well known since the early 1920s. They have attracted a lot of interest due to their unrivalled

ability to be utilised extensively in various areas of biomedical research activities [31]. They are dyes containing the π-electron conjugated system bearing an electron acceptor terminal group (ETG$_1$), electron donor terminal group (ETG$_2$), and the methine chain (MC) joining the two terminal groups.
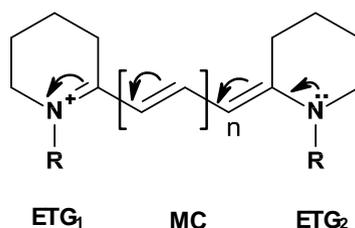
Figure 1.5: Polymethine dye.

The electron acceptor terminal group usually contains a highly electronegative atom adjoining to a double bond such as N$^+$=. The carbon atom =C integrated into the heterocyclic system is normally a monovalent residue. The electron donor terminal group contains an atom having a lone pair of electrons such as O, N, S joined to a divalent carbon atom. The polymethine chain is made up of sp^2- hybridised carbon atoms forming the π-electron conjugated system. The unsaturated nature of this part of the molecule allows electron movement between the heterocyclic termini, and for a given pairing, the maximum wavelength of absorption can be related to the length of the methine chain due to the fact that the vinylene shift amounts to about 100 nm [32]. Variation in the length of the polymethine chain and the identity of the terminal group allows for the alteration of the absorption and emission spectra throughout the visible and NIR regions of the electromagnetic spectrum. The conjugation between the electron donor terminal group and the electron acceptor terminal group results in the delocalisation of π-electron and bond order equalisation of the chromophore. Depending on the chemical constitution of the terminal end group, the polymethine dye can be categorised as being either symmetric or asymmetric. If the terminal end group possess the same chemical constitution, the polymethine dye is called symmetric. Figure 1.6 shows an example of symmetric trimethine (Cy3) polymethine dye called pinacyanol.

8
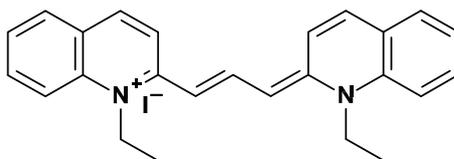
Figure 1.6: Symmetrical Cy3 dye (pinacyanol).

The electron density distribution within the chromophore system of such a dye is also symmetrical. Alternatively, if the terminal end groups differ in their chemical composition, the polymethine dye is called asymmetric. Figure 1.7 shows an example of an asymmetric polymethine dye called merocyanine 540 (MC 540).
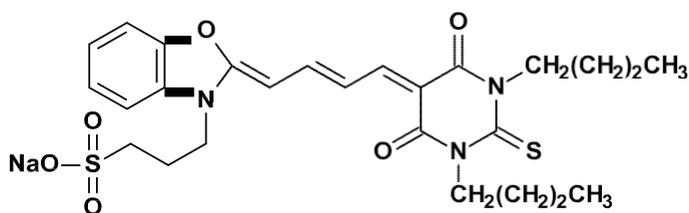
Figure 1.7: Asymmetrical polymethine (MC 540).

Amongst the different kinds of polymethine dye molecules e.g. squaraine derivatives (Figure 1.8), the cyanine family possess the greatest potential for being used in biomedical applications due to their excellent biocompatibility, superior photophysical and bio-distribution properties [33]. They also possess large molar extinction coefficients, moderate-to-high fluorescence quantum yields and a broad wavelength range that is chemically adjustable [33].
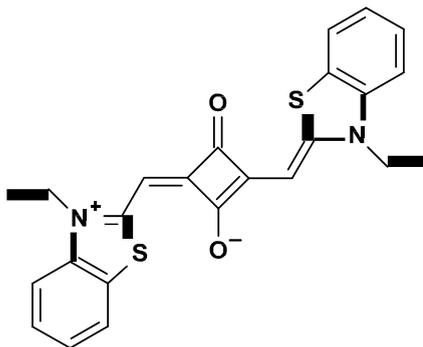
Figure 1.8: Squaraine derivative.

The name cyanine dyes was derived from the Latin word *cyanos,* meaning blue, which represent a unique class of charged π-electron organic compounds which generically consist of two heterocycles joined by an electron deficient conjugated methine chain [24, 34]. Cyanine dyes are among the oldest class of synthetic dyes commonly used today. They were first discovered by Williams in 1856 who obtained "corn flour" blue cyanine by treating quinolinium salts with amyl iodide followed by treatment with a base [35]. Since their discovery, they have been used extensively in numerous technical applications including their use as non-optical materials and photographic sensitisers. More recently they have been used as fluorescent probes for *in-vivo* molecular imaging activities due to their ability to emit light, i.e. fluoresce [36, 37].

The typical cyanine dye molecule (Figure 1.9) can be defined as being made up of two nitrogen-containing heterocyclic ring systems, in one of which the nitrogen atom is trivalent and in the other it is tetravalent; the two nitrogen atoms are joined by a conjugated chain of an uneven number of carbon atoms. In the early days, both the two heterocyclic rings were derived from quinolone; but nowadays they are also derived from pyridine, indole, benzothiazole, benzoselenazole and other heterocycles [38].
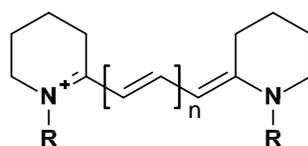
Figure 1.9: Generic cyanine dye.

The naming of cyanine dyes directly corresponds to the number of methine groups located in the methine chain joining the two heterocycles. Dyes having n = 0, 1, 2, and 3, are categorised as mono-, tri- (Cy3), penta- (Cy5) and hepta- (Cy7) methine cyanine dyes [39-41]. The structural versatility of cyanine dyes is such that analogue formation is relatively straight forward e.g. *via* variation in heteroatom, length of polymethine chain or *N*-alkylation. This has led to the synthesis of large number of various types of cyanine dyes over the last century. There are three main types of cyanine dyes (Figure 1.10) namely; streptocyanine, hemicyanine, and closed chain cyanine dyes [42].
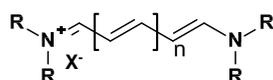
Streptocyanines
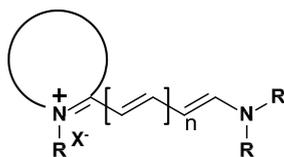
Hemicyanines
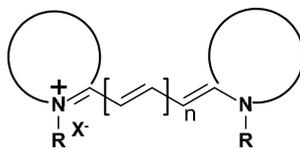
Closed-chain cyanines

Figure 1.10: Types of cyanine dyes.

Cyanine dyes are usually associated with intense colour, which is a result of the resonance interaction between the nitrogen atoms at the terminal ends of the conjugated methine chain, involving the movement of cationic charge [43]. The colour of cyanine dyes can be understood by considering the structural components of the dyes such as terminal groups, chromophoric systems and the sensitivity of the dyes to specific solvents [39, 40]. Generally,

cyanine dyes all have a sterochemical trans-geometry in their stable form although they do occasionally undergo photoisomerisation, a major route for deactivation of cyanine dyes [38]. They also show absorption and fluorescence that are a function of their molecular structure.

Generally, visible light absorption by a dye molecule depends on the possession of a conjugated π-system with the wavelength of the absorbed light depending on the charge distribution within the system. The λ_{max} for a given heptamethine dye can be increased by lengthening the polymethine chain [44]. However, this may result in photoisomerisation, a major deactivation pathway for most cyanine dyes. This deactivation process could lead to formation of singlet oxygen species [44]. Singlet oxygen has been proven to kill both healthy and tumour cells. Furthermore, increasing the polymethine chain length often leads to reduced solubility of the dye. Therefore, careful consideration and balance of these factors is needed when designing potential candidates for biomedical applications.

1.5 Chromophoric System of Cyanine Dyes

Resonance theories such as Pariser-Parr-Pole (PPP) Molecular Orbital (MO) theory have been applied in predicting the colour and other colour-related properties of the cyanine dyes in terms of the energy levels of the frontier orbitals and the π-electron density changes accompanying the first transition [45-47]. The absorption maximum of cyanine dyes usually exhibits a bathochromic shift of about 100 nm due to the presence of each extra vinylene conjugating unit. The effects of a heteroaromatic ring R on the λ_{max} of cyanine dyes depends on its structure as shown in Figure 1.11. A bathochromic shift can be gained by increasing the basicity of heteroatoms and enlarging the π- conjugated systems.

R=CH-(CH=CH)$_3$-R

920 nm   818 nm

X = Se   790 nm
X = S   763 nm
X = CMe$_2$ 741 nm
X = O   695 nm
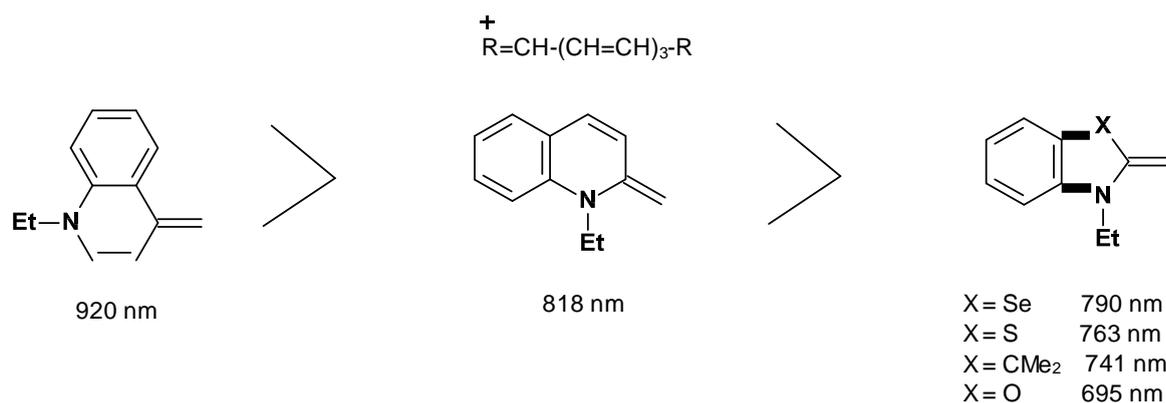
Figure 1.11: Structures of heteroaromatic ring R.

1.6 Synthesis of Cyanine Dyes

The base catalysed aldol type reaction is one of the major methods used to synthesise NIR fluorescent cyanine dyes due to its high level of stereo-selectivity and hence formation of stereo-controlled products [28]. Classical synthesis of cyanine dyes usually involves a heteroaromatic compound such as the quaternary pyridine derivative with a methyl group at position 2, 4 or 6 as the starting material. The electron-withdrawing nature of the quaternary nitrogen enhances the acidity the methyl proton, which then loses a proton. The proton abstraction step could also be promoted by the use of a base such as sodium acetate, pyridine or triethylamine to form the nucleophile or carbanion (Scheme 1.1). The nucleophile then attacks the dialdehyde or ketone through a nucleophile attack followed by subsequent dehydration to form the basic cyanine-type molecule.
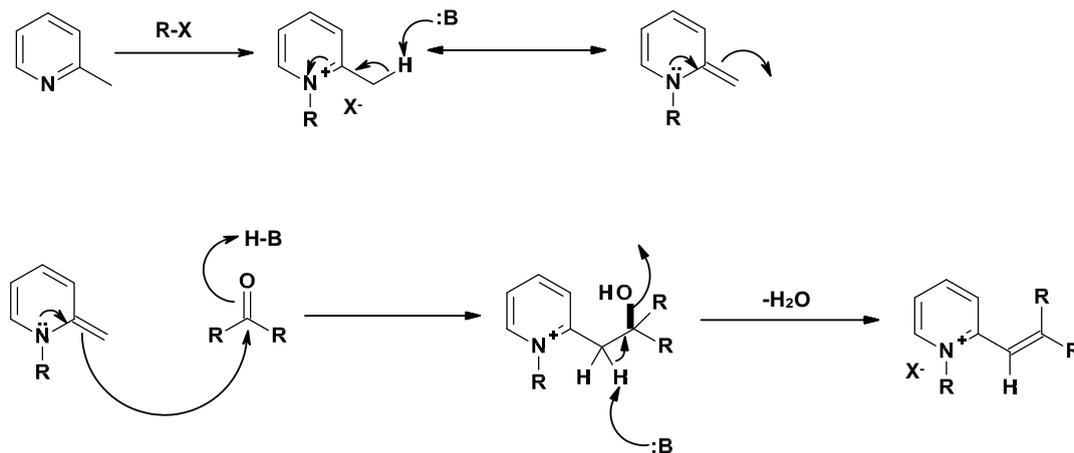
Scheme 1.1: General mechanism for cyanine dye synthesis [28].

1.7 Monomethine Cyanine Dyes

Deligeorgiev and co-workers developed a novel method for the preparation of symmetrical and asymmetrical monomethine cyanine dyes (Scheme 1.2) [48]. The novel synthetic method developed involves the reaction of quaternary salts of a heterocyclic 2- or 4-methyl compound and *N*-heterocyclic 2- or 4-sulfobetainic compounds by simply melting or boiling them in common polar solvents or solvent mixtures in the absence of a basic agent. The applicability of this method is highly dependent on the melting points of the starting materials and their thermostability [48].
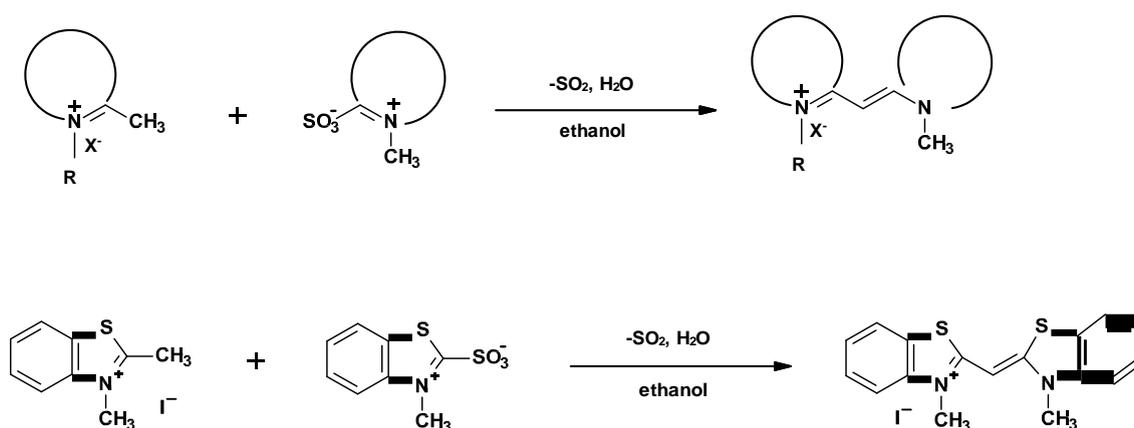
Scheme 1.2: Deligeorgiev novel method for the preparation of symmetrical and asymmetrical monomethine cyanine dyes [48].

1.8 Trimethine Cyanine Dyes (Cy3 Dyes)

Peng and co-workers have utilised the classical orthoester synthetic approach to synthesise a range of novel trimethine cyanine dyes. The approach involves the condensation of orthoesters with quaternary heterocyclic salts substituted with an activated methyl group under basic conditions (Scheme 1.3) [49].
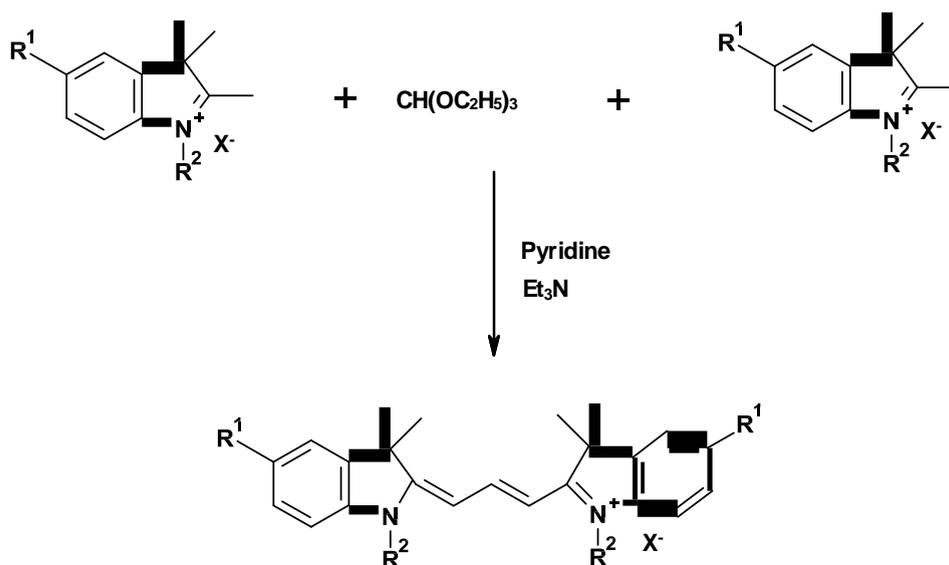
Scheme 1.3: Pengs synthetic route to yield trimethine cyanine dyes [49].

The synthetic route involves a condensation reaction using triethyl orthoformate with appropriately substituted 2-methyl-3*H*-indolium salts in the presence of triethylamine. The route was developed by successful optimisation of the reaction conditions, from a ratio of 2-methyl-3*H*-indolium : ortho ester : triethylamine of 2 : 3 : 4, the reaction mixture was then refluxed for 1 h at 120 °C in pyridine solution.

Using similar synthetic transformations, a central one-carbon constituent of the trimethine bridge can be derived from *N,N'*-diphenylformamidine [50, 51] or iodoform. The diphenylformamidine protocol allows for the synthesis of asymmetric dyes bearing two diverse end-heterocyclic subunits or two different *N*-subunits on the same heterocyclic systems [52]. The central methine group of the trimethine chain in dyes **A** and **B** can also be

made using a novel Vilsmeier-type reagent obtained from *N,N'*-dimethylformamide and hydrogen bromide (Scheme 1.4) [53].
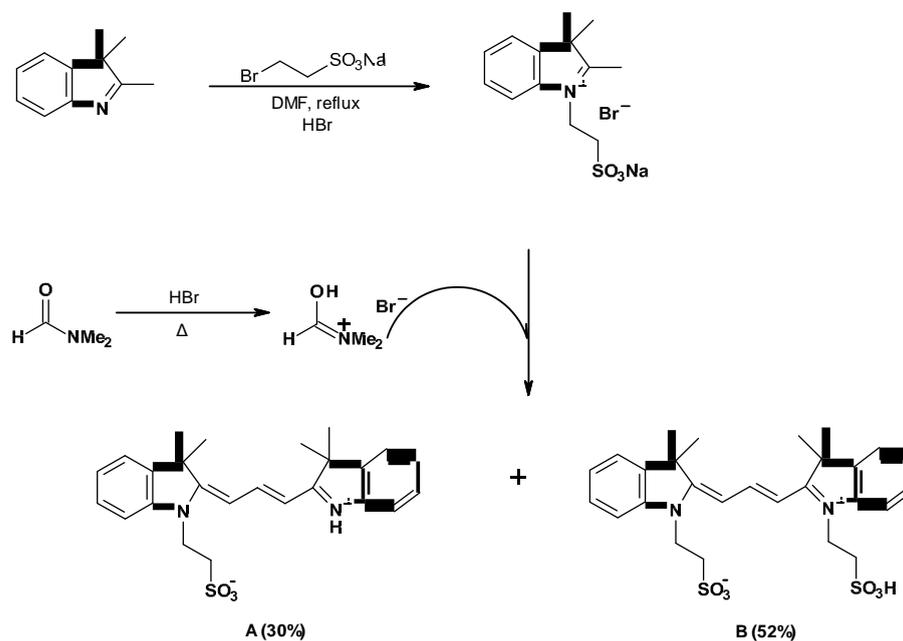
Scheme 1.4: Synthetic route to yield trimethine cyanine dyes using dimethylformamide protocol [53].

Post synthetic modifications can be carried out at the meso postion of a meso-methyl-substituted trimethine dye (Scheme 1.5) by condensation with an aldehyde to yield dye **C**. An ethyl analogue can also undergo the same condensation at the α-position of the ethyl group [54].
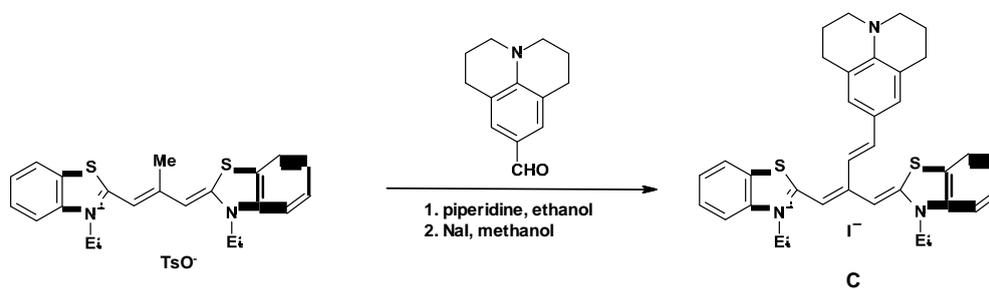
Scheme 1.5: Post synthetic modification to yield dye **C** [54].

1.9 Pentamethine Cyanine Dyes (Cy5 dyes)

One of the main synthetic routes to yield this class of polymethine dyes is the condensation of cationic heterocyclic compounds containing an activated methyl group with derivatives of malondialdehyde. Waggoner and co-workers have recently developed a novel synthetic method to yield a water soluble pentamethine cyanine dye **D** (Scheme 1.**6**) [55].
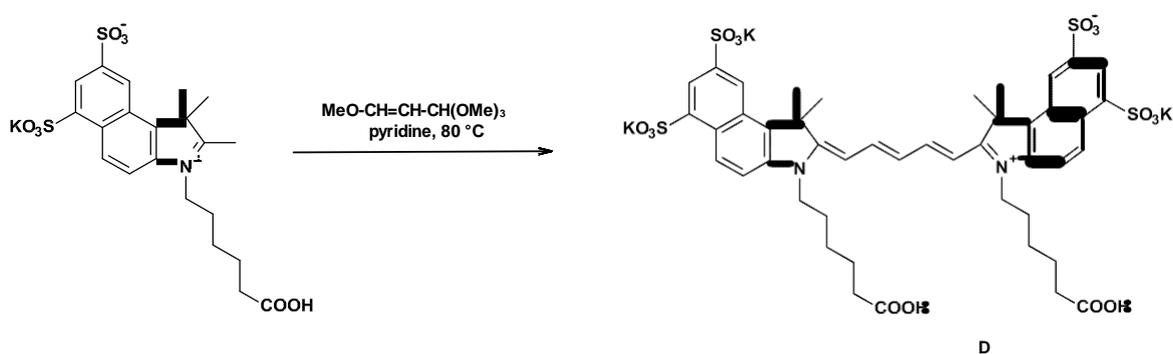
Scheme 1.6: Waggoner synthesis of water soluble pentamethine cyanine dye **16** [55].

Renard and co-workers have developed a new synthetic route (Scheme 1.7) for the preparation of a range of novel water soluble pentamethine cyanine dyes, using an effective acylation reaction with an original trisulfonated linker [56]. The structure of the intermediates were designed to create a scaffold bearing the two orthogonal reactive amino and carboxylic acid groups, which can be modified easily and selectively to yield pentamethine cyanine dye **E** bearing two different *N*-substituents [56]. Purification of pentamethine cyanine dye **E** is usually very difficult and challenging, due to their high level of polarity. Crystallisation rarely produces pure compounds and large amounts of the dye are irreversibly adsorbed by using the normal silica gel chromatography method. The most effective purification method for such highly polar dyes is reverse-phase chromatography utilising a commercial C18 adsorbent [50].
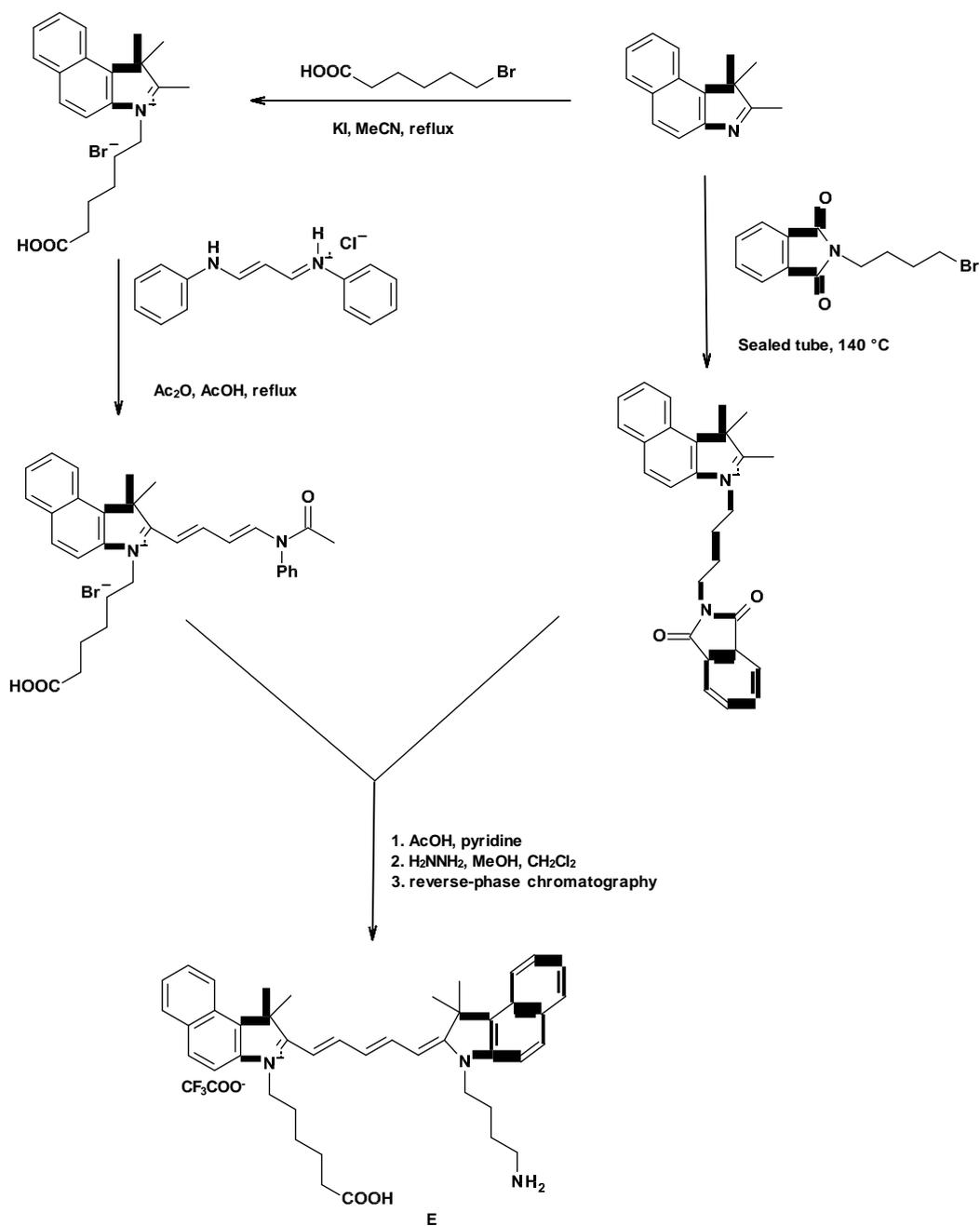
Scheme 1.7: Renard synthesis of pentamethine cyanine based amino acid [56].

1.10 Heptamethine Cyanine Dyes

Currently, there is a huge amount of interest in the chemistry of heptamethine cyanine dyes due to their application as fluorescence biomarkers in biomedical sciences [57-62]. A large

amount of these dyes possess a six-membered cyclohexene subsystem as part of the heptamethine chain e.g. compound **F** (Scheme 1.8). One of the advantages of this structural feature is that it helps to increase the rigidity of the compound, hence give an increase in the quantum yield of the molecule. Due to steric factors, the cyclohexene subsystem also decreases the level of dye aggregation in solution. The first series of heptamethine cyanine dyes were synthesised in 1977 by Makin and co-workers [60]. The synthesis involved the condensation of Vilsmeier-Haack intermediate (**VH1**) obtained from cyclohexanone and a heterocyclic salt bearing an activated methyl group (**MG1**) in the presence of base (Scheme 1.8).
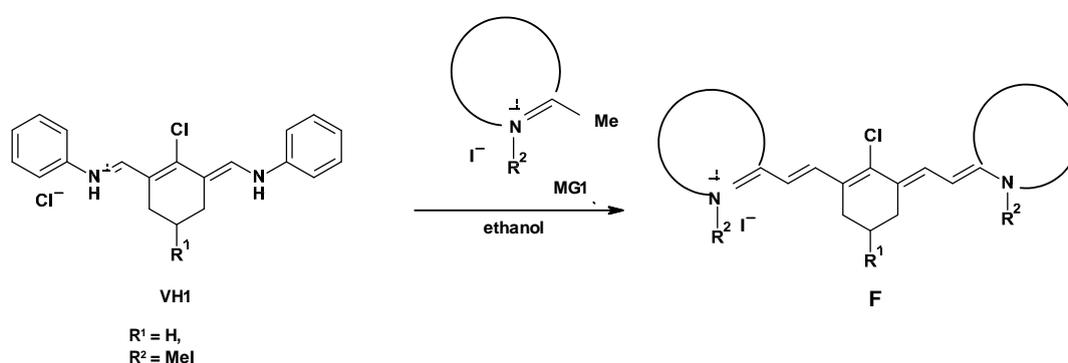
Scheme 1.8: Makins synthesis of heptamethine cyanine dye [60].

1.11 Application of Cyanine Dyes

Due to the recent advancement of specialised innovative or functionalised dyes, there has been increasing interest in the application of cyanine dyes. The biological and photophysical properties of cyanine dyes within different types of media have led to their use over a vast range of applications such as photorefractive materials [63], industrial paints, for trapping solar energy, as sensitisers for solar cells [64], in optical disk for recording media [65-67], as laser materials [68-72], as inorganic large band-gap semiconductor materials [73-78] and most recently as targeted and non-targeted probes for *in-vivo* imaging activities [79-86].

1.12 Sensitisers for solar cells

Much emphasis has been placed on the investigation of dye-sensitised solar cells due to the advent of green technology using solar energy [87]. Though an array of organic dyes such as merocyanine [88], polyenes [89] and coumarins [90] have been reported to show excellent solar-light to electricity conversion efficiency, little has been reported on near-infrared sensitisers [91]. Some heptamethine cyanine dyes are usually very stable under UV-irradaition as they contain the rigid cyclohexene moiety, and this makes them very interesting and attractive compounds for application as sensitisers for solar cells [91, 92].

Jianli and co-workers have designed and synthesised new fluoranthene-based asymmetric cyanine dye **G1** and **G2** (Figure 1.12) bearing a ethynyl unit for comparison purposes as sensitisers for applications in Dye-Sensitized Solar Cells (DSSC) [93]. The absorption spectra, electrochemical and photovoltaic properties of the dyes (**G1** and **G2)** were extensively investigated and reported. The DSSC based on the fluoranthene dye **G1** displayed the superior photovoltaic performance: a maximum monochromatic PCE of 67%, a short-circuit photocurrent density (*J*sc) of 7.83 mAcm^{-2}, an open-circuit photovoltage (*V*oc) of 0.476 V, and a fill factor (ff) of 0.63, conforming to an overall conversion efficiency of 2.34% under simulated AM 1.5G solar light conditions in comparison to cyanine dye **G2**. Also investigated were the effects of ChenoDeoxyCholic Acid (CDCA) in a solution as a co-adsorbate on the photovoltaic performance of DSSCs based on cyanine dyes. The presence of CDCA for 30 mins was reported to increase both the photovoltage and photocurrent of the DSSC in combination with **G1**, in which the photovoltage and photocurrent increase 9.3% and 20%, respectively. The above photovoltaic results indicate that co-adsorption of suitable amount of CDCA is effective in improving solar cell performance [88].
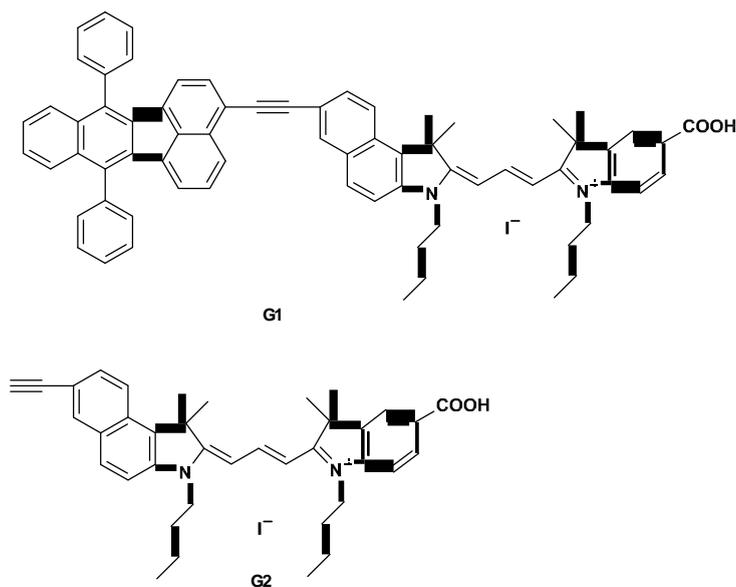
Figure 1.12: Molecular structures of cyanine-based dyes **G1** and **G2** [88].

1.13 Ion Sensors

A range of novel NIR ketocyanine dyes have been designed and synthesised by Julian and co-workers [94]. The dyes were evaluated as potential pH fluoroionophores to be utilised for the development of new Integrated Waveguide Fluorescence Optodes (IWFO). The ketocyanines (**H1**) upon protonation were transformed to meso hydroxyl substituted carbocyanine dyes (**H2**) (Scheme 1.9) and this process was accompanied by a large bathochromic shift (in the range of 200 nm) of the absorption band along with a considerable decrease in fluorescence intensity.

X, Y = CMe$_2$, S; R^1, R^2 = H, OH, COOEt, NH$_2$, NHA$_C$
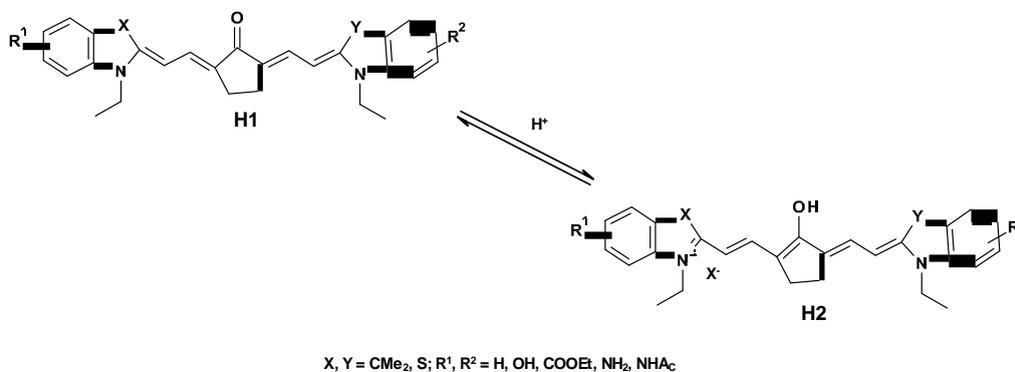
Scheme 1.9: Protonation of ketocyanine dyes [94].

21

The ketocyanine dyes also demonstrated their suitability for application as acidochromic fluoroionophores in bulk optodes for the design and development of IWFO. They show high fluorescence intensities in the far-visible region, an optimum pH sensitivity and sufficient photostability [89, 95].

1.14 Non-Linear Optics

With the increasing demand for optically non-linear organic chromophores and photorefractive materials [96, 97], a great deal of research has focused upon the molecular engineering requirements to improve the optical non-linearities in push-pull compounds [98, 99]. Non-linear optics is concerned with studies of the non-linear interactions of electromagnetic radiation and the media. The non-linear interaction indicates that matter reacts in a non-linear manner to the incident radiation fields. This gives the media the ability to change the wavelength, or the frequency of the incident electromagnetic waves. In general, this non-linear interaction is only observed when the incoming light is of high intensity (electric field) [100]. Boxer and co-workers have reported results of Stark and Electric-Field-Induced-Second-Harmonic (EFISH) measurements for a series of donor/acceptor merocyanine dyes which differ in their electron acceptor end group (Figure 1.13). These demonstrate the correlation between optical non-linearities along with a large solvent dependence of their electronic structure [101].
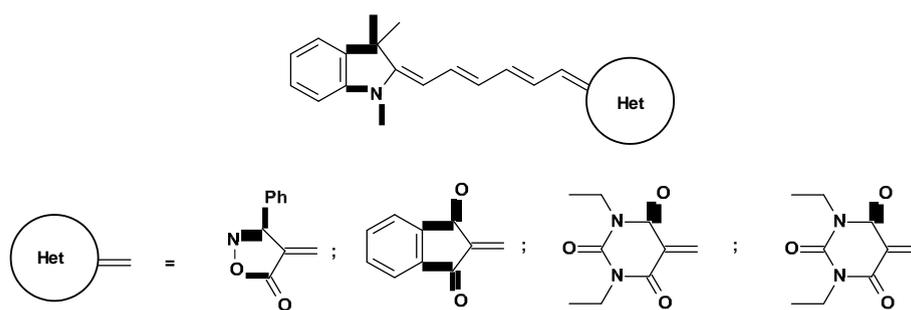
Figure 1.13: Merocyanine dyes synthesised by Boxer and co-workers [101].

Merocyanines have been known to show non-linear optical properties both in a polymer matrix and as crystals. However, most non-linear optical chromophores are usually difficult to crystallise [102]. Tsuboi and co-workers have utilised the Second-Harmonic Generation (SHG) to study the non-linear optical responses of a Self-Assembled Monolayer (SAM) bearing merocyanine chromophore (Figure 1.14) on gold in water and ethanol [103]. The pH dependence of the SHG clearly indicated a solvatochromic modification of the merocyanine from a protonated form to a zwitterionic form [103].
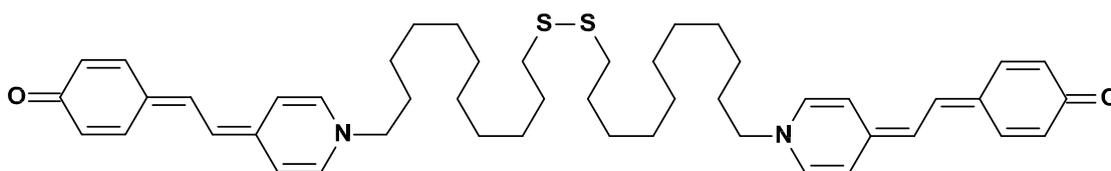
Figure 1.14: Merocyanine dye synthesisd by Tsuboi and co-workers [103].

1.15 Cyanine Dyes for Photodynamic Therapy (PDT)

Photodynamic Therapy (PDT) involves the use of a photosensitising agent and near-visible light to kill cancer cells [104]. After administration into the body, within a short period of time, the photosensitiser localises in the tumour in high concentrations, and then the treated area is irradiated with a light source. The light causes the photosensitising agent to react with molecular oxygen producing singlet oxygen, a powerful oxidant and a cytotoxic agent, that kills the cancer cells. PDT may also work by damaging the blood vessels that feed the cancer cells and by informing the immune system to attack the cancer [28]. The effectiveness of the photosensitiser depends on the initial singlet electronic excited state of the molecule possessing sufficient longevity to give enhanced intersystem crossing and electron spin inversion to yield the triplet excited state. This stimulate the interaction with the surrounding environment through either electron transfer (Type I photosensitisation) or energy transfer and singlet oxygen generation (Type II photosensitisation) (Scheme 1.10) [28]. Also, the absorption maximum and the wavelength of the laser source are important parameters that determine the strength of photodynamic action on malignant tissues. PDT possesses several advantages over some of the traditional cancer treatments like chemotherapy, radiation and hormone therapy. It can target specific cells and can be repeated several times at the same site

if the need arises. The treatment is less invasive and cancer patients treated with PDT have less, if any, long term side-effects. PDT has been approved by the Medicines and Healthcare products Regulatory Agency (MHRA) and United States Food Drug Administration (FDA) and is utilised worldwide for the treatment of lung cancer, obstructive oesophageal cancer and age-related macular degeneration [105-108].
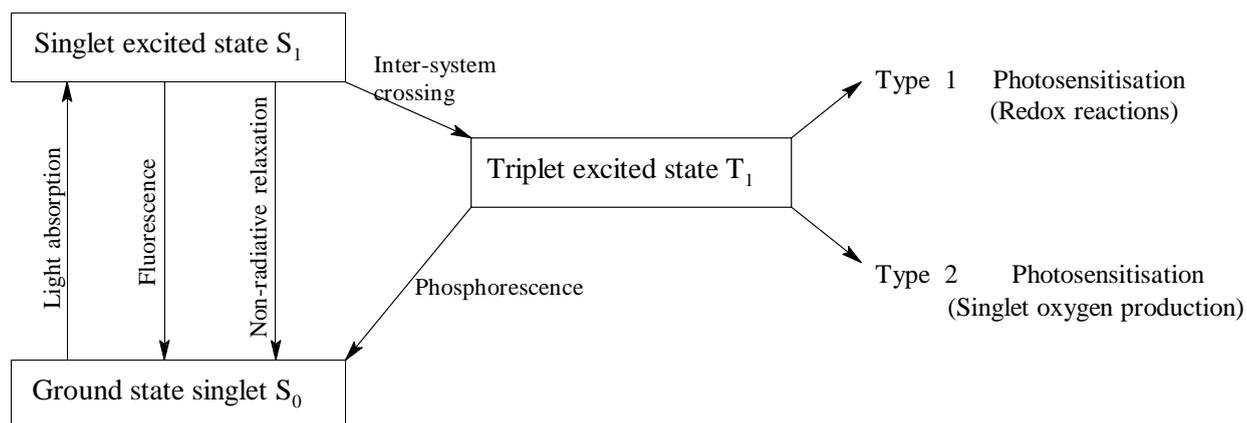
Scheme 1.10: Jablonski diagram showing the various stages involved in
photosensitisation process [24].

Cyanine dyes such as merocyanines and ketocyanines have been studied extensively as potential PDT tools for the treatment of solid tumours [102, 109]. They have also been utilised as radiation sensitizers for treatment of cancerous cells [110]. Harrimann and co-workers have proposed merocyanine as a reagent for both diagnosis and treatment of early stages of leukaemia by PDT as it has shown the potential for selective recognition of the leukaemia cells [110]. The intracellular merocyanine dye **I1-I7** (Figure 1.15) acts as a phototoxin to destroy the host cells under irradiation due to the long-lived triplet excited state of the dyes which plays an important role in the overall process [111].
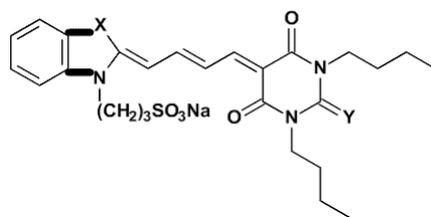
I1: X = O, Y = S (MC 540)
I2: X = C(CH₃)₂, Y = S
I3: X = S, Y = S
I4: X = Se, Y = S
I5: X = Se, Y = O
I6: X = Se, Y = Se
I7: X = O, Y = O

Figure 1.15: Intracellular merocyanine dye for PDT [111].

The photo-process involves isomerisation from the singlet excited state progressing from an all-*trans* configuration to a long-lived *cis*-isomer. Thus for merocyanine dye derivatives to be clinically useful, it is essential that:

a) The photoisomerisation is inhibited, since it competes with intersystem crossing and radiative deactivation.

b) Highly fluorescent dyes are photobleached in cellular media to recognise leukaemia cells [105].

The photobleaching process occurs via an oxidative attack of the singlet oxygen produced from the long-lived triplet excited state on the polymethine chain [112]. Therefore, a group of merocyanine dyes giving no triplet state, are hence suitable for detection purposes, and other analogues of such dyes displaying high triplet yield, are consequently useful as phototoxins, both of which are required.

It has also been observed that for a series of merocyanine dye derivatives, the presence of heavy atoms increases the triplet yield by spin-orbital coupling and alters the rate and yield of isomerisation [113]. Amongst the derivatives, merocyanine **I6**, containing Se, was shown to be a potent sensitiser. The lipophilicity also increases by the attachment of heavy atoms. It possesses high toxicity towards leukaemia cells due to high intracellular solubilisation, and also a faster rate of uptake into infected cells which improves its biological activity [114].

1.16 Protein Labelling

Protein labelling also known as probe technology involves the conjugation or attachment of a chromophore to a protein either covalently or non-covalently. The technology is advantageous because it allows for higher sensitivity and better detection limits since the detection of the extrinsic chromophore possess a higher molar absorptivity than the protein's intrinsic chromophore. Greater sensitivity is achieved when studies are carried out in the NIR region of the electromagnetic spectrum. Covalent and non-covalent labelling techniques can be used to study both quantitative and qualitative analysis [115-117].

The majority of covalent labels employed for biological applications are usually synthesised. Primary amines and thiols are typically the reactive moieties on the proteins that are targeted by dyes for conjugation by the reaction with functionalised dyes [118]. Hydrazide or amine groups on dyes have been used for the attachment to carboxylic acid groups on proteins. Dyes derived with iodoacetamide or maleimide can be reacted with protein thiols. In addition, dyes functionalised with an isothiocyanate (SCN) group or *N*-hydroxysuccinimidyl (NHS) ester have been widely used to target lysine moieties. Figure 1.16 illustrates the reactive pathways of some commonly available labelling reagents [50].
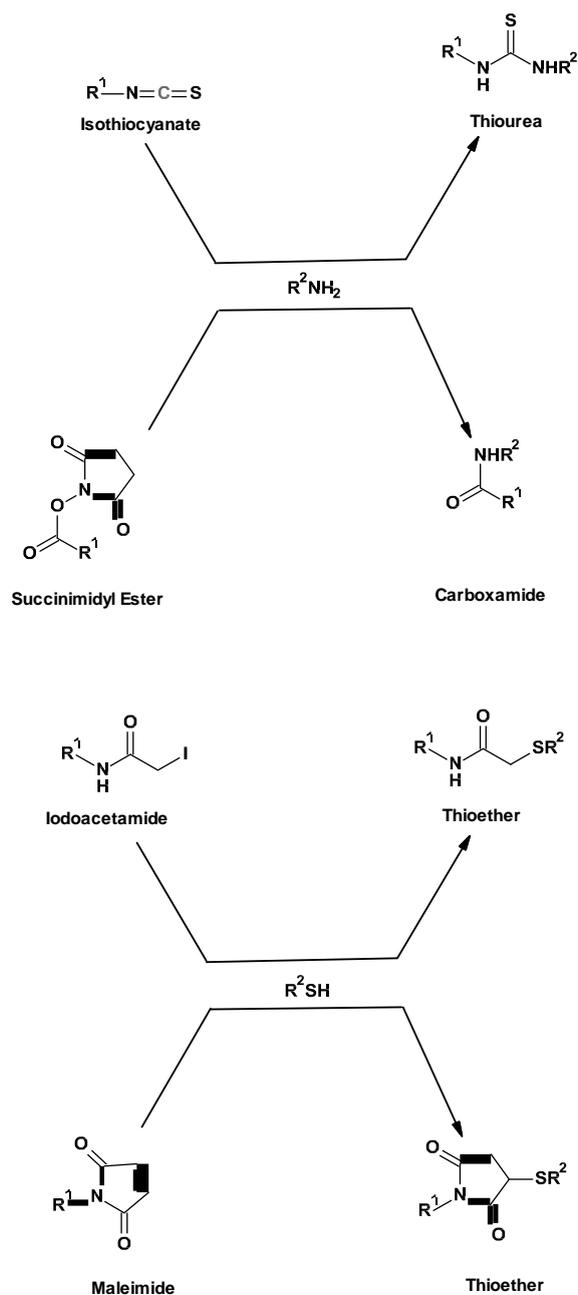
Figure 1.16: Covalent labelling of amine and thiol groups of proteins R^2NH_2 and R^2SH.

Reactions involving lysine functionalities of proteins occur readily under neat conditions with a variety of commercially available reagents. Covalently labelled complexes are generally very specific and stable, and the possibility for nonspecific interactions is significantly minimised [119]. Due to their excellent specificity, covalent labelling is often employed in quantitative analysis, where it is used to determine the number of reactive sites or degree of substitution. This particular characteristic of covalent labelling is suitable for determining the

number of functional groups (e.g. amines) present on the surface of a protein of interest [119]. Some fluorescent covalent labelling agents have shown excellent water solubility, good photostability, and favourable photophysical properties. Figure 1.17 shows a range of selected NIR reagents for labelling of proteins at the amino group [119].
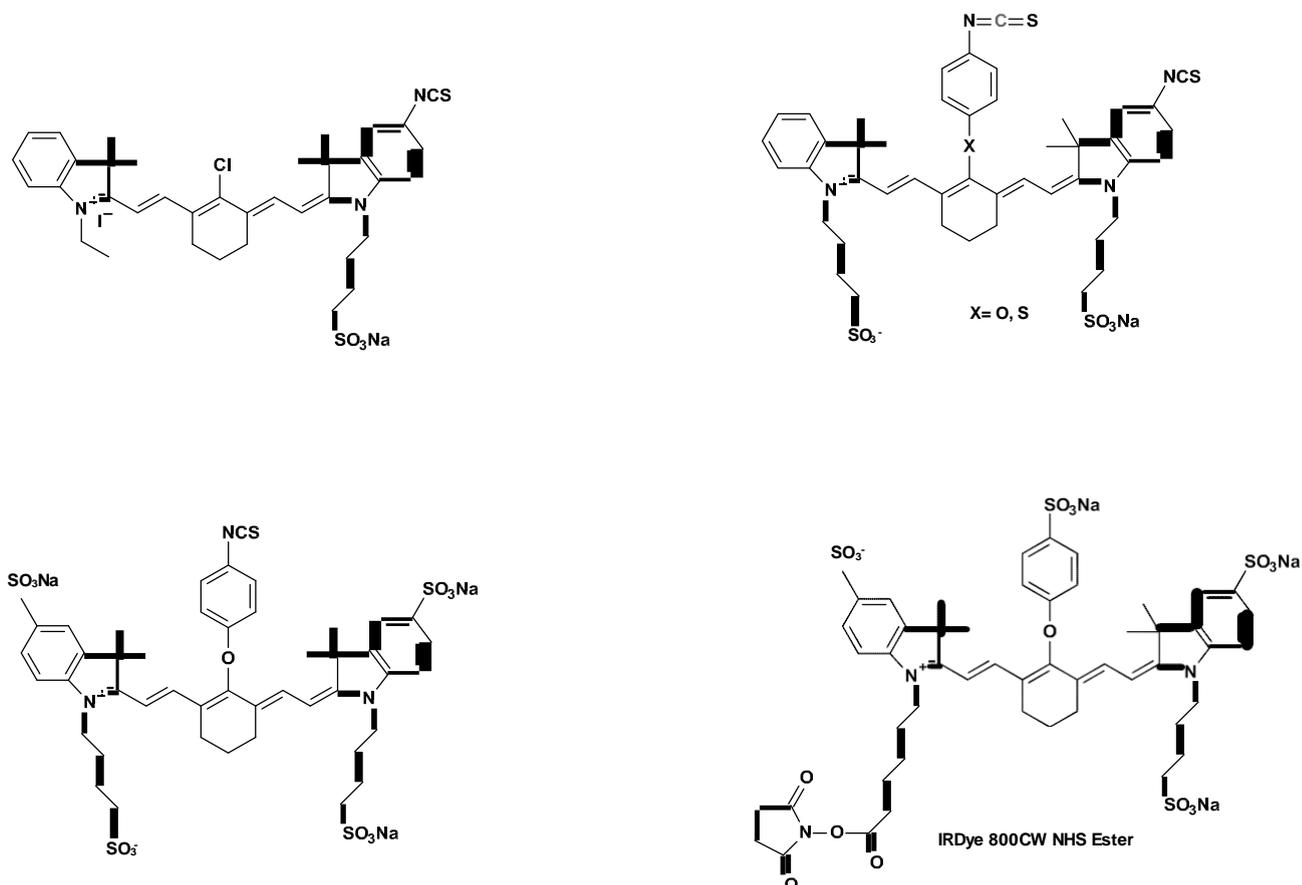
Figure 1.17: NIR cyanine dyes for covalent labelling of proteins at an amino group.

Frangioni and co-workers have investigated intraoperative NIR fluorescence imaging systems for small-animal surgery [120]. They labelled Human Serum Albumin (HSA) covalently with an IRDye78 to produce an HSA-dye conjugate (Figure 1.18) as a fluorescent lymph tracer [120, 121]. The tracer is suitable for use in intraoperative NIR fluorescence imaging studies since it is non-toxic and the excitation light source used is safe for animals. The tracer was reported to exhibit clearly resolved images. The properties of the NIR probe were also compared with that of Quantum Dots (QDs). It was discovered that the NIR probes possessed

superior properties such as high emission wavelengths and quantum yield indicating their better suitability for *in vivo* imaging applications.
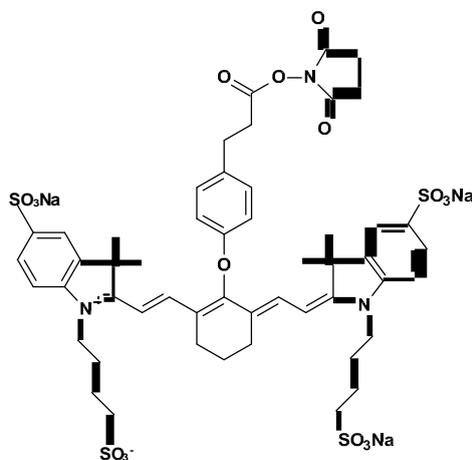
Figure 1.18: IRDye78-NHS.

1.17 Tumour Targeting and Imaging

Amongst the available NIR dyes, cyanine dyes have demonstrated promising potential for tumour targeting and imaging. A vast amount of research has focused on increasing the tumour-targeted specificity of cyanine dyes by conjugating them to targeting molecules known to bind to certain receptors having high expression in tumour cells [122]. Also, multifunctional dyes with Magnetic Resonance Imaging (MRI) and optical imaging properties are being developed. In a bid to develop tumour targeting specific fluorescent agents, Achilefu and co-workers conjugated NIR cyanine dye to small peptides for targeting Somatotatin (SST) receptors [123]. In their approach to prepare the tumour targeting agent **J3**, the NIR cyanine dye **J1** was conjugated to the C- terminus of a cyclic SST receptor avid octapeptide **J2** (Scheme 1.11). The absorption and fluorescence emission properties of the fluorescent probe **J3** were similar to that of the precursor NIR cyanine dye **J1**.
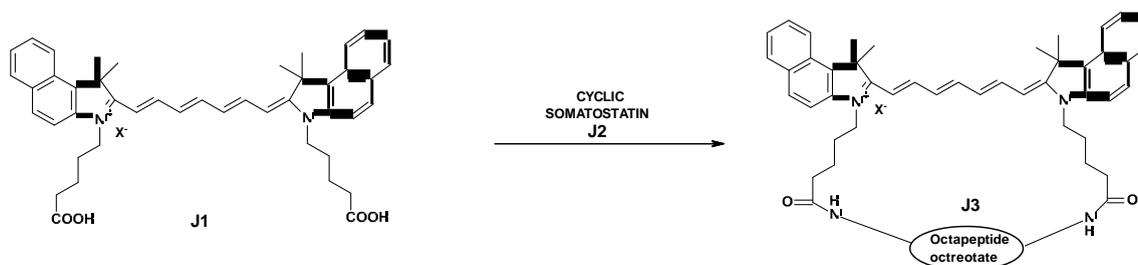
Scheme 1.11: NIR cyanine dye peptide conjugate.

In a similar study Licha and co-workers reported the synthesis and characterisation of SST receptor-specific peptide H$_2$N-($_d$-Phe)-cyclo[Cys-Phe-($_d$-Trp)-Lys-Thr-Cys]-Thr-OH, which was labelled with a carboxylated indodiacarbo and an indotriacarbocyanine NIR cyanine dye at the *N*-terminal amino group. The imaging agent was prepared by using automated solid-phase synthesis, with subsequent attachment of the cyanine dye and cleavage of the whole conjugate from the resin (Scheme 1.12) [124]. The resulting peptide-dye conjugates displayed high absorbance at 792 nm and emission at 811 nm, which are typical for cyanine dyes. Hence, these dyes are suitable receptor-targeted contrast agents for tumour targeting and imaging. The ability of the peptide-dye conjugates to target the SST receptor was demonstrated by flow cytometry *in vitro*, in which the indotricarbocyanine conjugate led to elevated cell-associated fluorescence on SST receptor-expressing tumour cells. While in contrast, the linear analogue of the sequence H$_2$N-($_D$-Phe)-Met-Phe-($_D$-Trp)-Lys-Thr-Met-Thr-OH produced only minimal cell fluorescence, thus confirming the specificity of the cyclic SST derivative [117].
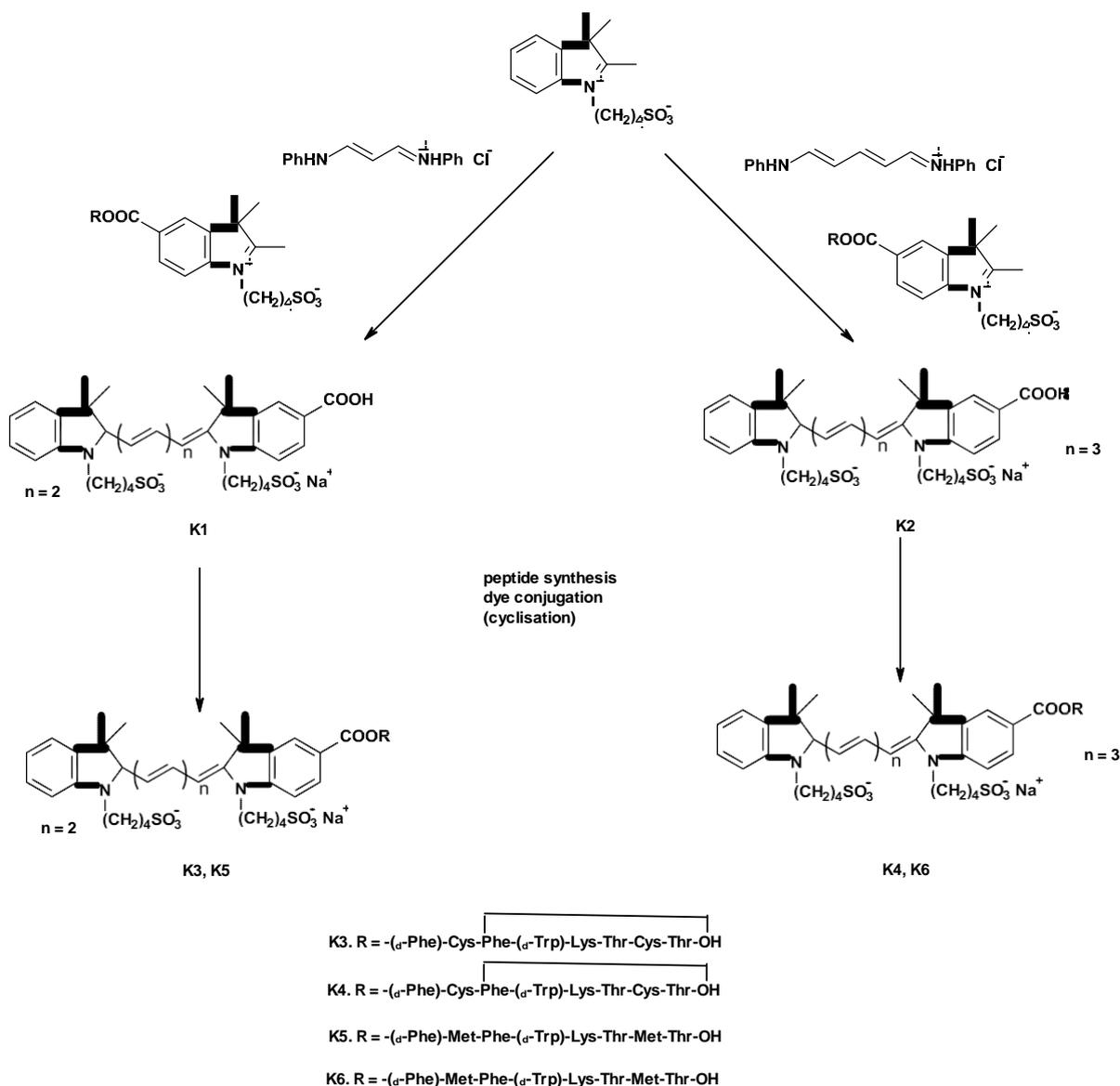
Scheme 1.12: Preparation of monocarboxylated indodicarbo (**K1**) and indiotricarbocyanine (**K2**), and the structures of the resulting peptide conjugates **K3**-**K6**.

Glunde and co-workers have reported the synthesis and development of two novel NIR cyanine dye fluorescent probes by linking a carbocyanine fluorophore and glucosamine through diverse linkers (Scheme 1.13) [125]. The probes demonstrated a high quantum yield, low cytotoxicity, reversible pH-dependent fluorescence in the physiological pH range, and a decreased aggregation tendency in aqueous solutions. Results from the *in vitro* NIR optical

imaging studies showed cellular uptake and strong intracellular NIR fluorescence for the two probes in four breast epithelial cell lines [125].
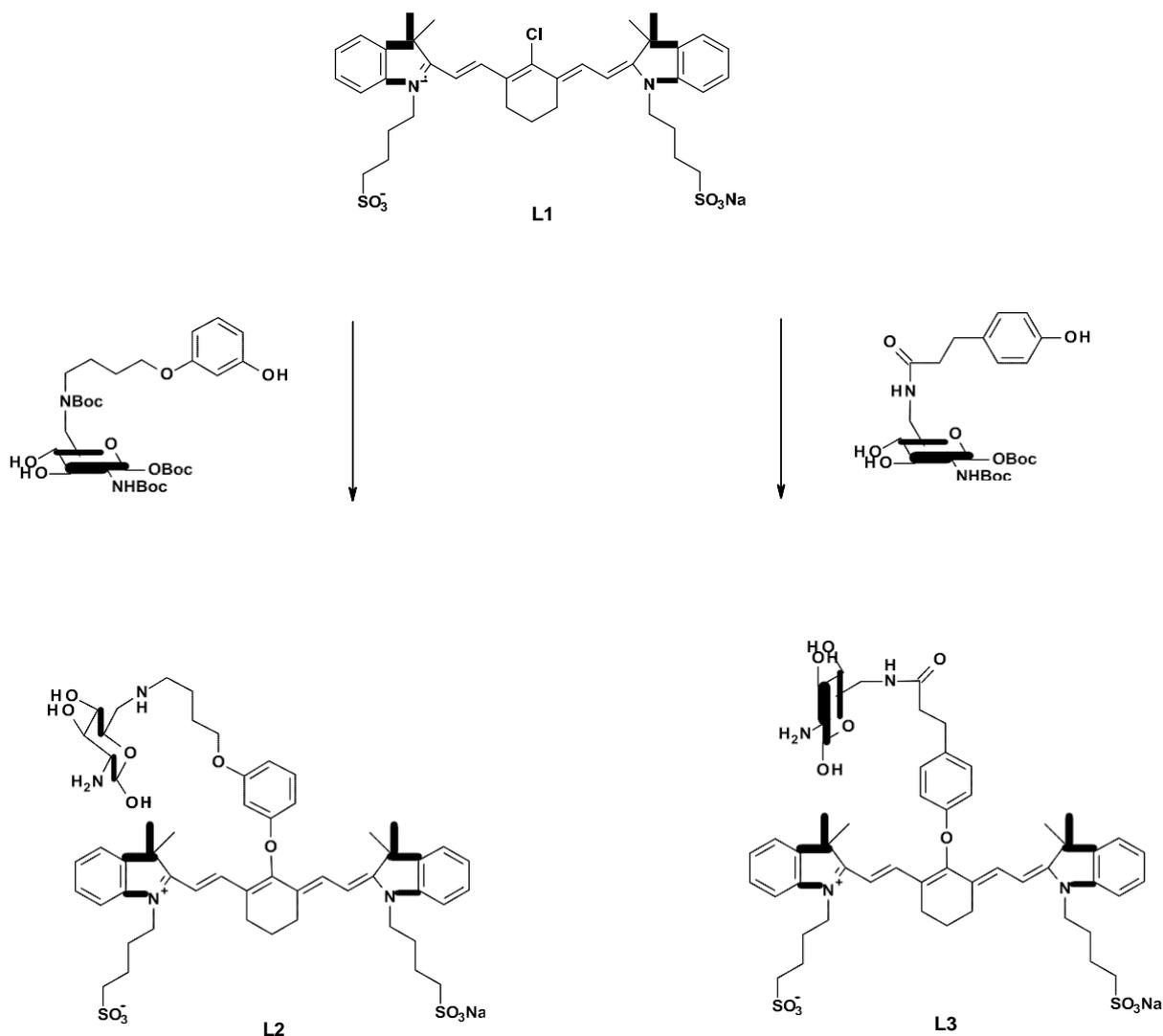
Scheme 1.13: Glucosamine fluorescent dye probes.

Kimura and co-workers have successfully coupled a NIR fluorescent ICG dye molecule to a nanocarrier for tumour imaging application [126]. A murine model for human liver cancer was established by injecting human hepatocellular carcinoma cells expressing luciferase into mice. The ICG coupled nanocarrier was then delivered parenterally. The ICG NIR fluorescence distribution pattern was reported to overlap with the luciferin bioluminescence, indicating the potential of the NIR fluorescent dye-coupled nanocarrier as a prospective

tumour imaging candidate [126]. In another approach, a NIR cyanine dye (Cy5.5) in conjugation with NHS with a potent Prostate-Specific Membrane Antigen (PSMA) inhibitor was utilised [127]. The probe was reported to display high potency against PSMA and demonstrated successful application for precisely labelling PSMA-positive prostate cancer cells in two and three dimensional cell culture conditions. The results indicated that a NIR Cy5.5-PSMA inhibitor conjugate (Figure 1.19) could be utilised for detection of prostate tumour cells by *in vivo* optical imaging [127].
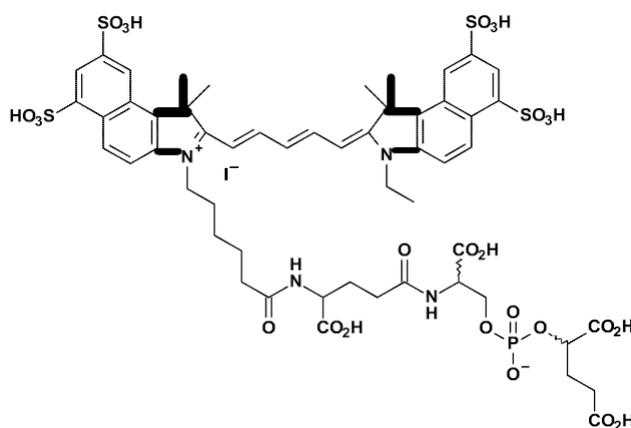
Figure 1.19: NIRF Conjugate Cy5.5-PSMA.

1.18 Click Chemistry

Improving and advancing the field of molecular imaging agents will require new chemistry techniques. Because imaging agents are often developed by the coupling of molecular entities with different but complementary functionality, the use of more refined and reliable covalent coupling reactions is necessitated [128]. Recently, a unique class of coupling reactions termed "click chemistry" has attracted tremendous amount of interest in the field of chemistry. Click chemistry was first fully introduced by Sharpless et al, and it can be defined as an integrated technique that utilises only the most feasible and consistent chemical transformations [129]. Its usage is often found in all aspects of drug discovery, starting from lead discovery through combinatorial chemistry to proteomics and DNA research, utilising bioconjugation reactions [130]. Click chemistry is predominantly used as a powerful linking reaction, due to its high level of specificity, dependability, and the complete bio-compatibility

of the reactants. The reactions are usually associated with high yields, with minimal side products that are easily removed by non-chromatographic techniques such as distillation or crystallisation. The reactions are also easy to perform being non sensitive to oxygen and water and utilise solvents that are easily removed or benign like water [130]. Though usually mistaken with a single reaction, 1,3-dipolar cycloaddition (CuAAC), "click chemistry" refers to a concept of how to do chemistry [131]. Numerous reactions including CuAAC, Diels-Alder reactions, nucleophilic substitution chemistry (such as the ring-opening chemistry of epoxides), carbonyl chemistry (such as thiourea formation), and oxidative additions to carbon-carbon multiple bonds (such as expoxidations) [132, 133] were identified to fulfil the click chemistry criteria such as minimal side products and hence can be categorised as click chemistry [126-131].

With the increasing interest in developing new synthetic approaches to construct chemically modified DNA for use in biological applications, it has quickly become apparent to researchers in the synthetic biology field that the Cu(I) catalysed [3+2] azides-alkyne cycloaddition reactions possess enormous potential [134]. The characteristics of click ligation reaction that are potentially useful for synthetic biology include:

- Azides and alkynes can be readily attached to nucleic acids without disturbing or changing their biophysical properties [132].
- The resulting triazole unit is particularly stable, being resistant to both hydrolysis and redox reactions [135].
- Azides and unactivated alkynes are almost totally unreactive towards the functional groups encountered in nature; they react only with each other. Figure 1.20 and Scheme 1.14 show the basic CuAAC click reaction and the Cu(I) catalysed click reaction cycle [132].
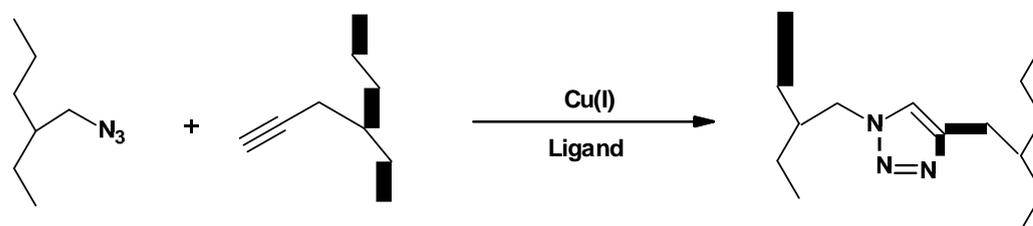
Scheme 1.14: The CuAAC reaction between an azide and a terminal alkyne to produce a 1,4-triazole [132].

34

The Cu(I) are usually introduced by the reduction of Cu(II) salts by sodium ascorbate or ascorbic acid (5-10 mol%). The Cu(II) salts are reasonably cheap making this synthetic route preferable [136].
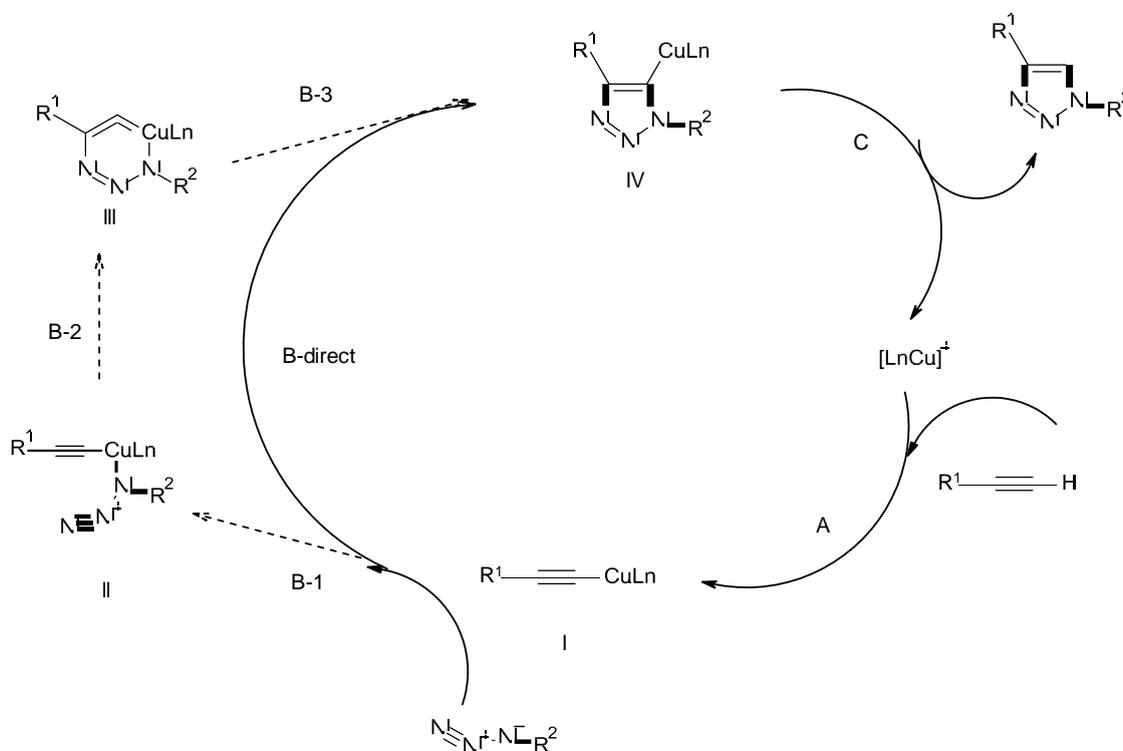
Figure 1.20: Proposed mechanism for Cu(l) catalysed click reaction between an azide and a terminal alkyne [136].

The reaction mechanism is divided into two pathways. The first pathway is the direct [2+3] cycloaddition and the second pathway is the stepwise progression (B1-B2-B3). Most recently, click chemistry has been used to incorporate alkyne functions into oligonucleotides and label them with dye azides. One strategy of carrying out this reaction is to introduce the fluorophore post-synthetically by reacting an alkyne-labelled DNA oligonucleotide with an azide derivative of a fluorescent dye, since the alkynes and azides are very stable functional groups except when reacting with each other. Wagnenknecht and co-workers have recently utilised this strategy, incorporating an alkyne moiety into oligonucleotides and labelling them with dye azides to give fluorescent dye oligonucleotide conjugate **M1** (blue) and **M2** (red) [137] (Scheme 1.15).
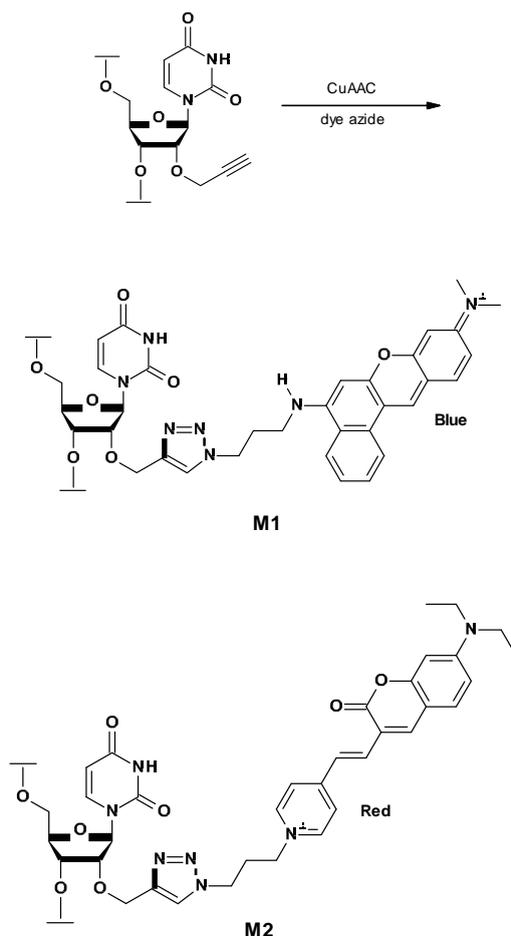
Scheme 1.15: Dye labelling at 2-position of ribose in DNA oligonucleotide using the CuAAC reaction [137].

Recent research has also shown that the CuAAC is a direct and robust method to couple a large variety of imaging agents to other functional entities [138]. Such entities include azide and alkyne–containing analogues of metabolic precursors such as monosaccharides and amino acids [138-140]. It is envisaged that in the future, there will be more novel molecular imaging applications of "click chemistry" and these applications will in turn help fuel the development of new and sophisticated molecular targeting imaging agents.

Literature Review:
Heptamethine Cyanine Dyes.

2.0 Near-Infrared Absorbing Heptamethine Cyanine Dyes

Near-infrared fluorescent dyes are molecules that absorb in the NIR region, 700-1000 nm. They can be efficiently used to visualise and study *in vivo* molecular targets because most tissues produce little autofluorescence in the NIR region [141]. NIR fluorescent dyes developed for *in vivo* imaging of cellular targets offer new opportunities in the field of molecular imaging [142]. The NIR fluorescent dyes have a highly conjugated molecular structural system with the energy gap between the ground and the excited state being lower than the dyes which absorbs in the visible region [141]. Currently, there are four main types of NIR fluorescent dyes commonly used in optical imaging, namely: cyanine dyes, squaraine dyes, thiazine and oxazine dyes [143-146]. The fluorescence mechanism of NIR fluorescent dyes relies on the transition of electrons between molecular electronic states. When an electron absorbs a photon from a radiation source of the right wavelength, the electron is promoted from its singlet ground state to its singlet excited state and the electron can return to its original state (singlet ground state) either directly or via molecular vibration. A photon is usually emitted when the electron returns directly to the singlet ground state and this is known as fluorescence. However, no radiation is produced when the electron returns by molecular vibration (Figure 2.1). In addition, energy is usually released when the electron returns to the singlet ground state. The energy change of excitation (ΔEex) is generally larger than the energy change of emission (ΔEem) thereby, generating a longer wavelength for the emission radiation than the excitation [147].
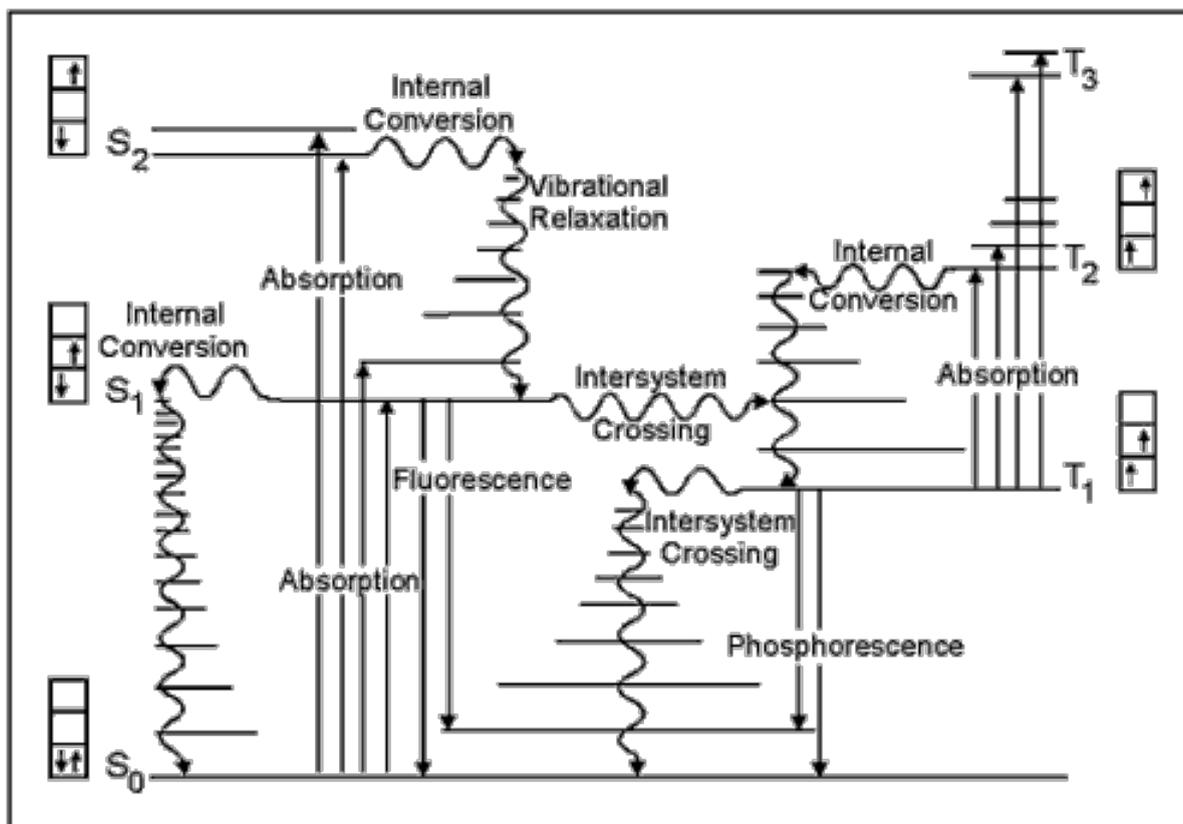
Figure 2.1: Jablonski diagram showing Electronic transition energy level [148].

2.1 NIR fluorescent cyanine dye characteristics

Indocyanine Green (Figure 2.2) has attracted a great deal of attention in the industrial and academic world. ICG is a typical non-targeting tricarbocyanine dye showing long-wavelength absorption around 800 nm and 830 nm emission maxima. It was first introduced into medicine in 1957 by Fox and co-workers [149] and its first application was in measuring cardiac output [150]. ICG was later adopted as a method of measuring hepatic blood flow and function [151]. When dissolved in blood, ICG has shown affinity for proteins such as Human Serum Albumin (HSA) and lipoproteins. Although ICG is a non-specific agent that is rapidly cleared from the blood, it frequently accumulates in regions of dense vascularity through extravasation [151].
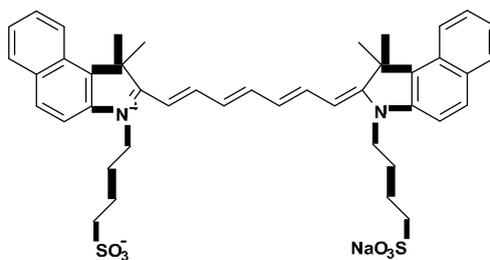
Figure 2.2: Indocyanine Green (ICG).

ICG and its analogues have also been explored as imaging agents in various aspect of surgical medicine [13, 152, 153]. For example, it has been applied for decades in ophthalmology for imaging retinal blood vessels, i.e. in retinal angiography [154, 155], for imaging sentinel node mapping in gastric cancer [156] and for evaluation of breast lymphatic pathways in patients with breast cancer [157]. Tumour targeting by fluorescence imaging is a result of a series of events occurring at the molecular level. The overall outcome is that a fluorescent molecule absorbs light within a molecular-specific absorption band and then emits light isotropically at a longer wavelength. The wavelength shift accompanying the fluorescence emission together with the isotropic nature of the emission facilitates discrimination between excited and emitted light in fluorescence imaging [158]. ICG has been used clinically for over 20 years with some drawbacks such as its cytotoxicity, non-specific binding and low fluorescence quantum yields (of 0.01) [159, 160]. Therefore, the development of new fluorescent dyes is important for medical research. Non-targeting NIR fluorescent heptamethine cyanine probe used for biomedical applications need to comply with several important criteria, as follows:

1) Wavelength: All potential NIR fluorescent dyes should be designed to absorb at wavelengths between 700-900 nm (diagnostic window) where there is enhanced tissue penetration (of approximately 5-10 mm) and less interference from other endogenous absorbers such as oxy and deoxyhaemoglobin, lipids and water. Below 700 nm, light does not penetrate to the maximum distance through tissues because of scattering and the presence of other endogenous absorbers. Above 900 nm water absorbs and therefore reduces the light penetration efficiency of the dye [161].

2) Quantum yield: Fluorescence quantum yield (ɸ) is one of the most important characteristics of a NIR fluorescent dye and having a high quantum yield is a major characteristic that the dye must possess. Fluorescence quantum yield can be defined as the level of effectiveness with which absorbed light creates the desired effect. It can also be defined as the percentage of photons emitted to those which are absorbed. The maximum fluorescence quantum yield is 1.0 (100%) indicating all photons emitted are absorbed [162].

3) Toxicity and Clearance: The safety of NIR fluorescent dyes is of paramount importance. It is critical to ensure that the imaging probe does not significantly interfere with the living subject in an acutely or chronically toxic manner. An optimal dye for biomedical application should have no toxic effects on cells and should clear rapidly, since uncleared free dye will interfere with the background light and hence affect its performance. Another important factor to be considered when designing tumour imaging dyes is the half-life of the dye in the human system. This is normally governed by the lipophilic or hydrophilic character of the dye. It is a well-established fact that hydrophilic dyes are rapidly cleared from the biological system but the lipophilic dyes are usually metabolised in order to generate more hydrophilic derivatives. This implies that a more lipophilic dye will remain for longer periods within the system, consequently increasing the chances of a deleterious event such as killing of normal cells [18, 159].

4) Solubility: NIR fluorescent dyes must have a high level of aqueous solubility before being administered into tissues for tumour visualization. A good level of solubility reduces the tendency of aggregates to form. One way of increasing the aqueous solubility of a dye is by the attachment of a sulfonic acid group on the dye structure [18, 199, 202].

5) Photobleaching: An ideal NIR fluorescent dye should be chemically stable under various conditions. Photobleaching, also known as fading, is a phenomenon which occurs when a dye loses its ability to fluoresce as a result of photon induced chemical damage. It results in a dramatic loss of the fluorescence emission intensity of most dyes [18, 197, 198].

2.2 Fission Yeast

To a test a number of the properties required by NIR dyes, non-targeting molecular probes can be tested *in vitro* (with extracts of cells) and *in vivo* using intact cells in cell assays. Testing the non-targeting probes with intact cells helps to determine some of the biological effects of the probes, such as toxicity. These techniques, in combination with modern molecular biology methods allows for a better understanding of the interactions between the molecular probes and the living subject [163].

In biology, the word yeast is usually used when referring to a wide variety of different single-celled fungi. Fission yeast (Figure 2.3) also known as *Schizosaccharomyces pombe* (*S. pombe*) is a species of yeast which has been extensively employed as a model organism in molecular and cell biology for investigating the fundamental processes significant to all living organisms [164]. There is a high degree of similarity between the cellular processes in yeast and those of human cells [164], which has resulted in the successful application of fission yeast as a model organism for mammalian diseases and pathways. These characteristics of yeast are considered in combination with its technical advantages, such as low cost, ease of growth and maintenance, reproducibility and the drive towards a reduction in the use of animal models in research. Fission yeast also gives the advantage of testing cell permeability and toxicity at the same time [165].

Yeast-based assays have been extensively used for measuring the activity of proteins and for detecting and characterising novel compounds with molecular interactions [166]. The easy genetic manipulation of yeast makes it an ideal system for investigating the effects of multiple mutations on cellular proliferation. These assays can immediately select against compounds that are cytotoxic and can also provide information on cell stability, permeability and solubility of the inhibitor [166]. Measurement of the reduction in cell proliferation has been used to characterise growth inhibition of established and new chemical entities such as chemical probes, which preferentially target proliferating cells [167].

Figure 2.3: The electron tomogram of a complete *S. pombe* yeast cell [168].

2.3 Recent Developments in Heptamethine Cyanine Dyes for Tumour Imaging

Amongst the available NIR dyes, heptamethine cyanine dyes have shown great potential for tumour imaging, due to their excellent biocompatibility and photophysical properties [169]. A vast amount of research is currently focused on increasing their tumour-targeted specificity by conjugating the fluorophores to targeting molecules known to bind to certain cell surface receptors that are expressed in tumour cells [171]. Also, on-going efforts are being made to develop targeted tumour photosensitisers conjugated to heptamethine cyanine dyes. The resulting bifunctional agents will be used for tumour imaging and photodynamic therapy. Such compounds which can be applied for imaging and therapeutic purposes would create a new paradigm for tumour diagnosis and therapy [191]. In this section, a perspective on the synthesis, photophysical characteristics, imaging and therapeutic potential of selected cyanine dyes will be briefly discussed.

Recent studies have focused on the design and development of new NIR fluorescent dyes with improved photophysical properties for *in vivo* imaging applications. For example in 2002, Tung and co-workers reported the synthesis of four new highly stable NIR dyes (Figure 2.4) with the aim of improving their photophysical and photochemical properties. The dyes were designed with a monoreactive carboxyl end group for labelling purposes [169].
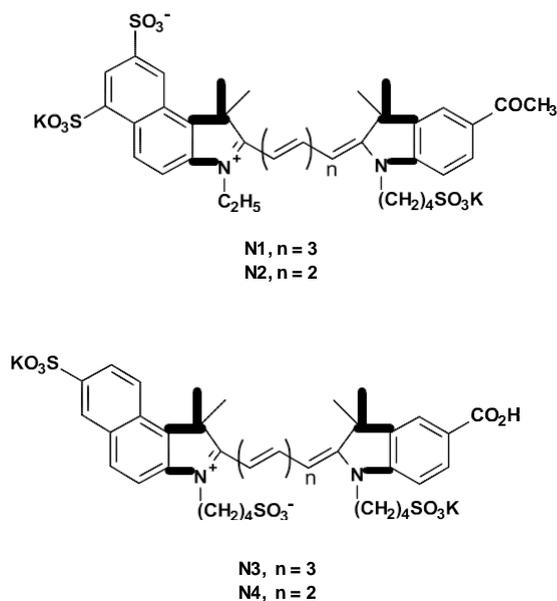
Figure 2.4: NIR dyes synthesised by Tung and co-workers [169].

The NIR dyes (Figure 2.4) contain multiple hydrophilic groups and were synthesised as monohydroxyl succinimide esters for binding to biomolecules such as proteins, metabolites and other affinity ligands. The synthesised dyes were characterised to be highly stable, possessing high quantum yields and excellent water solubility. In another report, Cheng and co-workers synthesised a series of novel NIR 3*H*-indocyanine dyes with varying *N*-substituents (Figure 2.5). The dyes were synthesised and tested to investigate the relationship between structures and photophysical properties in order to develop potential NIR dyes with excellent photostability for fluorescent imaging applications [170].

O1	O2	O3	O4	O5
X = Cl	X = Cl	X = Cl	X = Br	X = Cl
R = COOH	R = CH₃	R = F	R = NO₂	R = H

O6
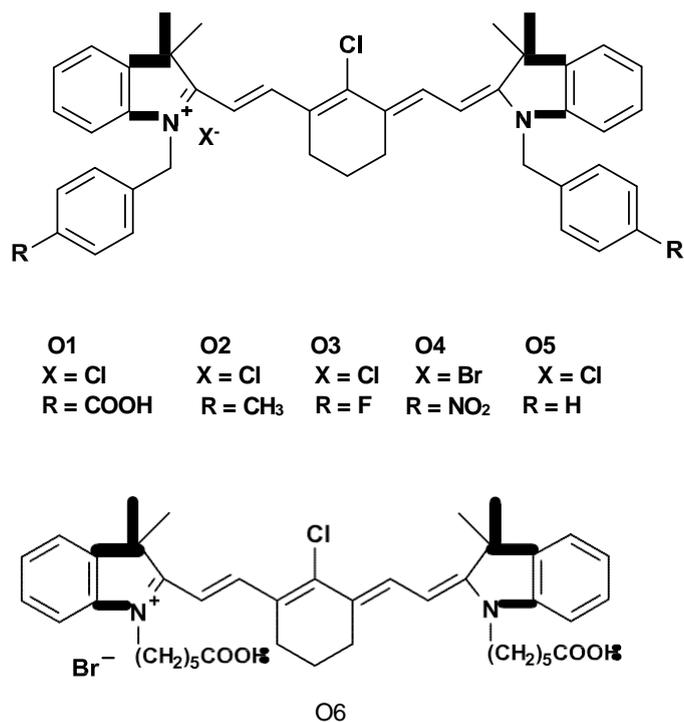
Figure 2.5: Structures of novel NIR cyanine dyes synthesised by Cheng and co-workers [170].

The NIR dyes which had an electron-donating group on the *N*-atom of the 3*H*-indolenine ring were reported to be effective in attaining greater resistance to photobleaching than those with electron-withdrawing groups. The NIR dyes showed absorption and emission maxima at 782-786 nm and 807-814 nm and fluorescence quantum yields ɸ within the range of 0.10-0.15 in methanol. The effects of varying the substitution pattern on the photostability for different substituents on the *N*-position was reported to decrease within the series from **O5**>**O2**>**O3**>**O1**>**O6**>**O4** [170]. Nagao and co-workers have described the synthesis and reactivity of a novel NIR fluorescent labeling reagent, ICG amide derivative of 1,3-thiazolidine-2-thione (ICG-ATT) possessing 3-acyl-1,3-thiazolidine-2-thione (ATT) (Figure 2.6) [171].
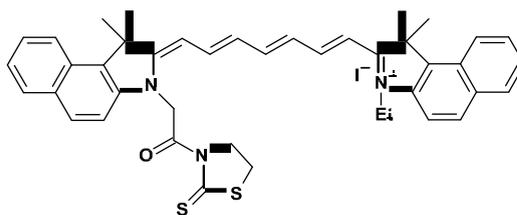
Figure 2.6: Novel NIR fluorescent labelling reagent synthesised by Nagao and co-workers [171].

It was concluded that ICG-labelled proteins can be utilised for tumor imaging applications due to their excellent fluorescence [171]. Recently, Aibin and Liping synthesised a heptamethine cyanine-based sensor. The sensor was designed by integrating a heptamethine cyanine fluorophore and methylpiperazine (Figure 2.7) [172].
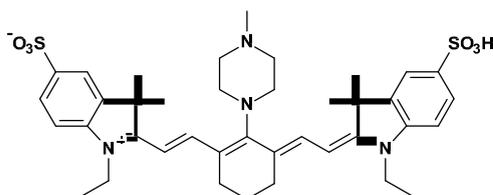
Figure 2.7: Heptamethine cyanine dye sensor synthesised by Aibin and Liping [172].

The sensor was reported to exhibit excellent responses to changes in pH levels (Scheme 2.1) and Stoke shift value of around 100 nm. Fluorescent imaging experiments were also performed in living cells to demonstrate the potential of the sensor for *in vivo* applications in biological systems [172].
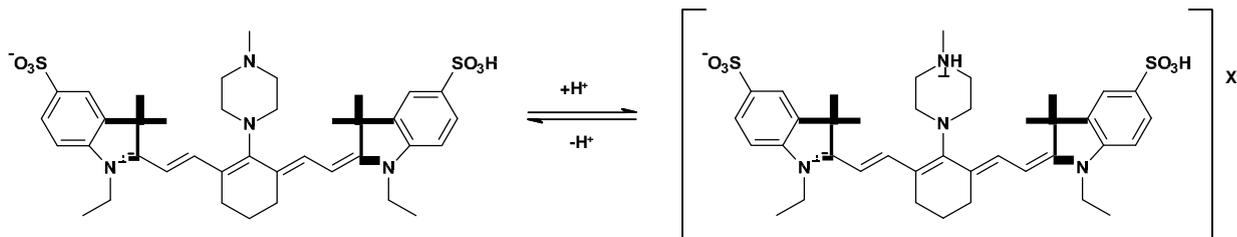
Scheme 2.1: Proposed binding mode between NIR sensor and H^+ [172].

The experiments in living cells were carried out using V79 379A Chinese hamster cells. The results obtained from the experiments indicated that the sensor penetrated the cell membrane and could be used for imaging of H^+ and detecting changes in H^+ concentration in biological systems [172]. The synthesis of a range of structurally diverse NIR absorbing dyes has been reported by Samuel Achilefu and co-workers [173]. Studies were carried out to primarily determine the effects of structural changes on the Fluorescent Life Times (FLT) of the dyes. Figure 2.8 shows the diverse range of dyes synthesised [173, 174]. The report indicated that the comparative FLT analysis based on solvent showed that the FLT of the polymethine dyes increased from polar to non-polar solvents. Also, analysis based on the heterocyclic structural system and modification of the methine chain length indicated that dye **P1** exhibited longer FLT than **P3** and this effect could be attributed to the influence of both the heterocyclic system and the short polymethine chain [145]. Nucleophilic substitution on the meso-chlorine atom in **IR 820** with a phenyl carboxyl to give compound **P1** was also reported to increase the FLT from 0.48 to 0.98 nm in dimethyl sulfoxide (DMSO). This result demonstrated that not only the presence of the heavy-atom mediated intersystem crossing but a combination of different criteria can also play a role in determining the FLTs of NIR dyes. It was also observed that the presence of a bulky ring system in dye **P1** gave shorter FLT than in dye **P4**, indicating the presence of the bulky phenyl group in **P1** destabilises the excited state in comparison to dye **P4** which has no phenyl group. The effect of different substituents at heterocyclic ring system of the NIR dyes was also investigated. The results obtained indicated that the presence of a heavy-atom plays an important role in the FLT of the NIR dyes, since the substitution of carbon with sulfur or selenium in **P5** and **P6** gave an increased

FLT. It was then concluded that the presence of heavy-atoms in the ring system facilitated inter system crossing [145].
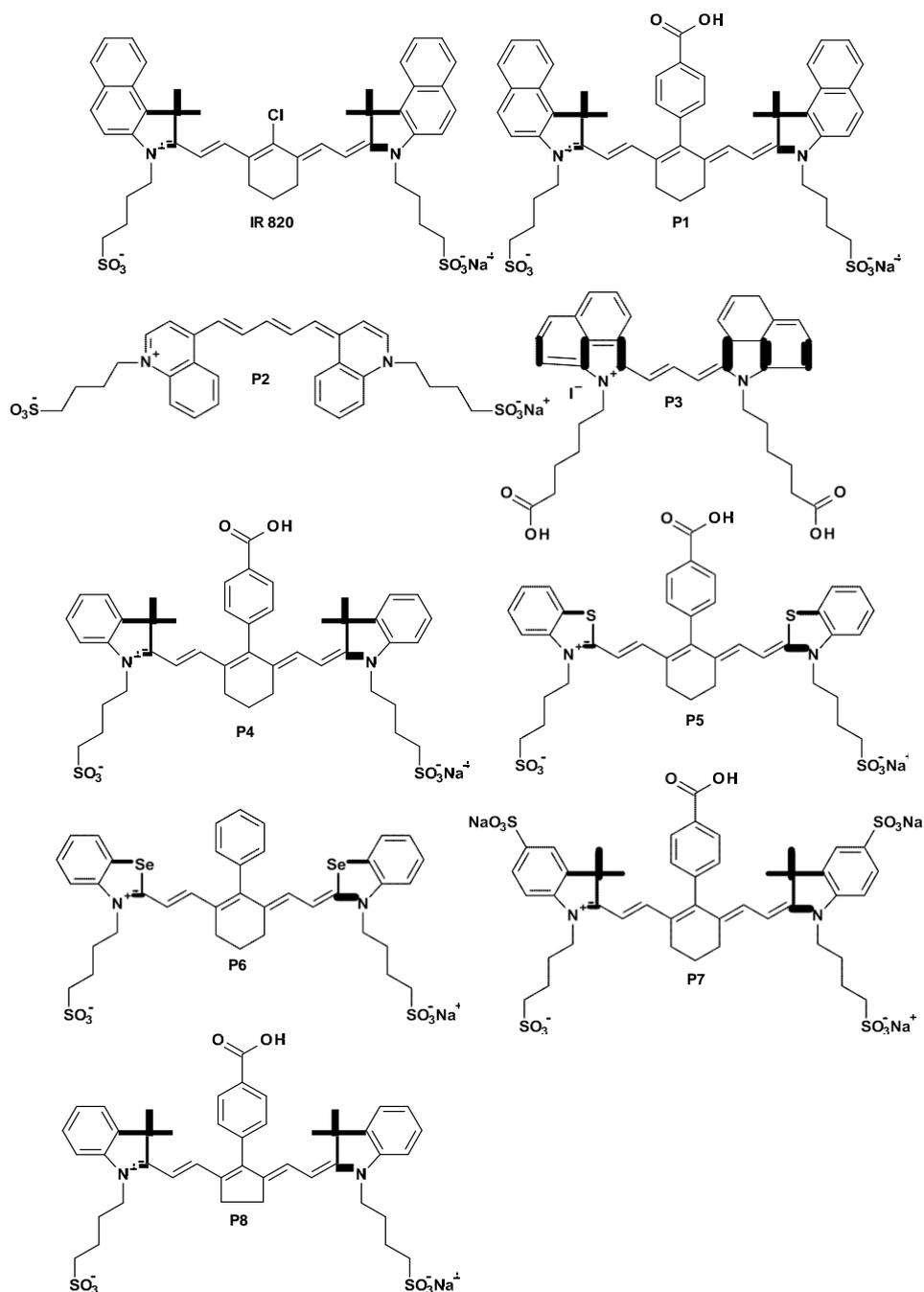
Figure 2.8: Structures of NIR fluorescent dyes synthesised by Achilefu and co-workers [173].

Patonay and co-workers have synthesised and investigated the effect of varying the alkyl group length substituted on the indole nitrogens on the spectroscopic properties of cyanine dyes [175]. The molar absorptivities (ε) were determined by the Beer-Lambert law and fluorescence quantum yields were calculated using the relative method [175]. Two diverse classes of cyanine dyes were investigated: pentamethine cyanine dyes and the ring-stabilised heptamethine cyanine dyes (Figure 2.9). The two classes of cyanine dyes with different "backbones" which differed mainly in terms of the substitution and length of the polymethine chain were selected as models to ensure that the observed results were broadly applicable to a variety of cyanine dyes.

MHI-85	R = (CH$_2$)$_4$SO$_3^-$ Na$^-$	
666	R = *n*-Butyl	X$^-$ = PF$_6$
829	R = Isopentyl	X$^-$ = PF$_6$
IR-676	R = Methyl	X$^-$ = I

MHI-71	R = *n*-Butyl	X$^-$ = I
IR-780	R = *n*-Propyl	X$^-$ = I
IR-786	R = Methyl	X$^-$ = ClO$_4$
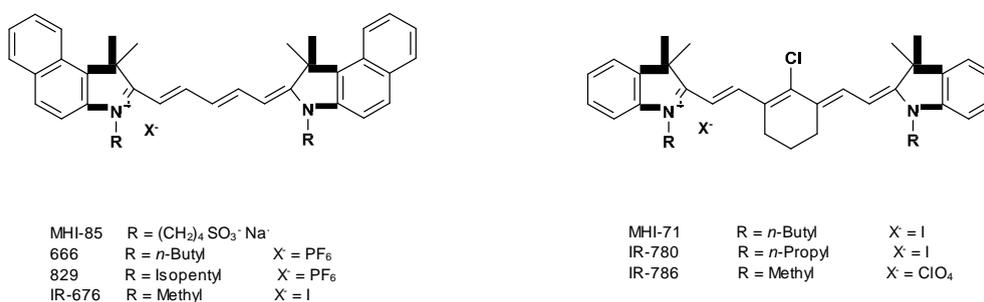
Figure 2.9: Structure of pentamethine and heptamethine cyanine dyes studied by Patonay and co-workers [175].

Based on the results obtained, the authors generalised that increasing the chain length of the R substituents on the heterocyclic indole nitrogen has little or no effect on the quantum yields and the molar absorptivities of the cyanine dyes. Likewise, the addition of sulfonate groups to the ends the alkyl *N*-substituents does not alter the quantum yield. The lack of influence on quantum yield may be attributed to the fact that the *N*-substituents are not directly conjugated to the chromophore and hence have little or no influence on the internal conversion-type energy loss. Also, the short chain substituents do not provide enough steric hindrance to interfere with photoisomerisation to *cis*-cyanine. The effects of these results are significant to the development and synthesis of new cyanine dyes [175].

Reactive Oxygen Species (ROS) have been reported to operate as signalling molecules under a wide range of physiological conditions. The over production of ROS results in oxidative stress and is involved in the pathogenesis of many diseases such as cancer and neurological

disorders [176-178]. Hence, fluorescent probes for visualising ROS offer new opportunities for the investigation of molecular mechanisms of physiological and pathological process and might also be suitable for diagnosis. To this end, Nagano and co-workers have reported the synthesis of a novel fluorescent probe, **FOSCY-1** (Figure 2.11) which operates in the physiologically favourable NIR region [179]. The probe consists of two cyanine dyes that react differentially with ROS connected by a linker. Reaction of the more labile dye with ROS results in intramolecular fluorescence quenching of the less labile dye. Firstly, they investigated whether cyanine dyes themselves react with various ROS by addition of hydroxyl radical ($^\bullet$OH), peroxynitrite (ONOO$^-$), or hypochlorite ($^-$OCl) to a phosphate buffered solution of commercially available cyanine dyes, **Cy5** and **Cy7** (Figure 2.10). The absorption of the dyes in the NIR region was lost, whilst little absorption spectral change was observed in the presence of oxygen and hydrogen peroxide (H_2O_2), which are weaker oxidants. The reactivity of the cyanine dyes with ROS in terms of the percentage absorbance was also investigated. This was reported to decrease at the maximum wavelength after ROS addition. There was a clear difference of reactivity between **Cy5** and **Cy7** with **Cy7** being more labile than **Cy5**.
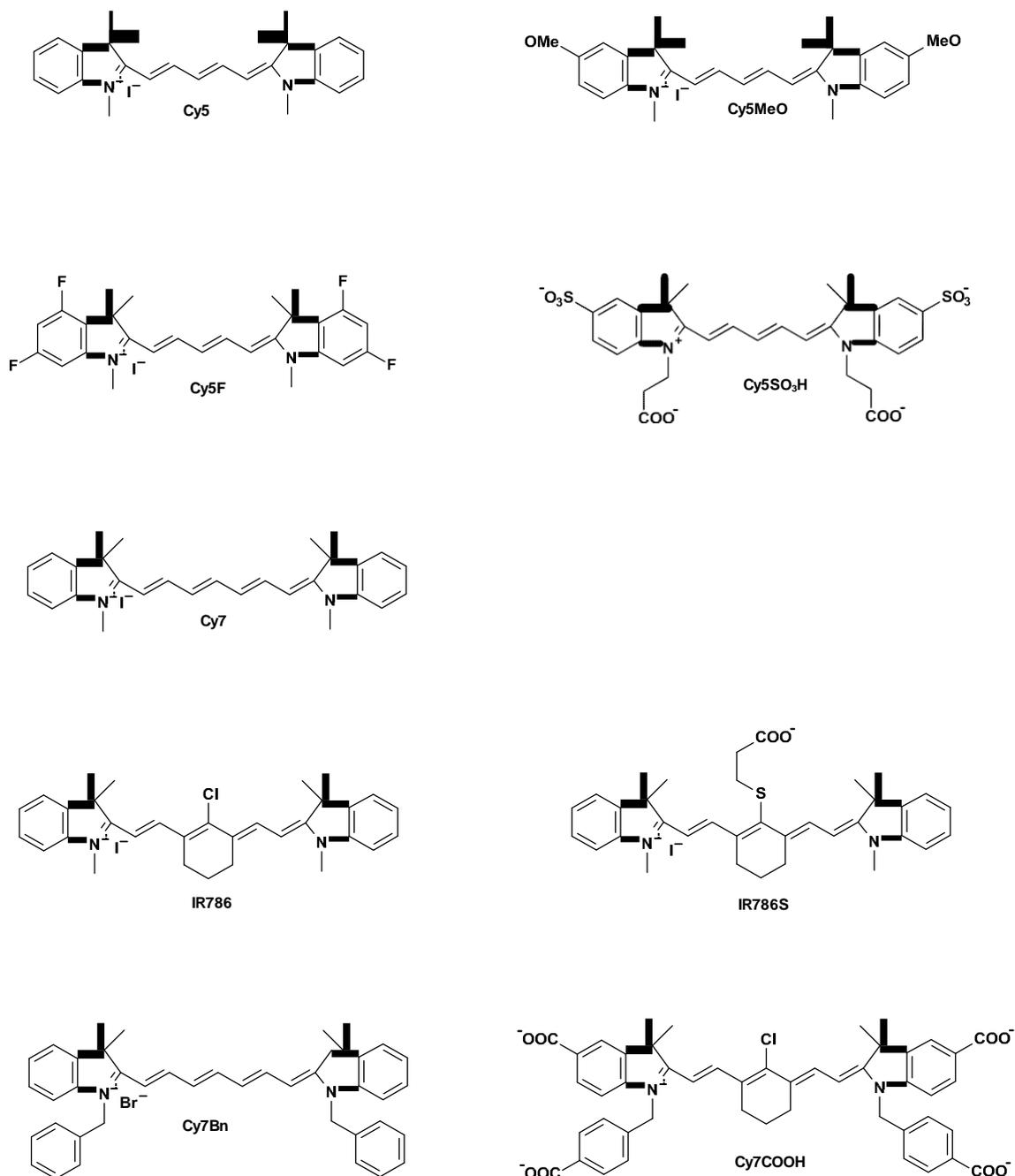
Figure 2.10: Structures of purchased or synthesised Cy5 derivatives and Cy7 derivatives by Nagano and co-workers [179].

The findings were also used to develop a novel NIR fluorescence probe. Emphasis focused on the differential reactivity of cyanine dyes using two linked cyanine dyes to obtain an

oxidative stress sensor (**FOSCY-1**) (Figure 2.11). Using this strategy, the two most suitable cyanine dyes with respect to reactivities were selected. **IR786S** and **Cy5SO₃H** showed a large difference in ROS reactivity, with **IR786S** reacting favourably with ROS in the presence of equal amounts of the two dyes. Hence, the two dyes were adopted and linked together through a cyclohexanediamine linker, yielding the sensor **FOSCY-1** [146,180].
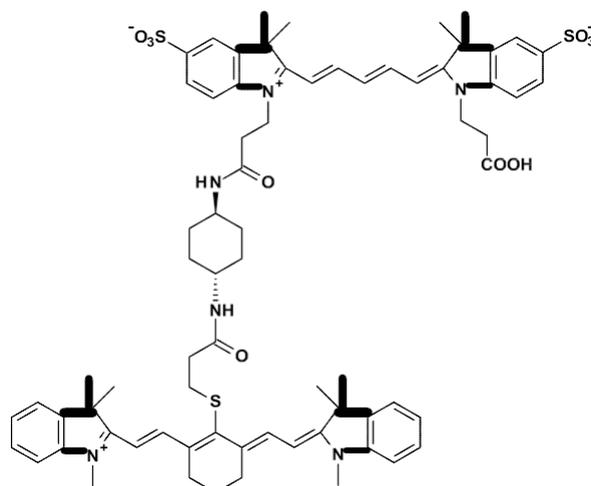
Figure 2.11: **FOSCY-1** [180].

The absorption peaks were observed at 644 and 792 nm indicating the presence of **Cy5SO₃H** and IR786S, respectively. The absorbance and fluorescence of **FOSCY-1** were very stable with respect to pH change or photooxidation, showing that **FOSCY-1** could detect ROS with high reliability in living cellular systems [179, 180]; thus, indicating its suitability for detection of ROS in chemical and enzymatic systems. The probe also demonstrated that it is suitable for detection of extracellular ROS as it appears to be almost membrane-impermeable [180]. Keli Han and co-workers have also developed a NIR reversible fluorescent probe bearing an organoselenium functional group that can be used for monitoring the highly sensitive and selective peroxynitrite oxidation and reduction events under physiological conditions [181]. ONOO⁻ is controlled by a cellular antioxidant defence system, the antioxidant enzyme glutathione peroxidase (GPx) in which selenium is a constituent of the active site [145, 182, 183]. GPx catalyses the reduction of ONOO⁻ using glutathione (GSH) via a unique ping-pong mechanism [184]. A NIR fluorescent cyanine dye with a high extinction coefficient, was selected as a signal transducer, whilst 4-(phenylselenyl)aniline

(PSe) was selected as modulator since it usually responds selectively to ONOO$^-$ [185, 186]. Using the ping-pong mechanism, the authors designed and synthesised a new NIR reversible fluorescent probe (Cy-PSe) (Scheme 2.2) for detection of ONOO$^-$ in living cells through a fast induced Photoinduced Electron Transfer (PET) process.

Scheme 2.2: Cy-PSe [185].
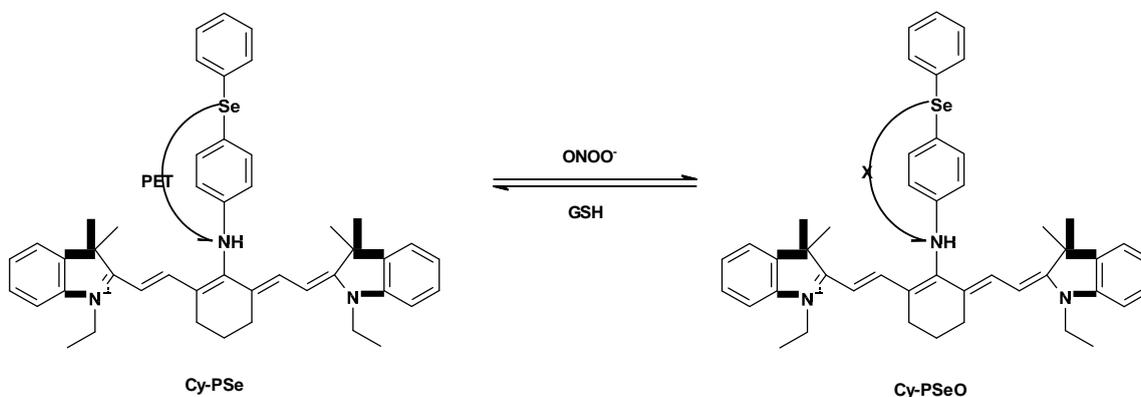
The probe demonstrates little autofluorescence in biological systems and also shows minimal toxicity to cells. It can also be utilised for the real-time imaging of living cells. In summary, the results indicated that the Cy-PSe probe can be used to visualise intracellular peroxynitrite levels with insignificant amount of background fluorescence and cellular toxicity [181]. Recently, a series of unique heptamethine cyanine dyes (**IR-783** and **MHI-148**) have been synthesised by Yang and co-workers (Figure 2.12a and b). The dyes were reported to be retained in cancer cells, and not normal cells, in tumour xenografts and transgenic mice [187]. They discovered that the dyes were localising in the mitochondria and lysosomes of cancer cells, possibly through Organic Anion Transporting Peptides (OATP), since the dye uptake and retention in cancer cells can be blocked totally by bromosulfophthalein (BSP). OATP are well established as routes for the transport of a wide range of substrates, including hormones, bile acids, xenobiotics, and their metabolites [188-191].
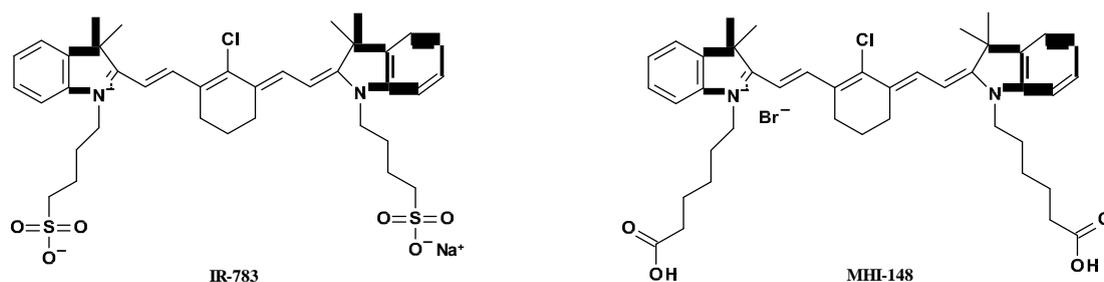
Figure 2.12(a) and (b): **IR-783** and **MHI-148** [187].

Tan and co-workers recently reported the improved chemical synthesis (Scheme 2.3) and biological activity of an already existing heptamethine cyanine dye (**IR-808**). The dye was shown for first time to exhibit intrinsic preferential tumour accumulation, photosensitising activity and NIR imaging without the need for chemical conjugation [192]. The advantages of the dye include excellent optical properties and photostability in serum. This allows for clear visualisation of cancer cells and tissues, with negligible background fluorescence from the host tissue, achieving superb signal to background ratio. The dye also possesses good pharmacokinetic properties and can be rapidly cleared from the host without any toxicity issues. The unique tumour accumulation and superior photosensitising characteristics make the dye particularly suited for targeting, imaging and PDT of minor tumours at their formation stage.
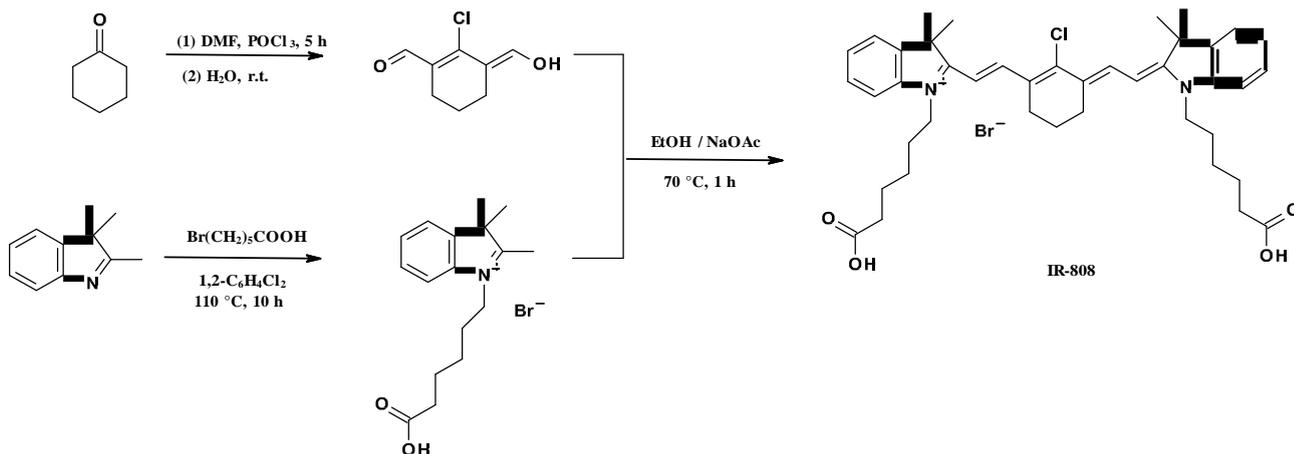
Scheme 2.3: Synthesis of IR-808 by Tan and co-workers [192].

Maged and co-workers recently synthesised three heptamethine cyanine dyes using a facile one-pot synthetic methodology (Scheme 2.4) [193]. The reaction protocol yielded a mixture of three symmetric and asymmetric heptamethine cyanine dyes bearing various *N*-indolenine substituents, a dicarboxylic acid (DA), a monoester (ME), and a diester (DE). The dyes were isolated and purified using column chromatography [193]. The biological activities of the dyes were also investigated to determine their tumour cell toxicity and uptake selectivity. It was discovered that the esterified heptamethine cyanine dyes (monoester and diester) were selectively cytotoxic to cancer cells and not to normal fibroblast cells. This effect could be attributed to the fact that esters are more readily transported across cellular membranes [193]. The heptamethine cyanine dyes were also used in confocal fluorescence imaging to confirm the tumour cell targeting potentials of the dyes.
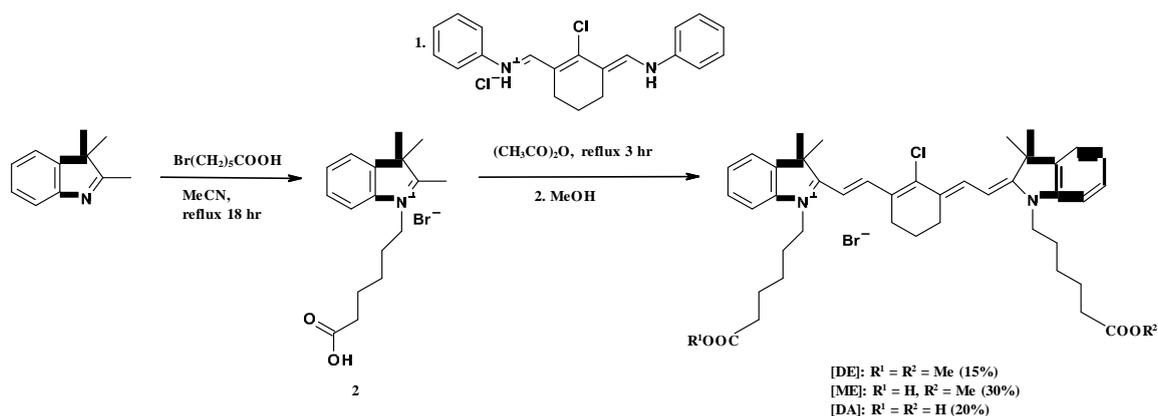
Scheme 2.4: Synthetic protocol for the one pot synthesis of symmetrical and unsymmetrical heptamethine cyanine dyes (DE, ME and DA) [192].

At present, there is still many on-going research aimed at developing new NIR heptamethine cyanine dyes that require no conjugation to targeting molecules for their delivery [194 -196]. Furthermore, these new developments will go a long way to assist primary tumour resection and improve the chances of complete removal of all tumour tissues while sparing surrounding healthy tissues during surgical procedures.

2.4 Aims and Concept

The aim of this project is to develop three different families of Cy7 dyes (linear, rigid and polymethine substituted) and experimentally compare their photophysical and growth inhibition characteristics against two classical NIR imaging dyes: The clinical standard ICG and IR-820.The focus will be on the dyes bearing sulfonic acids due to their close link with both ICG and IR-820. The project goal being to develop a range of non-targeted Cy7 imaging dyes which can be used alongside the clinical standards in biochemical research.

For these dyes to be considered for clinical application, dye candidates must have:

1. An economical and simplistic synthetic route, delivering the Cy7 dyes in good yields with straightforward purification.
2. Display better fluorescence quantum yields and comparable Stokes shifts to ICG and IR-820. All dyes must absorb and emit in the NIR region (700-900 nm).
3. Show less or comparative growth inhibition on cells upon comparison with ICG and IR-820.

With the above criterion in mind the specific objectives are:

1. The synthesis of linear, rigid and polymethine substituted heptamethine cyanine dyes. These synthesised dyes will contain a basic cyanine structure. Also, the dyes will also possess good leaving groups such as chlorine and bromine atoms making them potentially multifunctional agents for conjugation and functionalisation with biomolecules of interest.
2. Experimental photophysical evaluation of each dye by absorption and emission wavelengths, fluorescence quantum yields and Stokes shifts. The photophysical properties of dyes are important characteristics which determine their effective use as molecular probes for clinical applications.
3. Undertake comparative growth inhibitory studies, performed using *Schizosaccharomyces pombe* (*S. pombe*), a eukaryotic microorganism previously used for growth inhibitory screening and providing an important and valuable screening tool for determination of dye toxicity.

Synthesis and Characterisation.

3.0 Results and Discussion

This research project has been divided into three main sections which are outlined below:

1. Synthesis of non-targeted NIR heptamethine cyanine dyes.

   The rigid cyanine dyes were synthesised in accordance with published protocols [199, 259, 260] along with methodology which has been developed during this project. To expand, the *in-situ* cascade reaction within this novel methodology is a modification of the Zincke reaction and provides an elegant approach to the linear cyanine dyes, which can be tailored to develop more structurally sophisticated cyanine dyes, an example of which can be seen in Figure 3.15. Purification has been performed using either recrystallisation or column chromatography. Standard analytical techniques such as ^{1}H, ^{13}C NMR, ESI, HRMS, IR, UV and melting point analysis has been used for structural elucidation. 2D COSY NMR was also used to show coupling where required. One problem encountered with the characterisation part of this thesis was the difficulty in obtaining ^{13}C NMR for the rigid and linear dyes. These difficulties could be attributed to solubility issues and formation of aggregates in solution by the rigid and linear dyes.

2. Photophysical characterisations of the non-targeted NIR dyes.

   Photophysical characterisation for each dye was based upon, absorption and emission (excitation at 785 nm), fluorescence quantum yield (ϕ) and Stoke shifts. Each of the dyes was analysed alongside ICG and IR-820 due to their structural similarities.

3. Growth inhibition screening of the non-targeted NIR dyes.

   Comparative growth inhibition studies was performed using *Schizosaccharomyces pombe* (*S. pombe*), a eukaryotic microorganism used for growth inhibition screening [164]. It provides an important and valuable screening tool for determination of dye

toxicity [165]. This is important, should these dyes show potential for clinical applications. Using *S. pombe* as a model for mammalian cells is advantageous as many cellular processes are highly conserved between the two [164, 165]. Cell permeability and growth inhibition can be tested simultaneously and *S. pombe* strains are low in cost, easy to grow and the results obtained are highly reproducible [165]. The photophysical and growth inhibition data for each dye synthesised will be evaluated in chapter four.

The cyanines are *N*-substituted heterocyclic dyes with an extendable polymethine backbone which allows variations in their absorption profile; this is due to a bathochromic shift of approximately 100 nm per vinylene moiety (CH=CH) [38]. The heptamethine cyanine (Cy7) dyes in particular are among the most common NIR fluorescent dyes, showing high molar absorption coefficients and fluorescent quantum yields in organic solutions [40]. However, in aqueous solution many cyanine dyes suffer from poor photostability, low quantum yield, undesired aggregation and mild fluorescence [197]. Adapting these dyes to incorporate a rigid cyclohexenyl ring in the polymethine backbone increases their photostability and fluorescence quantum yield [39]. It has been recorded that addition of electron-donating/withdrawing groups on the nitrogen of 3*H*-indolenine affects the photostability of the cyanine dyes and by substituting the central chlorine atom on the cyclohexene ring for an electron-donor group such as amines can enhance the photostability of these dyes [198, 36, 41].

To this end, three classes of heptamethine cyanine dyes (rigid, linear and substituted polymethine linear dyes) (Figure 3.1) have been synthesised and their suitability as non-targeting probes for imaging in biological systems is evaluated and presented. Three distinct variations can be seen (X, R_1, R_2) with a final variation being shown along the polymethine backbone ($R_3 – R_4$). The reasons for such are highlighted below:

1. (X = S or 2 x C(CH$_3$)$_2$). It is well documented that sulfur moiety can exhibit a heavy atom effect and dramatically enhance intersystem crossing to the triplet state leading to alterations of the fluorescence quantum yield [145, 173]. It is also known that sulfur moiety can shift the absorption into the red by approx. 20 nm as shown in Table 4.4. The gem- dimethyl functionality on the

indolenine moiety allow comparisons to be made against the sulfur functionalities present in the benzothiazole moiety (Table 3.1)

2.   (R_1). Extending the alkyl chain length on the tertiary nitrogen (n=1 to 10, where n= alkyl salts). It has been shown in Table 4.1 that above n=4 the alkyl chains tend to make these compounds cytotoxic and as such, only alkylation from n=1 to 4 have been accomplished on the dyes synthesised. Many hepatmethine cyanine dye molecules tend to form aggregates in aqueous solution, specifically when inorganic salts are present. These aggregates typically have absorption bands shifted to the blue and, usually have a weak fluorescence [199]. It has been reported that cyanine dyes with a sulfonate group attached to the heterocyclic ring system of the dye have a minimal tendency to form these aggregates [202]. The sulfonate groups attached to the alkyl moiety of the indolenine nuclei of the dyes have little or no effect on the chromophore, but have been reported to increase the photostability, and aqueous solubility [197, 199, 202].

3.   (R_2). The potential heavy atom effects will be observed if different functional groups (such as Cl) are attached at this position.

4.   Its well noted that altering the rigidification of the polymethine chain is an established approach for improving the chemical and photostability of NIR dyes [173, 175].

Each of the dyes prepared are structurally related to each other so direct comparisons can be made.
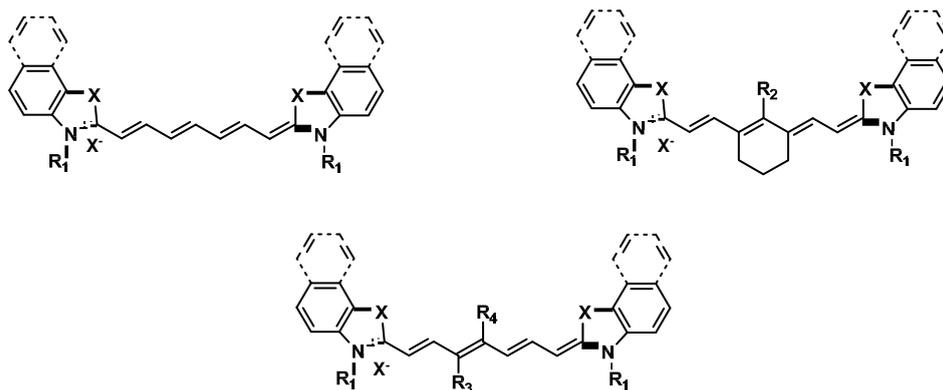
Figure 3.1: Structures of synthesised heptamethine cyanine dyes.
See Table 1.1 for values of X and R

3.1 *N*-Alkylation on the heterocyclic indole nitrogen

3.1.1 *N*-Alkylation of 2,3,3-trimethylindolenine and 2-methylbenzothiazole

The synthesis of the *N*-alkylated 2,3,3-trimethylindolenine (**1 a-m**) and 2-methylbenzothiazole (**2 a-m**) salts was straight forward and required no harsh or unusual methodology, as shown in Scheme 3.1. The salts were prepared by alkylation with the corresponding alkyl/benzyl halides or sultones, to afford the *N*-alkylated salts (bromides or iodides) in excellent to poor yields as shown in Table 3.1. For compounds with linear alkyl chains lengths less than n=4, the alkyl iodides (e.g. iodomethane) were used, whereas for chains greater than n=5, alkyl bromides (e.g. 1-bromopentane) were used [appendix]. It's interesting to note that compounds **1 a-d** and **k-m** precipitated from the reaction mixture and were isolated by vacuum filtration. This was also the case for all the *N*-alkylated 2-methylbenzothiazole salts (**2 a-m**). Compounds **1 e-j** however, show an increased hygroscopic nature which was attributed to the bromide counter ion. To counteract this problem, a counter ion exchange was performed based on the Finkelstein reaction to yield the iodide salts which are not as hygroscopic as the bromides; thus easier to handle and work with from a biological viewpoint. The counter ion exchange was straightforward and required refluxing the bromide salts with a stoichiometric amount of sodium iodide in acetone. Precipitation of sodium bromide followed, which was collected by filtration followed by evaporation of the liquor under reduced pressure yielded compounds **1 e-j** as the iodide salt. The synthesis of the full set of compounds (**1 a-m** and **2 a-m**) is shown in the experimental

section for clarity. The ^{1}H NMR spectra were consistent with the literature report and all synthesised compounds displayed downfield shifted signals (range: δ 3.90 – 4.05 ppm) corresponding to the CH$_2$-*N* moiety.

1 a-m and 2 a-m
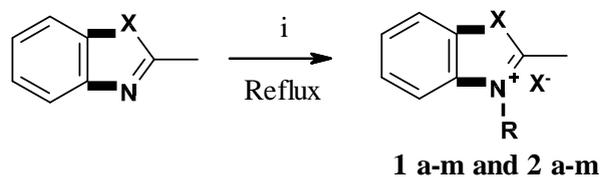
i. Alkyl halides in MeCN or Toluene or neat

Scheme 3.1: Synthetic route to yield *N*-alkylated salts (see Table 3.1 for values of X$^-$, X and R).

Number				Number			
	X$^-$	R	% Yield		X$^-$	R	% Yield
1a	I$^-$	CH$_3$	58	**2a**	I$^-$	CH$_3$	87
1b	I$^-$	CH$_2$CH$_3$	86	**2b**	I$^-$	CH$_2$CH$_3$	41
1c	I$^-$	CH$_2$CH$_2$CH$_3$	94	**2c**	I$^-$	CH$_2$CH$_2$CH$_3$	81
1d	I$^-$	CH$_2$(CH$_2$)$_2$CH$_3$	67	**2d**	I$^-$	CH$_2$(CH$_2$)$_2$CH$_3$	33
1e	I$^-$	CH$_2$(CH$_2$)$_3$CH$_3$	38 (99)	**2e**	I$^-$	CH$_2$(CH$_2$)$_3$CH$_3$	11
1f	I$^-$	CH$_2$(CH$_2$)$_4$CH$_3$	22 (99)	**2f**	I$^-$	CH$_2$(CH$_2$)$_4$CH$_3$	7
1g	I$^-$	CH$_2$(CH$_2$)$_5$CH$_3$	19 (86)	**2g**	I$^-$	CH$_2$(CH$_2$)$_5$CH$_3$	10
1h	I$^-$	CH$_2$(CH$_2$)$_6$CH$_3$	11 (40)	**2h**	I$^-$	CH$_2$(CH$_2$)$_6$CH$_3$	15
1i	I$^-$	CH$_2$(CH$_2$)$_7$CH$_3$	20 (27)	**2i**	I$^-$	CH$_2$(CH$_2$)$_7$CH$_3$	9
1j	I$^-$	CH$_2$(CH$_2$)$_8$CH$_3$	53 (99)	**2j**	I$^-$	CH$_2$(CH$_2$)$_8$CH$_3$	6

1k	Br⁻	$CH_2C_6H_5$	77	2k	Br⁻	$CH_2C_6H_5$	7
1l	-	$CH_2CH_2CH_2SO_3^-$	63	2l	-	$CH_2CH_2CH_2SO_3^-$	91
1m	-	$CH_2CH_2CH_2CH_2SO_3^-$	50	2m	-	$CH_2CH_2CH_2CH_2SO_3^-$	51

Table 3.1: Preparation of *N*-alkylated indolium/benzothiazole salts.

*N akylated salts 1e-m (C >5) data taken from allied project which has been published in *Eur. J. Med .Chem* which can be found in Appendix .

3.1.2 *N*-Alkylation of 1,1,2-trimethylbenz[e]indole

The synthesis of the *N*-alkylated 1,1,2-trimethylbenz[e]indole salts (**3 a-g**) was of strategic importance to the project, due to the fused benzene ring also being present in ICG and IR820. The synthetic route to these compounds is shown in Scheme 3.2 with Table 3.2 showing the % yields. Based on the cytotoxicity data collected (section 4.3) for the *N*-alkylated 2,3,3-trimethylindolenine (**1 a-m**) and 2-methylbenzothiazole (**2 a-m**) compounds, *N*-alkylation for these compounds was only to n=4.

3 a-g
(see Table 3.2 for values of X⁻ and R).

i. Alkyl halides in MeCN or Toluene or neat
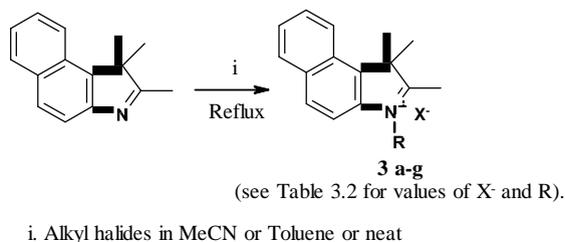
Scheme 3.2: Synthetic route to yield *N*-alkylated 1,1,2-trimethylbenz[e]indole salts.

Number			
	X⁻	**R**	**% Yield**
3a	I⁻	CH$_3$	91
3b	I⁻	CH$_2$CH$_3$	89
3c	I⁻	CH$_2$CH$_2$CH$_3$	81
3d	I⁻	CH$_2$(CH$_2$)$_2$CH$_3$	66
3e	Br⁻	CH$_2$C$_6$H$_5$	65
3f	-	CH$_2$CH$_2$CH$_2$SO$_3^-$	65
3g	-	CH$_2$CH$_2$CH$_2$CH$_2$SO$_3^-$	28

Table 3.2: Preparation of 1,1,2-trimethylbenz[e]indole salts.

3.1.3 *N*-Alkylation of 2-methylnaphtho[2,1-d]thiazole

N-Alkylation of 2-methylnaphtho[2,1-d]thiazole (Figure 3.2) was attempted, however only alkylation with iodomethane was observed in low yield. This was accomplished under microwave conditions (heating at 150 °C for 1 h under neat conditions) using iodomethane. It should be noted that normal wet conditions were attempted, however, no product was isolated from the reaction mixture. It is postulated that the nucleophilic nature of the sulfur group has an effect in the *N*-alkylation of the tertiary nitrogen and thus the presence of the aromatic ring causes enhanced steric bulk resulting in only a basic methyl iodide methylation being accomplished.
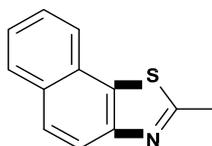
Figure 3.2: 2-Methylnaphtho[2,1-d]thiazole.

3.2 Activation of indolium or benzothiazole salts

For the rigid or linear heptamethine cyanine dyes to be synthesised, activation of the methyl group on position 2 of the indolium or benzothiazole salts must occur as shown in Scheme

3.3. This can be accomplished under Schotten-Baumann conditions, although this can also be done *in-situ*. Both conditions are explained further in 3.2.1 and 3.2.2 respectively.
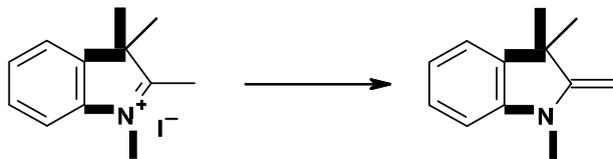
Scheme 3.3: Activation of the methyl group.

3.2.1 The Schotten-Baumann Method.

The Schotten-Baumann method is usually applied to the synthesis of amides as shown in Scheme 3.4. This historical method has been somewhat over-shadowed due to the potential problems of using an acid chloride in the presence of aqueous sodium hydroxide.
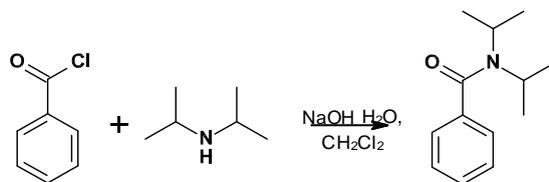
Scheme 3.4: Schotten-Baumann method of synthesis of amides.

Activation of the methyl group in position 2 of the indolium or benzothiazole salts can also be accomplished using this method as it does not suffer the same problems as the aforementioned acid chloride. The mechanism is shown in Scheme 3.5 and works using a biphasic set-up of 2M NaOH and toluene. The indolium salt dissolves first into the basic aqueous phase and following deprotonation, the newly formed 1,3,3-trimethyl-2-methyleneindoline is driven into the organic toluene layer. Isolation of the toluene layer and concentration under reduced pressure yields activated methylene groups in high yield usually being deep red in colour.
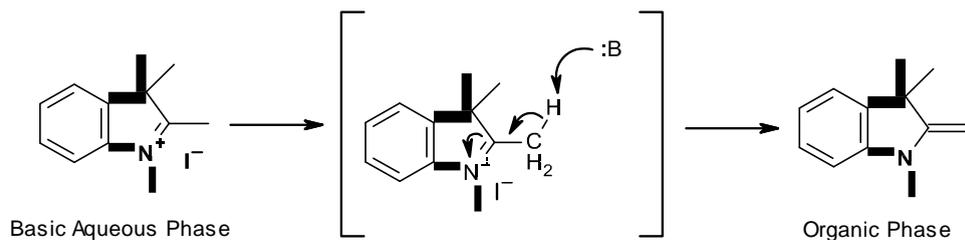
Scheme 3.5: Synthetic route to yield 2-methyleneindoline. :B = Base

Problems do however exist with this method; the composition of the product is often very sticky and tar-like, thus leading to subsequent handling problems.

3.2.2 The *in situ* method

Alternatively, this reaction can be done *in situ* during the synthesis of the dye, with the base being added during reflux (for the rigid dyes) or at room temperature (for the linear or substituted polymethine). This is usually the best way of preparing these types of dyes and as such has been used during this project. One drawback of this method is that unlike the Schotten-Baumann method, the activation of the methyl group does not always go to completion, affording lower dye yields.

3.3 Synthesis of the Rigid Heptamethine Cyanine Dyes

Rigidification of the polymethine chain is accomplished by incorporating a rigid cyclohexane moiety, examples of which are shown in Table 3.3. In order for this to be done a Vilsmeier-Haack (**VH1**) intermediate must be synthesised as highlighted in section 3.3.1.

3.3.1 Synthesis of Vilsmeier-Haack intermediate (VH1)

i. POCl$_3$ / DMF; ii. Aniline / EtOH; iii H$_2$O / HCl
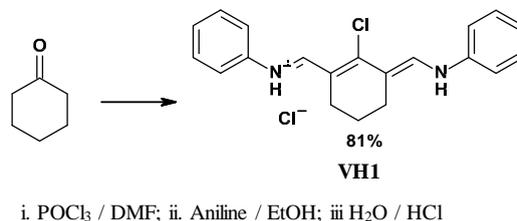
Scheme 3.6: Synthetic route to yield VH1.

The Vilsmeier-Haack intermediate (**VH1**) was synthesised using a previously reported procedure [199]. The Vilsemeier-Haack reagent is an iminium salt which possesses a weak electrophilic characteristic and is formed in the reaction between POCl$_3$ and an amide as shown in Scheme 3.6. The Vilsemeier-Haack reagent is then added with cyclohexanone and aniline, followed by an acid workup affords **VH1**. The reaction as whole involves the drop wise addition of POCl$_3$ (acid chloride) to a solution of anhydrous DMF and stirring them together at room temperature to form the reaction intermediate (*Vilsmeier reagent*) as a dark yellow solution. The next step is the addition of the cyclohexanone, followed by refluxing the combined mixture together to form a dark red mixture which is then allowed to cool down to room temperature. The final step is an exothermic reaction involving the drop wise addition of aniline in ethanol, followed by the acidic hydrolysis of the reaction mixture using dilute HCl and water to form the product in good yield of 81% (Scheme 3.6). The ^{1}H NMR was consistent with the literature report and the NH peaks were noticed as broad singlet peaks at δ 11.5 ppm. Further support for the structure was given by [M+H] peak in the ESIMS.

The structures and codes of the dyes with the rigid cyclohexane moieties are shown in Table 3.3 for clarity.

Code	Structure	Code	Structure
4 (a-g)		**7 (a-f)**	
5 (a-g)		**8 (a-e)**	
6 (a-g)			

Table 3.3: Structure of dyes with rigid cyclohexane moiety.
$X^- = I^-$ or Br^-

3.3.2 Synthesis of rigid dyes 4 a-g

The rigid cyanine dyes (**4 a-g**) were synthesised using an aldol-like condensation reaction as shown in Scheme 3.7.

i. **VH1**, NaOAc, EtOH
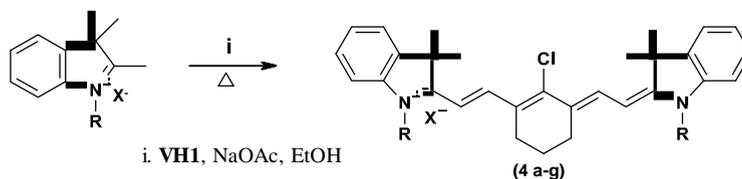
Scheme 3.7: Synthesis of the rigid meso-chloro indolium heptamethine cyanine dyes (**4 a-g**).
$X^- = I^-$ or Br^-

The crude dyes were purified by crystallisation from hexane or using flash chromatography to afford the dyes all in solid forms (Table 3.4).

Code			
	4 a-g		
	X⁻	**R**	**% Yield**
4a	I⁻	CH$_3$	36
4b	I⁻	CH$_2$CH$_3$	64
4c	I⁻	CH$_2$CH$_2$CH$_3$	54
4d	I⁻	CH$_2$(CH$_2$)$_2$CH$_3$	25
4e	Br⁻	CH$_2$C$_6$H$_5$	14
4f	-	CH$_2$CH$_2$CH$_2$SO$_3^-$	69
4g	-	CH$_2$CH$_2$CH$_2$CH$_2$SO$_3^-$	46

Table 3.4: Preparation of rigid indolium heptamethine cyanine dyes (**4 a-g**).

This reaction involves refluxing **4 a-g** with **VH1**, in ethanol in the presence of sodium acetate as shown in Scheme 3.7. Sodium acetate acts as a base catalyst forcing the deprotonation or proton abstraction of the methyl proton in the indolium salts to form the nucleophile. This step was accompanied by a colour change (yellow to red) during the reaction, indicating the formation of the nucleophile, which attacks the Vilsmeier-Haack salt acting as the electrophile in the reaction to form the crude heptamethine cyanine dye. During the nucleophilic attack step, the reaction mixture changed colour to a green solution indicating the slow formation of the dye. It should also be noted that the electron-withdrawing effect of the quaternary nitrogen plays a significant role in the deprotonation step and this is evident from the proposed mechanism for **4a** (Scheme 3.8).
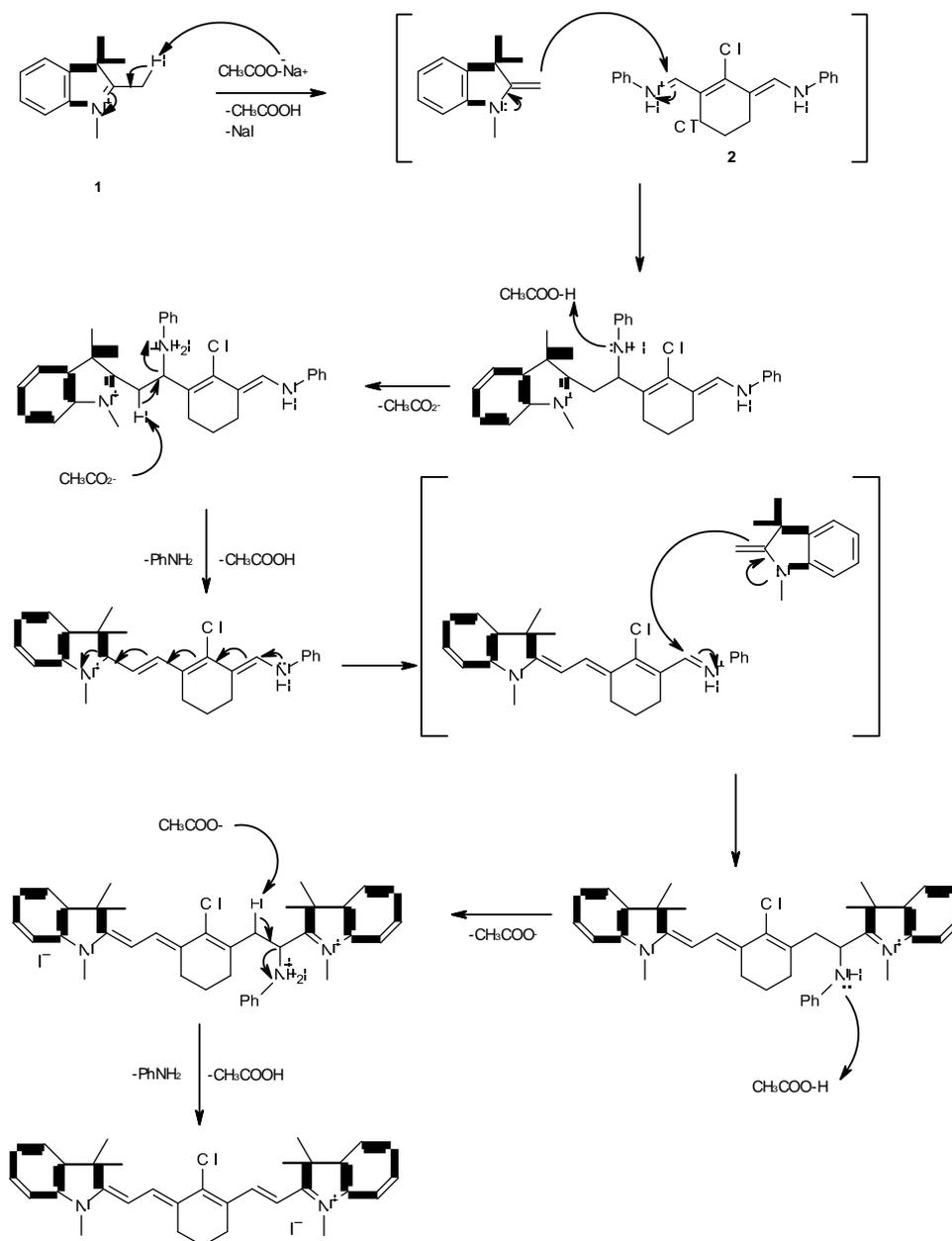
Scheme 3.8: Proposed mechanism for formation of heptamethine cyanine dye.

It is apparent from the reaction mechanism, the reaction for dye production will proceed in a 2 (quaternary ammonium salt) to 1 (**VH1**) stoichiometric ratio, to obtain the heptamethine cyanine dyes (**4 a-g**). The ^{1}H NMR splitting pattern shown for each dye in this family (**4 a-g**) is very precise (due to its symmetrical nature), each showing the expected 4H protons present on the polymethine backbone as doublets, each with a *trans*-coupling constant of 12 - 15 Hz. Also shown, is the 12H proton integral (4 x CH₃) as a large singlet between 1.5 - 1.8 ppm and

the 6H protons for rigid cyclohexene moiety, often observed as multiplets around 1.8 - 3.0 ppm. Each member of this family differs only in the *N*-alkylation substituents attached onto the quaternary nitrogen. To visually expand on this, Figure 3.3 shows the ^{1}H NMR spectrum of compound **4f**. Due to solubility issues, all the dyes within this thesis have been analysed using d$_6$-DMSO as solvent.
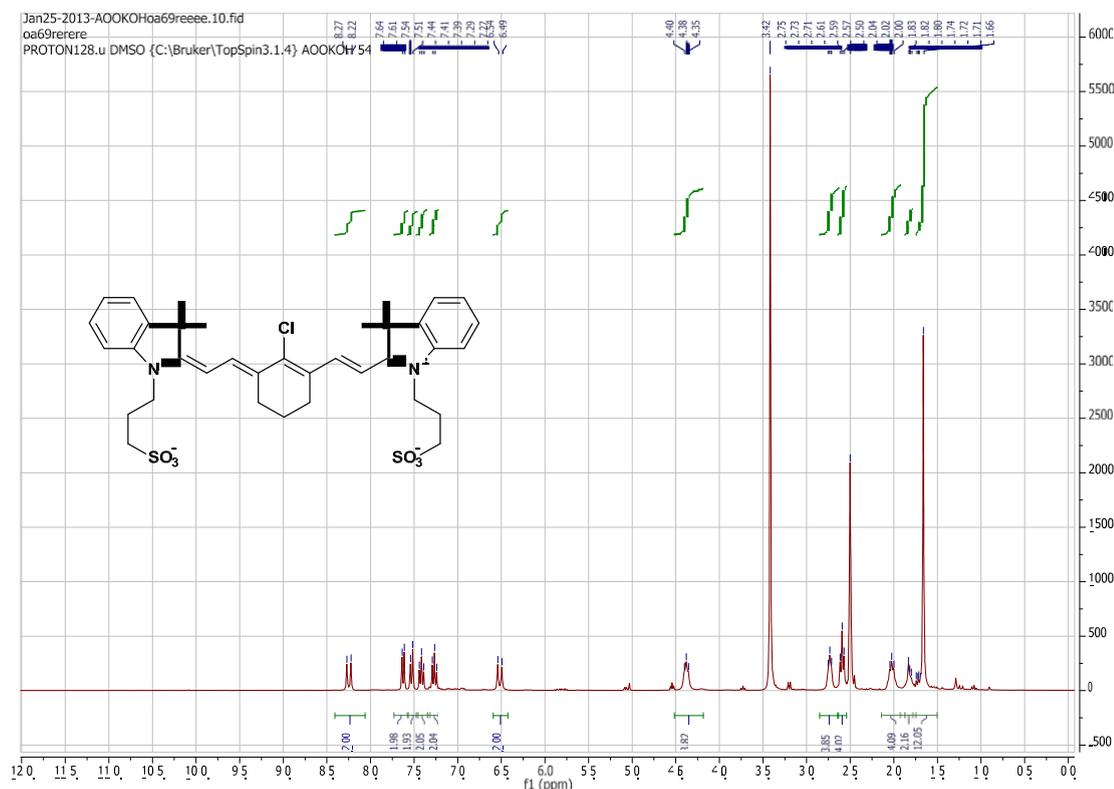
Figure 3.3: ^{1}H NMR spectra of **4f** in d$_6$-DMSO.

To expand further on the ^{1}H NMR of compound **4f**, the protons in the conjugated polymethine chain, gives two unique separate doublets at 6.49 ppm (*J* = 14.0 Hz) and 8.22 ppm (*J* = 14.0 Hz). The degree of the vicinal coupling constant indicates the all-*trans* characteristics of the polymethine chain. The large difference in the chemical shifts of the polymethine protons is due to the variation of charge along the conjugated cationic π-electron system. The *N*-alkylated side chain defines each dye within this family with **4f** having a linear propyl sulfonic acid side chain. Due to the molecular symmetry, the linear chain shows a well-defined set of signals when looking at the ^{1}H NMR with the N-*CH$_2$* signals.

3.3.3 Synthesis of rigid dyes 5 a-g

The synthesis of the rigid benzothiazole cyanine dyes (**5 a-g**) was accomplished using the same reaction methodology and stoichiometry as for compounds **4 a-g** and is shown in Scheme 3.9.

i. **VH1**, NaOAc, EtOH

(**5 a-g**)
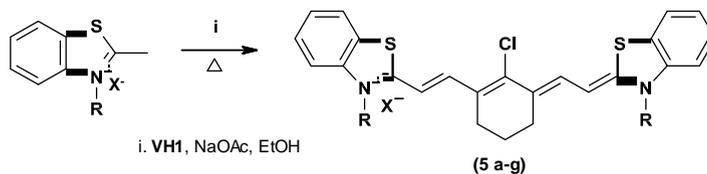
Scheme 3.9: Synthesis of the rigid meso-chloro benzothiazolium heptamethine cyanine dyes (**5 a-g**), X⁻ = I⁻ or Br⁻.

Purification either by recrystallisation or flash chromatography yielded the pure dyes in moderate to low yields (Table 3.5). This reaction proceeded faster in comparison to the indolenine dyes as noted by the rapid colour change of the reaction mixture from pale red to dark green. A possible explanation of this could be down to the nucleophilic character of the sulfur group.

The benzothiazole heptamethine cyanine dyes featuring two benzothiazole rings linked by a polymethine chain, possess the greatest potential for use in visualisation of cellular changes occurring *in-vivo* due to their excellent biocompatibility [200]. Patonay and coworkers have previously reported that heptamethine cyanine dyes bearing sulfur atoms within their heterocyclic ring system bind preferentially to human serum albumin (HSA) binding sites and furthermore, the sulfur atom on the heterocyclic ring system could enhance the specificity of the dye molecule [201]. Waggoner and coworkers have also reported that the presence of sulfonate groups on the aromatic rings of the dyes helps to increase aqueous solubility and thereby reduces aggregation [202].

Number			
	X⁻	**R**	**% Yield**
5a	I⁻	CH_3	51
5b	I⁻	CH_2CH_3	60
5c	I⁻	$CH_2CH_2CH_3$	63
5d	I⁻	$CH_2(CH_2)_2CH_3$	38
5e	Br⁻	$CH_2C_6H_5$	54
5f	-	$CH_2CH_2CH_2SO_3^-$	15
5g	-	$CH_2CH_2CH_2CH_2SO_3^-$	42

Table 3.5: Prepartion of rigid benzothiazolium heptamethine cyanine dyes (**5 a-g**).

Upon comparing the ^{1}H NMR of **5e** to **4f** it is clear to see differences in their structrual features. Noteably the 12H proton integral (4 x CH_3) as a large singlet between 1.5 - 1.8 ppm in **4f** is now absent in **5e** owing to the replacement of the sulfur moiety. It is also notable that the 6H cyclohexane protons which were shown as non-defined multiplets in **4f** are now shown as very prominent multiplets. The main difference comes from the 10H proton integral from the aromatic *N*-benzyl moiety off the benzothiazole ring. The Ph-*CH₂*-N protons in the ^{1}H NMR spectra of **5e** are equivalent and appear as a prominent singlet at δ 5.74 ppm, while the aliphatic region only indicates the presence of the cyclohexane protons confirming the presence of the benzothiazole dye. **5e** was further subjected to 2D COSY NMR analysis (Figure 3.4) to show further confirmation of the structure. Accurate mass analysis (HRMS) was also performed on **5e** to further emphasise on the purity of the compound. Figure 3.4b shows the accurate mass spectra for **5e**
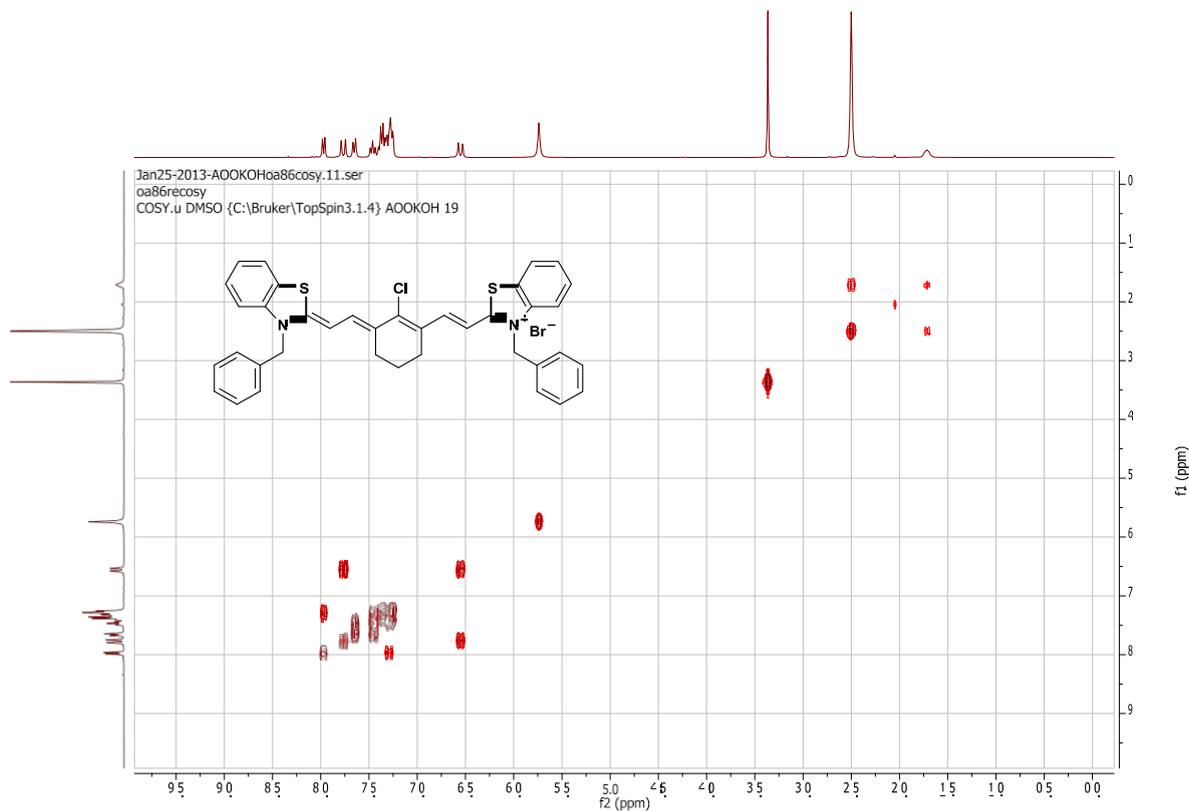
Figure 3.4: 2D COSY spectra of **5e** in d$_6$-DMSO.
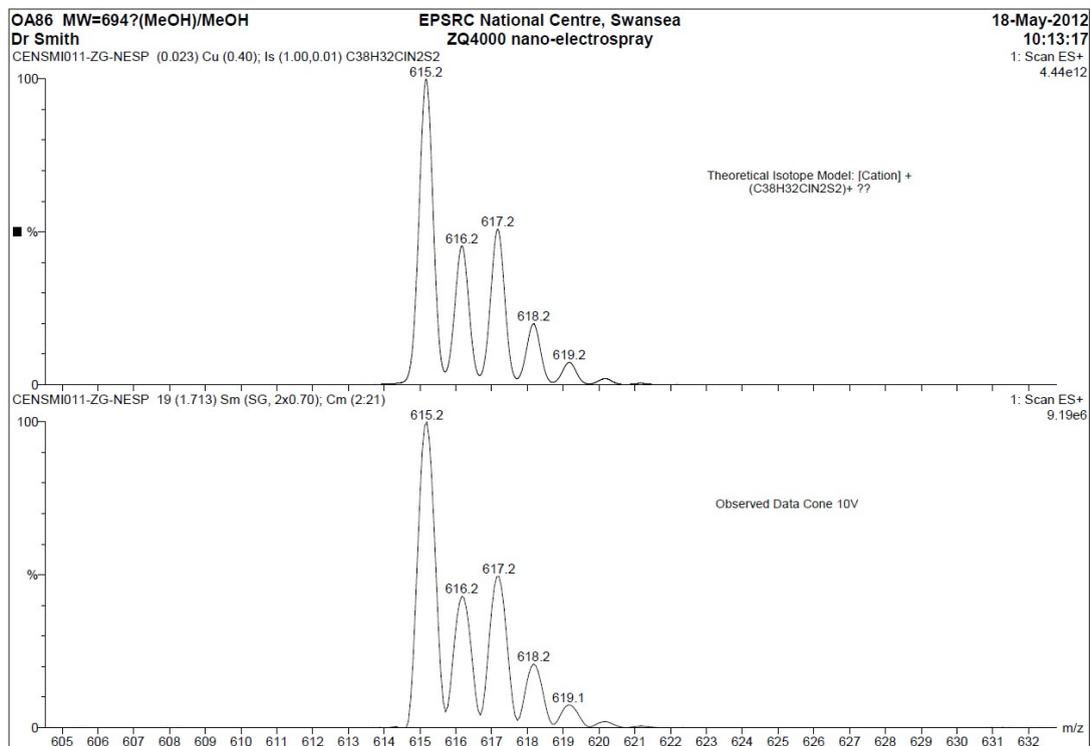
Figure 3.4b: Accurate mass spectra of **5e**.

3.3.4 Synthesis of rigid dyes 6 a-g

The synthesis of the benz[e]indolium heptamethine cyanine dyes was carried out by heating various *N*-substituted 2,3,3-trimethyl benz[e]indolium salts (**3 a-g**) with **VH1** in the presence of sodium acetate and ethanol under reflux (Scheme 3.10). The crude dyes were purified by silica gel column chromatography to afford the dyes all in solid forms (Table 3.6).
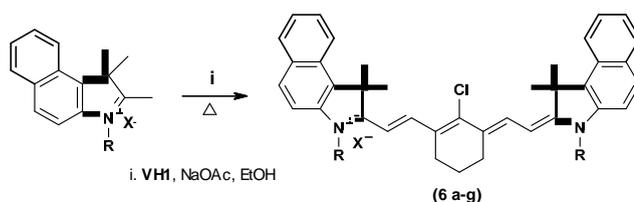
Scheme 3.10: Synthetic route to yield benz[e] indolium heptamethine cyanine dyes (**6 a-g**).
$X^- = I^-$ or Br^-

Number			
	6 a-g		
	X⁻	**R**	**% Yield**
6a	I⁻	CH_3	29
6b	I⁻	CH_2CH_3	58
6c	I⁻	$CH_2CH_2CH_3$	72
6d	I⁻	$CH_2(CH_2)_2CH_3$	45
6e	Br⁻	$CH_2C_6H_5$	20
6f	-	$CH_2CH_2CH_2SO_3^-$	70
6g	-	$CH_2CH_2CH_2CH_2SO_3^-$	79

Table 3.6: Preparation of Benz[e] indolium heptamethine cyanine dyes (**6 a-g**).

The benz[e]indolium based heptamethine cyanine dyes have been reported to increase the extent of π-electron conjugation of the heptamethine scaffold [173]. The increase in conjugation shifts the absorption wavelength of the dyes to the longer wavelength region

[175]. The presence of the extra phenyl ring on the dye molecule increases the planarity of the molecule, which reduces the chances of aggregation and in turn decreases the fluorescence excited state of the dye. As previously mentioned these dyes were strategically made as these structurally mimic IR-820 due to the fused benzene ring. The fused benzene ring leads to an increased bathochromic shift by approximately 20 nm into the red when compared to **4 a-g**.

The ^{1}H NMR spectra indicates the presence of extra aromatic protons belonging to the benz[e]indolium aromatic moiety (see Chapter 6).

3.3.5 Synthesis of rigid functionalised dyes 7 a-g

Previously Peng and co-workers had reported that tricarbocyanine dyes bearing an amine group at the central position of the polymethine bridge possess larger Stokes shifts than the non-substituted tricarbocyanines, owing to intramolecular charge transfer (ICT) [203, 204]. The large Stokes shift characteristic of the amine-substituted cyanine dyes renders them useful as NIR platforms for the development of a wide range of non-targeting fluorescent probes [203]. This will be discussed further in Section 4.4.4. It was envisaged that the presence of secondary nitrogen at the *meso*-position would improve the spectral properties and also have an effect on the growth inhibition properties of the synthesised dyes. The heptamethine cyanine dye structures are frequently modified at the *meso*-position to enhance and improve their cellular uptake, binding interactions, pH sensitivity and solubility [204]. Understanding the chemistry of how these modifications may impact the activity and spectral properties of the dyes is an important criterion for designing novel compounds with specific functional and binding properties.

The synthesis of dyes with the aniline moiety in place of the chlorine atom, involves the treatment of the heptamethine cyanine dyes **4 a-g** in anhydrous DMF under an atmosphere of nitrogen with ten equivalents of aniline (Scheme 3.11). A polar aprotic solvent such as DMF is suitable for this reaction since it helps in increasing the rate of the reaction.
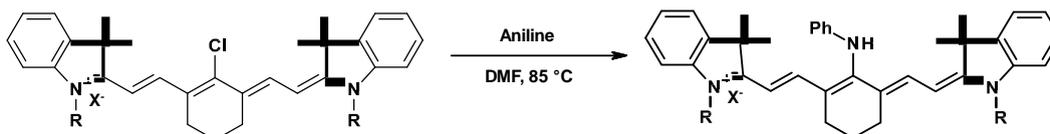
Scheme 3.11: Synthetic route to yield *meso*-anilino derivatives of indolium based heptamethine cyanine dyes (**7 a-f**), X⁻ = I⁻ or Br⁻.

The crude dyes were purified by flash chromatography to afford the dyes all in solid forms with moderate to poor yields (Table 3.7) and in high purity.

Number			
	X⁻	**R**	**% Yield**
7a	I⁻	CH_3	30%
7b	I⁻	CH_2CH_3	35%
7c	I⁻	$CH_2CH_2CH_3$	43%
7d	Br⁻	$CH_2C_6H_5$	17%
7e	-	$CH_2CH_2CH_2SO_3^-$	33%
7f	-	$CH_2CH_2CH_2CH_2SO_3^-$	40%

Table 3.7: Preparation of *meso*-anilino derivatives of indolium based heptamethine cyanine dyes (**7 a-f**).

Upon the addition of aniline to the dye, the reaction mixture was heated under reflux at 85 °C overnight to afford the crude product. The progress of the reaction was monitored continuously by TLC and visual appraisal due to a hypsochromic (shortwave) colour shift from green to blue as the electron-withdrawing chloro group is being replaced by an electron-donating amino group (Figure 3.5). The crude product was purified by column chromatography on silica gel to give the product with yields in the range of 17% to 43%. The conjugate dyes were stable at room temperature. The ¹H NMR data (Figure 3.6) supports the

presence of a bound aniline molecule, which is best exemplified by the Ph-NH signal appearing at 8.62 ppm as a broad singlet peak (see Chapter 6). Inspection of the IR spectra of **7a-f** shows N-H stretches at 2920 - 2928 cm^{-1} appearing in form of a shoulder band. The C-N stretch appears at around 1232 - 1240 cm^{-1} rather than at lower wave numbers due to the presence of the bound aniline molecule.
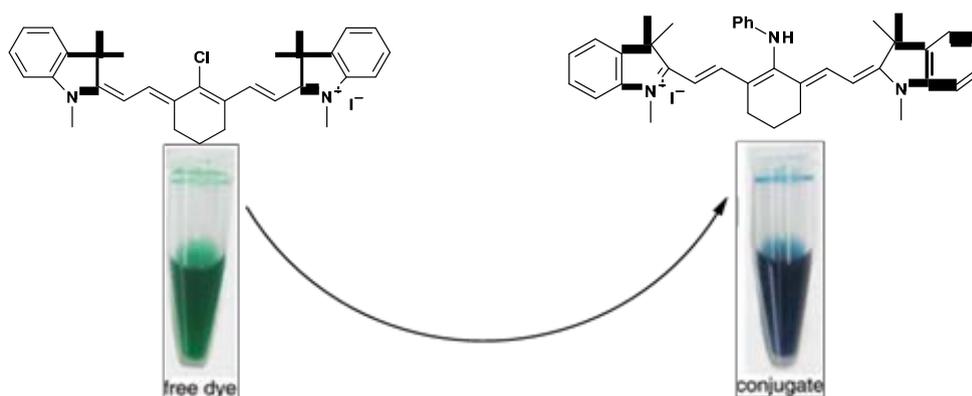
Figure 3.5: Colour change accompanying the substitution process.

The proposed mechanism for the reaction (Scheme 3.12) proceeds by the direct addition of the nucleophile to the cationic π-system followed by the subsequent elimination of the chlorine ion. The reaction occurs slowly upon gradual heating and prolonged reaction time.
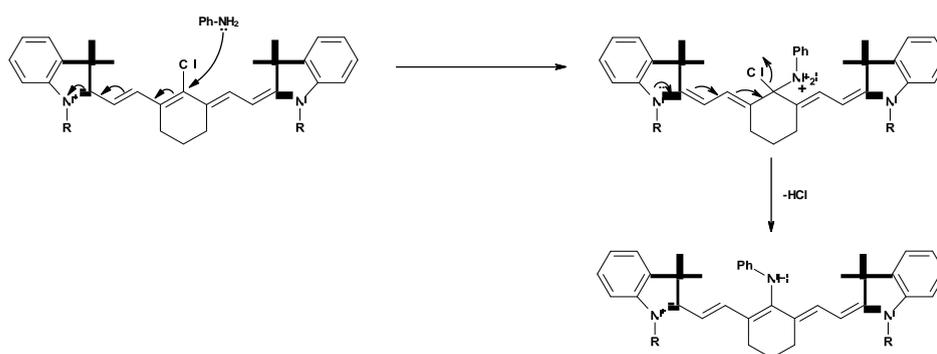
Scheme 3.12: Proposed mechanism to yield *meso*-anilino derivatives of indolium based heptamethine cyanine dyes.

3.3.6 Synthesis of rigid functionalised dyes 8 a-g

The *meso*-chlorine atom on the heptamethine scaffold of the benz[e]indolium heptamethine cyanine dye was treated with aniline in the presence of DMF to furnish the resulting anilio derived benz[e]indolinium heptamethine cyanine dyes (**8 a-e**) (Scheme 3.13). The butyl iodide and propanesultone derived *meso*-anilino dyes were unable to be synthesised due to solubility and purification issues. The crude products were purified by column chromatography on silica gel (chloroform/methanol 90:10) to give the pure products (Table 3.8). All the synthesised dye conjugates were stable at room temperature.
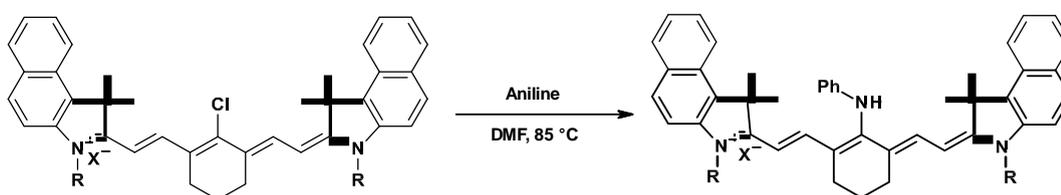
Scheme 3.13: Synthetic route to yield *meso*-anilino derived benz[e]indolinium heptamethine cyanine dyes (**8 a-e**), $X^- = I^-$ or Br^-.

Number				
	X⁻	**R**		**% Yield**
8a	I⁻	CH_3		44%
8b	I⁻	CH_2CH_3		34%
8c	I⁻	$CH_2CH_2CH_3$		38%
8d	Br⁻	$CH_2C_6H_5$		38%
8e	-	$CH_2CH_2CH_2CH_2SO_3^-$		40%

Table 3.8: Preparation of *meso*-anilino derivatives of benz[e]indolinium heptamethine cyanine dyes (**8 a-e**).

The ^{1}H NMR spectra (Figure 3.6) shows the presence additional aromatic proton and Ph-NH signal belonging to the aniline moiety.
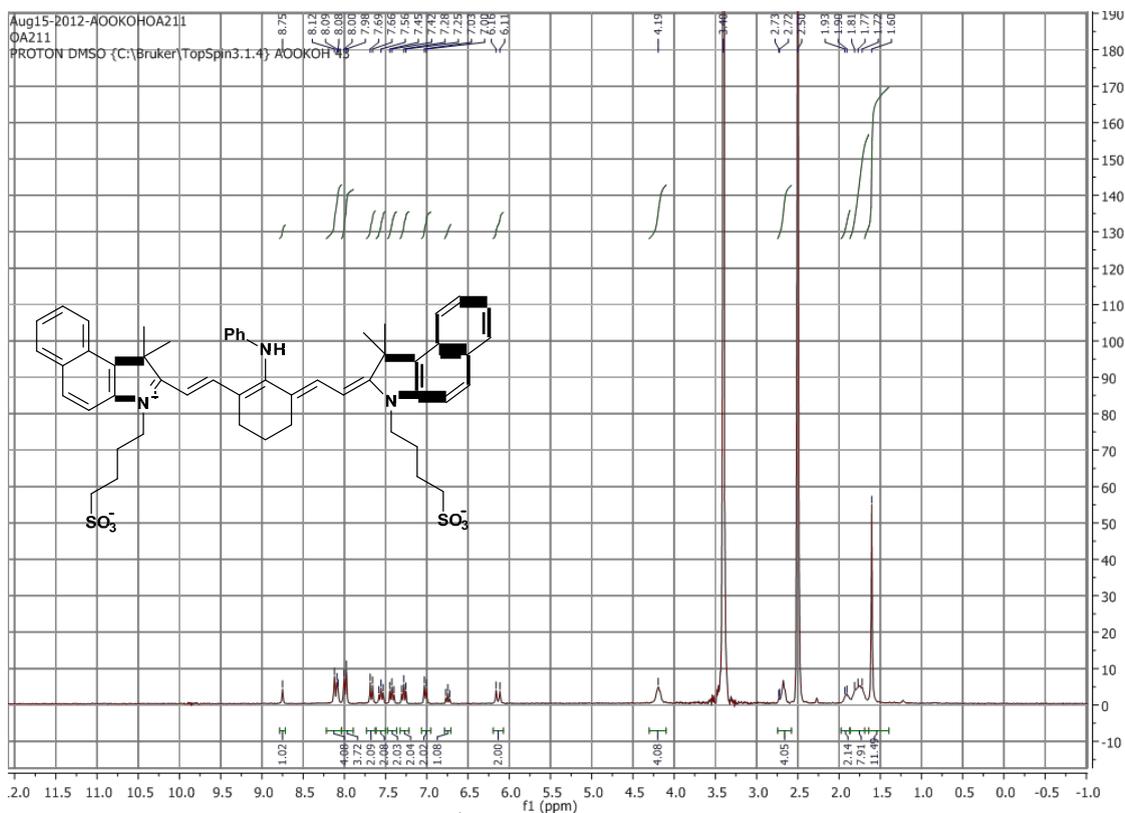
Figure 3.6: ^{1}H NMR spectra of **8e** in DMSO.

3.3.7 Attempted synthesis of *meso*-anilino derivatives of benzothiazole based heptamethine cyanine dyes.

Several attempts to synthesise the *meso*-anilino derivatives of the benzothiazole based heptamethine cyanine dyes (Scheme 3.14) failed. It is postulated that this effect could be due the nucleophilic nature of the sulfur atom in the heterocyclic ring system. The synthesis of the derivative was therefore discontinued.
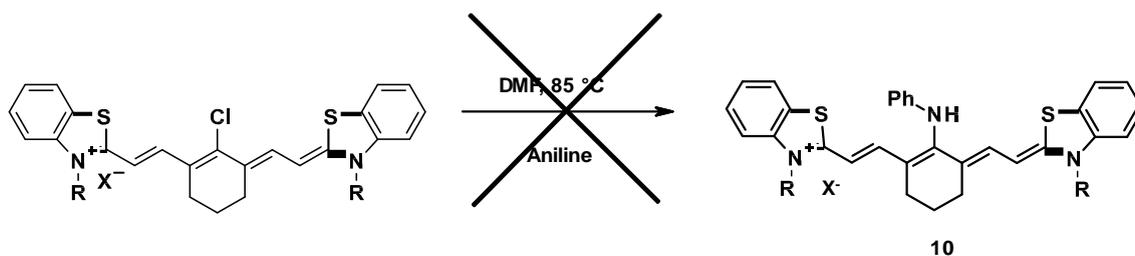
Scheme 3.14: Attempted synthesis of *meso*-anilino derivatives of benzothiazole based heptamethine cyanine dyes.

3.4 Synthesis of the linear heptamethine cyanine Dyes.

The linear or straight chain polymethine dyes are widely used in a large range of applications due to their excellent photophysical properties and low toxicity [205]. ICG (Figure 3.7) is a commercially available symmetrical Cy7 dye approved by the Medicines and Healthcare Products Regulatory Agency and the United States Food and Drug Administration. It is used in clinical applications, in particular, evaluating blood flow [205-207] and clearance [1]. Although it also has the potential as a tool for fluorescence-guided management and treatment of cancer [208, 209].
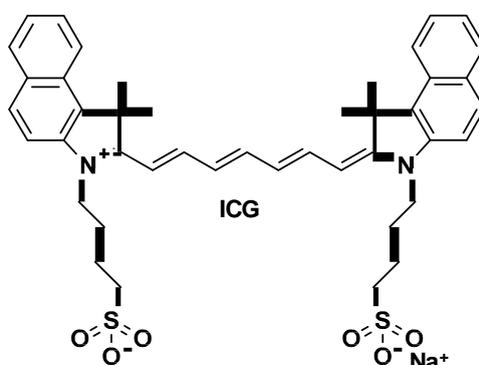
Figure 3.7: ICG

Symmetrical Cy7 dyes are usually prepared using a one-step condensation reaction with the appropriate indolium salt containing an activated methyl group in the 2-position in the presence of glutaconaldehyde dianil monohydrochloride (Figure 3.8).
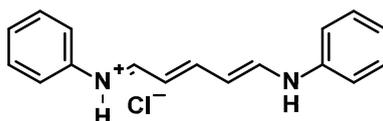
Figure 3.8: Glutaconaldehyde dianil monohydrochloride

The glutaconaldehyde dianil monohydrochloride is usually purchased as the *trans* isomer. In the presence of the indolium salts (2 molar stoichiometric ratio) under basic conditions yields the symmetrical Cy7. Scheme 3.15 shows the synthetic route to yield ICG.
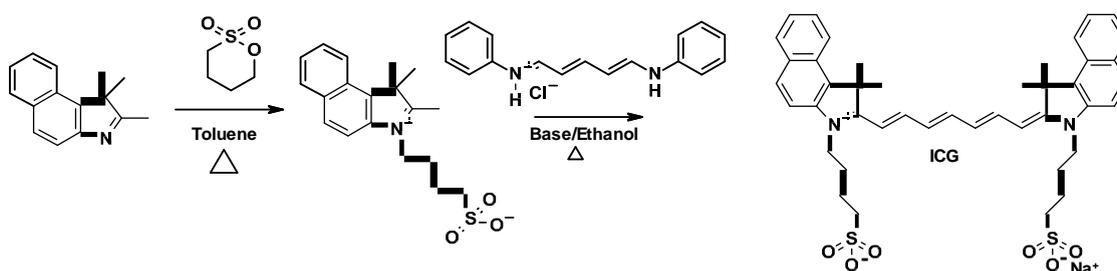
Scheme 3.15: Synthetic route to yield ICG.

Asymmetrical Cy7 dyes on the other hand require a modification to their synthesis. Such dyes are generally synthesised in accordance with Scheme 3.16 below, as per the literature methodology (step 1) [210], (step 2) [211], (step 3) [212]. The asymmetric Cy7 dyes require a slightly different synthetic approach, requiring two condensation reactions as shown in Scheme 3.16. The first step is straight forward and requires activation of the indolium salt using base catalysis to yield the activated methyl group in position 2. This is usually accomplished using Schotten-Baumann conditions as previously discussed, which subsequently reacts with glutaconaldehyde dianil monohydrochloride in the presence of acetic acid and acetic anhydride to yield intermediate **IO** (Scheme 3.16). It should be noted that asymmetric dyes are useful labelling agents (usually via a Azide-Alkyne Huisgen Cycloaddition) due to the large amount of selectivity which can be obtained.
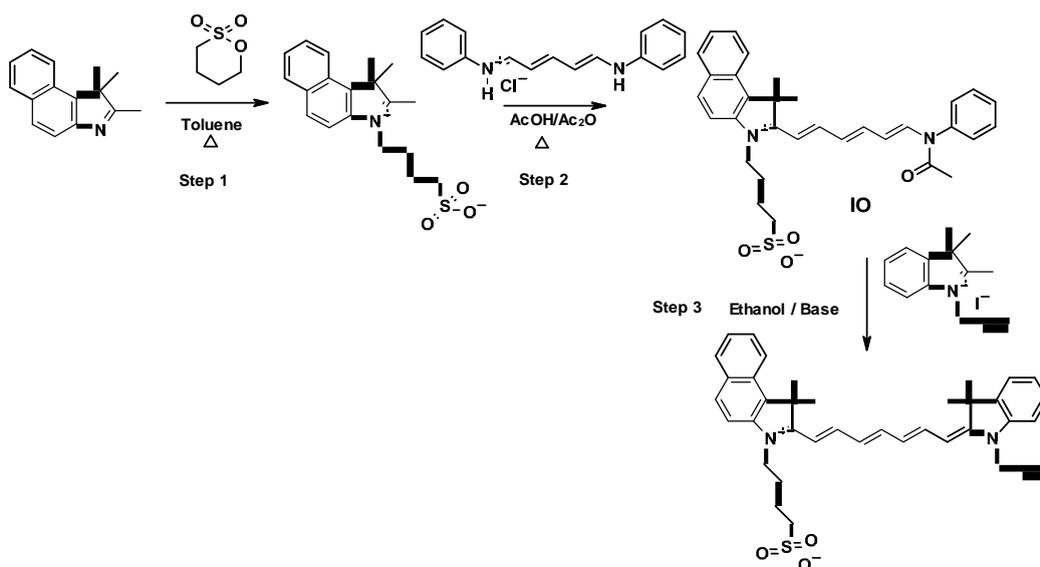
Scheme 3.16: Synthetic route to yield asymmetrical Cy7 dyes.

3.4.1 Linear cyanine dyes *via* an *in-situ* cascade reaction

The Cy7 dyes are very expensive to buy/produce, partly owing to the high cost of the glutaconaldehyde dianil monohydrochloride. There has long been a need for an improved synthetic methodology to reduce the costs of manufacturing such dyes. In particular, current synthetic methodologies to develop the Cy7 dyes suffer from the following drawbacks:

- Low yields of the final dye compounds.

- Low purity of the final dye compounds.

- Prevalence of the less desirable cis-isomer (*Z*-isomer) of the dye compound.

- Purification difficulties with respect to both the glutaconaldehyde dianil monohydrochloride and the dye compound.

- Complexities of isolating intermediates.

- Difficulties and inconsistencies on scale-up.

- Laborious and complex processing.

- Large energy input required (*e.g. heating at reflux in Step 2).*

- Long reaction times.

Having mentioned all these limitations, there is need for the development of a new and improved synthetic methodology to solve the aforementioned problems. As a result, the inspiration to develop a more efficient synthesis has led us to the development of a cascade reaction based on the Zincke reaction [218, 219] (Scheme 3.17).
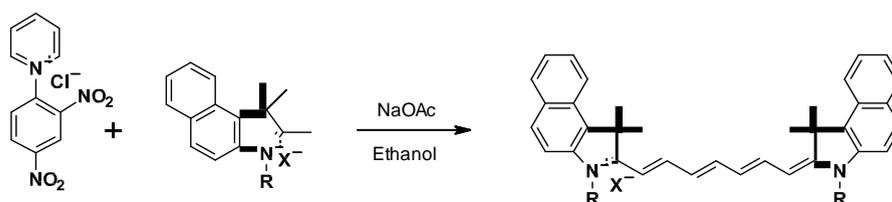
Scheme 3.17: Novel synthetic route to linear or straight chain heptamethine cyanine dye.
$X^- = I^-$ or Br^-.

The cascade reaction provides a one-pot process, in which the reactive intermediate is formed *in situ*, which in turn reacts *in situ* with the activated alkylated salts. The pyridinium salt ring opens to give the activated Zincke salt. This produces the linear heptamethine cyanine dyes (Table 3.10) in moderate yields, and in a manner which avoids undesirable by-product formation.

The new synthetic methodology takes place in a protic solvent system such as ethanol. Also, the reaction according to the newly developed synthetic protocol is base catalysed (Scheme 3.17). The base increases the reactivity between the alkylated salts and the pyridinium salt (or reactive intermediates derived there from e.g. Zincke-type intermediates). The base is preferably a weak base (i.e. sodium acetate). The reaction takes place substantially at ambient room temperature. This is significantly advantageous over existing methodologies, which require a significant amount of heat to effect the reaction between the alkylated salts and a Zincke-type intermediate. This method was used during the synthesis of all the linear dyes reported in this thesis.

The newly developed synthetic methodology is also a cheap and efficient route to producing the linear heptamethine cyanine dyes which are otherwise very expensive to produce or purchase commercially. It is envisaged that the newly developed synthetic methodology will

help fuel further research in the development of distinct heptamethine cyanine molecular probes. The solution to the drawbacks of the existing synthetic methodologies essentially involves combining Steps 1, 2 and 3 (shown in Scheme 3.15) into a single one-pot process. Scheme 3.21 illustrates the postulated mechanism for the newly developed synthetic methodology. The success of this "one-pot" procedure was particularly surprising given that multiple by-products were expected.

The newly developed synthetic methodology advantageously provides:

- Compounds in moderate yield (over the three steps).

- Compounds in high purity.

- Compounds which are easier to purify to produce a product specification suitable for use in medical applications due to the versatility of the synthetic protocol.

- Resource efficient and simple processing.

- A process which requires no burdensome isolation of intermediates.

- A low energy route to the yield the linear heptamethine cyanine dyes (e.g. which requires no heat input).

- A very fast process, since reaction times are very fast (4 – 10 h).

Another excellent characteristic of this cascade reaction is that the polymethine chain can be functionalised by using a wide range of commercially available pyridines (Schemes 3.18, 3.19 and 3.20).
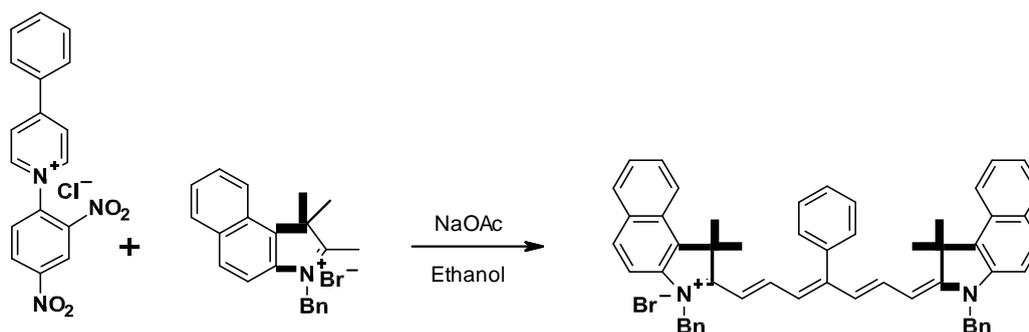
Scheme 3.18: Synthetic route to yield distinct novel Cy7 dye bearing a phenyl ring on the polymethine chain.
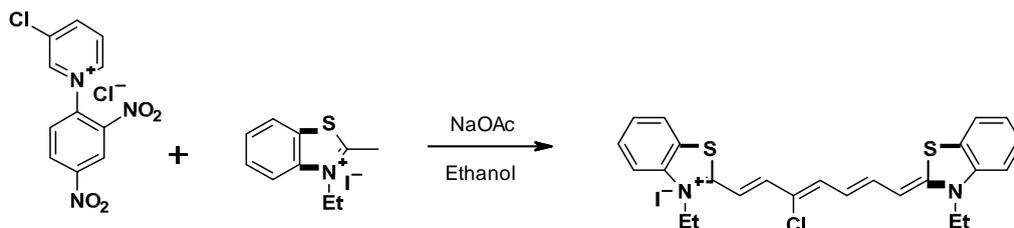
Scheme 3.19: Synthetic route to yield distinct novel Cy7 dye bearing a chloro group on the polymethine chain.
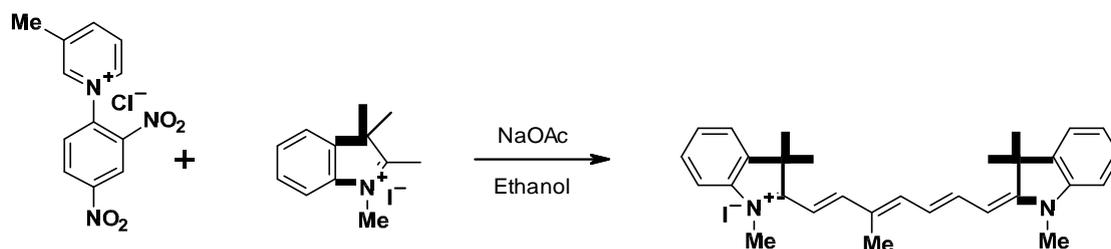
Scheme 3.20: Synthetic route to yield distinct novel Cy7 dye bearing a methyl group on the polymethine chain.

Until now regioselective functionalisation was not possible on the polymethine backbone. There are of course limitations to these reactions. Nucelophilic functional groups (amines, hydroxyl and thiols) cannot be used during this reaction, also due to the nature of the Zincke reaction, carbonyls also cannot be used. However this can be overcome by functional group protection. This allows scope to accomplish the addition of carbohydrates since cancer cells need more energy to divide and thus take in sugar to create this energy. Furthermore, DNA aptamers and antibodies could also be added to the polymethine backbone.
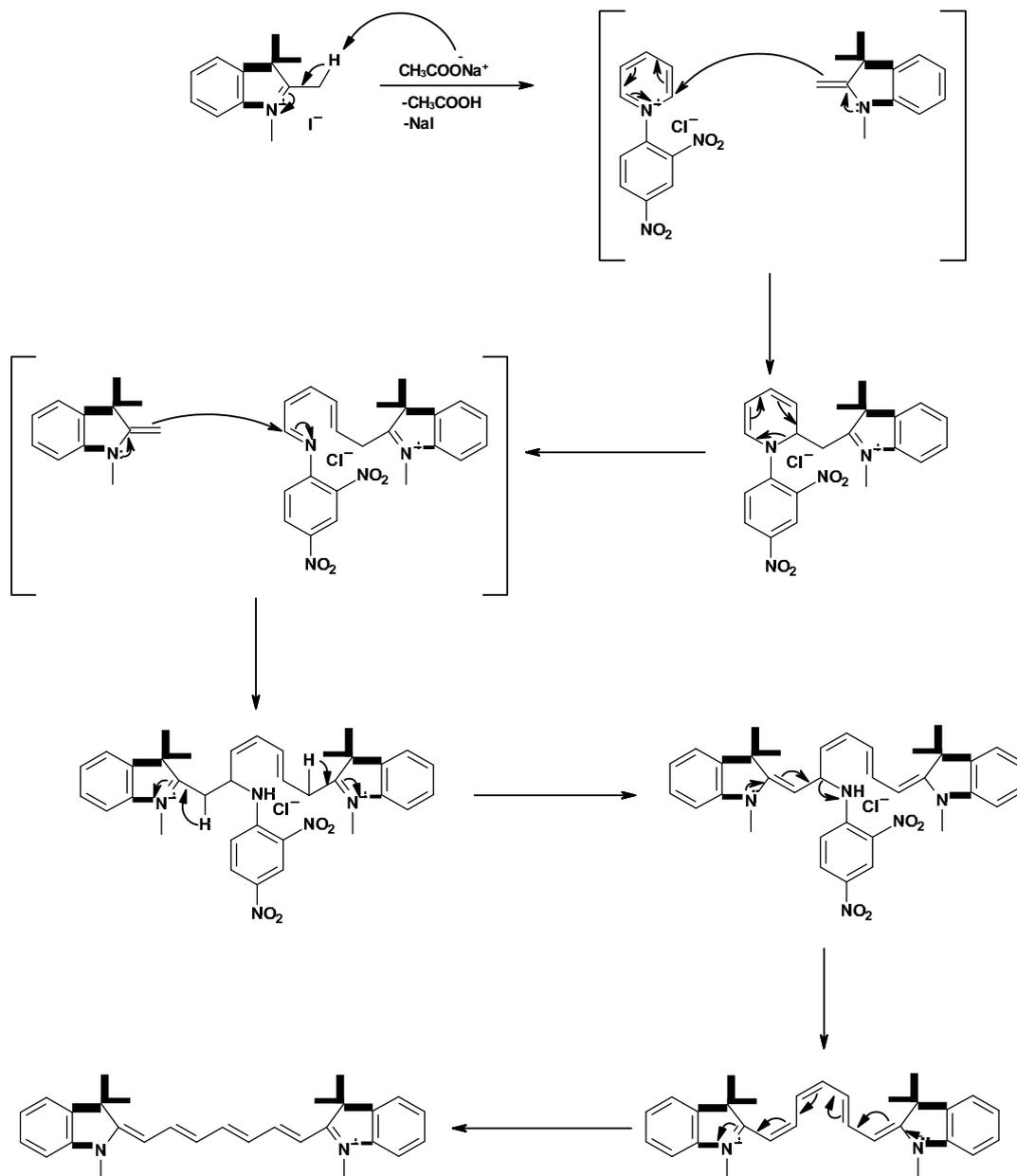
Scheme 3.21: Proposed mechanism for formation of linear heptamethine cyanine dye (**9a**).

3.4.2 Pyridine Salt formation

Pyridinium salts are versatile class of compounds utilised as cationic surfactants [213], initiators of cationic polymerisation [214], antimicrobials [215], acylating agents [216] and precursors to the formation of Zincke salts used in the synthesis of NIR dyes [217-219]. The Zincke salts are valuable group of conjugated dienes, derived from the ring opening reaction of pyridinium salts [220]. The ring-opening reaction itself dates back to more than a century to the pioneering work of Zincke and Konig [217-219]. The pyridinium salts resulting from the ring-opening reaction have proven to be useful synthetic building block and versatile precursor to many biologically active compounds. The Zincke reaction (Scheme 3.22) is overall an amine exchange process that converts pyridinium salts to the Zincke salts upon treatment with aniline [220]. It should be noted at this point that the glutaconaldehyde dianil monohydrochloride can be synthesised using the pyridinium salt as shown in Scheme 3.22 in the presence aniline in 80% aqueous ethanol. However this reaction is problematic and if not controlled carefully, leads to the unwanted bi-product 2,4-dinitroaniline usually after ten minutes of adding the aniline. Our method removes the use of aniline and as mentioned previously allows the pyridine to be further functionalised.
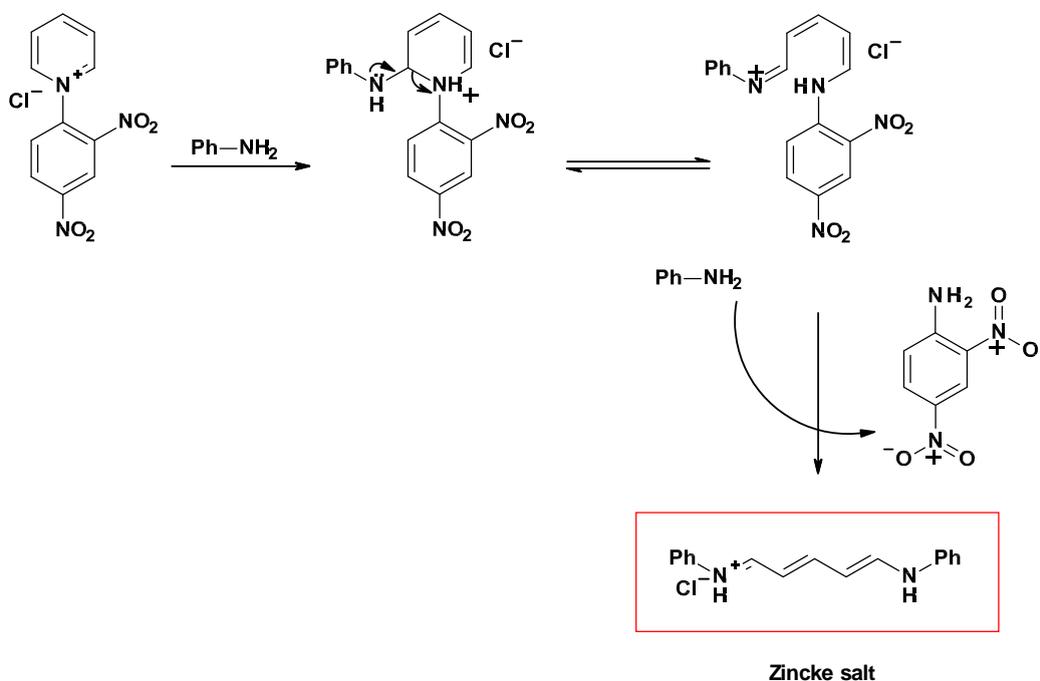
Scheme 3.22: Zincke reaction.

The formation of the pyrdinium salts (Scheme 3.23) is straightforward and high yielding as indicated by the synthesis of (2,4-dinitrophenyl)pyridinium chloride. The salts precipitated directly from the reaction mixture in high purity, in this instance, 76%.
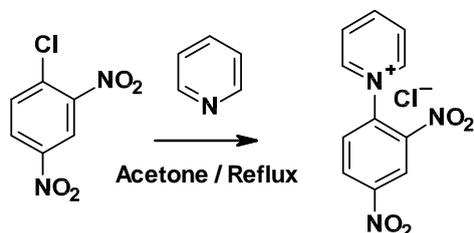
Scheme 3.23: Synthetic route to yield pyrdinium salts

To highlight the versatility of this reaction, a small selection of polymethine substituted cyanine dyes were prepared. These are highlighted in Section 3.4.7. Table 3.9 highlights the structures and yields of the pyridinium salts used to making the linear Cy7 dyes.

Number			
	R1	**R2**	**% Yield**
PY1	H	H	76%
PY2	Me	H	69%
PY3	Br	H	79%
PY4	Cl	H	79%
PY5	H	Ph	81%

Table 3.9: Pyridinium salts.

The cyanine dyes formed from the functionalised pyridinium salts (**PY1**-**PY5**) were *N*-alkylated with alkyl sulfonic acids in order for photophysical and biological comparisons to be made between the synthesised Cy7 dyes and ICG. A typical structure for these types of dyes is shown in Figure 3.9 below and highlights the use of **PY3** in the reaction.
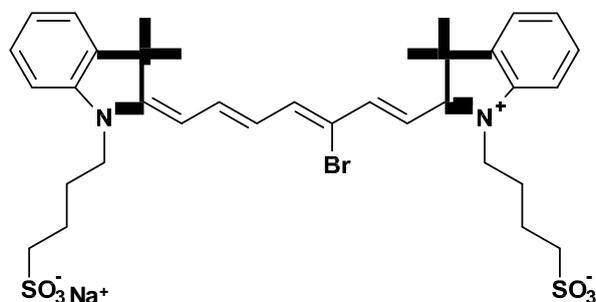
Figure 3.9: Substituted Polymethine linear Cy7 dye (**13**).

3.4.3   Synthesis of linear dyes 9 a-g

The structures and codes of the linear Cy7 dyes are shown in Table 3.10 for clarity. See Tables 3.11, 3.12 and 3.13 for values of R.

Code	Structure
9 (a-g)	
10 (a-g)	
11 (a-g)	

Table 3.10: Synthesised linear Cy7 dyes.
$X^- = I^-$ or Br^-.

The dyes were synthesised and purified by silica gel column chromatography to afford the dyes in good to moderate yields as shown Table 3.11

Number			
	X⁻	R	% Yield
9a	I⁻	CH_3	28%
9b	I⁻	CH_2CH_3	47%
9c	I⁻	$CH_2CH_2CH_3$	66%
9d	I⁻	$CH_2(CH_2)_2CH_3$	31%
9e	Br⁻	$CH_2C_6H_5$	21%
9f	-	$CH_2CH_2CH_2SO_3^-$	60%
9g	-	$CH_2CH_2CH_2CH_2SO_3^-$	73%

Table 3.11: Synthesised linear indolium heptamethine Cy7 dyes.

The ^{1}H NMR spectra of **9a** is shown in Figure 3.10
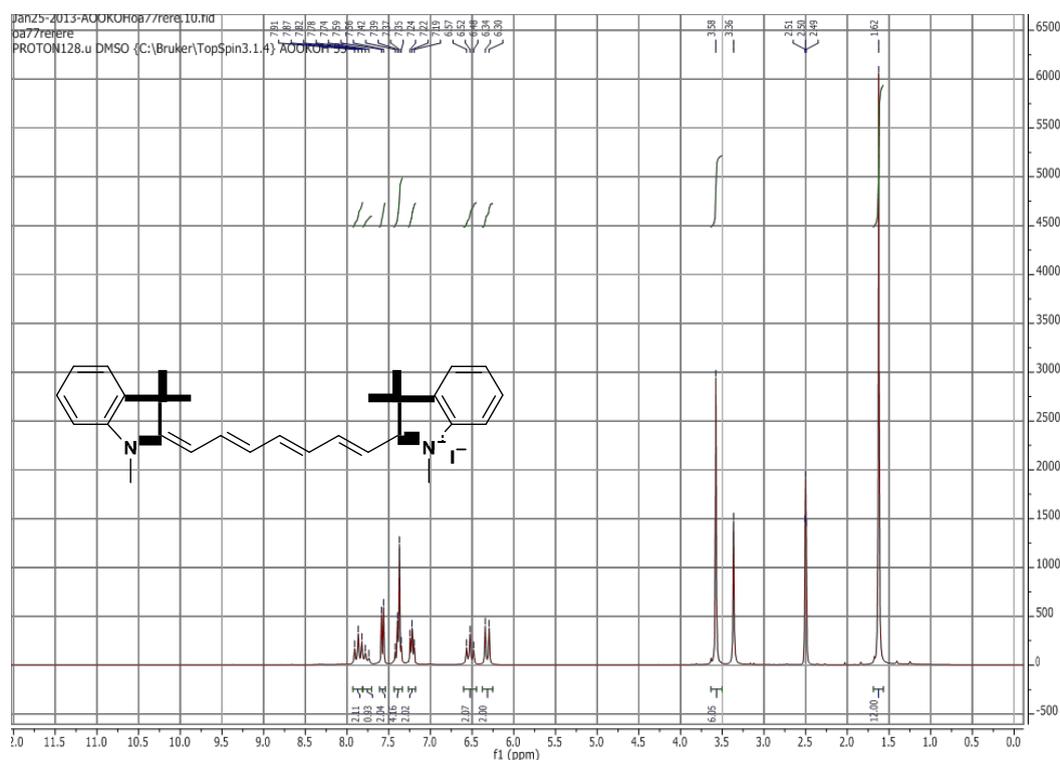
Figure 3.10: ^{1}H NMR spectra of **9a** in d$_6$-DMSO.

The molecular structures of **9 a-g** are closely related and will be discussed together. In regards to the ^{1}H NMR spectrum of **9a**, the molecular symmetry of the structure is highly evident from the coupling patterns of the protons within the molecule. The signals of the alkyl hydrogen moiety are easily recognised, *N*-CH$_3$ protons (s, 6H) at 3.58 and gemdimethyl (s, 12H) at 1.62 ppm. The signals shown for the polymethine backbone exhibited *trans* coupling constants indicating that the electronic charges are distributed alternately on the conjugated on the polymethine chain. Further views of **9a** are depicted in 2D COSY NMR (Figure 3.11) indicating the coupling patterns of the molecule.
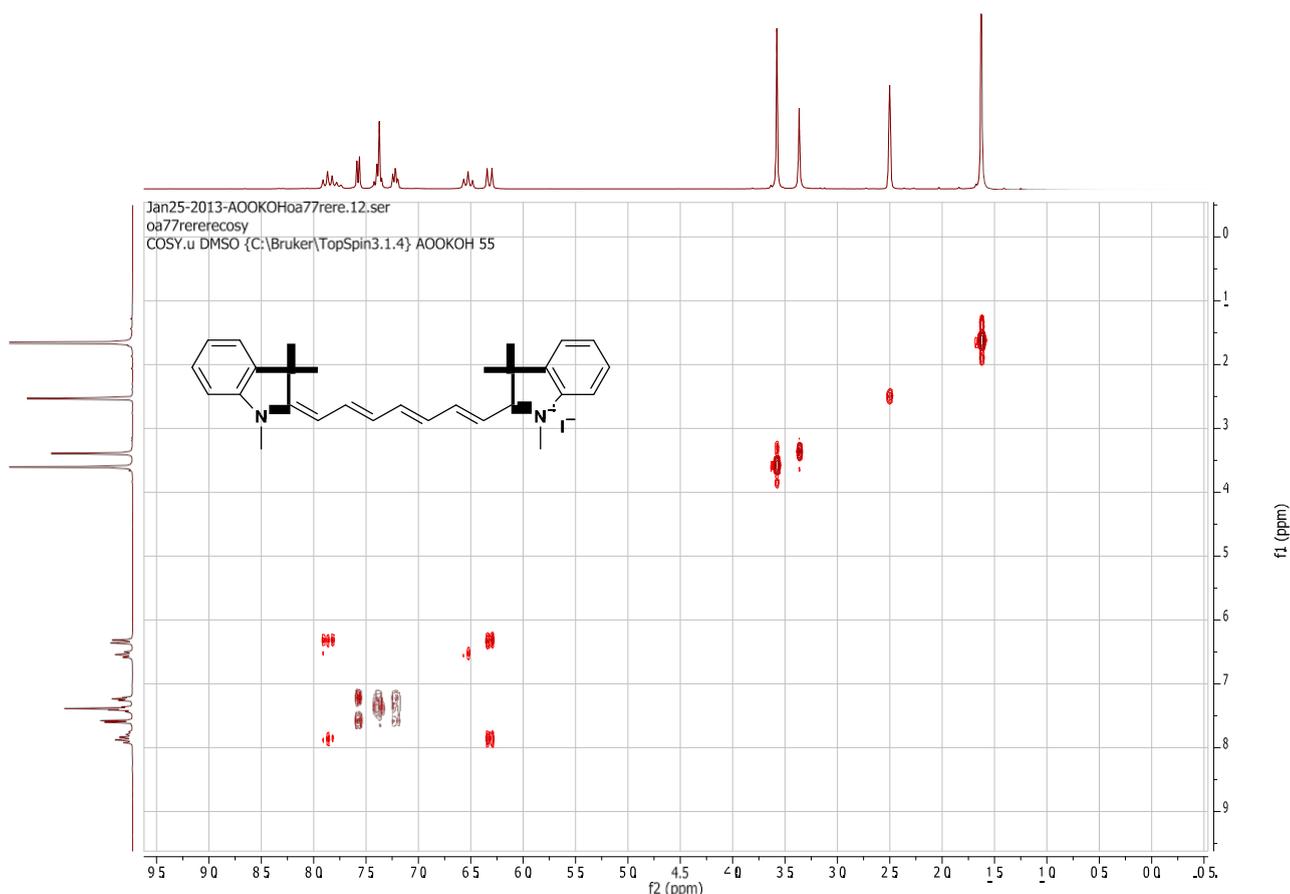
Figure 3.11: 2D COSY spectra of **9a** in d$_6$-DMSO.

3.4.4   Synthesis of linear dyes 10 a-g

The linear cyanine dyes (**10 a-g**) were synthesised once again using the Zincke type cascade reaction as shown in Scheme 3.24. The reactions progressed more rapidly in comparison to

dyes **9 a-g** and this can possibly be attributed to the nucleophilic nature of the sulfur in the benzothiazole subunit.
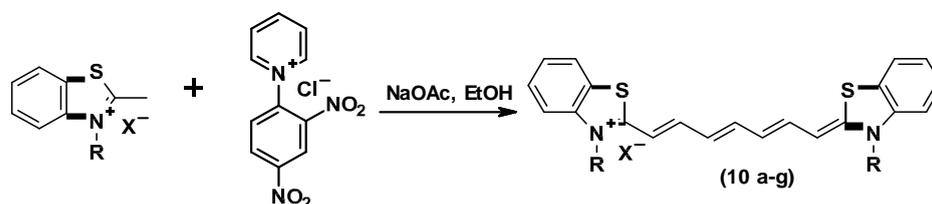
Scheme 3.24: Synthetic route to yield linear benzothiazole heptamethine cyanine dyes.

The dyes were synthesised and purified by silica gel column chromatography to afford the dyes in good to moderate yields as shown Table 3.12

Number			
	X⁻	**R**	**% Yield**
10a	I⁻	CH_3	78%
10b	I⁻	CH_2CH_3	46%
10c	I⁻	$CH_2CH_2CH_3$	66%
10d	I⁻	$CH_2(CH_2)_2CH_3$	44%
10e	Br⁻	$CH_2C_6H_5$	60%
10f	-	$CH_2CH_2CH_2SO_3^-$	46%
10g	-	$CH_2CH_2CH_2CH_2SO_3^-$	47%

Table 3.12: Synthesised linear benzothiazole Cy7 dyes.

The ^{1}H NMR spectra data (Figure 3.12) was consistent with the structure of the linear benzothiazole heptamethine cyanine dye.
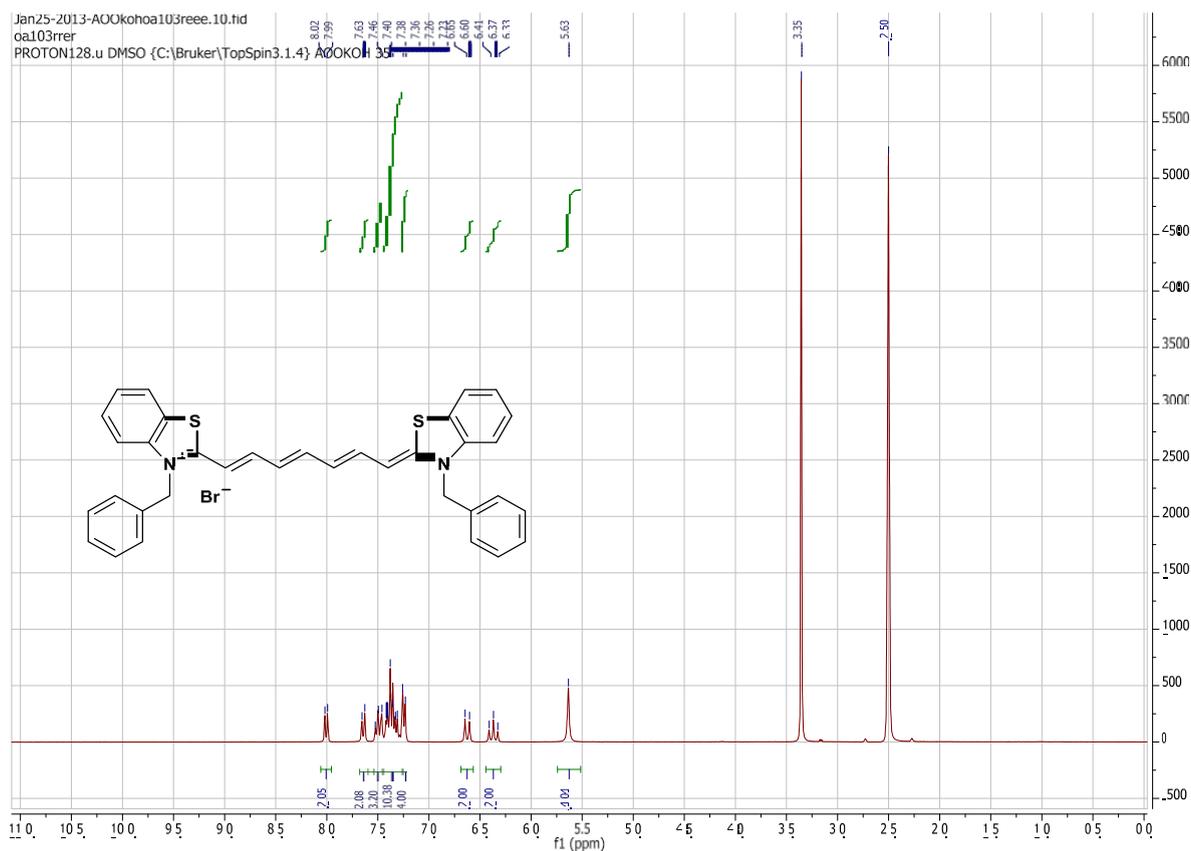
Figure 3.12: ^{1}H NMR spectra of **10e** in d$_6$-DMSO.

3.4.5 Synthesis of linear dyes 11a-g
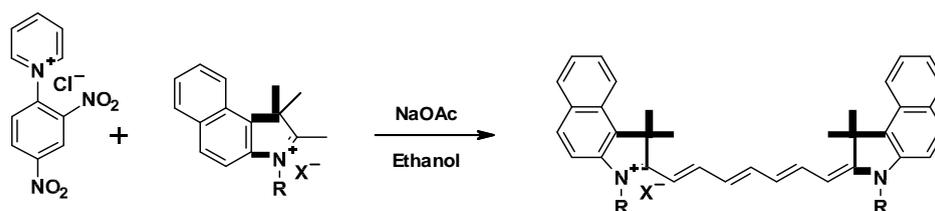
Scheme 3.25: Synthetic route to yield benz[e]indolium heptamethine cyanine dyes.

The synthesis of the linear benz[e]indolium heptamethine cyanine dyes (**11 a-g**) was accomplished using the various *N*-substituted 2,3,3-trimethyl benz[e]indolenine salts (**3 a-g**) with the pyridinium chloride salt in the presence of sodium acetate and ethanol at room

temperature. The crude dyes were purified by silica gel column chromatography to afford the dyes all in solid forms with moderate to poor yields as shown in Table 3.13.

Number			
	X⁻	**R**	**% Yield**
11a	I⁻	CH_3	37%
11b	I⁻	CH_2CH_3	19%
11c	I⁻	$CH_2CH_2CH_3$	20%
11d	I⁻	$CH_2(CH_2)_2CH_3$	28%
11e	Br⁻	$CH_2C_6H_5$	17%
11f	-	$CH_2CH_2CH_2SO_3^-$	32%
11g	-	$CH_2CH_2CH_2CH_2SO_3^-$	28%

Table 3.13: Synthesised linear benz[e]indolium Cy7 dyes (**11 a-g**).

The ^{1}H NMR spectra (Figure 3.13) confirms the presence of extra aromatic protons belonging to the benz[e]indolium aromatic moiety.
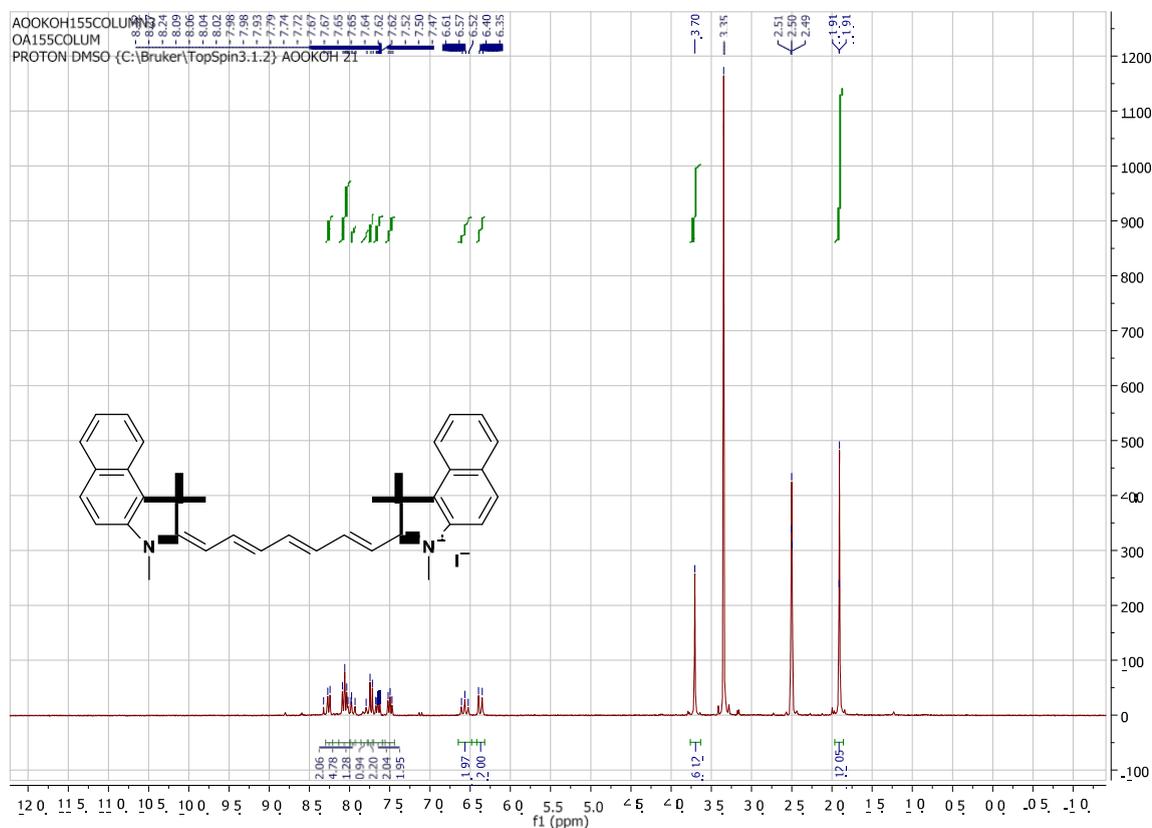
Figure 3.13: ^{1}H NMR spectra of **11a** in $_{d6}$-DMSO.

The IR spectra of the linear dyes are quite similar and therefore they will be discussed together. Although the IR spectra of heptamethine cyanine dyes have been reported to be complex [222], the characteristic functional absorption bands can be relatively assigned. The aromatic absorption appears at 1620-1590, 1580-1520, (^{v}C=C) and 860-800 (^{v}C=H), 770-730. In addition, the resonance-conjugated unsaturated stretching modes in the chromophore appear at 1520-1480 and 1440-1420 cm^{-1}. The chromophoric CH out-of-plane bending (^{v}-CH=CH-) appears around 980-920 cm^{-1}.

3.4.6 Substituting across the polymethine backbone

Additional compounds bearing substituents on the polymethine backbone were also synthesised to further illustrate the applicability of the novel one pot synthetic methodology as highlighted in Section 3.4.1.

The synthetic route is shown in Scheme 3.26 and has the potential to allow a great deal of new dyes to be synthesised. As already discussed, there are limitations to this method, however these could be dealt with using functional group protection.
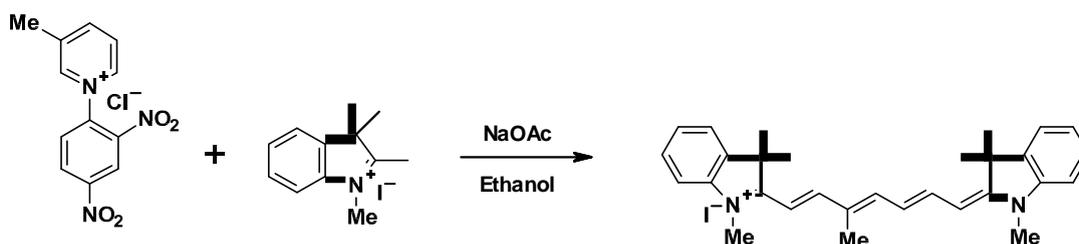
Scheme 3.26: Synthetic route to yield substituted heptamethine cyanine dye bearing methyl group on the polymethine chain.

Table 3.13 shows the structure of some of the diverse dyes synthesised. Emphasis was placed on altering the nature of the substituting group on the polymethine chain, but keeping the *N*-alkyl chains as sulfonic acids. This allowed direct comparisons to be made against ICG. It was anticipated that having different electron donating and electron withdrawing groups on the polymethine chain would affect the photophysical and growth inhibitory properties of the dyes. It is was envisaged that these new dyes would possess better spectral properties than the currently available commercial dye (ICG), thereby leading to the development of new non-targeting heptamethine cyanine molecular probes bearing various conjugation points for linking of targeting molecules.

Although these novels dyes were synthesised, the reactions suffered from low yields as judged by Table 3.14. The synthesised dyes were all stable at room temperature and have been characterised using a combination of HRMS, IR, and NMR (^{1}H and ^{13}C) spectroscopy (see Chapter 6). The ^{1}H NMR of **16** is shown in Figure 3.16. The methylene N-*CH₂* protons

in the ^{1}H NMR spectra of **16** are inequivalent and appear as two distinct triplets at 4.47 and 4.67 ppm indicating the unsymmetrical character of the dye molecule.

Figure 3.14 shows the HRMS for cyanine dye **15** indicating the purity of the compound and the presence of an extra phenyl ring.
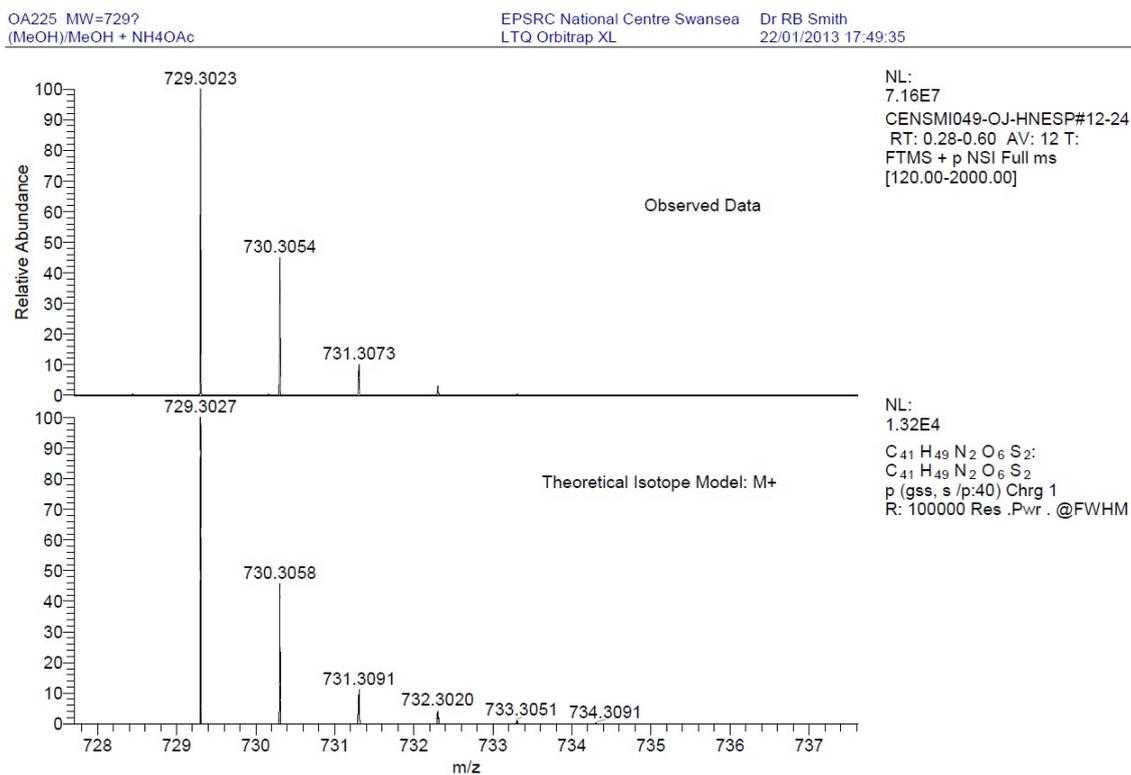
Figure 3.14: HRMS for substituted heptamethine cyanine dye **15**.

Code	Structure	Yields	Code	Structure	Yields
12		19%	17		22%
13		19%	18		20%
14		18%	19		24%
15		20%	20		36%
16		18%	21		21%
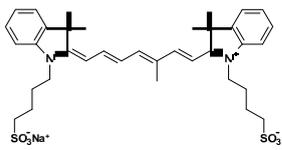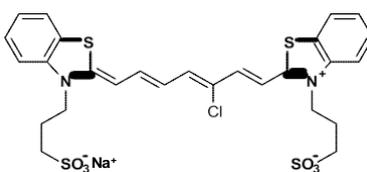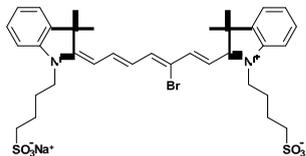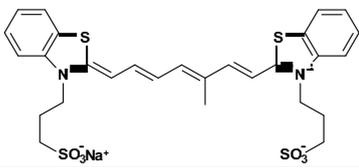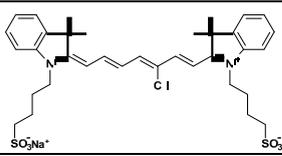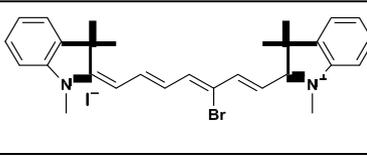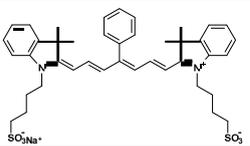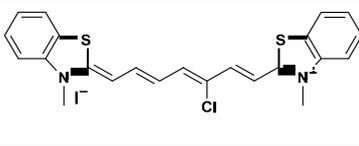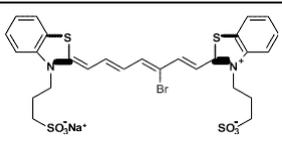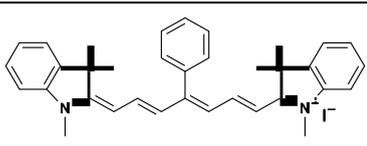
Table 3.14: Substituted heptamethine cyanine dyes.

Using this methodology further sophisticated Cy7 dyes could be prepared for instance attachment of substituted isoalloxazine molecule as shown in Figure 3.15. This would be advantageous from a PDT viewpoint.
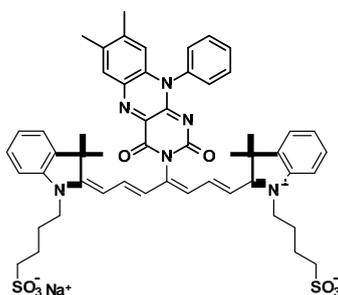
Figure 3.15: Conjugate Cy7 dyes.

98

In conclusion, a total of 40 linear and substituted heptamethine cyanine dyes were synthesised using the novel one-pot synthetic method, which we believe offers a better alternative to the existing methods.
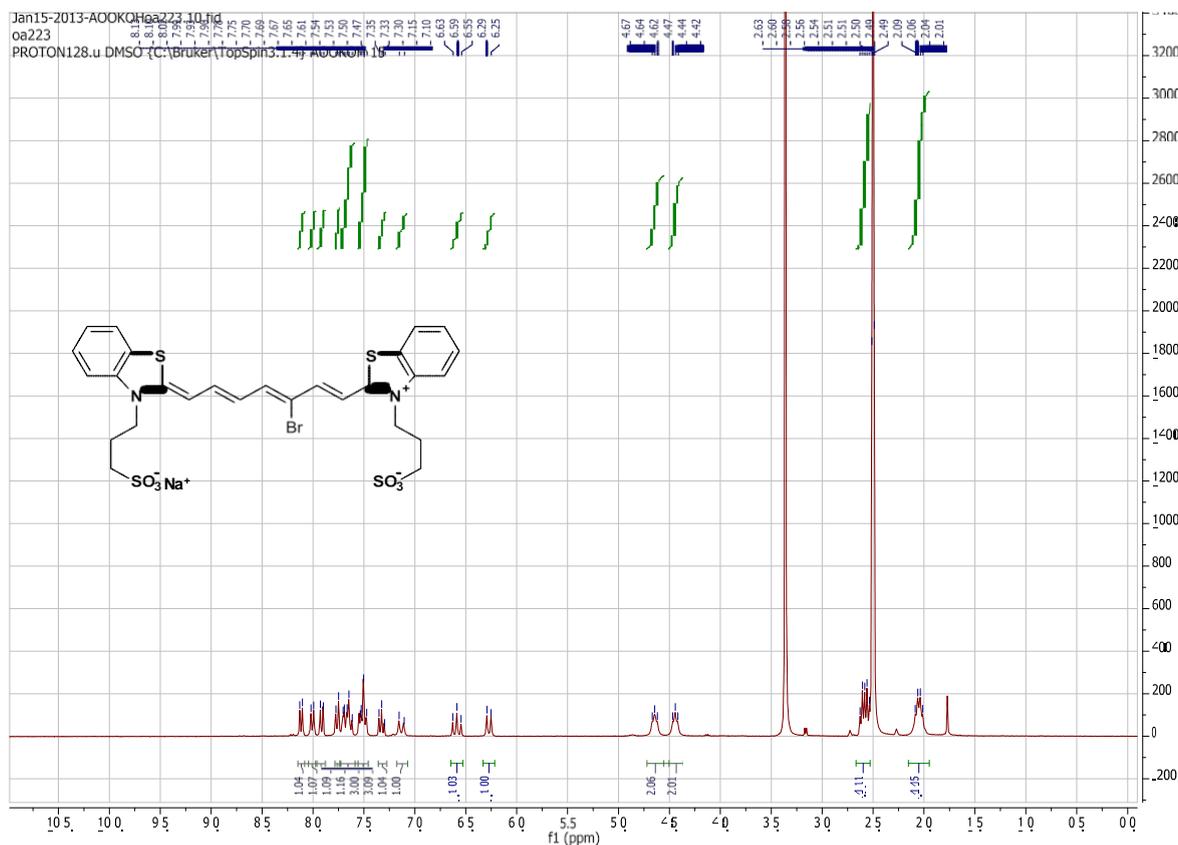
Figure 3.16: ^{1}H NMR spectra of **16** in d[6]-DMSO.

3.4.7 Synthesis of linear specific dyes for Click Chemistry

The *in vitro* and *in vivo* labelling of biomolecules by the use of fluorescent dyes represents a significant tool in order to study complex biological processes often *via* molecular or optical imaging [223]. One of the important characteristics of the fluorescent dye utilised for this purpose is their high sensitivity. The conjugation of the fluorescent dye relies on their selective and efficient reaction under aqueous conditions with functional groups available at the biomolecule of interest [209]. Amongst the known ligation reactions, the click reaction Cu(I)-catalyzed azide-alkyne cycloaddition (CuAAC) is the most concise method for

synthetically designing labelling biomolecules bearing alkyne and azide functional groups[224, 225]. The Huisgen's 1,3-dipolar cycloaddition of alkynes and azides yielding triazoles is undeniably the foremost example of a click reaction. The Huisgen's 1,3-dipolar cycloaddition offers several advantages such as the easy preparation of alkynes and azides, their ease of attachment to biomolecules. Also their inertness toward biological molecules and the reaction conditions within the living system makes it an ideal reaction for a wide range of *in vitro* and *in vivo* bio-conjugation applications [130, 131].

The recently discovered dramatic rate acceleration of the azide–alkyne coupling reaction using copper-(I) catalysis and the beneficial effects of water as the reaction solvent [130] has led to the utilisation of this unique connection process to design and synthesis variety of benzothiazole NIR heptamethine cyanine dye azide conjugates (Scheme 3.27).
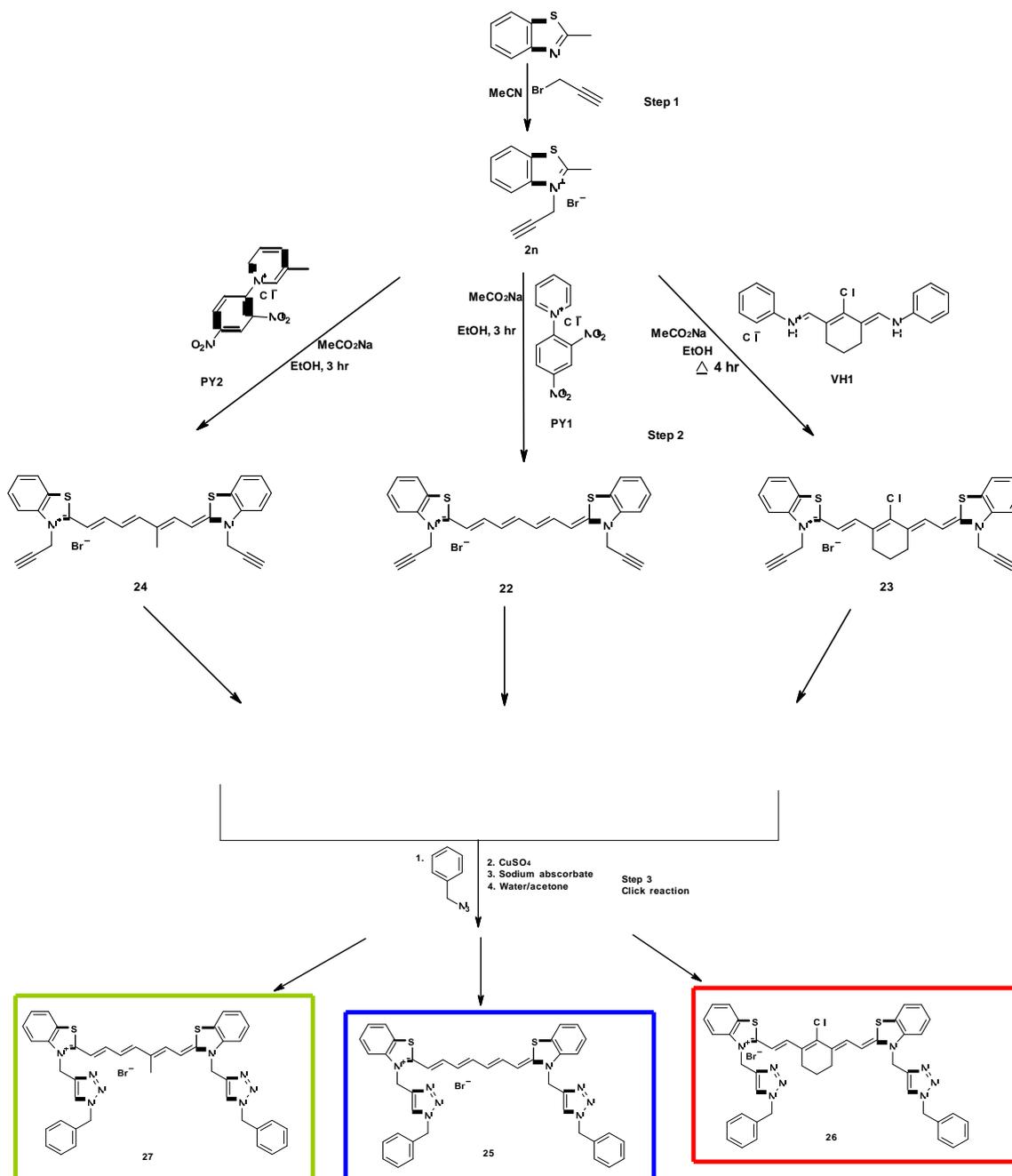
Scheme 3.27: Synthetic route to yield azide dye conjugates.

The first step in the above synthetic route (Scheme 3.27) was the synthesis of the benzothiazole salt (**2n**) bearing the alkyne functional group moiety. This strategy of incorporating the alkyne moiety at the first stage of the synthetic scheme was employed in order to avert the potential problems of steric interference and the tedious purification step encountered during the post synthetic modifications of cyanine dyes. The next step was the dye formation reaction between the benzothiazole salts and the corresponding pyridinium salts (**PY2**, **PY1**) and the iminium salt (**VH1**), in the presence of sodium acetate as the base to afford the crude dyes. These were purified by column chromatography to obtain the pure dyes (**24**, **22**, **23**) bearing the alkyne moiety. The ^{1}H NMR spectra obtained were consistent with the expected structure. Figure 3.17 shows the ^{1}H NMR spectrum of **22**.
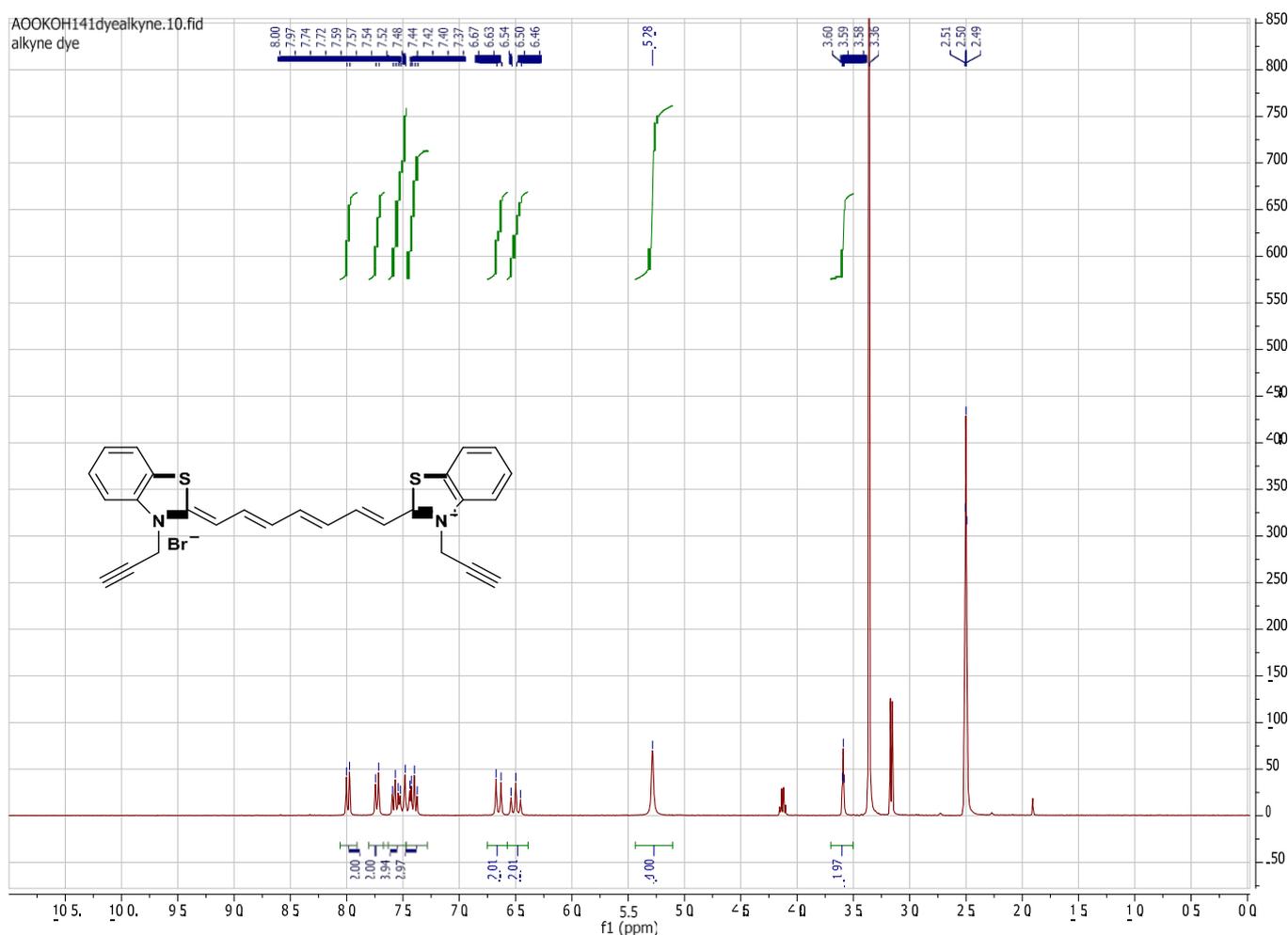
Figure 3.17: ^{1}H NMR spectra of **22** in d_6-DMSO.

The final step in the synthetic scheme is the click reaction between the benzothiazole cyanine dyes (**24**, **22**, **23**) bearing the alkyne moiety with a benzyl azide bearing the azide functional group in the presence $CuSO_4$. $5H_2O$, sodium ascorbate and a mixture of 80% water/acetone. The sodium ascorbate enhances the reduction of the Cu^{II} salts to Cu^{I} salts [225]. The crude dye azide conjugates obtained were purified by column chromatography to yield the pure product in solid forms. It is suggested that the above synthetic route (Scheme 3.27) will provide a blueprint for the future design and synthesis of symmetrical heptamethine cyanine dyes conjugated to biomolecules, since to our knowledge this is first time heptamethine cyanine dyes bearing the same conjugated group at the heterocyclic ring terminals has been synthesised. Figure 3.18 shows the ^{1}H NMR spectrum of **25**.
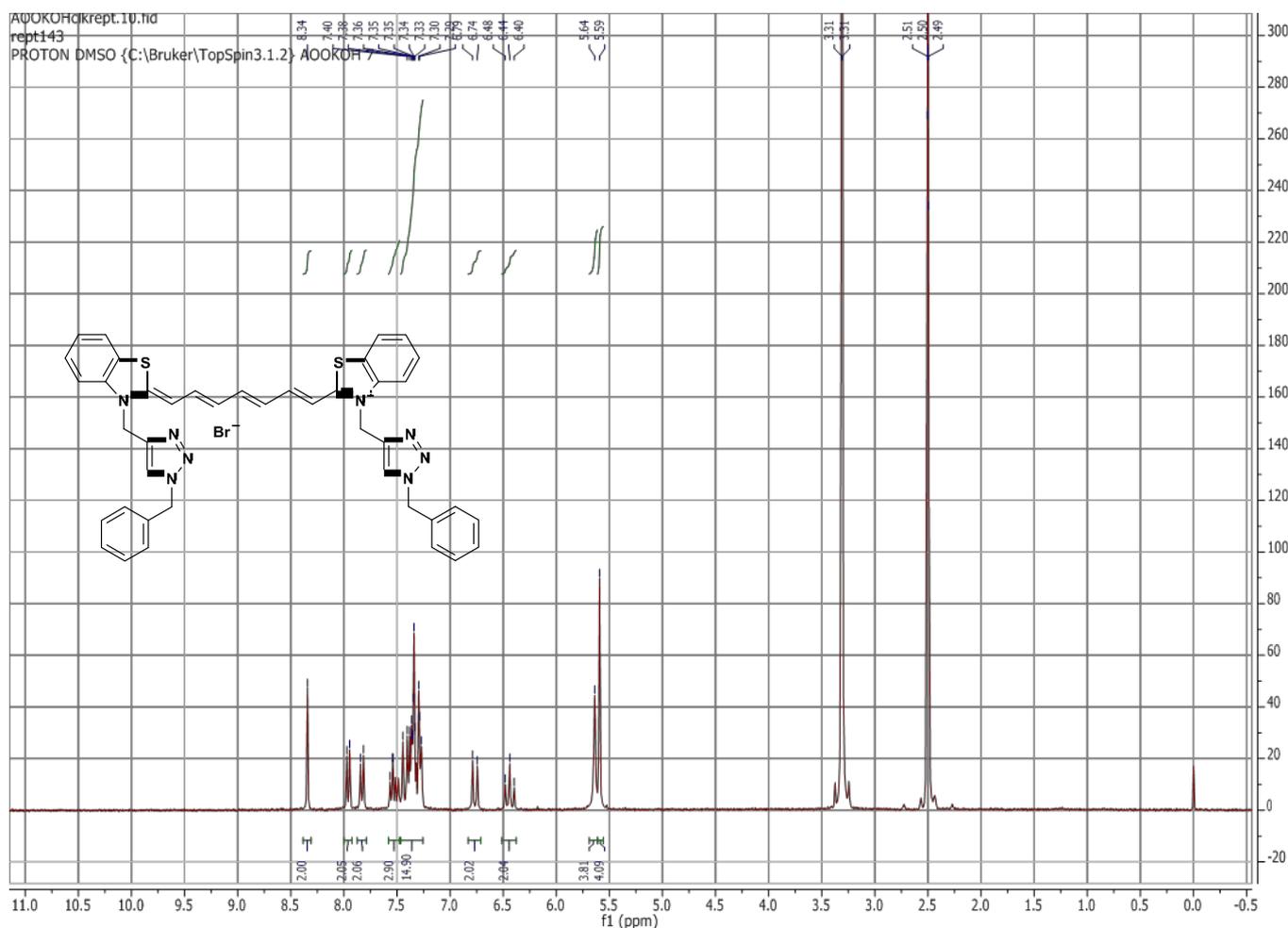
Figure 3.18: ^{1}H NMR spectra of **25** in d_6-DMSO.

The above ^{1}H NMR spectra (Figure 3.18) confirms the formation of the dye azide conjugate when compared to the ^{1}H NMR spectra of **22** (Figure 3.16) (dye bearing only the alkyne functional group). The protons in the triazole ring give a unique singlet at 8.34 ppm which is absent in Figure 3.17 (spectra of **22**). The N-CH_2 protons linked to the triazole ring and the phenyl ring both gives a prominent singlet peaks at 5.63 and 5.59 ppm respectively. Further evidence for the structure is illustrated by the presence of extra aromatic proton belonging to the phenyl rings linked to the triazole rings.

The proposed catalytic cycle for the Cu(I) catalysed ligation process is shown below (Figure 3.19) [136].
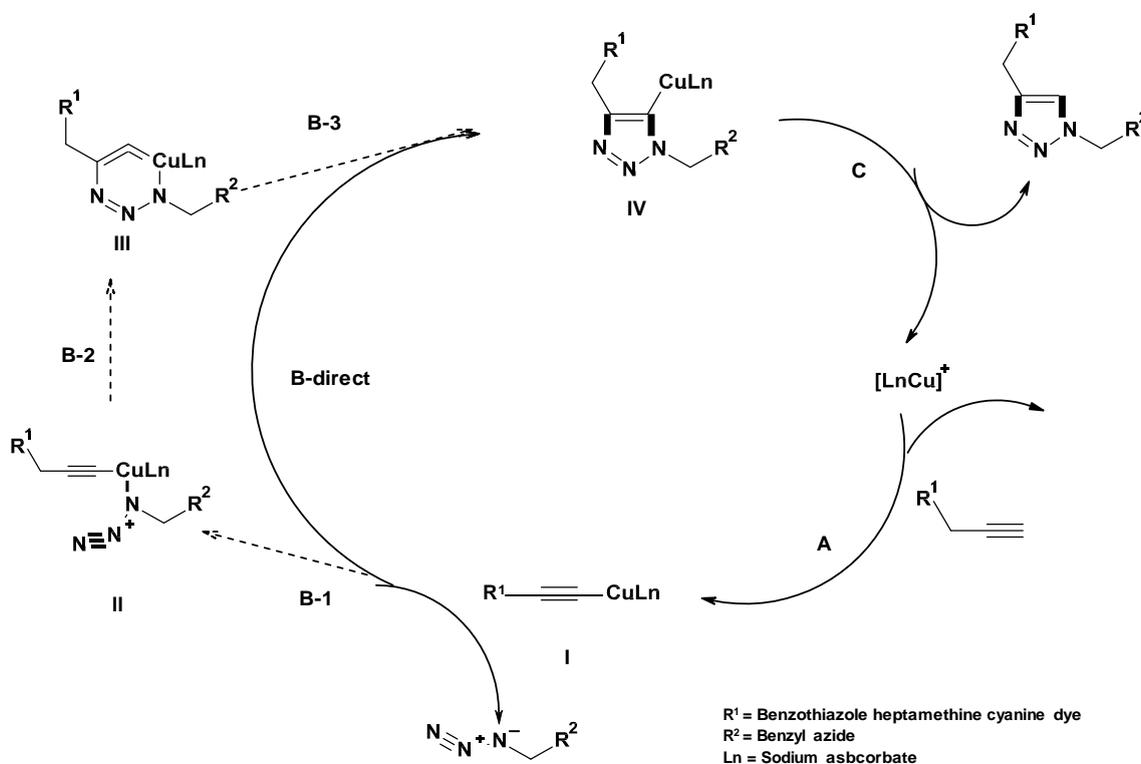
Figure 3.19: Proposed catalytic cycle for Cu^I catalysed ligation.

The reaction mechanism is divided into two pathways. The first pathway is the direct [2+3] cycloaddition and the second one is the stepwise progression (B1-B2-B3) pathway. The Cu^I are usually introduced by the reduction of Cu^{II} salts by sodium ascorbate or ascorbic acid (5-

10 mol%). The Cu^{II} salts are reasonably cheap, reliable and readily available making them a preferred choice for the process. The proposed reaction mechanism of the benzothiazole heptamethine cyanine dye with the benzyl azide in theory should provide a model for the design of future long-wavelength absorbing cyanine dyes azide conjugated absorbing biomolecule.

Potential problems with the Huisgen's 1,3-dipolar cycloaddition of alkynes and azides do exist upon scale-up and these are associated with the explosive nature of the azides in the presence of copper.

Chapter four of this thesis will focus on the photophysical properties and growth inhibition studies using the newly synthesised Cy7 dyes.

*Photophysical and
Growth Studies.*

4.0 Photophysical and Growth Studies.

4.1 Photophysical properties of structurally diverse heptamethine cyanine dyes.

Much attention has been focused on the photophysical properties of heptamethine cyanine dyes including their absorption and emission wavelengths, fluorescence quantum yields, Stokes shifts and effect of solvent polarity. Several strategies have been attempted to improve the overall photophysical properties of heptamethine cyanine dyes. It is well noted that rigidification of the polymethine chain is an established approach for improving the chemical and photostability of NIR dyes [226]. Two classical NIR probes are ICG and New Indocyanine Green IR-820 are currently being used for clinical applications [227, 228]. One of the main draw backs of ICG is its low fluorescence quantum yield [229-231]. IR-820 is structurally related to ICG except with the incorporation of a rigid cyclohexane moiety providing improved *in vitro* and *in vivo* stability. However, it is documented that IR-820 has a notably lower quantum yield than ICG [232].

With the increasing importance of NIR heptamethine cyanine dyes in biological imaging applications, dyes with unique structural features are being designed and synthesised to improve spectral properties. Inspired by this, the photophysical properties (absorption and fluorescence spectra, fluorescence quantum yields and Stokes shift) of the dyes synthesised in this project has been compared against those of the standard fluorophores ICG and IR-820. This comparison is based on structural similarities such as length and substitution pattern of the polymethine chain, nature of the substituting group on the nitrogen of the heterocyclic

ring system. As shown in figure 4.1, the established ICG (linear chain) and IR-820 (rigidified chain) dyes have terminal dimethyl-indolyl groups with an additional fused benzene ring.
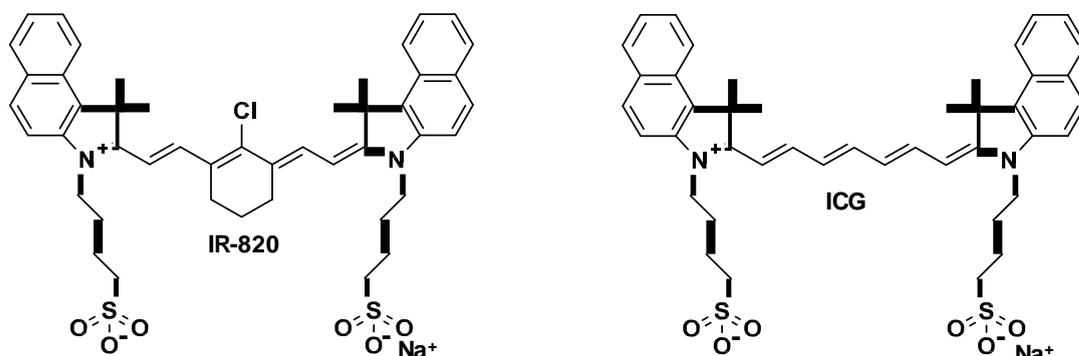
Figure 4.1: The structures of **IR-820** and **ICG**.

The heterocyclic ring system and the polymethine chain linking the heterocyclic rings generally determine the spectral characteristics of heptamethine cyanine dyes. The photophysical properties of the heptamethine cyanine dyes synthesised in this project are summarised in Tables 4.3 - 4.14.

4.2 Growth Inhibition Screening

Apart from the photophysical properties of the dyes, the growth inhibition and lipophilicity properties are important characteristics which determine the practical use of the dyes in living cells. The Log*P* is an estimate of a compound's overall lipophilicity and it is usually linked to potency. It is envisaged that the vast structural diversity of the dyes synthesised in this project should play a major role in their solubility and growth inhibition characteristics. To this end, dyes synthesised were screened in order to identify and select the best set of dyes as potential candidates for clinical applications. For the experiment, we employed the eukaryotic, unicellular organism, fission yeast *Schizosaccharomyce spombe* (*S. pombe*), as a medium for establishing growth inhibition screening due to a high degree of similarity between the cellular processes in yeast and those of human cells [164].

The growth inhibition screening procedure involved the inoculation of *S. pombe* wild-type cells (NJ2 *h- ura4-D18 leu1-32 ade6-M210 his7-366*) into 0.5% w/v yeast extract broth (YE),

3% w/v glucose, 0.025% w/v adenine, histidine, leucine, uracil+lysine, as previously reported [235]. The culture was then incubated overnight at 30 °C with shaking at 200 rpm. Stock solutions of the dyes were prepared in 20% DMSO and diluted in YE, resulting in a final concentration of 10% DMSO, a concentration known not to inhibit yeast growth. DMSO and YE were used as controls for the experiment. 3×10^{4} yeast cells were transferred into the wells of a 96-well plate. A 1:2 serial dilution of the dyes was then performed (Figure 4.2). The well plates were visually inspected for growth after 24 h of incubation at 30 °C. Growth was indicated by full or partial appearance of yeast on the bottom of the wells. The minimum growth inhibition concentration of the dyes was estimated to be the concentration of the compound in the well before yeast growth was first seen. The experiment was repeated three times to ensure reproducibility of the results. For a number of dyes, no growth was observed at the lowest concentration tested. These are included in Tables 2.3.1-2.3.10, where the lowest concentration tested is indicated. In addition, a number of dyes had limited solubility; the values within the tables indicate the highest possible concentration tested. Wells containing 10% DMSO and only YE showed 100% yeast growth. The effect on cell growth of the synthesised dyes was compared to available commercial dyes such as ICG, IR-820 and acridine orange (AO) (Figure 4.2). AO is a well-known commercially available toxic dye, possessing strong inhibitive actions by intercalation and hence was used as a negative control [233, 234]. The synthesised dyes were graded based on their Minimal Inhibitory Conentration (MIC) values alongside AO. MIC in the range of < 4 μM indicated by red bars exhibited high levels of inhibition against the *S. pombe* yeast strain. IR-820/ICG MIC in the range of greater >8 μM indicated by green bars show low levels of inhibition against the aforementioned strain. MIC values in the range of 4 - 8 μM are classified as intermediates and indicated by yellow bars which represent an intermediate level of inhibition (Figure 4.3 - 4.14).
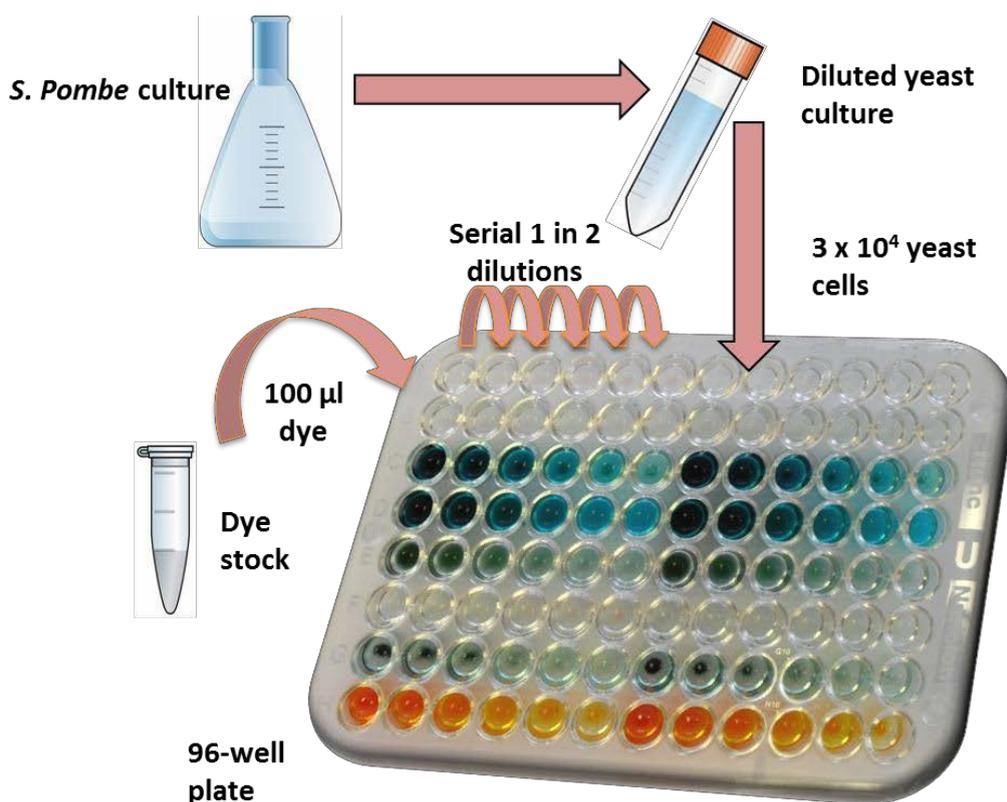
Figure 4.2: Schematic diagram of growth inhibition process using 96 Well plates showing growth inhibitory effect of heptamethine cyanine dyes on yeast cells and structure of AO.

4.3 *N*-Alkyled 2,3,3-trimethylindolenine and 2-methylbenzothiazole

A major step during this work was to determine to what extent the alkyl chain length affected growth inhibition and to determine if the *N*-alkylated salts were toxic. It was necessary to investigate the growth inhibition effects of the *N*-alkylated salts since we cannot however, rule out the possibility of photodegradation of the dyes occurring in solution. Degradation of cyanine dyes in solution in the presence of light and air has been a recurrent problem over the years [236, 237]. Lepaja and co-worker have reported one major photoproduct in the degradation pathway of heptamethine cyanine dyes as 2,3,3-trimethylindolenine [237]. To this end, the growth inhibitive effects of the *N*-alkylated salts were investigated. To

understand this both 2,3,3-trimethylindolenine and 2-methylbenzothiazole were alkylated up to a chain length of C=10. Also both compounds were *N*-alkylated with benzyl bromide and 1,3-propanesultone and 1,4-butanesultone. The growth inhibition was determined against *S. pombe*, fission yeast. Table 4.1 shows the MICs for the *N*-alkylated 2,3,3-trimethylindolenine and Table 4.2 for the *N*-alkylated 2-methylbenzothiazoles. It should be noted that the full MICs for N-Alkylations being C5-10 can be found in the Appendix (*Eur. J. Med. Chem*)
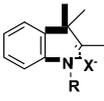
Number					MIC (μM)
	R	X⁻	% Yield	Log*P*	*S. pombe*
1a	CH$_3$	I⁻	58	-0.691	500
1b	CH$_2$CH$_3$	I⁻	86	-0.315	500
1c	CH$_2$CH$_2$CH$_3$	I⁻	85	0.188	250
1d	CH$_2$(CH$_2$)$_2$CH$_3$	I⁻	67	0.747	250
1k	CH$_2$C$_6$H$_5$	Br⁻	77	0.904	1000
1l	CH$_2$CH$_2$CH$_2$SO$_3$⁻	-	58	-4.33	1000
1m	CH$_2$CH$_2$CH$_2$CH$_2$SO$_3$⁻	-	50	-4.114	1000
1n	NA (control)	-	-	3.286	250

Table 4.1: Growth Inhibition Evaluation for *N*-alkylated 2,3,3-trimethylindolenine.

MIC of synthesised compounds tested in *S. pombe*. Cells were innoculated at a concentration of 3 x 10^4 cells. Culture media tested were in YE for *S. pombe*. Growth of yeast was determined visually after 24 hours incubation at 30 °C. The MICs of the compounds were determined to be the well before yeast growth was first seen. The experiments were repeated three times.
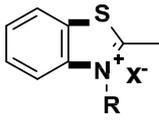
Number		X⁻	% Yield	Log*P*	MIC (μM)
	R	X⁻	% Yield	Log*P*	*S. pombe*
2a	CH$_3$	I⁻	87	-1.077	500
2b	CH$_2$CH$_3$	I⁻	41	-0.701	250
2c	CH$_2$CH$_2$CH$_3$	I⁻	44	-0.199	250
2d	CH$_2$(CH$_2$)$_2$CH$_3$	I⁻	51	0.36	250
2k	CH$_2$C$_6$H$_5$	Br⁻	90	0.517	1000
2l	CH$_2$CH$_2$CH$_2$SO$_3$⁻	-	50	-4.576	1000
2m	CH$_2$CH$_2$CH$_2$CH$_2$SO$_3$⁻	-	7	-4.411	1000
2n	NA (control)	-	-	2.085	250

Table 4.2: Growth Inhibition Evaluation for *N*-alkylated 2-methylbenzothiazoles

MIC of synthesised compounds tested in *S. pombe.* Cells were innoculated at a concentration of 3 x 10⁴ cells. Culture media tested were in YE for *S. pombe.* Growth of yeast was determined visually after 24 hours incubation at 30 °C. The MICs of the compounds were determined to be the well before yeast growth was first seen. The experiments were repeated three times.

The quaternary *N*-alkylated derivatives of both 2-methylbenzothiazole and 2,3,3-trimethylindolenine salts show varying degrees of growth inhibitive actions with the longer chain substituents being more potent against *S. pombe.* As shown in Appendix 1. This is evident when comparing **1j** (15.6 μM) to **1a** (500 μM) and **2j** (7.8 μM) to **2a** (500 μM) and indeed these results were consistent throughout the experiment. It was suggested that the growth inhibition can be attributed to the charged *N*-alkylated compounds with the increasing linear chain lengths. We postulate that these compounds are attracted to the negatively charged yeast membrane, with the longer lipophilic chains being absorbed into and subsequently distorting the lipid membrane [238].

It is concluded from this data that only *N*-alkyl chains up to the length of C4 should be used for the growth inhibition evaluation of the dyes due to the high level of growth inhibitive activity shown by the compounds possessing *N*-alkyl chain lengths of >C5. It is also noted that the sulfonic acid salts of both the 2,3,3-trimethylindolenine and the 2-methylbenzothiazole (**1 l-m & 2 l-m**) showed no growth inhibition activity, it is assumed that the presence of the sulfonic acid groups tends to increase their solubility and reduce their growth inhibition characteristics, possibly through suppressing membrane permeability and cellular uptake. It is also noted that the benzyl substituent also showed no activity against *S.*

pombe and this could possibly be due to the molecule having little membrane permeability due to the sp^2 hybridised ring system and steric factors.

4.4.0 Rigid Heptamethine Cyanine

Section 4.4 will focus on analysis of the photophysical and growth inhibition data for families of compounds **4 – 8**. Each of these compounds will be compared against IR-820 due to the high level of their structural similarities (the presence of the rigid cyclohexene backbone on the polymethine chain). During these experiments AO has been used as a negative control since it's a well-known commercially available toxic dye possessing strong inhibitive effect [233, 234].

4.4.1 Compounds 4 a-g

Compounds		Fluorescence Studies				Growth Inhibition Studies	
Code	R	Absorption λ_{max} (nm)	Fluorescence Emission (nm)	Fluorescence Quantum Yield (Φ)	Stokes Shift (nm)	Minimum Growth Inhibition (μM)	Log *P*
4a	Me	775	793	0.073	18	0.64[a]	4.928
4b	Et	777	796	0.080	19	0.61[a]	5.680
4c	*n*-Pr	781	798	0.074	17	0.58[a]	6.686
4d	*n*-Bu	780	799	0.076	19	0.70[a]	7.804
4e	Bn	775	793	0.084	18	0.61[a]	7.922
4f	$CH_2(CH_2)_2SO_3^-$	782	802	0.082	20	17.9[b]	-0.364
4g	$CH_2(CH_2)_3SO_3^-$	782	802	0.085	20	17.2[b]	-0.178
IR-820	Commercial Dye	820	840	0.032	20	15.1[b]	1.441
AO	Commercial Dye	-	-	-	-	<1.47[a]	3.321

Table 4.3: Photophysical and growth inhibition evaluation for indolium-based rigid heptamethine cyanine dyes.
Quantum yields ± 10%, λ_{max} ± 1 nm. Relative to IR-820.
Excitation at 785 nm.
[a]Indicates no visible yeast growth observed at this concentration of dye.
[b]Indicates highest possible concentration tested, visible yeast growth observed.
X$^-$ = I$^-$ or Br$^-$

The photophysical properties of compounds **4 a-g** are summarised in Table 4.3. It's clear to see that the indolium-based rigid heptamethine cyanine dyes exhibited absorption spectra maxima all absorbing in the NIR region between 775 - 782 nm. Rigidification of the polymethine backbone shifts the absorption and fluorescence maxima approximately 30 - 40 nm to the red when comparing **4a** (775 and 793 nm respectively) with **9a** (740 and 770 nm). The fused benzyl rings on IR-820 leads to an increased bathochromic shift by approximately 30 - 50 nm into the red which can be seen when comparing **4g** (782 nm) with IR-820 (820 nm) and **4e** with **6e** (775 and 822 nm respectively). Furthermore the similarities in the absorbance wavelength of the dyes in Table 4.3 could be attributed to the fact that the *N*-donor and *N*-acceptor substituting groups are too far away from the chromophore and as such have very little influence on the spectroscopic properties of the dyes.

An interesting observation is noted that compounds **4 a-g** demonstrated an approximate 2.5 to 3-fold increase in quantum yield when compared with IR-820. This result clearly indicates that presence of the extra phenyl group in IR-820 and dyes in Table 4.5 (**6 a-g**) destabilises the excited state of the NIR dyes relative to **4 a-g**. We note the Stokes shifts for the rigid dyes **4 a-g** show comparable shifts when compared against IR-820 and are also relatively small (17 – 20 nm). This indicates minor structural changes between the ground and excited states of the dyes.

The growth inhibition data can also be viewed in Table 4.3 and shows that compound **4 a-d** which possess linear alkyl chains give MIC values from 0.58 - 0.70 μM. When linked to the Log*P* its clear to see that higher degrees of lipophilicity are linked to cytotoxicity. However **4f** and **4g** with the sulfonic acid groups give MIC values of approximately 18 μM, thus we postulate that the presence of the sulfonic acid group on the dyes tends to increase their solubility and reduce their growth inhibition characteristics, possibly through reduced membrane permeability and cellular uptake. The growth inhibition is also shown graphically in Figure 4.3. The results from Figure 4.3 indicate that the synthesised heptamethine cyanine dyes (4 **a-g**) have a growth inhibition effect at different concentrations. The dyes coloured in green were the dyes which showed no inhibitory effect on the growth of the yeast cell (i.e. non-toxic) at the concentration tested. The results obtained were comparable to the result obtained for IR-820, a well-known commercially available non-toxic dye. Those bars coloured in red showed inhibitory effect on the growth of the yeast cells (i.e. prevented the

growth of the cells) and the results were similar to results obtained for AO, a well-known commercially available toxic dye.
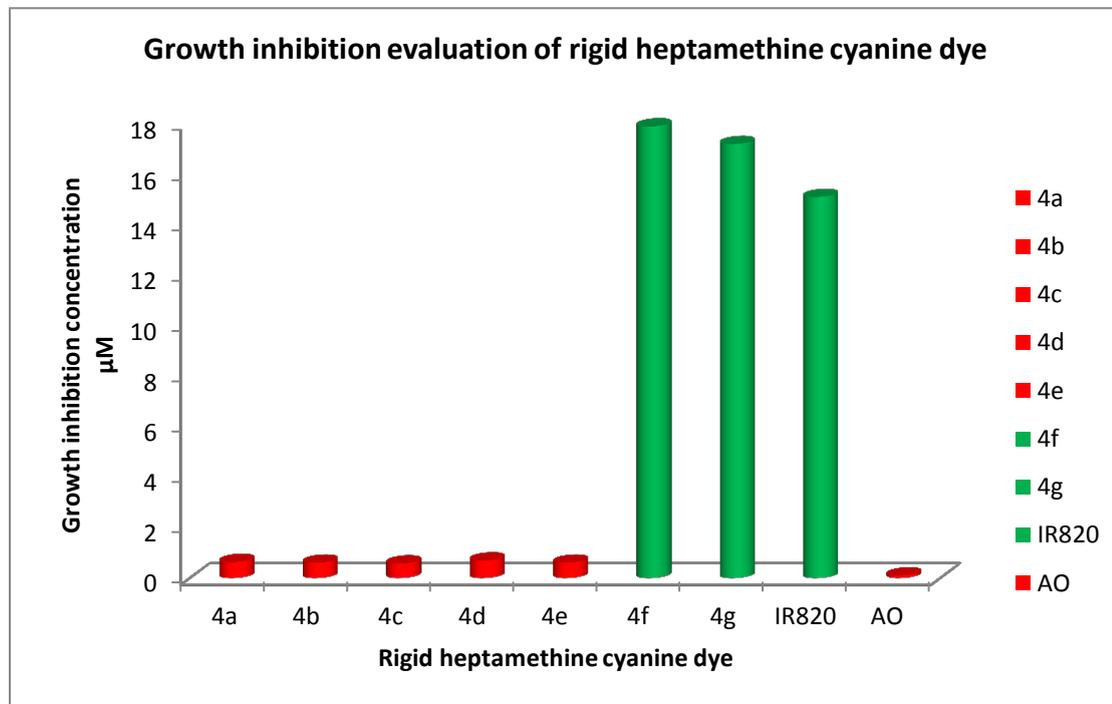
Figure 4.3: Growth inhibition evaluation of rigid heptamethine cyanine. Green bars indicate growth inhibition was comparable to IR-820. Red bars indicate growth was comparable to AO.

4.4.2 Compounds 5a - g

Compounds		Fluorescence Studies				Growth Inhibition Studies	
Code	R	Absorption λ_{max} (nm)	Fluorescence Emission (nm)	Fluorescence Quantum Yield (Φ)	Stokes Shift (nm)	Minimum Growth Inhibition (μM)	Log *P*
5a	Me	796	812	0.087	16	0.66[a]	3.923
5b	Et	796	812	0.087	16	0.63[a]	4.675
5c	*n*-Pr	797	814	0.091	17	0.60[a]	5.68
5d	*n*-Bu	796	813	0.093	17	0.05[a]	6.799
5e	Bn	804	820	0.093	16	0.89[a]	9.176
5f	$CH_2(CH_2)_2SO_3^-$	798	815	0.066	17	18.43[b]	-2.422
5g	$CH_2(CH_2)_3SO_3^-$	800	817	0.082	17	17.71[b]	-1.883
IR-820	Commercial Dye	820	840	0.032	20	15.1[b]	1.441
AO	Commercial Dye	-	-	-	-	<1.47[a]	3.321

Table 4.4: Photophysical and growth inhibition evaluation for rigid benzothiazole heptamethine cyanine dyes.

Quantum yields ± 10%, λ_{max} ± 1 nm. Relative to IR-820.

Excitation at 785 nm.

[a]Indicates no visible yeast growth observed at this concentration of dye.

[b]Indicates highest possible concentration tested, visible yeast growth observed.

$X^- = I^-$ or Br^-

The results in Table 4.4 indicates that the replacement of the 3,3-dimethylindolenine ring with a benzothiazole ring, shifts the absorption and fluorescence maxima deeper into the red as shown by comparing **5a** (796 and 812 nm) with **4a** (775 and 793 nm). Indeed, this comparison is seen throughout the series in Tables 4.4 and 4.4. This result suggests that the heavy atom effect plays an important role, since replacement of carbon with sulfur in the heterocyclic ring system facilitates the intersystem crossing resulting in increased shifts as previously reported [173]. Also the similarities in the absorbance and emission wavelength of the dyes in Table 4.4 could still be attributed to the fact that the *N*-donor and *N*-acceptor

substituting groups are too far away from the chromophore to have any influence on their spectral properties.

Furthermore, it was noted that the dyes in Table 4.4 (**5 a-g**) demonstrated an approximate 2.5 to 3-fold increase in quantum yield when compared with IR-820. This is also attributed to the heavy atom effect in the heterocyclic ring system increased the quantum yield and this is seen when comparing **5a** ($\Phi = 0.087$) and **4a** ($\Phi = 0.073$). The Stokes shifts values remained fairly consistent when comparing dyes in Table 4.4 (**5 a-g**) and dyes in Table 4.3 (**4 a-g**). This demonstrated that substituting the indolinium moiety with sulfur atom had no effect on the Stokes shifts of the dyes.

The growth inhibition values show that compounds **5 a-e** (bearing the sulfur moiety) (Table 4.4) show similar MIC values upon comparison with compounds **4 a-e** (bearing the indolium group) (Table 4.3). It's interesting to note that compounds **5f** and **5g** show slightly higher MIC values. This is evident when comparing **5f** (18.43 μM) and **5g** (17.71 μM) with **4f** (17.9 μM) and **4g** (17.2 μM) respectively. Hence, it is therefore suggested that the observed effect could be attributed to the excellent biocompatibility characteristics of the benzothiazole moiety [200]. The results from Figure 4.4 indicate that the synthesised heptamethine cyanine dyes have different growth inhibitory effect at different concentration. The dyes coloured in green were the dyes which showed no inhibitory effect on the growth of the yeast cell (i.e. non-toxic) at the concentration tested. The results obtained indicated that **5f** (18.43 μM) and **5g** (17.71 μM) showed better MIC values when compared to **IR-820** (15.1 μM), indicating their suitability for possible clinical applications. Those bars coloured in red showed inhibitory effect on the growth of the yeast cells (i.e. prevented the growth of the cells) and the results were similar to results obtained for AO.
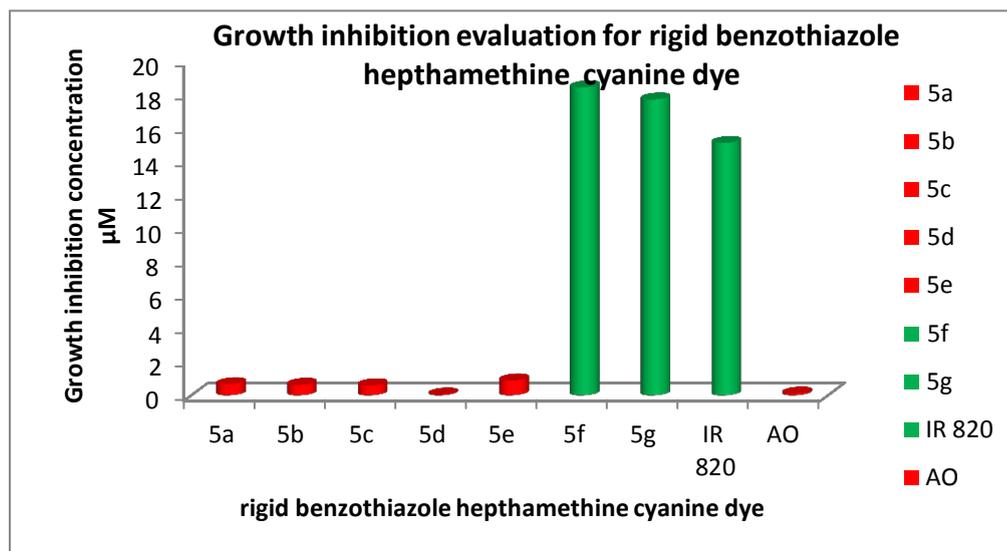
Figure 4.4: Growth inhibition evaluation for rigid benzothiazole heptamethine cyanine. Green bars indicate growth inhibition was comparable to IR-820. Red bars indicate growth was comparable to AO.

4.4.3 Compounds 6 a-g

Compounds		Fluorescence Studies				Growth Inhibition Studies	
Code	R	Absorption λ_{max} (nm)	Fluorescence Emission (nm)	Fluorescence Quantum Yield (Φ)	Stokes Shift (nm)	Minimum Growth Inhibition (μM)	Log *P*
6a	Me	813	834	0.028	21	0.02[a]	7.247
6b	Et	815	833	0.035	18	0.05[a]	7.999
6c	*n*-Pr	818	838	0.029	20	0.02[a]	8.695
6d	*n*-Bu	838	818	0.032	20	0.03[a]	9.139
6e	Bn	822	845	0.029	23	3.06[a]	9.176
6f	$CH_2(CH_2)_2SO_3^-$	820	841	0.032	21	15.6[b]	0.9
6g	$CH_2(CH_2)_3SO_3^-$	820	840	0.032	20	15.1[b]	1.441
IR-820	Commercial Dye	820	840	0.032	20	15.1[b]	1.441
AO	Commercial Dye	-	-	-	-	<1.47[a]	3.321

Table 4.5: Photophysical and growth inhibition evaluation evaluation for rigid benzo[e] heptamethine cyanine dyes.

Quantum yields $\pm$ 10%, $\lambda_{max} \pm$ 1 nm. Relative to IR-820.

Excitation at 785 nm.
[a]Indicates no visible yeast growth observed at this concentration of dye.
[b]Indicates highest possible concentration tested, visible yeast growth observed.
$X^- = I^-$ or Br^-

Perspective views of **6 a-g** are depicted in Table 4.5. Table 4.5 outlines the spectral properties of the indolinum based heptamethine cyanine dyes bearing the extra phenyl ring. Regardless of the substituting groups attached to the indolinium nuclei, the fluorescence quantum yield and Stoke shifts of the dyes (**6 a-g**) were practically identical. However on comparing the absorption and emission wavelengths of **6a** (813 nm and 834 nm) with **4a** (775 nm and 793 nm), it was noted that the presence of the extra fused phenyl ring on the heterocyclic system resulted in an increase shift of absorption and emission wavelength to red which is as a result of increase in conjugation in the π-electron system. Indeed this result is consistent when comparing the values in Table 4.3 (**4 a-g**) with Table 4.5 (**6 a-g**) respectively. Also it should be noted that the quantum yields are around the same value as for IR-820 highlighting the close structural relationship.

The MIC and Log*P* values were consistent with the results obtained from the previous series of compounds due to their structural similarities, with dyes bearing the *N*-alkylated linear chain possessing higher toxicity and higher degrees of lipophilicity. It is interesting to observe that the compound **6e** which has the *N*-benzylic group shows a higher MIC value when compared with **4e** and **5e** this could be attributed to the extra fused phenyl moiety having an effect on its spatial arrangement between itself and the cell wall of the *S. pombe*. Figure 4.5 further illustrates the results obtained for the growth inhibition evaluation.
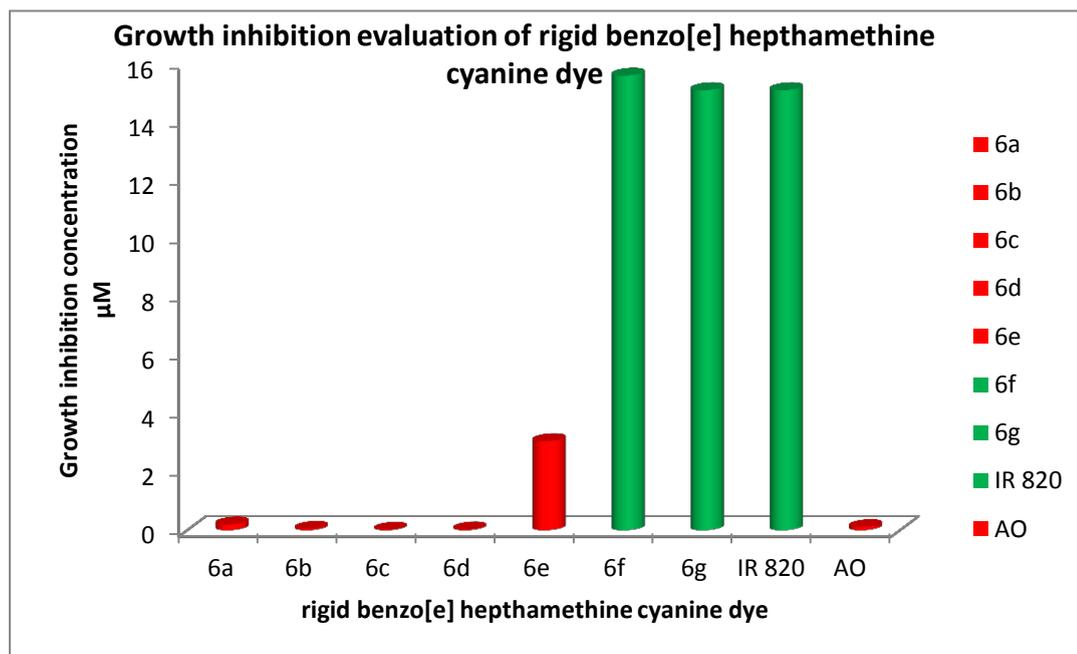
Figure 4.5: Growth inhibition evaluation of rigid benzo[e] heptamethine cyanine dyes. Green bars indicate growth inhibition was comparable to IR-820. Red bars indicate growth was comparable to AO.

4.4.4 Compounds 7 a- f

	Compounds	Fluorescence Studies				Growth Inhibition Studies	
Code	**R**	**Absorption λ_{max} (nm)**	**Fluorescence Emission (nm)**	**Fluorescence Quantum Yield (Φ)**	**Stokes Shift (nm)**	**Minimum Growth Inhibition (μM)**	**Log *P***
7a	Me	736	786	0.030	50	0.58[a]	6.185
7b	Et	735	786	0.027	51	0.56[a]	6.937
7c	*n*-Pr	746	795	0.054	49	0.54[a]	7.942
7d	Bn	736	794	0.015	58	0.80[a]	8.778
7e	$CH_2(CH_2)_2SO_3^-$	745	793	0.045	48	16.5[b]	-0.162
7f	$CH_2(CH_2)_3SO_3^-$	745	791	0.047	46	15.9[b]	0.379
IR-820	Commercial Dye	820	840	0.032	20	5.1[b]	1.441
AO	Commercial Dye	-	-	-	-	<1.47[a]	3.321

Table 4.6: Photophysical and growth inhibition evaluation for functionalised indolium-based rigid heptamethine cyanine dyes.

Quantum yields $\pm$ 10%, λ_{max} $\pm$ 1 nm. Relative to IR-820.
Excitation at 785 nm.
[a]Indicates no visible yeast growth observed at this concentration of dye.
[b]Indicates highest possible concentration tested, visible yeast growth observed.
$X^- = I^-$ or Br^-

Due to unusual synthetic problems, the *n*-butyl derivative of these dyes could not be made and this synthesis was abandoned. Thus the comparison with this compound with **4d** was unable to take place.

Addition of aniline to the rigid cyclo-hexene central subunit shows a profound effect on the photophysical activities and this can be seen when comparing **7 a-f** with **4 a-f**. To highlight this, comparisons between **4a** and **7a, 4e** and **7d** and **4g** with **7f** have been made. It's interesting to note that each of the three sets of compounds shows unusually high Stokes shifts (~50 nm). This is related to the decrease in absorption across the spectrum of compounds which can be highlighted when comparing **4a** to **7a** (775 nm to 736 nm), **4e** to **7d** (775 nm to 736 nm) and **4g** to **7f** (745 nm to 787 nm) respectively. Also there is no defined pattern for the quantum yields and it is noted that compounds **7a**, **b** and **d** all show a decrease when compared to **IR-820**. It's interesting to note that compounds **7 e-f** show higher quantum yields to that of **IR-820**. The increase in Stoke shift is advantageous for this type of work since it renders the amine-substituted cyanine dyes useful as NIR platforms for the development of a wide range of non-targeting fluorescent probes [203].

The growth inhibition data once again shows the same trend in comparison with the other sets of compounds **4-6**. Once again the compounds **7e** and **f** show lower MIC values when compared to **IR-820** which of course go hand in hand with a decrease in Log*P* for both compounds. And this is evident in Figure 4.6
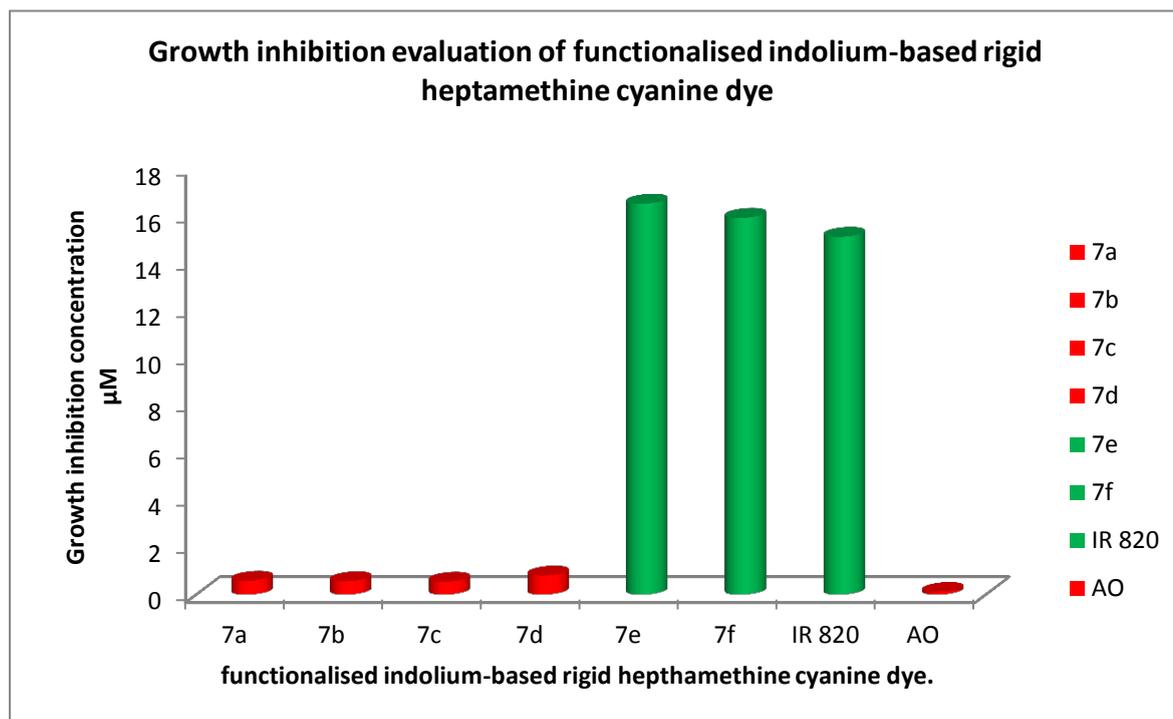
Figure 4.6: Growth inhibition evaluation of functionalised indolium-based rigid heptamethine cyanine dyes. Green bars indicate growth inhibition was comparable to ICG. Red bars indicate growth was comparable to acridine orange AO.

4.4.5   Compounds 8 a-e

Compounds		Fluorescence Studies				Growth Inhibition Studies	
Code	R	Absorption λ_{max} (nm)	Fluorescence Emission (nm)	Fluorescence Quantum Yield (Φ)	Stokes Shift (nm)	Minimum Growth Inhibition (μM)	Log *P*
8a	Me	780	818	0.049	38	0.10[a]	8.488
8b	Et	776	820	0.062	44	0.10[a]	8.813
8c	*n*-Pr	778	823	0.063	45	0.20[a]	9.182
8d	Bn	769	826	0.048	57	1.43[a]	9.503
8e	$CH_2(CH_2)_3SO_3^-$	779	824	0.067	45	14.15[b]	2.698

| IR-820 | Commercial Dye | 820 | 840 | 0.032 | 20 | 15.1[b] | 1.441 |
| AO | Commercial Dye | - | - | - | - | <1.47[a] | 3.321 |

Table 4.7: Photophysical and growth inhibition evaluation for functionalised rigid benzo[e] heptamethine cyanine dyes.

Quantum yields ± 10%, λ_{max} ± 1 nm. Relative to IR-820.

Excitation at 785 nm.

[a]Indicates no visible yeast growth observed at this concentration of dye.

[b]Indicates highest possible concentration tested, visible yeast growth observed.

$X^- = I^-$ or Br^-

The structural and spectral characteristics of dyes in Table 4.6 (**7 a-f**) and Table 4.7 (**8 a-e**) are closely related and can also be discussed together. The dyes in Tables 4.6 and 4.7 are similar in terms of their structural features which differ most noticeably with presence of the extra phenyl ring on dyes **8 a-e**. As can be seen in Tables 4.6 and 4.7, the Stoke shifts values of rigid heptamethine cyanine dyes **7 a-f** and **8 a-e** range from 38 to 57 nm and this is quite high and this increase is evident when comparing **7d** (58 nm) with **4e** (18 nm) and **8d** (57 nm) with **6e** (23 nm). Indeed, this comparison is seen throughout the series in Tables 4.3, 4.5, 4.6 and 4.7. And it is postulated that the observed increase could be as a result of the substitution of the meso-chlorine atom with an aromatic moiety, indicating a large structural change between the ground and the excited singlet state of the dyes owing to an intramolecular charge transfer (ICT) effect. Figure 4.7 indicates the structures of the compared rigid heptamethine cyanines dyes for the Stokes shift studies.
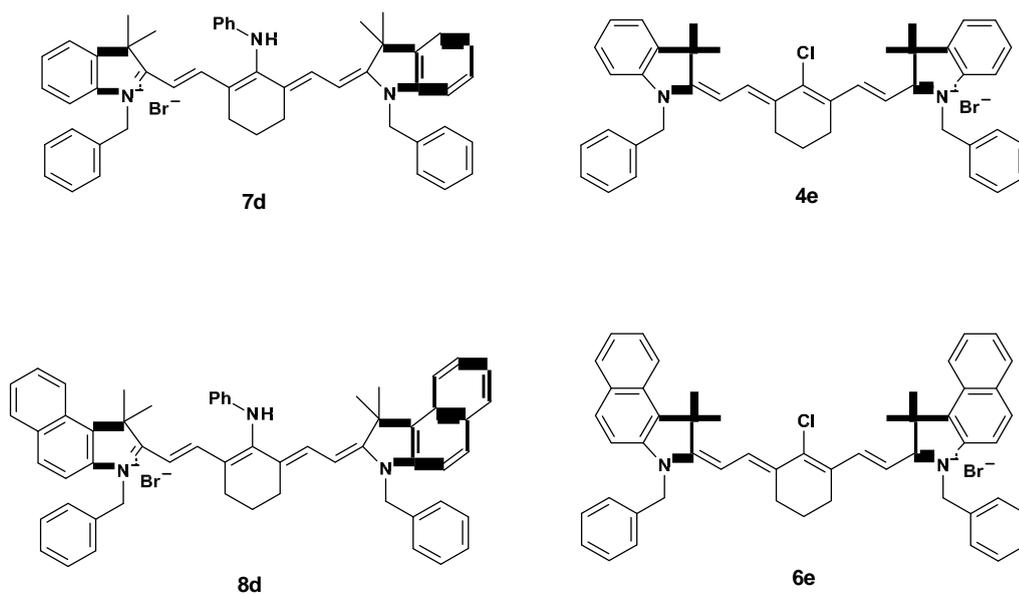
Figure 4.7: Structures of heptamethine cyanine dyes.

The MIC values remained fairly consistent with *N*-sulfonic acid dyes showing MIC values in the range of 14.1 to 16.5 µM. Also the values were parallel to results obtained for IR-820. While the *N*-linear alkyl chains gave MIC values from 0.10 - 0.80 µM relating to their Log*P* values and the values were corresponding to results obtained for 1AO. This is illustrated in Figure 4.8
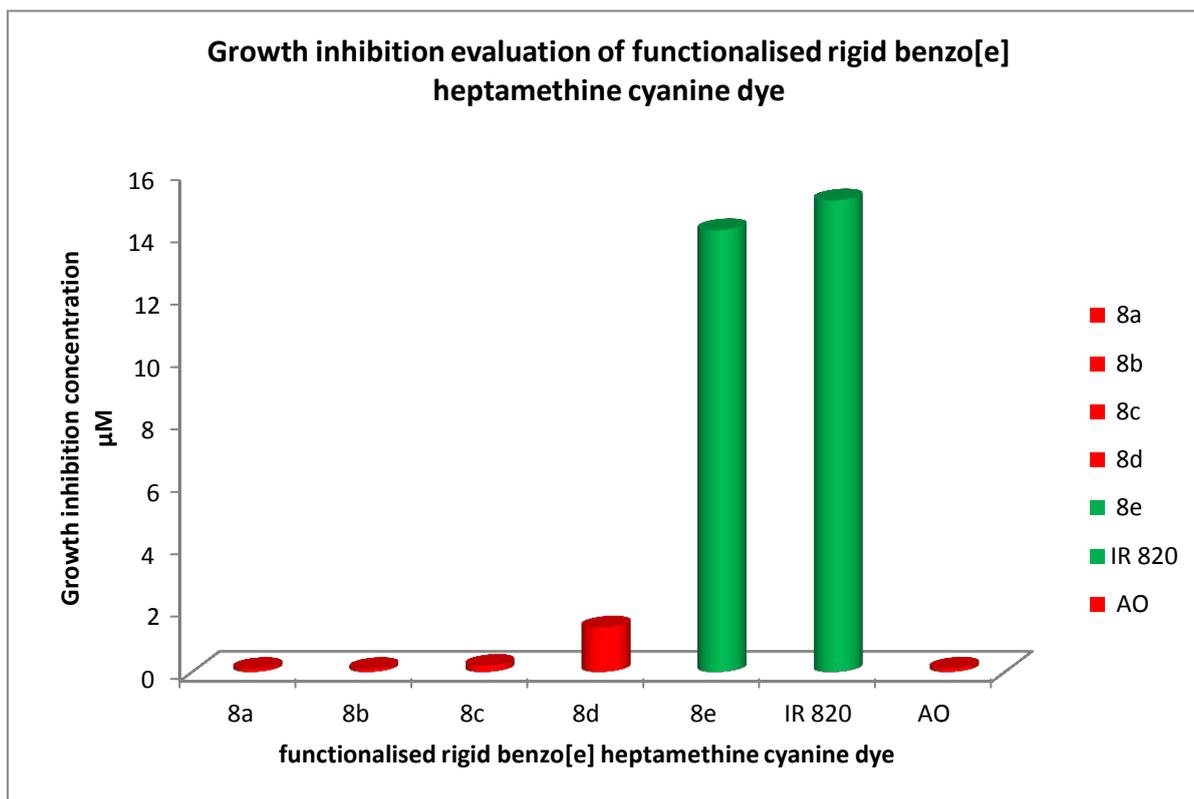
Figure 4.8: Growth inhibition evaluation for functionalised rigid benzo[e] heptamethine cyanine dyes. Green bars indicate growth inhibition was comparable to IR-820. Red bars indicate growth was comparable to AO.

4.5.0 Linear Heptamethine Cyanine

Section 4.5 will focus on analysis of the photophysical and growth inhibition data for families of compounds **9 – 11**. Each of these compounds will be compared against ICG due to the high level of their structural similarities such as the absence of the rigid cyclohexene backbone on the polymethine chain. During these experiments, AO has been used as a negative control [234].

4.5.1   Compounds 9 a-g

Compounds		Fluorescence Studies				Growth Inhibition Studies	
Code	**R**	**Absorption λ_{max} (nm)**	**Fluorescence Emission (nm)**	**Fluorescence Quantum Yield (Φ)**	**Stokes Shift (nm)**	**Minimum Growth Inhibition (μM)**	**Log *P***
9a	Me	740	770	0.09	30	0.58[a]	3.810
9b	Et	742	770	0.11	28	0.55[a]	4.562
9c	*n*-Pr	746	776	0.13	30	0.52[a]	5.567
9d	*n*-Bu	746	776	0.13	30	0.76[a]	6.686
9e	Bn	748	776	0.15	28	0.48[a]	6.804
9f	$CH_2(CH_2)_2SO_3^-$	747	773	0.13	26	16.0[b]	-2.537
9g	$CH_2(CH_2)_3SO_3^-$	747	775	0.13	28	15.3[b]	-1.995
ICG	Commercial Dye	785	814	0.072	29	16.6[b]	1.591
AO	Commercial Dye	-	-	-	-	<1.47[a]	3.321

Table 4.8: Photophysical and growth inhibition evaluation for indolium-based linear heptamethine cyanine dyes.

 Quantum yields $\pm$ 10%, $\lambda_{max} \pm 1$ nm. Relative to ICG.
 Excitation at 785 nm.
[a]Indicates no visible yeast growth observed at this concentration of dye.
[b]Indicates highest possible concentration tested, visible yeast growth observed.
$X^- = I^-$ or Br^-

Due to the remarkable and distinct variations between compounds **9 a-g** and **10 a-g** which include the replacement of 2,3,3-trimethylindolenine with a benzothiazole moiety**,** comparisons between both sets will be made on the next page.
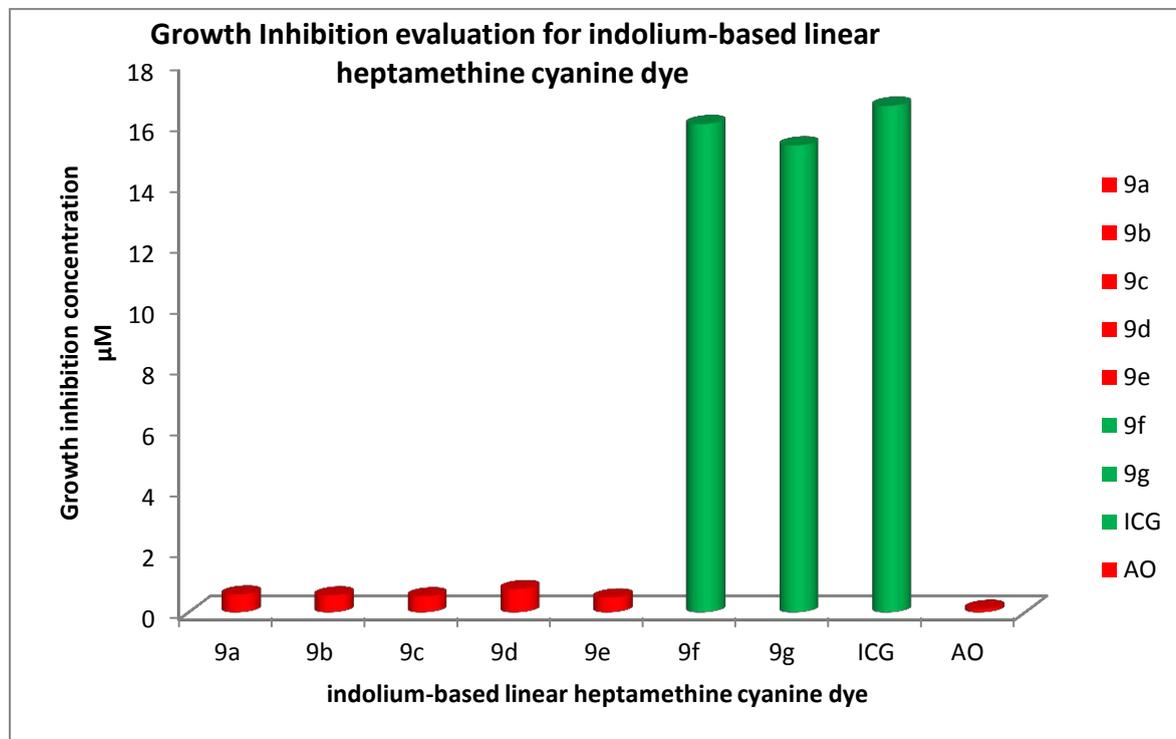
Figure 4.9: Growth inhibition evaluation for linear indolium based heptamethine cyanine dyes. Green bars indicate growth inhibition was comparable to ICG. Red bars indicate growth was comparable to AO.

4.5.2 Compound 10 a-g

Compounds		Fluorescence Studies				Growth Inhibition Studies	
Code	R	Absorption λ_{max} (nm)	Fluorescence Emission (nm)	Fluorescence Quantum Yield (Φ)	Stokes Shift (nm)	Minimum Growth Inhibition (μM)	Log P
10a	Me	756	783	0.165	27	1.21[a]	2.805
10b	Et	759	785	0.161	26	0.57[a]	3.557
10c	*n*-Pr	761	786	0.176	25	0.54[a]	4.562
10d	*n*-Bu	761	787	0.181	26	0.06[a]	5.681

10e	Bn	765	791	0.229	26	4.62[b]	5.994
10f	$CH_2(CH_2)_2SO_3^-$	762	789	0.146	27	16.58[b]	-3.542
10g	$CH_2(CH_2)_3SO_3^-$	762	789	0.166	27	15.85[b]	-3.001
ICG	Commercial Dye	785	814	0.072	29	6.6[b]	1.591
AO	Commercial Dye	-	-	-	-	<1.47[a]	3.321

Table 4.9: Photophysical and growth inhibition evaluation for linear benzothiazole heptamethine cyanine dyes.
Quantum yields $\pm$ 10%, λ_{max} $\pm$ 1 nm. Relative to ICG.
Excitation at 785 nm.
[a]Indicates no visible yeast growth observed at this concentration of dye.
[b]Indicates highest possible concentration tested, visible yeast growth observed.
$X^- = I^-$ or Br^-

The molecular structural backbone of dyes **9 a-g** and **10 a-g** are very similar with the only difference being the replacement of the 3,3-dimethylindolenine ring with a benzothiazole ring. The spectral properties collected for the dyes are summarised in Tables 4.8 and 4.9. It is noted that the benzothiazole ring shifts the absorption and fluorescence maxima deeper into the red as shown by comparing **9e** (748 nm and 776 nm) with **10e** (765 nm and 791 nm), however the Stokes shift remains constant for both at 28 nm and 26 nm respectively. An interesting observation is that the linear benzothiazole heptamethine cyanine dyes (**10 a-g**) show a 2-fold increase in quantum yield when compared with **ICG**. It was also discovered, that rigidification of the polymethine chain reduces the quantum yields by approximately 50%, as shown by comparing **10a** ($\Phi = 0.165$) with **5a** ($\Phi = 0.087$). This reduction in quantum yield is also seen when comparing ICG ($\Phi = 0.072$) with IR-820 ($\Phi = 0.032$) and also when comparing dyes (**9 a-g**) with dyes (**4 a-g**). This finding is in contrast to the typical observations that rigidifying chromophore systems in organic molecules is an established strategy to stabilise and optimise the spectral properties of fluorescent dyes [239]. Also it was observed that the linear dyes (**10 a-g**) bearing the benzothiazole moiety showed higher quantum yield values when compared with the linear dyes (**9 a-g**) bearing the 3,3-dimethylindolenine moiety. Based on the results obtained from this comparison, it could be suggested that a combination of different factors all play a role in the quantum yield of the dyes rather than just the presence of the rigid cyclo-hexene ring. And such factors include the substitution pattern of the indolium ring system and length of polymethine chain. Furthermore, large Stokes shift values were noticed when comparing the linear dyes (**9 a-g**, **10 a-g**) with Stokes shift values in the range 25-30 nm to the dyes (**4 a-g**, **5 a-g**) bearing the rigid

cyclohexene moiety with Stokes shift values in the range of 16-20 nm. This characteristic is not unusual and could be attributed to the replacement of the rigid cyclohexene unit with the linear chain indicating a major structural change, which in turn affects the ground state and the excited singlet states of the dyes.

The growth inhibition data can also be viewed in Table 4.8 and 4.9 and the results indicate that the dyes (**9 a-d**, **10 a-d**) bearing the linear alkyl chains on the nitrogen of the indolenine nuclei gave MIC values from 0.06-0.76 μM. While the dyes (**9 f-g**, **10 f-g**) bearing the sulfonic acid group gave MIC values from 15.3-16.58 μM. When considered against the Log$P$ values its clear to see that higher degrees of lipophilicity are linked to toxicity and vice versa. Furthermore, the results in Figure 4.10 indicate that the synthesised linear heptamethine cyanine dyes have different growth inhibition effect at different concentration. The dyes coloured in green were the dyes which showed no inhibition effect on the growth of the yeast cell (i.e. non-toxic) at the concentration tested and the results obtained were corresponding to result obtained for ICG. Those bars coloured in red showed inhibitory effect on the growth of the yeast cells (i.e. prevented the growth of the cells) and the results were parallel to results obtained for AO.
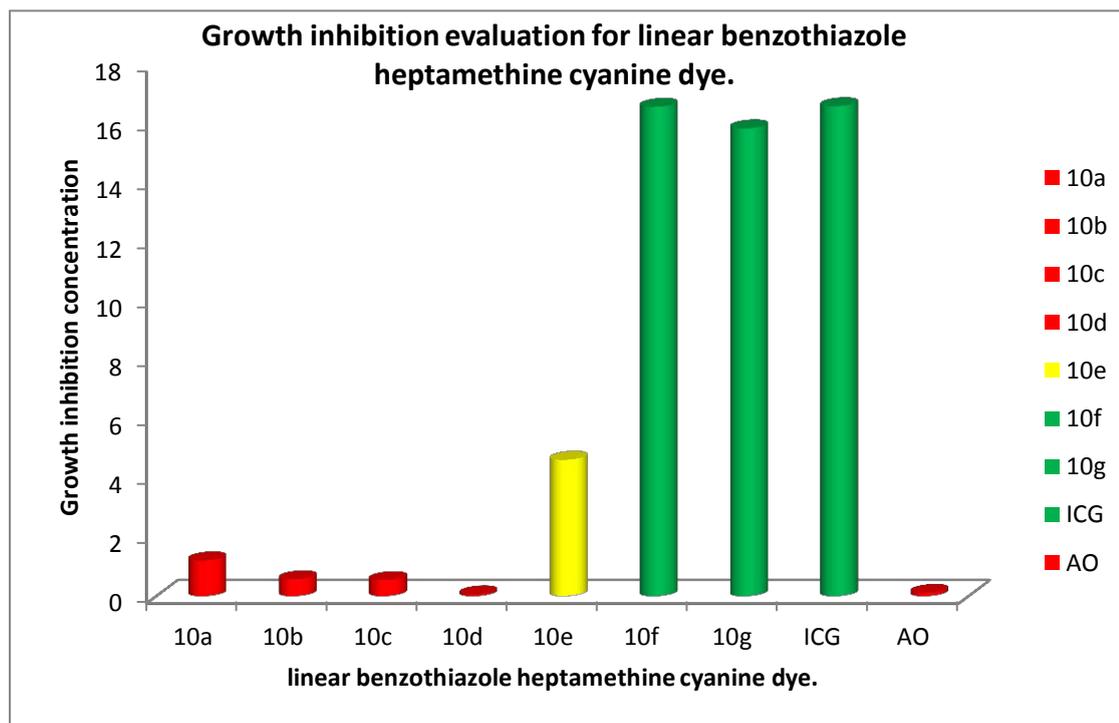
Figure 4.10: Growth inhibition evaluation for linear benzothiazoleheptamethine cyanine dyes. Green bars indicate growth inhibition was comparable to ICG. Red bars indicate growth was comparable to AO. Yellow bar indicate growth in the intermediate range.

4.5.3   Compound 11 a-g

Compounds		Fluorescence Studies				Growth Inhibition Studies	
Code	R	Absorption λ_{max} (nm)	Fluorescence Emission (nm)	Fluorescence Quantum Yield (Φ)	Stokes Shift (nm)	Minimum Growth Inhibition (μM)	Log P
11a	Me	778	807	0.064	29	0.007[a]	6.129
11b	Et	781	809	0.072	28	0.029[a]	6.881
11c	n-Pr	782	811	0.071	29	0.028[a]	7.881
11d	n-Bu	783	811	0.075	28	0.027[a]	8.696
11e	Bn	786	814	0.076	28	6.74[b]	8.753

11f	$CH_2(CH_2)_2SO_3^-$	784	812	0.073	28	17.2^b	-0.218
11g	$CH_2(CH_2)_3SO_3^-$	785	814	0.072	29	16.6^b	0.323
ICG	Commercial Dye	785	814	0.072	29	16.6^b	1.591
AO	Commercial Dye	-	-	-	-	$<1.47^a$	3.321

Table 4.10: Photophysical and growth inhibition evaluation for linear benzo[e] heptamethine cyanine dyes.

Quantum yields $\pm$ 10%, $\lambda_{max} \pm 1$ nm. Relative to ICG.
Excitation at 785 nm.
[a]Indicates no visible yeast growth observed at this concentration of dye.
[b]Indicates highest possible concentration tested, visible yeast growth observed.
$X^- = I^-$ or Br^-

The photophysical and growth inhibition characteristics for the linear benzo[e] heptamethine cyanine dyes are summarised in Table 4.10 above. The properties studied and data collected are similar to previous results obtained and discussed for dyes having similar structural characteristics.
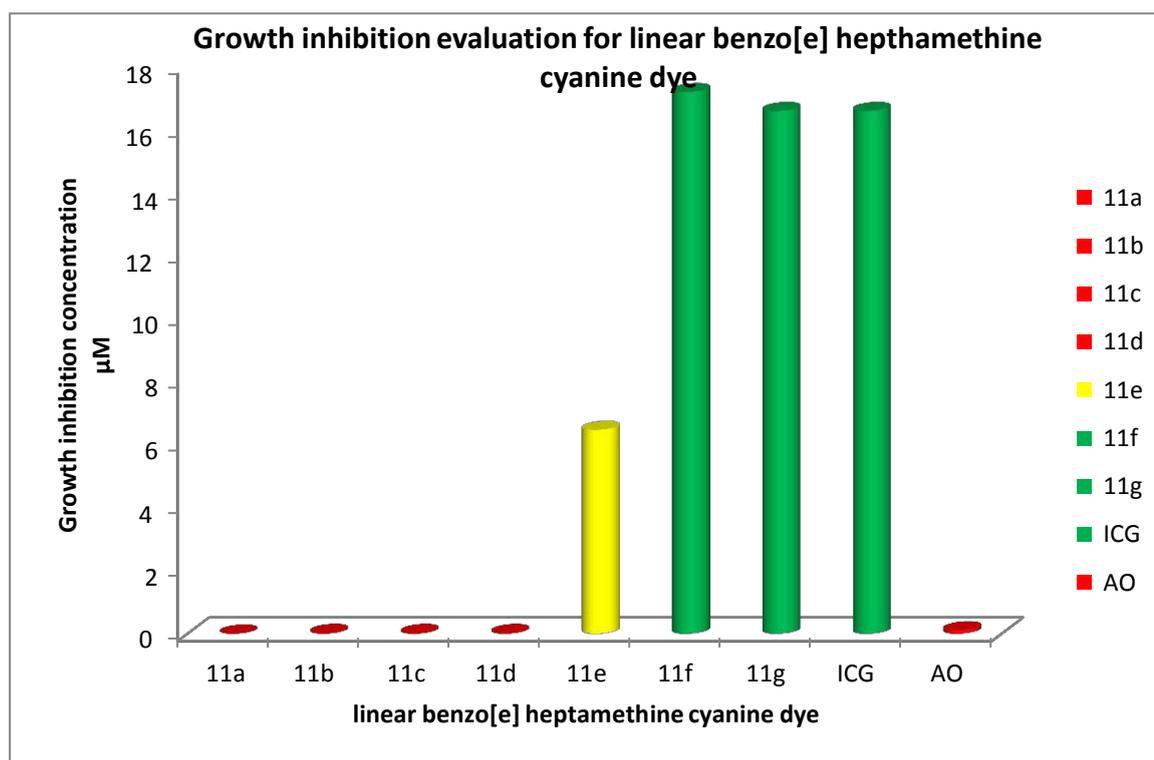
Figure 4.11: Growth inhibition evaluation for linear benzo[e] heptamethine cyanine dyes. Green bars indicate growth inhibition was comparable to ICG. Red bars indicate growth was comparable to AO. The yellow bar indicates growth in the intermediate range.

4.6 Substituted Polymethine Linear Heptamethine Cyanine

Section 4.6 will focus the analysis of the photophysical and growth inhibition data for compounds **12 - 20**. Because of the linear nature of these dyes comparisons will be made against ICG rather than IR-820. During these experiments AO has been used as a negative control.

Compounds		Fluorescence Studies				Growth Inhibition Studies	
Code	R	Absorption λ_{max} (nm)	Fluorescence Emission (nm)	Fluorescence Quantum Yield (Φ)	Stokes Shift (nm)	Minimum Growth Inhibition (μM)	Log *P*
12		784	814	0.072	30	9.39[b]	0.361
13		743	769	0.091	26	8.54[b]	0.279
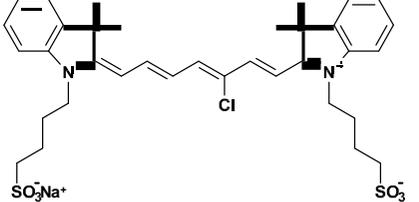
14		747	774	0.116	27	9.09[b]	0.148
15		758	782	0.144	24	17.1[b]	1.15
16		753	779	0.129	26	9.16[b]	-1.267
17		758	783	0.158	25	9.81[b]	-1.398
18		61	784	0.148	23	10.1[b]	-1.185
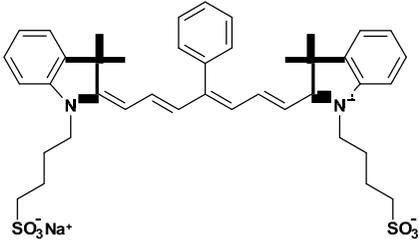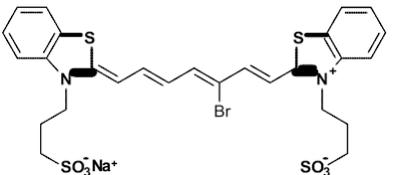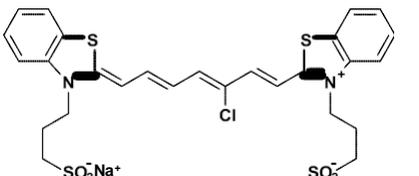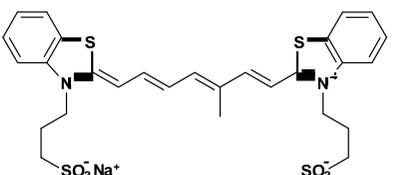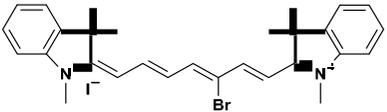
19		737	764	0.071	27	1.01[a]	4.276
20		752	777	0.154	25	1.13[a]	3.139
ICG	Commercial Dye	785	814	0.072	29	16.6[b]	1.591
AO	Commercial Dye	-	-	-	-	<1.47[a]	3.321
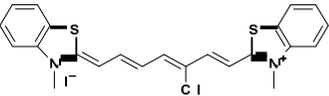
Table 4.11: Photophysical and Growth Inhibition evaluation for substituted linear heptamethine cyanine dyes.

*[1] Quantum yields $\pm$ 10%, $\lambda_{max} \pm 1$ nm. Relative to ICG.

*[2] Excitation at 785 nm.

[a]Indicates no visible yeast growth observed at this concentration of dye.
[b]Indicates highest possible concentration tested, visible yeast growth observed.

The spectral and growth inhibition characteristics for the diverse range of heptamethine cyanine dyes (**12 – 20**) are summarised in Table 4.11 above. It's clear to see that all dyes exhibited absorption spectra maxima in the NIR region between 743 - 784 nm. They also demonstrated higher fluorescence quantum yields than ICG. The fluorescence quantum yield for the dyes bearing the 3,3-dimethylindolenine ring increased in the order Cl>Br>CH$_3$.While that of the dyes bearing the benzothiazole ring increased in the order Cl>CH$_3$>Br. The results collected indicates that the dyes (**17** and **20**) bearing the benzothiazole ring with their linear polymethine chain linked to a chlorine atom showed the highest quantum yield **20** (Φ = 0.154), **17** (Φ = 0.158). It is uncertain as to the mechanism or exact reason for the observed effect. Previous reports in the literature have suggested that the fluorescence life times and quantum yields of organic dyes increased with increasing molecular weight of the intramolecular heavy atom modifications [240]. It would therefore seem plausible that the presence of the chlorine, sulfur atom and substitution pattern of the polymethine chain may all have contributed to the increased quantum yields. We cannot however, rule out the possibility that heavy atom modification did increase the efficiency of crossing into the triplet state, since heavy atoms show larger rate of intersystem crossing. The growth inhibition data shows that the substituted linear heptamethine cyanine dyes demonstrated MIC values from 1.01 - 17.1 µM based on their structural characteristics. Due to the intense colour of the dyes, it was difficult to accurately judge the growth of yeast. Therefore, the assay for the substituted linear heptamethine cyanine dyes may under estimate the MIC values. The dyes may not be growth inhibitive as the data suggests, since the MIC values were calculated from the second wells in which growth was more visible. The dyes bearing the alkyl chains on the nitrogen of the indolenine nuclei gave MIC values comparable to AO (Table 4.11 and Figure 4.12). While the dyes bearing the sulfonic acid group gave MIC values comparable to ICG (Table 4.11 and Figure 4.12). Also when the MIC values are related to the Log*P* it's clear to see that higher degrees of lipophilicity are linked to toxicity. Due to these interesting quantum yields and MIC values, the diverse range of synthesised heptamethine cyanine dyes show potential for clinical applications when compared with the clinical standard ICG.
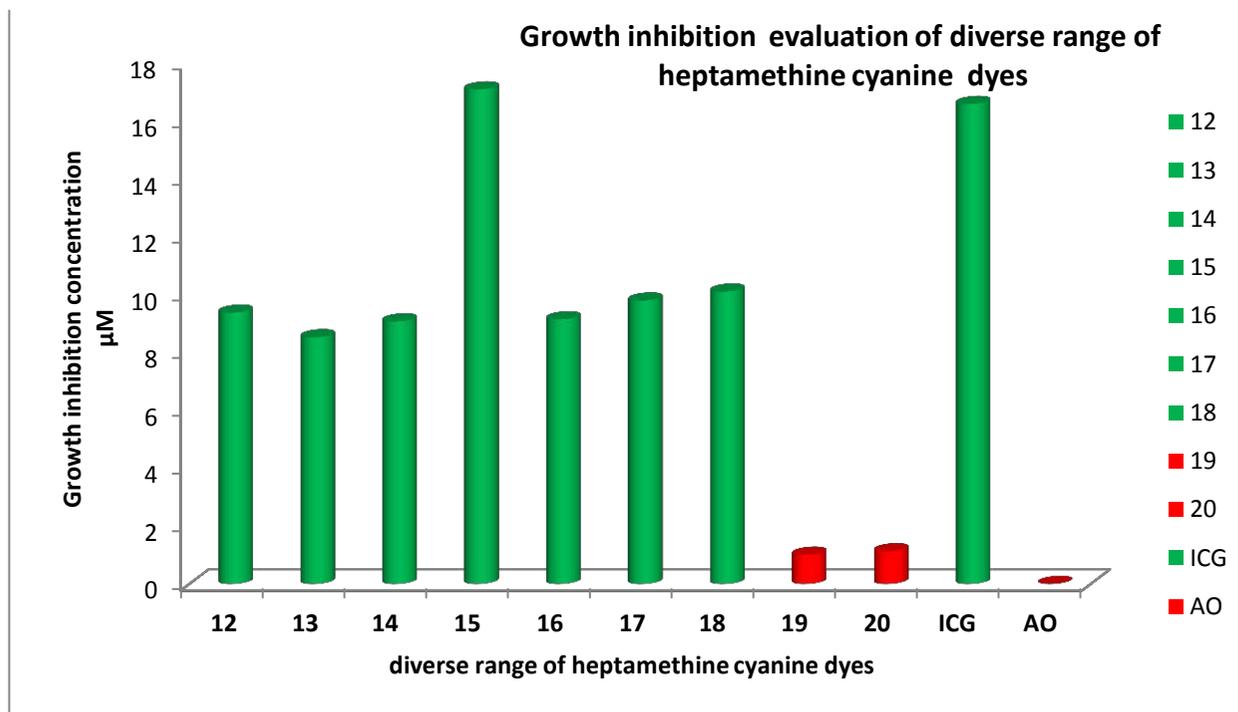
Figure 4.12: Growth inhibition evaluation for substituted linear heptamethine cyanine dyes. Green bars indicate growth inhibition was comparable to ICG. Red bars indicate growth was comparable to AO.

Compounds		Fluorescence Studies				Growth Inhibition Studies	
Code	R	Absorption λ_{max} (nm)	Fluorescence Emission (nm)	Fluorescence Quantum Yield (Φ)	Stokes Shift (nm)	Minimum Growth Inhibition (μM)	Log P
22		758	786	0.17	28	4.83[b]	3.124
23		800	818	0.09	18	1.05[a]	4.242
24		759	782	0.15	23	4.70[b]	3.672
ICG	Commercial Dye	785	814	0.072	29	16.6[b]	1.591
AO	Commercial Dye	-	-	-	-	<1.47[a]	3.321
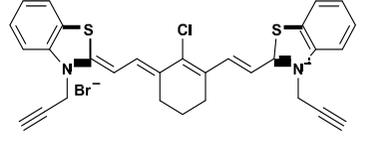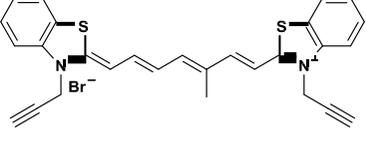
Table 4.12: Photophysical and Growth Inhibition evaluation for click intermediate dyes.

Quantum yields ± 10%, λ_{max} ± 1 nm. Relative to ICG.
Excitation at 785 nm.
[a]Indicates no visible yeast growth observed at this concentration of dye.
[b]Indicates highest possible concentration tested, visible yeast growth observed.
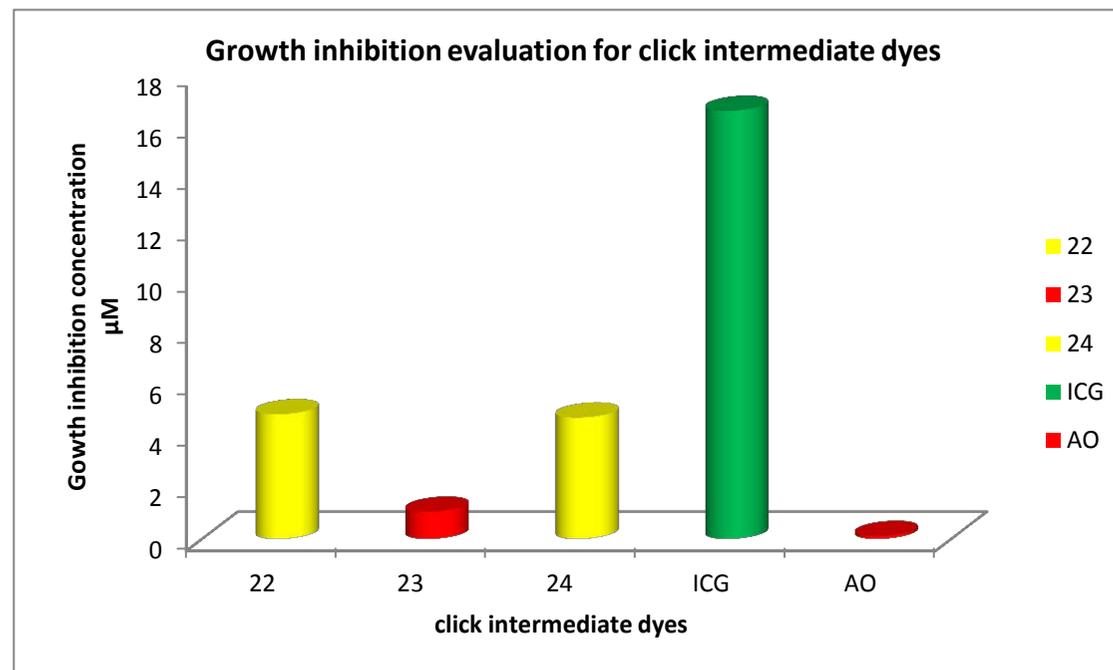
Figure 4.13: Growth inhibition evaluation for click intermediate cyanine dyes. Green bars indicate growth inhibition was comparable to ICG. Red bars indicate growth was comparable to AO. Yellow bar indicate growth in the intermediate range.

Compounds		Fluorescence Studies				Growth Inhibition Studies	
Code	R	Absorption λ_{max} (nm)	Fluorescence Emission (nm)	Fluorescence Quantum Yield (Φ)	Stokes Shift (nm)	Minimum Growth Inhibition (μM)	Log *P*
25		764	791	0.17	27	6.38[b]	5.493
26		804	821	0.09	17	2.91[a]	6.611
27		759	786	0.12	27	6.27[b]	6.041
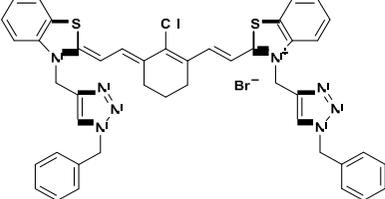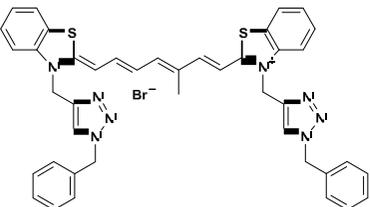
ICG	Commercial Dye	785	814	0.072	29	16.6[b]	1.591
AO	Commercial Dye	-	-	-	-	<1.47[a]	3.321

Table 4.13: Photophysicaldatas for heptamethine cyanine dye-azide conjugates.

Quantum yields $\pm$ 10%, λ_{max} $\pm$ 1 nm. Relative to ICG.
Excitation at 785 nm.
[a]Indicates no visible yeast growth observed at this concentration of dye.
[b]Indicates highest possible concentration tested, visible yeast growth observed.

The spectral characteristics of the cyanine dye triazole conjugates (**25 - 27**) and alkyne intermediates (**22 – 24**) will be discussed together. The spectral properties collected are summarised in Table 4.12 and 4.13. It is worth noting that the click intermediates compounds and the cyanine dye azide conjugates showed higher fluorescence quantum yield when compared ICG and IR-820 indicating their suitability as potential labelling agents. Also the spectral characteristics of the intermediate cyanine dyes and the cyanine dye azide conjugates are similar because the modification occurs at the nitrogen of the benzothiazole, which is too far away from the chromophore to exert any influence on the spectral characteristics of the compounds.

The growth inhibition data is interesting denoting that the trizaoles are less cytotoxic towards *S. pombe* in comparison to the linear alkyl chains and this seen when comparing **25** (6.38 μM) with **23** (1.05 μM) and **27** (6.27 μM) with **27** (4.70 μM) respectively (Tables 4.12, 4.13 and Figures 4.13, 4.14). This in part is understandable as the linear alkyl chains have the ability to penetrate and subsequently disrupt the lipid membrane [241].
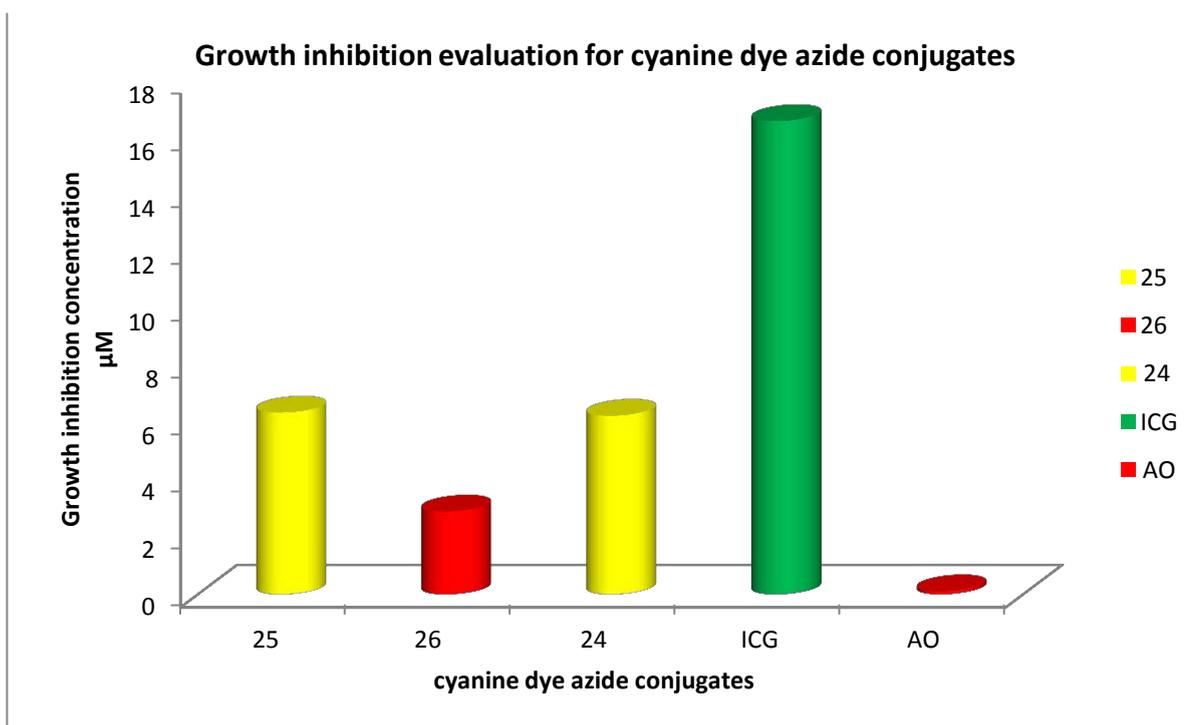
Figure 4.14: Growth inhibition evaluation for cyanine dye azide conjugates. Green bars indicate growth inhibition was comparable to ICG. Red bars indicate growth was comparable to AO. Yellow bar indicate growth in the intermediate range.
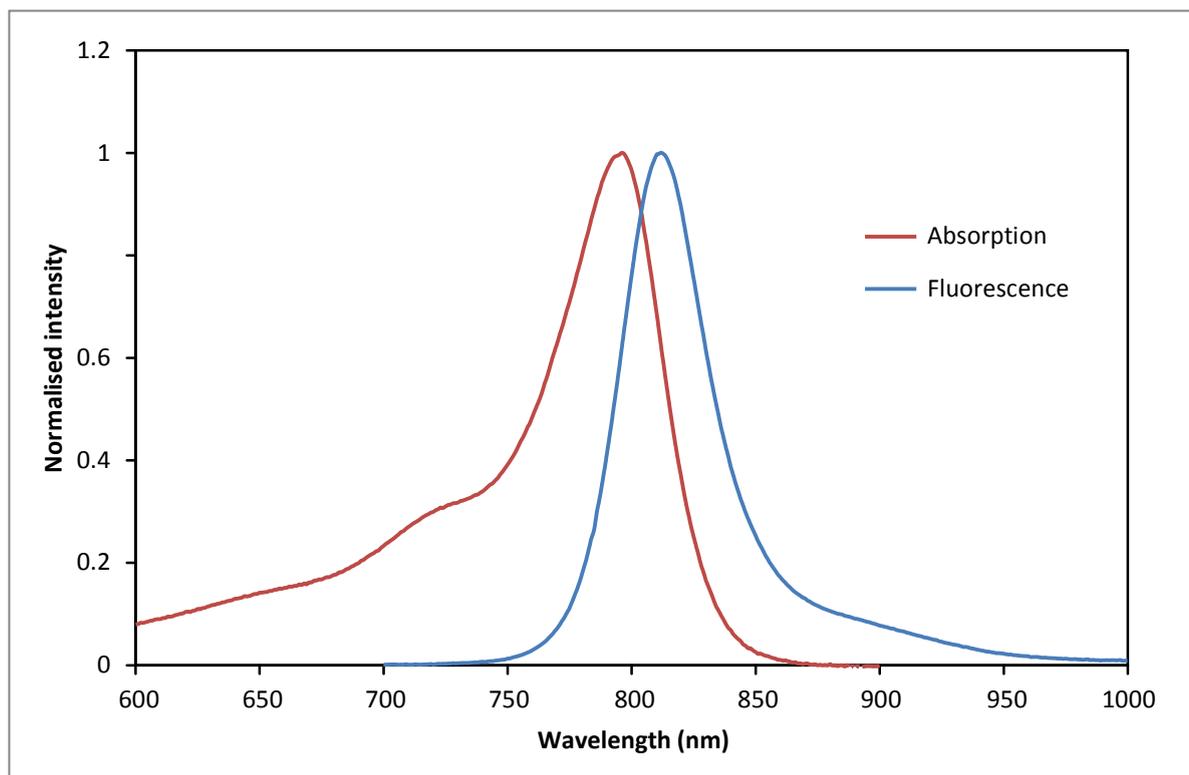
Figure 4.15:**7b** in MeOH excited at 785 nm showing absorption and emission spectra with Stokes fluorescence.

Finally the dependence of the spectral properties of these dyes on various solvents was also investigated in order to investigate their performances in different solvent environments (Table 4.14).

Table 4.14: **7a** in various solvent.
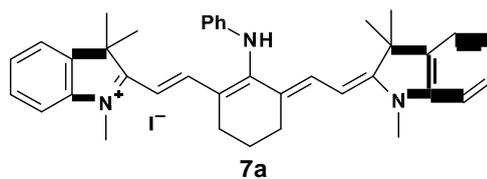
Dye	Solvent	Absorption λ_{Amax} (nm)	Fluorescence Emission λ_{Amax} (nm)	Fluorescence quantum yield Φ	Stoke Shift (nm)
7a	Methanol	736	786	0.030	50
7a	DMSO	757	799	0.023	42
7a	Propan-1-ol	739	791	0.053	52
7a	Chloroform	754	799	0.156	45
7a	Dichloromethane	757	798	0.184	41

Based on the results (Table 4.14) obtained from the analysis, it is difficult to determine which of the solvent properties such as polarity, viscosity and hydrogen bonding has the most dominant effect on the spectral properties of the dye. Several conflicting results on the effects of different solvent on the spectral properties of heptamine cyanine dyes have already been reported in the literature [242, 240]. The most consistent data from the results obtained from this experiment indicates that the quantum yield of the dyes increased from polar solvents to non-polar solvents in the order DMSO<methanol<propan-1-ol<chloroform<dichloromethane. It should be noted that the values of ICG and IR-820 can be found in the Appendix (*Journal of sulfur chemistry*).

Conclusion and Future work.

The use of molecular probes for detecting and quantifying biomolecules is an area of emerging interest and importance [1]. Using dyes which fluoresce in the visible region for this type of research can be challenging and can cause considerable problems, such as auto-fluorescence of a sample matrix [81]. The use of near-infrared (NIR) probes (700 – 1000 nm) has generated a vast array of interest, as these can be efficiently used to visualise and investigate *in-vivo* molecular targets as most tissues generate little NIR fluorescence [23]. Also probes operating in the NIR region offer deeper tissue penetration and low toxicity, which is beneficial for cell and tissue imaging [23]. Furthermore, the instrumentation techniques used for NIR Imaging is compact and relatively inexpensive; this is advantageous in terms of clinical applications [13].

Motivated by this, the synthesis, photophysical properties and growth inhibition characteristics of a series of structurally related non-targeting NIR heptamethine cyanine dyes have been investigated. The study first began with the synthesis of a series of heptamethine cyanine dyes (rigid and linear heptamethine cyanine dyes). The synthesised dyes were characterised by ^{1}H, ^{13}C NMR, ESI, HRMS, IR, UV and melting point analysis.   The rigid indolium heptamethine cyanine dyes (**4 a-g** and **6 a-g**) were further functionalised by substitution of their meso-chlorine atom with an aniline molecule with the aim of improving their photophysical and growth inhibitory properties. However, in contrast to the indolium rigid heptamethine cyanine dyes, the benzothiazole dyes (**5 a-g**) were inert to treatment with aniline under various experimental conditions. Therefore the synthesis of the functionalised benzothiazole dyes was discontinued. The synthesis of the linear heptamethine dyes is in itself significant, this *in-situ* cascade reaction is a modification of the Zincke reaction [218] and provides an elegant approach to the linear dyes which can be tailored to develop more structurally sophisticated cyanine dyes. The impact of the novel approach for the synthesis of the linear dyes (**9 a-g**, **10 a-g** and **11 a-g**) and linear substituted heptamethine cyanine dyes (**12-21**) is timely, highlighting the development of cost effective molecular probes with

enhanced photo-physical and toxicity characteristics when compared against the current clinical standards ICG and IR-820 [265].

The synthesis of NIR benzothiazole heptamethine cyanine dye azide conjugates (**25-27**) using the Cu(I)-catalyzed azide-alkyne cycloaddition (CuAAC) provides a prototype for the design of future long-wavelength absorbing cyanine dyes conjugated to biomolecules. Also, this further illustrates the structural versatility and applicability of the dyes synthesised in this research project.

With the increasing importance of NIR heptamethine cyanine dyes in biological imaging applications, dyes with unique structural features and improved spectral properties are desired. Several approaches have been attempted to improve the overall photophysical properties (absorption and emission wavelengths, fluorescence quantum yields, Stokes shifts and effect of solvent polarity) of heptamethine cyanine dyes [226]. To this end, the photophysical properties of the dyes synthesised in this research project were evaluated and compared against those of the standard fluorophores ICG and IR-820. Structures of the heptamethine cyanine dyes investigated were broadly categorised into nine main groups based on their heterocyclic ring system and the substitution pattern of their polymethine chain; indolium-based rigid heptamethine cyanine dyes (**4 a-g**), rigid benzothiazole heptamethine cyanine dyes (**5 a-g**), rigid benzo[e] heptamethine cyanine dyes (**6 a-g**), functionalised indolium-based rigid heptamethine cyanine dyes (**7 a- g** and **8 a-e**), indolium-based linear heptamethine cyanine dyes (**9 a-g**), linear benzothiazole heptamethine cyanine dyes (**10 a-g**), linear benzo[e] heptamethine cyanine dyes (**11 a-g**), substituted linear heptamethine cyanine dyes (**12-21**), and heptamethine cyanine dye-azide conjugates (**25-27**). On evaluation it was discovered that all the dyes exhibited absorption wavelength in the NIR region (700 -900 nm) indicating their suitability for deep tissue imaging applications. The absorption and emission wavelengths, fluorescence quantum yields and Stokes shifts for the synthesised dyes showed no significant change in terms of the substituting group on the indolium nitrogen. These observations could be attributed to the fact that the *N*-donor and *N*-acceptor substituting groups are too far away from the chromophore and as such have very little influence on the spectroscopic properties of the dyes. However, the quantum yields studies showed that the dyes bearing the benzothiazole moiety had higher quantum yield values when compared with the linear dyes bearing the 3,3-dimethylindolenine moiety.

145

Furthermore, it was also noted that the benzothaizole dyes in (**5 a-g** and **10 a**-**g**) demonstrated an approximate 2.5 to 3-fold increase in quantum yield when compared with IR-820 and ICG. These excellent quantum yield values indicate the suitability of the benzothiazole dyes as potential candidates for molecular imaging applications in clinical research [266]. It was also discovered that rigidification of the polymethine chain reduces the quantum yields by approximately 50%, and this was confirmed by comparing the rigid heptamethine dyes with the linear dyes. Dyes (**7 a-g**, **8 a-e**) bearing the aniline moiety on their polymethine chain gave the highest Stokes shift values. The observed increase could be as a result of the substitution of the *meso*-chlorine atom with an aromatic moiety, resulting in a large structural change between the ground and the excited singlet state of the dyes. The increase in Stokes shifts is desired for this type of research since it renders the amine-substituted cyanine dyes useful as NIR platforms for the development of a wide range of feature targeting and non-targeting fluorescent probes [203].

Apart from the photophysical characteristics of the dyes, the growth inhibition and Log*P* properties are important characteristics which determine the practical use of these fluorophores in living cells. The effect of the synthesised dyes on cell growth was compared to ICG**,** IR-820 and AO. The results obtained in this research indicated that most of the dyes which exhibited no growth inhibition effects were dyes bearing the sulfonic acid group on their *N*-donor and *N*-acceptor system. Most of the dyes that exhibited growth inhibition were the dyes bearing the alkyl or benzyl group at their *N*-donor and *N*-acceptor system. It was therefore postulated that the growth inhibition effect of these dyes could be attributed to the nature of substituent on the *N*-donor and *N*-acceptor system. Further support for these observations was seen using a virtual method, the log*P*. The presence of the sulfonic acid group on the dyes tends to increase their aqueous solubility and reduce their growth inhibition characteristics, possibly through reduced membrane permeability and cellular uptake. The dyes bearing the sulfonic acid groups are structurally very similar to ICG, IR820. The presence of the alkyl group tends to reduce the solubility and increase the growth inhibitory characteristic of the dyes due to their lipophilic characteristics.

In conclusion, the results from this research work offer a strong platform for the development of a wide range of future targeting and non-targeting fluorescent probes. Also the dyes reported in this research show huge potential as new fluorescent probes for potential clinical

applications. In particular the benzothiazole dyes (**10f**, **10g**, **16**, **17**, **18**) (Figure 5.1) bearing the sulfonic acid group on their heterocyclic ring systems manifested the most promising potentials in terms of their photophysical and growth inhibition properties. Dyes **16** and **17** in particular offer the opportunity to carry out more synthetic modifications, which can be tailored to develop more structurally sophisticated dyes.
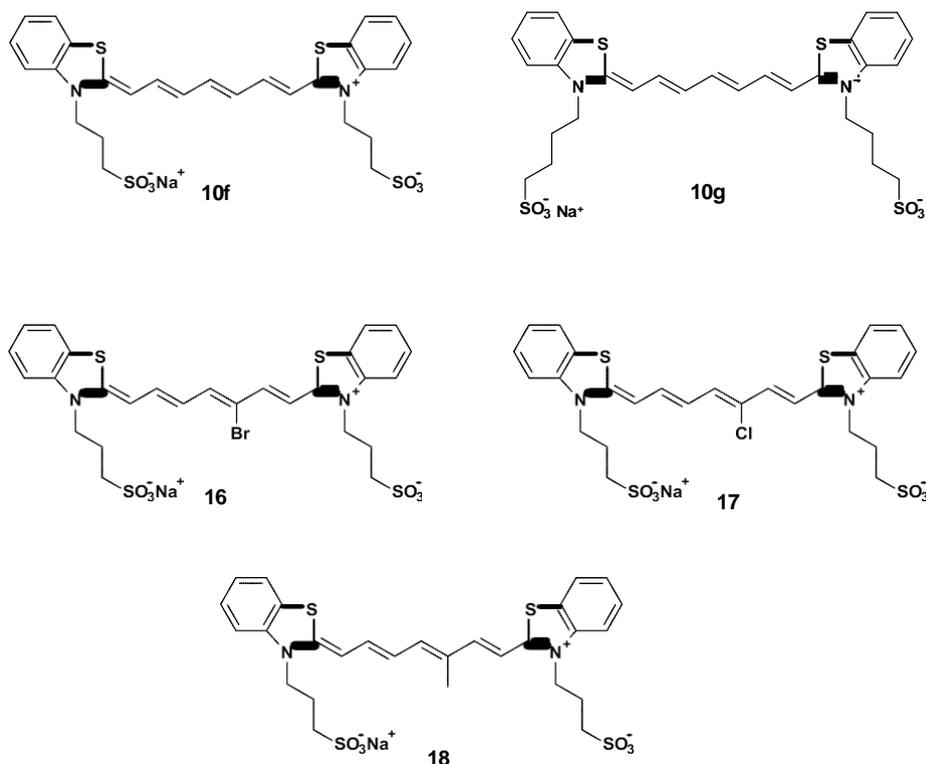
Figure 5.1: Promising benzothiazole heptamethine cyanine dyes.

In the future, more detailed assays involving yeast cells should be performed to fully characterise more biological properties of these dyes. This could be extended into mammalian cells lines. Furthermore, *in vivo* studies investigating potential targeting mechanisms such as aptamers and antibodies should be performed. Finally, the dyes should also be investigated as potential multifunctional agents for both molecular imaging and PDT applications.

Experimental

^{1}H and ^{13}C NMR spectra were measured on either a Bruker DPX 250 MHz, Bruker Avance-III 300 MHz or a Bruker Avance 400 MHz spectrometer at ambient temperature with tetramethylsilane (TMS) as internal standard for ^{1}H NMR and deuteriochloroform (CDCl$_3$, δ_C 77.23 ppm) and deuteriodimethylsulfoxide (d$_6$-DMSO, δ_C 39.51 ppm) for ^{13}C NMR unless otherwise stated. All chemical shifts are quoted in δ (ppm) and coupling constants in Hertz (Hz) using the high frequency positive convention. Coupling constants were rounded up into whole numbers. Low and high resolution mass spectra were obtained using electrospray ionization (ESI) mass spectrometry on a hybrid linear ion trap-fourier transform mass spectrometer. Accurate mass measurements were carried out for novel compounds by EPSRC National mass spectrometry service research group using the Thermofisher LTQ Orbitrap XL. Infrared spectra were recorded on a Specac ATR with a He Ne -633 nm laser. Stock solutions for UV-Vis spectroscopy of dyes were prepared in methanol. The absorbance and fluorescence spectra of each of the dyes were measured sequentially to reduce photobleaching and solubility issues. The fluorescence quantum yields of the dyes were calculated using the relative method i.e. integrated fluorescence peak area versus fraction of light absorbed at the excitation wavelength were plotted for both the standards and cyanine dyes [175]. Fluorescence quantum yields (φ) were measured using a fluorimeter based on an Innovative Photonic Solutions 785 nm diode laser, operating with a power output of 8 mW, an Andor Shamrock SR-303i spectrograph and an Andor iDus CCD detector (model DU420A-BR-DD). Fluorescence was detected at right angles without any filters. The spectral response of the system was corrected following the method outlined by Kosch and coworkers [267]. Absorbance values (A) of solutions at 785 nm were measured using a Perkin Elmer Lambda 25 spectrophotometer. Corrected fluorescence spectra for a series of solutions of increasing concentration were rescaled in energy and the integrated intensity was plotted

versus 1-10-A, with A (785 nm) ≤ 0.1. The quantum yields were obtained from the relative slopes of such plots compared with that from solutions of ICG in dimethyl sulfoxide. For determinations in different solvents, the refractive index (n2) correction was applied. Log*P* values were obtained using the virtual method (the base 10 logarithm) [268]. Thin Layer Chromatography (TLC) was carried out on Machery-Nagel polygramSil/G/UV$_{254}$ pre-coated plates. Melting point (m.p) analysis was carried out using a Griffin melting point apparatus. All chemicals were purchased from commercial sources and used without further purification.

1,2,3,3-Tetramethyl-3H-indol-1-ium iodide (1a) was synthesised according to a reported procedure [243].
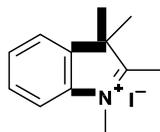
2,3,3-Trimethylindolenine (1.00 g, 6.30 mmol) was dissolved in iodomethane (10.0 mL, 168 mmol) with constant stirring, and the solution was heated under reflux for 17 h. The precipitate produced was filtered under suction, washed with *n*-hexane and dried *in vacuo* to give the product **1a** (1.12 g, 58%) as a pink solid; m.p. 257-259 °C, literature m.p. 258 °C [244]: ^{1}H NMR (d$_6$-DMSO, 250 MHz) δ 7.91-7.84 (m, 1H, Ar-H̲), 7.83-7.74 (m, 1H, Ar-H̲), 7.62-7.53 (m, 2H, Ar-H̲), 3.92 (s, 3H, N-CH̲$_3$), 2.71 (s, 3H, N-C-CH̲$_3$), 1.47 (s, 6H, C-(CH̲$_3$)$_2$). ^{13}C NMR (d$_6$-DMSO, 62.8 MHz) δ 195.2, 142.3, 142.1, 122.9, 122.3, 121.9, 118.3, 57.2, 38.4, 22.2, 15.1. IR (ATR) 2965, 1630, 1481, 938, 776, 588 cm^{-1}. MS (ESI) m/z: 174 [M]$^+$.

1-Ethyl-2,3,3-trimethyl-3H-indol-1-ium iodide (1b).
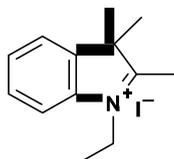
1b was synthesised as for **1a** using 2,3,3-trimethylindolenine (1.00 g, 6.30 mmol) and iodoethane (13.0 mL, 168 mmol) to give the product **1b** (1.70 g, 86%) as a pink solid; m.p. 228-230 °C, literature m.p. 226-228 °C [245] : ^{1}H NMR (d$_6$-DMSO, 250 MHz) δ 7.69-7.65 (m, 1H, Ar-H̲), 7.56- 7.53(m, 1H, Ar-H̲), 7.35-6.92 (m, 2H, Ar-H̲), 4.15 (q, *J*=8.0 Hz, 2H, N-CH̲$_2$-CH$_3$), 2.51 (s, 3H, N-C-CH̲$_3$), 1.31 (s, 6H, C-(CH̲$_3$)$_2$), 1.12 (t, *J*=8.0 Hz, 3H, CH$_2$-CH̲$_3$). ^{13}C NMR (d$_6$-DMSO, 62.8 MHz) δ 196.0, 141.9, 140.7, 129.37, 128.9, 123.5, 115.2, 54.1, 43.0, 21.8, 13.7, 12.6. IR (ATR) 2969, 1630, 1459, 1364, 1129, 928, 772, 583 cm^{-1}. MS (ESI) m/z: 188 [M]$^+$.

2,3,3-Trimethyl-1-propyl-3H-indol-1-ium iodide (1c).
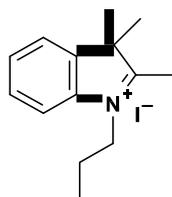
1c was synthesised as for **1a** using 2,3,3-trimethylindolenine (1.00 g, 6.30 mmol) and iodopropane (13.0 mL, 168 mmol) to give the product **1c** (1.95 g, 94%) as a brown solid; m.p. 131-133 °C, literature m.p. 159 °C [246]: ^{1}H NMR (d$_6$-DMSO, 400 MHz) δ 8.02-7.99 (m, 1H, Ar-$\underline{H}$), 7.87-7.81 (m, 1H, Ar-$\underline{H}$), 7.64-7.58 (m, 2H, Ar-$\underline{H}$), 4.48 (t, *J*=6.0 Hz, 2H, N-C$\underline{H}_2$-CH$_2$), 2.50 (s, 3H, N-C-C$\underline{H}_3$), 1.92 (sex, *J*=6.0 Hz, 2H, CH$_2$-C$\underline{H}_2$-CH$_3$), 1.55 (s, 6H, C-(C$\underline{H}_3$)$_2$), 1.02 (t, *J*=6.0 Hz, 3H, CH$_2$-C$\underline{H}_3$). ^{13}C NMR (75.4 MHz, CDCl$_3$): δ 195.7, 141.5, 140.8, 130.2, 129.5, 123.5, 115.5, 54.7, 51.2, 23.3, 21.6, 17.1, 11.4. IR (ATR) 2970, 1641, 1456, 1367, 1132, 920, 768, 572 cm^{-1}. MS (ESI) m/z: 203 [M]$^+$.

1-Butyl-2,3,3-trimethyl-3H-indol-1-ium iodide (1d).
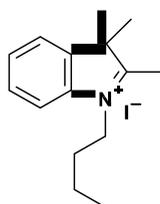
1d was synthesised as for **1a** using 2,3,3-trimethylindolenine (5.00 g, 31.4 mmol) and iodobutane (20.0 mL,168 mmol) to give the product **1d** (7.13 g, 67%) as a brown solid; m.p. 139-141 °C, literature m.p. 136 °C [246]: ^{1}H NMR (d$_6$-DMSO, 300 MHz) δ 8.03 (d, *J*=9.0 Hz, 1H, Ar-$\underline{H}$), 7.88 (d, *J*=9.0 Hz, 1H, Ar-$\underline{H}$), 7.63-7.60 (m, 2H, Ar-$\underline{H}$), 4.50 (t, *J*=6.0 Hz, 2H, N-C$\underline{H}_2$-CH$_2$), 2.89 (s, 3H, N-C-C$\underline{H}_3$), 1.85 (quin, *J*=6.0 Hz, 2H, N-CH$_2$-C$\underline{H}_2$-CH$_2$), 1.55 (s, 6H, C-(C$\underline{H}_3$)$_2$), 1.47 (sex, *J*=6.0 Hz, 2H, CH$_2$-C$\underline{H}_2$-CH$_3$), 0.95 (t, *J*=6.0 Hz, 3H, CH$_2$-C$\underline{H}_3$). ^{13}C NMR (75.4 MHz, CDCl$_3$): δ 196.8, 144.1, 142.3, 141.5, 129.8, 129.4, 124.0, 116.0, 54.6, 29.8, 22.5, 19.8, 14.9, 14.1. IR (ATR) 2862, 1593, 1458, 1371, 1296, 925, 776, 596 cm^{-1}. MS (ESI) m/z: 216 [M]$^+$.

1-Benzyl-2,3,3-trimethyl-3H-indol-1-ium bromide (1k) was synthesised according to a reported procedure [247].
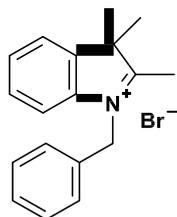
Benzyl bromide (0.80 mL, 6.80 mmol) dissolved in acetonitrile (20.0 mL) was stirred with constant heating under reflux. 2,3,3-trimethylindolenine (1.00 g, 6.30 mmol) was dissolved in acetonitrile (20.0 mL) and added drop wise to the reaction mixture from a dropping funnel. The reaction was stirred for 39 h with constant heating. The precipitate produced was filtered under suction, washed with *n*-hexane and dried *in vacuo* to give the product **1k** (1.65 g, 77%) as a red hygroscopic solid; m.p. 226-228 °C. ^{1}H NMR (d$_6$-DMSO, 250 MHz) δ 7.89 (d, *J*=7.0 Hz, 1H, Ar-H̲), 7.84 (d, *J*=7.0 Hz, 1H, Ar-H̲), 7.67-7.59 (m, 2H, Ar-H̲), 7.45-7.38 (m, 5H, Ar-H), 5.87 (s, 2H, N-CH̲$_2$), 3.59 (s, 3H, N-C-CH̲$_3$), 1.55 (s, 6H C-(CH̲$_3$)$_2$). ^{13}C NMR (d$_6$-DMSO, 62.8 MHz) δ 198.7, 142.5, 141.6, 132.7, 130.1, 129.5, 129.3, 128.1, 124.2, 116.5, 55.1, 51.2, 22.7, 15.1, 9.8. IR (ATR) 2969, 1603, 1454, 931, 741, 701, 567 cm^{-1}. MS (ESI) m/z: 250 [M]$^+$.

2,3,3-Trimethyl-1-(3-sulfonatopropyl)-3H-indol-1-ium (1l) was synthesised according to a reported procedure [248].
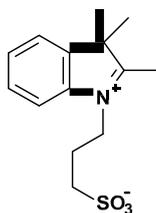
To a solution of 2,3,3-trimethylindolenine (9.92 g, 62.3 mmol) in toluene (50 mL) was added 1,3-propanesultone (11.4 g, 93.5 mmol) with constant stirring, and the solution was heated under reflux for 18 h. The precipitate produced was filtered under suction, washed with toluene and dried *in vacuo* to give the product **1l** (11.0 g, 63%) as a purple solid; m.p. 241-243 °C. ^{1}H NMR (d$_6$-DMSO, 400 MHz) δ 8.47 (d, *J*=7.0 Hz, 1H, Ar-H̲), 8.25 (d, *J*=8.0 Hz,

1H, Ar-<u>H</u>), 8.04-7.99 (m, 2H, Ar-<u>H</u>), 4.53 (t, *J*=7.0 Hz, 2H, N-C<u>H</u>$_2$-CH$_2$), 3.01-2.95 (m, 2H, C<u>H</u>$_2$-SO$_3$), 2.73 (s, 3H, N-C-C<u>H</u>$_3$), 2.29-2.21 (m, 2H, CH$_2$-C<u>H</u>$_2$-CH$_2$), 1.45 (s, 6H, C-(C<u>H</u>$_3$)$_2$). ^{13}C NMR (d$_6$- DMSO, 75.4 MHz) δ 207.08, 177.75, 177.72, 141.35, 129.61, 128.51, 125.01, 117.31, 47.80, 47.78, 31.17, 24.72, 17.21. IR (ATR) 2817, 1566, 1444, 1143, 1012, 770, 717, 662 cm^{-1}. MS (ESI) m/z: 282 [M+H]$^+$.

2,3,3-Trimethyl-1-(4-sulfonatobutyl)-3H-indol-1-ium (1m).
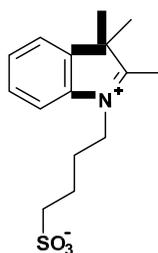
1m was synthesised as for **1l** using 2,3,3-trimethylindolenine (9.92 g, 62.3 mmol) and 1,4-butanesultone (12.7 g, 93.5 mmol) to give the product **1m** (9.33 g, 50%) as a white solid; m.p. 241-243 °C. ^{1}H NMR (D$_2$O, 400 MHz) δ 7.68 (d, *J*=6.0 Hz, 1H, Ar-<u>H</u>), 7.62 (d, *J*=6.0 Hz, 1H, Ar-<u>H</u>), 7.52-7.41 (m, 2H, Ar-<u>H</u>), 4.40 (t, *J*=7.0 Hz, 2H, N-C<u>H</u>$_2$), 2.85 (t, *J*=7.0 Hz, 2H, -CH$_2$-C<u>H</u>$_2$-SO$_3$), 2.70 (s, 3H, N-C-C<u>H</u>$_3$), 2.00-1.97 (m, 2H, N-CH$_2$-C<u>H</u>$_2$-CH$_2$), 1.77-1.69 (m, 2H, CH$_2$-C<u>H</u>$_2$-CH$_2$-SO$_3$), 1.44 (s, 6H, C-(C<u>H</u>$_3$)$_2$). ^{13}C NMR (D$_2$O, 62.8 MHz) δ 196.4, 141.7, 140.8, 129.8, 129.0, 123.3, 115.0, 54.4, 49.9, 47.3, 25.3, 21.6, 21.4, 1112. IR (ATR) 2857, 1560, 1460, 1183, 1032, 780, 727, 666 cm^{-1}. MS (ESI) m/z: 296 [M+H]$^+$.

2-Methyl-3-(methyl)-benzothiazolium iodide (2a) was synthesised according to a reported procedure [249].
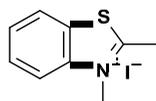
To a solution of 2-methylbenzothiazole (0.94 g, 6.30 mmol) in toluene (50.0 mL), was added iodomethane (10.0 mL, 168 mmol) with constant stirring, and the solution was heated under reflux for 18 h. The precipitate produced was filtered under suction, washed with *n*-hexane and dried *in vacuo* to give the product **2a** (1.64 g, 87%) as a white solid; m.p. 227-229 °C,

literature m.p. 225-226 °C [250]: ^{1}H NMR (d$_6$-DMSO, 250 MHz) δ 8.46 (d, *J*=8.0 Hz, 1H, Ar-<u>H</u>), 8.31 (d, *J*=9.0 Hz, 1H, Ar-<u>H</u>), 7.96 (t, *J*=9.0 Hz, 1H, Ar-<u>H</u>), 7.81 (t, *J*=8.0 Hz, 1H, Ar-<u>H</u>), 4.23 (s, 3H, N-C<u>H</u>$_3$), 3.11 (s, 3H, N-C-C<u>H</u>$_3$). ^{13}C NMR (d$_6$-DMSO, 62.8 MHz) δ 177.2, 141.5, 129.2, 128.6, 128.0, 124.4, 116.7, 36.1, 17.1. IR (ATR) 2965, 1548, 1441, 1336, 1210, 1131, 1011, 764, 717, 579 cm^{-1}. MS (ESI) m/z: 164 [M]$^+$.

2-Methyl-3-(ethyl)-benzothiazolium iodide (2b).
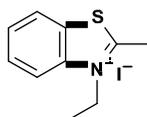
2b was synthesised as for **2a** using 2-methylbenzothiazole (0.94 g, 6.30 mmol) and iodoethane (13.5 mL, 168 mmol) to give the product **2b** (0.84 g, 41%) as a white solid; m.p. 196-200 °C, literature m.p. 198-200 °C [251]: ^{1}H NMR (d$_6$-DMSO, 250 MHz) δ 8.49 (d, *J*=7.0 Hz, 1H, Ar-<u>H</u>), 8.40 (d, *J*=7.0 Hz, 1H, Ar-<u>H</u>), 7.83 (t, *J*=8.0 Hz, 1H, Ar-<u>H</u>), 7.79 (t, *J*=7.0 Hz, 1H, Ar-<u>H</u>), 4.75 (t, *J*=7.0 Hz, 2H, N-C<u>H</u>$_2$-CH$_3$), 3.19 (s, 3H, N-C-C<u>H</u>$_3$), 1.45 (t, *J*=7.0 Hz, 3H, C-C<u>H</u>$_3$). ^{13}C NMR (d$_6$-DMSO, 62.8 MHz) δ 176.8, 140.4, 129.3, 129.1, 128.1, 124.7, 116.6, 44.7, 16.7, 13.2. IR (ATR) 2912, 1613, 1513, 1445, 1329, 1270, 1203, 1100, 777, 713, 670 cm^{-1}. MS (ESI) m/z: 178 [M]$^+$.

2-Methyl-3-(propyl)-benzothiazolium iodide (2c).
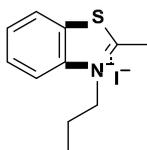
2c was synthesised as for **2a** using 2-methylbenzothiazole (0.94 g, 6.30 mmol) and iodopropane (13.5 mL, 168 mmol) to give the product **2c** (1.62 g, 81%) as a white solid; m.p. 199-201 °C: ^{1}H NMR (d$_6$-DMSO, 400 MHz) δ 8.51 (d, *J*=6.0 Hz, 1H, Ar-<u>H</u>), 8.42 (d, *J*=6.0 Hz, 1H, Ar-<u>H</u>), 7.93 (t, *J*=9.0 Hz, 1H, Ar-<u>H</u>), 7.84 (t, *J*=6.0 Hz, 1H, Ar-<u>H</u>), 4.74 (t, *J*=6.0 Hz, 2H, N-C<u>H</u>$_2$- CH$_2$), 3.25 (s, 3H, N-C-C<u>H</u>$_3$), 1.93 (sex, *J*=6.0 Hz, 2H, CH$_2$-C<u>H</u>$_2$-CH$_3$), 1.05 (t, *J*=6.0 Hz, 3H, CH$_2$-C<u>H</u>$_3$). ^{13}C NMR (d$_6$-DMSO, 75.4 MHz): δ 177.6, 141.3, 129.8, 129.5,

128.5, 125.1, 117.4, 50.8, 21.8, 17.3, 11.2. IR (ATR) 2919, 1607, 1518, 1449 cm^{-1}. MS (ESI) m/z: 192.21 [M]$^{+}$.

2-Methyl-3-(butyl)-benzothiazolium iodide (2d).
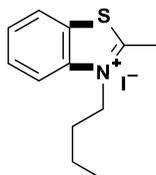
2d was synthesised as for **2a** using 2-methylbenzothiazole (5.00 g, 33.5 mmol) and 1-iodobutane (20.0 mL, 175 mmol) to give the product **2d** (3.63 g, 33%) as a cream solid; m.p. 189-191 °C, literature m.p. 186-187 °C [252]: ^{1}H NMR (d$_6$-DMSO, 300 MHz) δ 8.48 (d, *J*=6.0 Hz, 1H, Ar-H), 8.37 (d, *J*=6.0 Hz, 1H, Ar-H), 7.92 (t, *J*=6.0 Hz, 1H, Ar-H), 7.83 (t, *J*=6.0 Hz, 1H, Ar-H), 4.74 (t, *J*=6.0 Hz, 2H, N-CH$_2$-CH$_2$), 3.23 (s, 3H, N-C-CH$_3$), 1.86-1.71 (m, 2H, N-CH$_2$-CH$_2$-CH$_2$), 1.49-1.31 (m, 2H, N-CH$_2$-CH$_2$-CH$_2$), 0.96 (t, *J*=9.0 Hz, 3H, CH$_2$-CH$_3$). ^{13}C NMR (75.4 MHz, CDCl$_3$): δ 177.5, 141.3, 129.8, 129.5, 128.5, 125.1, 117.3, 49.5, 30.2, 19.7, 17.4, 14.0. IR (ATR) 2951, 1577, 1439, 1378, 1280, 948, 764 cm^{-1}. MS (ESI) m/z: 206.09 [M]$^{+}$.

2-Methyl-3-(2-benzyl)-benzothiazolium (2k) [245].
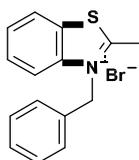
To a solution of 2-methylbenzothiazole (0.94 g, 6.30 mmol) in toluene (20.0 mL) was added benzyl bromide (1.16 g, 93.5 mmol) with constant stirring, and the solution was heated under reflux for 36 h. The precipitate produced was filtered under suction, washed with *n*-hexane and dried *in vacuo* to give the product **2k** (0.12 g, 7%) as a pink solid; m.p. 94-96 °C, literature m.p. 93 °C [253]: ^{1}H NMR (d$_6$-DMSO, 250 MHz) δ 8.47 (d, *J*=7.0 Hz, 1H, Ar-H), 8.12 (d, *J*=7.0 Hz, 1H, Ar-H), 7.45-7.40 (m, 2H, Ar-H), 7.32-7.11 (m, 5H, Ar-H), 6.12 (s, 2H, CH$_2$-Ph), 3.21 (s, 3H, C-CH$_3$). ^{13}C NMR (d$_6$-DMSO, 62.8 MHz) δ 186.4, 178.4, 140.9, 132.7,

129.5, 129.2, 128.1, 127.5, 126.9, 124.8, 117.0, 51.8, 17.2. IR (ATR) 2938, 1578, 1455, 1339, 1021, 808, 748, 577 cm^{-1}. MS (ESI) m/z: 240 [M]$^+$.

2-Methyl-3-(4-sulfopropyl)-benzothiazolium (2l).
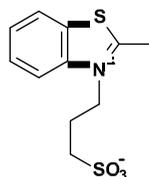
2l was synthesised as for **2a** using 2-methylbenzothiazole (9.30 g, 62.3 mmol), and 1,3-propanesultone (11.4 g, 93.5 mmol) to give the product **2l** (15.0 g, 91%) as a white solid; m.p. 258-260 °C, literature m.p. 276-278 °C [254]: ^{1}H NMR (d$_6$-DMSO, 250 MHz) δ 8.23-7.80 (m, 2H, Ar-$\underline{H}$), 7.28 (t, *J*=7.0 Hz, 1H, Ar-$\underline{H}$), 7.67 (t, *J*=7.0 Hz, 1H, Ar-$\underline{H}$), 4.72 (t, *J*=7.0 Hz, 2H, N-C$\underline{H}_2$), 3.08 (s, 3H, N-C-C$\underline{H}_3$), 3.02 (t, *J*=7.0 Hz, 2H, CH$_2$-C$\underline{H}_2$-SO$_3$), 2.28-2.20 (m, 2H, N-CH$_2$-C$\underline{H}_2$). ^{13}C NMR (D$_2$O, 75.4 MHz) δ 176.2, 140.7, 129.6, 128.8, 128.4, 123.6, 116.1, 47.6, 47.2, 23.0, 16.1. IR (ATR) 2917, 1511, 1413, 1353, 1263, 1032, 756, 663 cm^{-1}. MS (ESI) m/z: 272 [M+H]$^+$.

2-Methyl-3-(4-sulfobutyl)-benzothiazolium (2m).
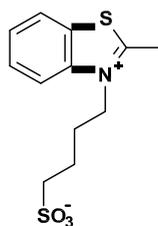
2m was synthesised as for **2a** using 2-methylbenzothiazole (9.30 g, 62.3 mmol), and 1,4-butanesultone (12.7 g, 93.5 mmol) to give the product **2m** (9.24 g, 51%) as a white solid; m.p. 258-260 °C, literature m.p. 294 °C [255]: ^{1}H NMR (d$_6$-DMSO, 300 MHz): δ 8.42 (d, *J*=9.0 Hz, 2H, Ar-$\underline{H}$), 7.87 (t, *J*=9.0 Hz, 1H, Ar-$\underline{H}$), 7.78 (t, *J*=9.0 Hz, 1H, Ar-$\underline{H}$), 4.91 (t, *J*=9.0 Hz, 2H, N-C$\underline{H}_2$), 3.20 (s, 3H, N-C-C$\underline{H}_3$), 3.16 (br s, 2H, C-C$\underline{H}_2$), 2.67 (t, *J*=6.0 Hz, 2H, C-C$\underline{H}_2$) 2.17 (q, *J*=9.0 Hz, 2H, C-C$\underline{H}_2$). ^{13}C NMR (D$_2$O, 62.8 MHz) δ 175.9, 140.9, 129.6, 128.9, 128.4, 123.6, 116.4, 50.0, 48.9, 26.3, 21.4, 16.2. IR (ATR) 2947, 1523, 1443, 1343, 1283, 1175, 1032, 796, 777, 714, 683 cm^{-1}. MS (ESI) m/z: 286 [M+H]$^+$.

1,1,2,3-Tetramethyl-1H-benzo[e]indol-3-ium iodide (3a) [243].
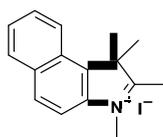
To a solution of 1,1,2-trimethyl-1*H*-benzo[e]indole (3.90 g, 18.6 mmol) in toluene (50.0 mL) was added iodomethane (20.0 mL, 481 mmol) with constant stirring, and the solution was heated under reflux for 18 h. The precipitate produced was filtered under suction, washed with *n*-hexane and dried *in vacuo* to give the product **3a** (6.03 g, 91%) as a brown solid; m.p. 230-232 °C, literature m.p. 221-223 °C [256]. ^{1}H NMR (d$_6$-DMSO, 300 MHz) δ 8.38 (d, *J*=9.0 Hz, 1H, Ar-<u>H</u>), 8.31 (d, *J*=9.0 Hz, 1H, Ar-<u>H</u>), 8.23 (d, *J*=9.0 Hz, 1H, Ar-<u>H</u>), 8.13 (d, *J*=9.0 Hz, 1H, Ar-<u>H</u>), 7.81-7.69 (m, 2H, Ar-<u>H</u>), 4.10 (s, 3H, N-C<u>H</u>$_3$), 2.88 (s, 3H, N-C-C<u>H</u>$_3$), 1.75 (s, 6H, C-(C<u>H</u>$_3$)$_2$). ^{13}C NMR (75.4 MHz, CDCl$_3$): δ 196.1, 139.9, 137.8, 136.9, 133.4, 130.9, 130.2, 129.3, 128.6, 127.5, 113.6, 55.7, 21.7, 21.5, 14.5. IR (ATR) 3012, 1635, 1464, 1391, 1225, 991, 895, 739 cm^{-1}. MS (ESI) m/z: 224 [M]$^+$.

3-Ethyl-1,1,2-Trimethyl-1H-benzo[e]indol-3-ium iodide (3b).
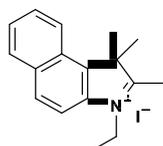
3b was synthesised as for **3a** using 1,1,2-trimethyl-1*H*-benzo[e]indole (3.90 g, 18.6 mmol) and iodoethane (30.0 mL, 375 mmol) to give the product **3b** (6.06 g, 89%) as a white solid; m.p. 215-217 °C, literature m.p. 213-218 °C [257]. ^{1}H NMR (d$_6$-DMSO, 300 MHz) δ 8.39 (d, *J*=6.0 Hz, 1H, Ar-<u>H</u>), 8.32 (d, *J*=9.0 Hz, 1H, Ar-<u>H</u>), 8.24 (d, *J*=9.0 Hz, 1H, Ar-<u>H</u>), 8.18 (d, *J*=9.0 Hz, 1H, Ar-<u>H</u>), 7.81-7.70 (m, 2H, Ar-<u>H</u>), 4.61 (q, *J*=7.0 Hz, 2H, N-C<u>H</u>$_2$-CH$_3$), 2.95 (s, 3H, N-C-C<u>H</u>$_3$), 1.76 (s, 6H, C-(C<u>H</u>$_3$)$_2$), 1.50 (t, *J*=7.0 Hz, 3H, CH$_2$-C<u>H</u>$_3$). ^{13}C NMR (75.4 MHz, CDCl$_3$): δ 196.4, 138.6, 137.4, 133.4, 131.1, 130.1, 128.8, 127.7, 125.5, 123.9, 113.6, 55.9, 43.8, 21.9, 14.1, 13.3. IR (ATR) 2978, 1583, 1461, 1388, 1215, 969, 874, 753 cm^{-1}. MS (ESI) m/z: 238 [M]$^+$.

1,1,2-Trimethyl-3-propyl-1H-benzo[e]indol-3-ium iodide (3c).
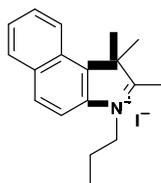
3c was synthesised as for **3a** using 1,1,2-trimethyl-1*H*-benzo[e]indole (3.90 g, 18.6 mmol) and iodopropane (30.0 mL, 309 mmol) to give the product **3c** (5.74 g, 81%) as a brown solid; m.p. 165-167 °C. ^{1}H NMR (d$_6$-DMSO, 300 MHz) δ 8.39 (d, *J*=6.0 Hz, 1H, Ar-$\underline{H}$), 8.31 (d, *J*=9.0 Hz, 1H, Ar-$\underline{H}$), 8.23-8.17 (m, 2H, Ar-$\underline{H}$), 7.85-7.70 (m, 2H, Ar-$\underline{H}$), 4.60 (t, *J*=6.0 Hz, 2H, N-C$\underline{H}_2$-CH$_2$), 2.97 (s, 3H, N-C-C$\underline{H}_3$), 1.97 (sex, *J*=6.0 Hz, 2H, N-CH$_2$-C$\underline{H}_2$), 1.77 (s, 6H, C-(C$\underline{H}_3$)$_2$), 1.05 (t, *J*=6.0 Hz, 3H, CH$_2$-C$\underline{H}_3$). ^{13}C NMR (75.4 MHz, CDCl$_3$): δ 196.9, 139.0, 137.8, 133.4, 130.1, 129.3, 128.8, 127.7, 125.7, 123.9, 113.8, 55.9, 44.0, 22.1, 21.5, 14.4, 11.2. IR (ATR) 2970, 2161, 2030, 1580, 1461, 1389, 1210, 1146, 993, 869, 742 cm^{-1}. MS (ESI) m/z: 252 [M]$^+$.

3-Butyl-1,1,2-trimethyl-1H-benzo[e]indol-3-ium iodide (3d).
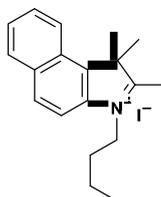
3d was synthesised as for **3a** using 1,1,2-trimethyl-1*H*-benzo[e]indole (3.90 g, 18.6 mmol) and iodobutane (30.0 mL, 263 mmol) to give the product **3d** (4.82 g, 66%) as a yellow brownish solid; m.p. 166-168 °C, literature m.p. 165-168 °C [258]. ^{1}H NMR (d$_6$-DMSO, 300 MHz) δ 8.25 (d, *J*=6.0 Hz, 1H, Ar-$\underline{H}$), 8.17 (d, *J*=9.0 Hz, 1H, Ar-$\underline{H}$), 8.09 (dd, *J*=6.0 Hz, 2H, Ar-$\underline{H}$), 7.67-7.55 (m, 2H, Ar-$\underline{H}$), 4.47 (t, *J*=6.0 Hz, 2H, N-C$\underline{H}_2$-CH$_2$), 2.82 (s, 3H, N-C-C$\underline{H}_3$), 1.76 (quin, *J*=6.0 Hz, 2H, N-CH$_2$-C$\underline{H}_2$-CH$_2$), 1.62 (s, 6H, C-(C$\underline{H}_3$)$_2$), 1.36 (sex, *J*=6.0 Hz, 2H, C$\underline{H}_2$-CH$_3$), 0.82 (t, *J*=6.0 Hz, 3H, CH$_2$-C$\underline{H}_3$). ^{13}C NMR (75.4 MHz, CDCl$_3$): δ 196.7, 139.9, 138.9, 137.4, 136.9, 133.4, 132.8, 131.1, 130.9, 130.1, 128.9, 55.9, 55.7, 48.2, 22.2, 21.7, 21.5, 14.1. IR (ATR) 2866, 1577, 1460, 1387, 1206, 1131, 992, 870, 752 cm^{-1}. MS (ESI) m/z: 266 [M]$^+$.

3-Benzyl-1,1,2-trimethyl-1H-benzo[e]indol-3-ium bromide (3e).
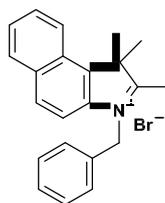
3e was synthesised as for **3a** using 1,1,2-trimethyl-1*H*-benzo[e]indole (3.90 g, 18.6 mmol) and benzyl bromide (3.10 mL, 25.2 mmol) to give the product **3e** (4.63 g, 65%) as a light yellow solid; m.p. 236-238 °C. ^{1}H NMR (d$_6$-DMSO, 300 MHz) δ 8.42 (d, *J*=6.0 Hz, 1H, Ar-H), 8.25 (d, *J*=9.0 Hz, 1H, Ar-H), 8.19-8.11 (m, 3H, Ar-H), 7.99 (d, *J*=9.0 Hz, 1H, Ar-H), 7.83-7.60 (m, 5H, Ar-H), 5.99 (s, 2H, N-CH$_2$-Ph), 3.09 (s, 3H, N-C-CH$_3$), 1.75 (s, 6H, C-(CH$_3$)$_2$). IR (ATR) 2965, 1609, 1459, 929, 748, 712, 560 cm^{-1}. MS (ESI) m/z: 301.51[M]$^+$.

1,1,2-Trimethyl-3-(3-sulfonatopropyl)-1H-benzo[e]indol-3-ium (3f).
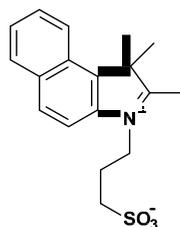
3f was synthesised as for **3a** using 1,1,2-trimethyl-1*H*-benzo[e]indole (3.25 g, 15.5 mmol) and 1,3-propanesultone (2.10 mL, 23.3 mmol) to give the product **3f** (3.35 g, 65%) as a white solid; m.p. 268-270 °C. ^{1}H NMR (d$_6$-DMSO, 300 MHz) δ 8.37-8.20 (m, 4H, Ar-H), 7.70-7.71 (m, 2H, Ar-H), 4.77 (t, *J*=7.0 Hz, 2H, N-CH$_2$-CH$_2$), 2.93 (s, 3H, N-C-CH$_3$), 2.69 (t, *J*=9.0 Hz, 2H, CH$_2$-CH$_2$-SO$_3$), 2.23 (br s, 2H, CH$_2$-CH$_2$-SO$_3$), 1.75 (s, 6H, C-CH$_3$). IR (ATR) 2978, 1582, 1463, 1389, 1181, 1030, 930, 874, 759 cm^{-1}. MS (ESI) m/z: 332 [M+H]$^+$.

1,1,2-Trimethyl-3-(4-sulfonatobutyl)-1H-benzo[e]indol-3-ium (3g).
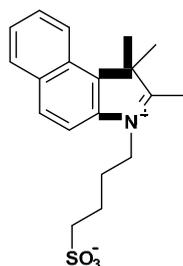
3g was synthesised as for **3a** using 1,1,2-trimethyl-1*H*-benzo[e]indole (3.25 g, 15.5 mmol) and 1,4-bultanesultone (4.10 mL, 25.1 mmol) to give the product **3g** (1.52 g, 28%) as a grey solid; m.p. 270-272 °C. ^{1}H NMR (d$_6$-DMSO, 300 MHz) δ 8.25 (d, *J*=8.0 Hz, 1H, Ar-<u>H</u>), 8.17 (d, *J*=9.0 Hz, 1H, Ar-<u>H</u>), 8.10 (d, *J*=9.0 Hz, 2H, Ar-<u>H</u>), 7.66-7.59 (m, 2H, Ar-<u>H</u>), 4.36 (t, *J*=9.0 Hz, 2H, N-C<u>H</u>$_2$-CH$_2$), 2.95 (s, 3H, N-C-C<u>H</u>$_3$), 2.08-2.02 (m, 6H, (C<u>H</u>$_2$)$_3$-SO$_3$), 1.75 (s, 6H, C-C<u>H</u>$_3$). IR (ATR) 2964, 1582, 1468, 1350, 1152, 1032, 930, 874, 727 cm^{-1}. MS (ESI) m/z: 346 [M+H]$^+$.

N-[5-Anilino-3-chloro-2,4-(propane-1,3-diyl)-2,4-pentadiene]anilinium   chloride   (VH1) was synthesised according to a reported procedure [259], [199].
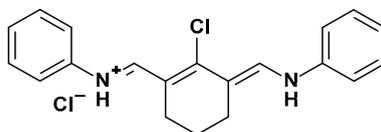
At 0 ºC POCl$_3$ (11.0 mL, 120 mmol) was added dropwise to anhydrous DMF (13.0 mL, 170 mmol) with constant stirring. After 30 min, cyclohexanone (5.50 mL, 53.0 mmol) was added, and the mixture was heated under reflux for 1 h. The reaction was cooled to 20 ºC and with constant stirring a mixture of aniline/EtOH [1:1 (v/v), 18.0 mL] was added dropwise. The reaction was continued for 30 min at 20 ºC with vigorous stirring, then the deep purple mixture was poured into H$_2$O/HCl [10:1 (v/v), 110 mL]. Crystals were allowed to form for 2 h in an ice bath; the reaction was filtered, washed with cold H$_2$O and Et$_2$O, and then dried *in vacuo* to give the product **VH1** (15.4 g, 81%) as a dark purple solid; m.p. 226-228 °C, literature m.p. 220 °C [254]. ^{1}H NMR (d$_6$-DMSO, 250 MHz) δ 11.2 (br s, 2H, NH), 8.55 (d, *J*=14.0 Hz, 2H, C<u>H</u>$_{alkene}$), 7.68 (d, *J*=7.0 Hz, 4H, Ar-<u>H</u>), 7.44 (t, *J*=7.0 Hz, 4H, Ar-<u>H</u>), 7.30-

7.28 (m, 2H, Ar-<u>H</u>), 3.03 (t, *J*=6.0 Hz, 4H, CH$_2$-C<u>H</u>$_2$), 2.05-1.98 (m, 2H, C<u>H</u>$_2$-CH$_2$). IR (ATR) 1609, 1562, 1457, 1267, 1179, 752, 683, 565 cm^{-1}. MS (ESI) m/z: 323.22 [M]$^+$.

2-[(E)-2-[(3E)-2-Chloro-3-{2-[(2E)-3,3-dimethyl-1-(4-sulfonatobutyl)-2,3-dihydro-1H-indol-2-ylidene]ethylidene}cyclohex-1-en-1-yl]ethenyl]-3,3-dimethyl-1-(4-sulfonatobutyl)-3H-indol-1-ium (4g) was synthesised according to a reported procedure [260].
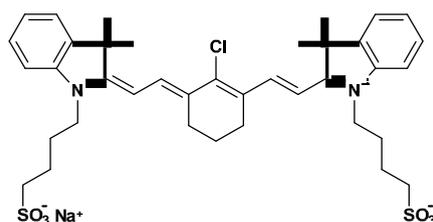
To a solution of **1l** (1.77 g, 6.00 mmol) and anhydrous sodium acetate (0.60 g, 6.00 mmol) in EtOH (60.0 mL) was added **VH1** (1.08 g, 3.00 mmol) with constant stirring, and the solution was heated under reflux for 4 h, cooled and then rotor evaporated to dryness. After removing the solvent, the crude product was purified by silica gel column chromatography (eluent solvent; chloroform:methanol = 7:3) to give the product **4g** (1.01 g, 46%) as a shiny purple solid; m.p. 253-255 °C: ^{1}H NMR (d$_6$-DMSO, 400 MHz) δ 8.21 (d, *J*=14.0 Hz, 2H, C<u>H</u>$_{alkene}$), 7.67 (d, *J*=7.0 Hz, 2H, Ar-<u>H</u>), 7.39-7.31 (m, 4H, Ar-<u>H</u>), 7.12-7.06 (m, 2H, Ar-<u>H</u>), 6.31 (d, *J*=14.0 Hz, 2H, C<u>H</u>$_{alkene}$), 4.89 (t, *J*=5.0 Hz, 4H, N-C<u>H</u>$_2$-CH$_2$), 3.01-2.96 (m, 4H, CH$_2$-C<u>H</u>$_2$), 2.68-2.60 (m, 4H, CH$_2$-C<u>H</u>$_2$), 1.70-1.61 (m, 8H, (C<u>H</u>$_2$)$_4$-SO$_3$), 1.50 (s, 12H, C-C<u>H</u>$_3$), 1.30-1.09 (m, 2H, CH$_2$-C<u>H</u>$_2$). IR (ATR) 2921, 1541, 1240, 1004, 889, 707, 565 cm^{-1}. MS (ESI) m/z: 727 [M+2H]$^+$. UV abs λ$_{max}$ = 770 nm.

2-[(E)-2-[(3E)-2-Chloro-3-{2-[(2E)-1,3,3-trimethyl-2,3-dihydro-1H-indol-2-ylidene]ethylidene}cyclohex-1-en-1-yl]ethenyl]-1,3,3-trimethyl-3H-indol-1-ium iodide (4a).
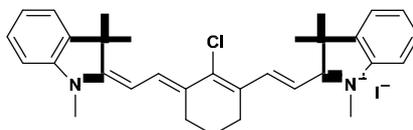
4a was synthesised as for **4g** using **1a** (0.602 g, 2.00 mmol) and anhydrous sodium acetate (0.16 g, 2.00 mmol) in EtOH (20.0 mL) and was added **VH1** (0.36 g, 1.00 mmol) to give the crude product which was purified by silica gel column chromatography (solvent; chloroform: methanol=9:1) to obtain cyanine dye **4a** (0.22 g, 36%) as a green solid; m.p. 253-255 °C: ^{1}H NMR (d$_6$-DMSO, 400 MHz) δ 8.27 (d, *J*=14.0 Hz, 2H, C$\underline{\text{H}}_{alkene}$), 7.64 (d, *J*=7.0 Hz, 2H, Ar-$\underline{\text{H}}$), 7.46-7.40 (m, 4H, Ar-$\underline{\text{H}}$), 7.32-7.29 (m, 2H, Ar-$\underline{\text{H}}$), 6.32 (d, *J*=14.0 Hz, 2H, C$\underline{\text{H}}_{alkene}$), 3.51 (s, 6H, N-C$\underline{\text{H}}_3$), 2.73 (t, *J*=6.0 Hz, 4H, C$\underline{\text{H}}_2$-CH$_2$), 1.86-1.79 (m, 2H, CH$_2$-C$\underline{\text{H}}_2$-CH$_2$), 1.67 (s, 12H, C-C$\underline{\text{H}}_3$). IR (ATR) 2922, 1556, 1508, 1486, 1437, 1363, 1301, 1244, 1151, 1093, 924, 854, 788, 752 cm^{-1}. MS (ESI) m/z: 483 [M]$^+$. UV abs λ$_{max}$ = 766 nm.

2-[(E)-2-[(3E)-2-Chloro-3-{2-[(2E)-1-ethyl-3,3-dimethyl-2,3-dihydro-1H-indol-2-ylidene]ethylidene}cyclohex-1-en-1-yl]ethenyl]-1-ethyl-3,3-dimethyl-3H-indol-1-ium iodide (4b).
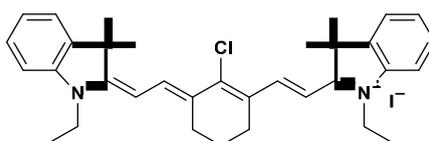
4b was synthesised as **4g** using **1b** (0.63 g, 2.00 mmol) and anhydrous sodium acetate (0.16 g, 2.00 mmol) in EtOH (20.0 mL) and was added **VH1** (0.36 g, 1.00 mmol) to give the crude product which was purified by impregnation on silica and eluting with ethyl acetate to remove the first band of impurities. The silica was then washed with methanol to remove the product and the solvent was rotor evaporated off to obtain cyanine dye **4b** (0.41 g, 64%) as a green solid; m.p. 246-248 °C: ^{1}H NMR (d$_6$-DMSO, 400 MHz) δ 8.29 (d, *J*=14.0 Hz, 2H, C$\underline{\text{H}}_{alkene}$), 7.66 (d, *J*=8.0 Hz, 2H, Ar-$\underline{\text{H}}$), 7.46-7.41 (m, 4H, Ar-$\underline{\text{H}}$), 7.30-7.27 (m, 2H, Ar-$\underline{\text{H}}$),

6.35 (d, J=14.0 Hz, 2H, C$\underline{H}_{alkene}$), 4.27 (q, J=7.0 Hz, 4H, N-C$\underline{H}_2$-CH$_3$), 2.68 (t, J=6.0 Hz, 4H, C$\underline{H}_2$-CH$_2$), 1.78-1.68 (m, 2H, CH$_2$-C$\underline{H}_2$-CH$_2$), 1.62 (s, 12H, C-C$\underline{H}_3$), 1.30 (t, J=7.0 Hz, 6H, CH$_2$-C$\underline{H}_3$). IR (ATR) 2957, 1552, 1509, 1478, 1397, 1282, 1249, 1208, 1034, 913, 828, 742, 579 cm^{-1}. MS (ESI) m/z: 511 [M]$^+$. UV abs λ_{max} = 778 nm.

2-[(E)-2-[(3E)-2-Chloro-3-{2-[(2E)-3,3-dimethyl-1-propylindol-2-ylidene]ethylidene}cyclohex-1-en-1-yl]ethenyl]-3,3-dimethyl-1-propylindol-1-ium iodide (4c).
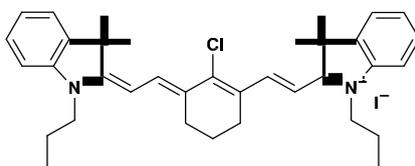
4c was synthesised as for **4g** using **1c** (1.31 g, 4.00 mmol) and anhydrous sodium acetate (0.33 g, 4.00 mmol) in EtOH (30.0 mL) and was added **VH1** (0.72 g, 2.00 mmol) to give the crude product which was purified by silica gel column chromatography (solvent; chloroform:methanol=8:2) to obtain cyanine dye **4c** (0.72 g, 54%) as a green solid; m.p. 246-248 °C: ^{1}H NMR (d$_6$-DMSO, 400 MHz) δ 8.17 (d, J=14.0 Hz, 2H, C$\underline{H}_{alkene}$), 7.50 (d, J=7.0 Hz, 2H, Ar-$\underline{H}$), 7.38-7.16 (m, 4H, Ar-$\underline{H}$), 7.20 (t, J=7.0 Hz, 2H, Ar-$\underline{H}$), 6.26 (d, J=14.0 Hz, 2H, C$\underline{H}_{alkene}$), 4.12 (t, J=6.0 Hz, 4H, N-C$\underline{H}_2$-CH$_2$), 2.61-2.57 (m, 4H, CH$_2$-C$\underline{H}_2$-CH$_3$), 1.75-1.64 (m, 6H, (C$\underline{H}_2$)$_3$), 1.57 (s, 12H, C-C$\underline{H}_3$), 0.87 (t, J=7.0 Hz, 6H, CH$_2$-C$\underline{H}_3$). IR (ATR) 2925, 1549, 1397, 1241, 1159, 1041, 925, 750, 707 cm^{-1}. MS (ESI) m/z: 539.29 [M]$^+$. UV abs λ_{max} = 781 nm.

Synthesis of 1-butyl-2-[(E)-2-[(3E)-3-{2-[(2E)-1-butyl-3,3-dimethylindol-2-ylidene]ethylidene}-2-chlorocyclohex-1-en-1-yl]ethenyl]-3,3-dimethylindol-1-ium iodide (4d).
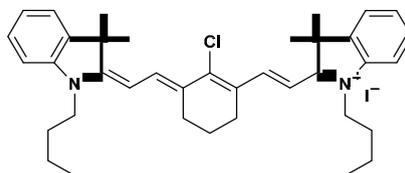
4d was synthesised as for **4g** using **1d** (1.37 g, 4.00 mmol) and anhydrous sodium acetate (0.33g, 4.00 mmol) in EtOH (30 mL) and was added **VH1** (0.72 g, 2.00 mmol) to give the crude product which was purified by silica gel column chromatography (eluent solvent; chloroform:methanol=8:2) to obtain cyanine dye **4d** (0.35 g, 25%) as a green solid; m.p. 219-221 °C: ^{1}H NMR (d$_6$-DMSO, 300 MHz) δ 8.28 (d, *J*=15.0 Hz, 2H, C$\underline{H}_{alkene}$), 7.66 (d, *J*=6.0 Hz, 2H, Ar-$\underline{H}$), 7.49 (dd, *J*=9.0 Hz, 4H, Ar-$\underline{H}$), 7.31 (d, *J*=6.0 Hz, 2H, Ar-$\underline{H}$), 6.36 (d, *J*=15.0 Hz, 2H, C$\underline{H}_{alkene}$), 4.25 (t, *J*=6.0 Hz, 4H, N-C$\underline{H}_2$-CH$_2$), 2.73 (quin, *J*=6.0 Hz, 4H, CH$_2$-C$\underline{H}_2$-CH$_2$), 1.88 (t, *J*=6.0 Hz, 2H, C$\underline{H}_2$-CH$_2$), 1.76 (t, *J*=6.0 Hz, 4H, CH$_2$-C$\underline{H}_2$), 1.67 (s, 12H, C-C$\underline{H}_3$), 1.44 (sex, *J*=9.0 Hz, 4H, C$\underline{H}_2$-CH$_3$), 0.96 (t, *J*=9.0 Hz, 6H, CH$_2$-C$\underline{H}_3$). IR (ATR) 2926, 1548, 1394, 1227, 1149, 1088, 911, 751 cm^{-1}. MS-EI: 567 [M]$^+$. UV abs λ$_{max}$ = 780 nm.

1-Benzyl-2-[(E)-2-[(3E)-3-{2-[(2E)-1-benzyl-3,3-dimethyl-2,3-dihydro-1H-indol-2-ylidene]ethylidene}-2-chlorocyclohex-1-en-1-yl]ethenyl]-3,3-dimethyl-3H-indol-1-ium bromide (4e).
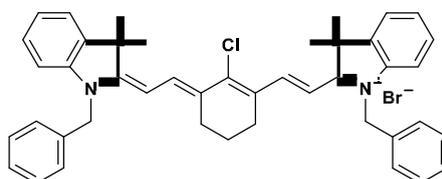
4e was synthesised as for **4g** using **1k** (0.66 g, 2.00 mmol) and anhydrous sodium acetate (0.16 g, 2.00 mmol) in EtOH (30.0 mL) and was added **VH1** (0.36 g, 1.00 mmol) to give the crude product which was purified by silica gel column chromatography (solvent; chloroform:methanol=9:1) to obtain cyanine dye **4e** (0.10 g, 14%) as a shiny purple solid; m.p. 254-256 °C: ^{1}H NMR (d$_6$-DMSO, 400 MHz) δ 8.25 (d, *J*=14.0 Hz, 2H, C$\underline{H}_{alkene}$), 7.41-

7.28 (m, 18H, Ar-$\underline{H}$), 6.35 (d, J=14.0 Hz, 2H, C$\underline{H}$*alkene*), 4.95 (br s, 4H, N-C$\underline{H}_2$-Ph), 2.50-2.45 (m, 4H, CH$_2$-C$\underline{H}_2$), 1.69 (s, 12H, C-C$\underline{H}_3$), 1.30-1.26 (m, 2H, CH$_2$-C$\underline{H}_2$-CH$_2$). IR (ATR) 1543, 1363, 1225, 1099, 896, 784, 668, 597 cm^{-1}. MS (ESI) m/z: 635 [M]$^+$. UV abs λ_{max} = 760 nm.

2-[(E)-2-[(3E)-2-Chloro-3-{2-[(2E)-3,3-dimethyl-1-(3-sulfonatopropyl)-2,3-dihydro-1H-indol-2-ylidene]ethylidene}cyclohex-1-en-1-yl]ethenyl]-3,3-dimethyl-1-(3-sulfonatopropyl)-3H-indol-1-ium (4f).
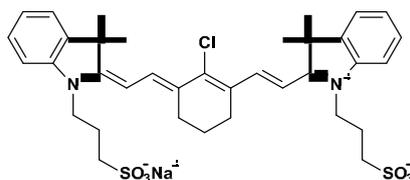
4f was synthesised as for **4g** using **1l** (1.69 g, 6.00 mmol) and anhydrous sodium acetate (0.49 g, 6.00 mmol) in EtOH (60.0 mL) and was added **VH1** (1.08 g, 3.00 mmol) to give the crude product which was purified by silica gel column chromatography (solvent; chloroform:methanol=9:1) to obtain cyanine dye **4f** (1.44 g, 69%) as a green solid; m.p. 249-251 °C: ^{1}H NMR (d$_6$-DMSO, 250 MHz) δ 8.27 (d, J=15.0 Hz, 2H, C$\underline{H}$*alkene*), 7.81 (d, J=7.0 Hz, 2H, Ar-$\underline{H}$), 7.74 (d, J=7.0 Hz, 2H, Ar-$\underline{H}$), 7.38 (t, J=7.0 Hz, 2H, Ar-$\underline{H}$), 7.12 (d, J=7.0 Hz, 2H, Ar-$\underline{H}$), 6.48 (d, J=15.0 Hz, 2H, C$\underline{H}$*alkene*), 4.49 (t, J=5.0 Hz, 4H, N-C$\underline{H}_2$-CH$_2$), 2.73 (t, J=5.0 Hz, 4H, CH$_2$-C$\underline{H}_2$-SO$_3$), 2.53-2.47 (m, 4H, CH$_2$-C$\underline{H}_2$-CH$_2$-SO$_3$), 1.98-1.89 (m, 6H, (C$\underline{H}_2$)$_2$), 1.66 (s, 12H, C-C$\underline{H}_3$). IR (ATR) 1542, 1390, 1454, 1390, 1003 cm^{-1}. MS (ESI) m/z: 699.20 [M+2H]$^+$. UV abs λ_{max} = 760 nm.

2-[(E)-2-[(3E)-2-Chloro-3-{2-[(2Z)-3-methyl-2,3-dihydro-1,3-benzothiazol-2-ylidene]ethylidene}cyclohex-1-en-1-yl]ethenyl]-3-methyl-1,3-benzothiazol-3-ium iodide (5a).
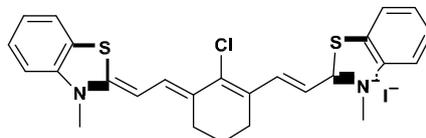
5a was synthesised as for **4g** using **2a** (0.58 g, 2.00 mmol) and anhydrous sodium acetate (0.16 g, 2.00 mmol) in EtOH (20.0 mL) and was added **VH1** (0.36 g, 1.00 mmol). The precipitate produced was filtered under suction, washed with *n*-hexane and dried *in vacuo* to give cyanine dye **5a** (0.30 g, 51%) as a green solid; m.p. 255-257 °C: ^{1}H NMR (d$_6$-DMSO, 400 MHz) δ 7.95 (d, *J*=7.0 Hz, 2H, Ar-<u>H</u>), 7.70 (d, *J*=13.0 Hz, 2H, C<u>H</u>$_{alkene}$), 7.70 (d, *J*=8.0 Hz, 2H, Ar-<u>H</u>), 7.52-7.48 (m, 2H, Ar-<u>H</u>), 7.34 (t, *J*=8.0 Hz, 2H, Ar-<u>H</u>), 6.47 (d, *J*=13.0 Hz, 2H, C<u>H</u>$_{alkene}$), 3.85 (s, 6H, N-C<u>H</u>$_3$), 2.66 (t, *J*=6.0 Hz, 4H, C<u>H</u>$_2$-CH$_2$), 1.08-1.03 (m, 2H, CH$_2$-C<u>H</u>$_2$-CH$_2$). IR (ATR) 2936, 1652 , 1506, 1423, 1384, 905, 849, 563 cm^{-1}. MS (ESI) m/z: 463 [M]$^+$. UV abs λmax = 796 nm.

2-[(E)-2-[(3E)-2-Chloro-3-{2-[(2Z)-3-ethyl-2,3-dihydro-1,3-benzothiazol-2-ylidene]ethylidene}cyclohex-1-en-1-yl]ethenyl]-3-ethyl-1,3-benzothiazol-3-ium iodide (5b).
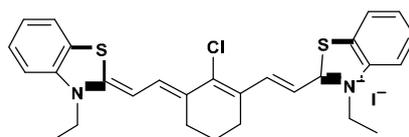
5b was synthesised as for **4g** using **2b** (0.62 g, 2.00 mmol) and anhydrous sodium acetate (0.16 g, 2.00 mmol) in EtOH (20.0 mL) and was added **VH1** (0.36 g, 1.00 mmol). The precipitate produced was filtered under suction, washed with *n*-hexane and dried *in vacuo* to give cyanine dye **5b** (0.37g, 60%) as a green solid; m.p. 246-248 °C: ^{1}H NMR (d$_6$-DMSO, 400 MHz) δ 8.01 (d, *J*=14.0 Hz, 2H, C<u>H</u>$_{alkene}$), 7.66 (d, *J*=7.0 Hz, 2H, Ar-<u>H</u>), 7.46-7.38 (m, 4H, Ar-<u>H</u>), 7.30-7.25 (m, 2H, Ar-<u>H</u>), 6.35 (d, *J*=14.0 Hz, 2H, C<u>H</u>$_{alkene}$), 4.28 (t, *J*=7.0 Hz, 4H, N-C<u>H</u>$_2$-CH$_2$), 2.63-2.59 (m, 4H, C<u>H</u>$_2$-CH$_2$), 2.51-2.48 (m, 2H, CH$_2$-C<u>H</u>$_2$-CH$_2$), 1.51 (t, *J*=7.0

Hz, 6H, CH$_2$-C$\underline{H}_3$). IR (ATR) 2957, 1552, 1509, 1478, 1397, 1282, 1249, 1208, 1034, 913, 828, 742, 579 cm^{-1}. MS (ESI) m/z: 491 [M]$^+$. UV abs λ_{max} = 796 nm.

2-[(E)-2-[(3E)-2-Chloro-3-{2-[(2Z)-3-propyl-2,3-dihydro-1,3-benzothiazol-2-ylidene]ethylidene}cyclohex-1-en-1-yl]ethenyl]-3-propyl-1,3-benzothiazol-3-ium iodide (5c).


5c was synthesised as for **4g** using **2c** (1.27 g, 4.00 mmol) and anhydrous sodium acetate (0.33 g, 4.00 mmol) in EtOH (30.0 mL) and was added **VH1** (0.72 g, 2.00 mmol) to give the crude product which was purified by silica gel column chromatography (solvent; chloroform:methanol=8:2) to obtain cyanine dye **5c** (0.81 g, 63%) as a green solid; m.p. 245-247 °C: ^{1}H NMR (d$_6$-DMSO, 400 MHz) δ 7.82 (d, *J*=8.0 Hz, 2H, Ar-$\underline{H}$), 7.63 (d, *J*=13.0 Hz, 2H, C$\underline{H}_{alkene}$), 7.58(brs, 2H, Ar-H), 7.39 (t, *J*=7.0 Hz, 2H, Ar-$\underline{H}$), 7.20 (t, *J*=7.0 Hz, 2H, Ar-$\underline{H}$), 6.38 (d, *J*=13.0 Hz, 2H, C$\underline{H}_{alkene}$), 4.25 (t, *J*=6.0 Hz, 4H, N-C$\underline{H}_2$-CH$_2$), 2.51-2.47 (m, 4H, C$\underline{H}_2$-CH$_2$), 1.63-1.57 (m, 6H, (C$\underline{H}_2$)$_2$), 0.85 (t, *J*=7.0 Hz, 6H, CH$_2$-C$\underline{H}_3$). IR (ATR) 2950, 1528, 1496, 1387, 1274, 1216, 1055, 983, 844, 740 cm^{-1}. MS (ESI) m/z: 519 [M]$^+$. UV abs λ_{max} = 797 nm.

3-Butyl-2-[(E)-2-[(3E)-3-{2-[(2Z)-3-butyl-2,3-dihydro-1,3-benzothiazol-2-ylidene]ethylidene}-2-chlorocyclohex-1-en-1-yl]ethenyl]-1,3-benzothiazol-3-ium iodide (5d).
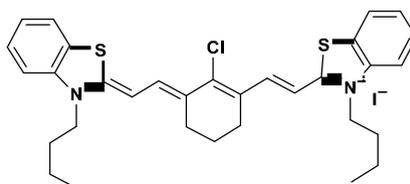
5d was synthesised as for **4g** using **2d** (0.88 g, 3.00 mmol) and anhydrous sodium acetate (0.24 g, 3.00 mmol) in EtOH (30.0 mL) and was added **VH1** (0.57 g, 1.50 mmol) to give the

crude product which was purified by silica gel column chromatography (solvent; chloroform:methanol=8:2) to obtain cyanine dye **5d** (0.38g, 38%) as a green solid; m.p. 212-214 °C: ^{1}H NMR (d$_6$-DMSO, 400 MHz) δ 7.99 (d, *J*=6.0 Hz, 2H, Ar-H), 7.83 (d, *J*=15.0 Hz, 2H, CH$_{alkene}$), 7.77 (d, *J*=6.0 Hz, 2H, Ar-H), 7.59 (t, *J*=6.0 Hz, 2H, Ar-H), 7.43 (t, *J*=9.0 Hz, 2H, Ar-H), 6.52 (d, *J*=15.0 Hz, 2H, CH$_{alkene}$), 4.47 (t, *J*=6.0 Hz, 4H, N-CH$_2$-CH$_2$), 2.67-2.60 (m, 4H, CH$_2$-CH$_2$), 1.84-1.80 (m, 2H, CH$_2$-CH$_2$-CH$_2$), 1.74 (t, *J*=9.0 Hz, 4H, CH$_2$-CH$_2$), 1.44 (sex, *J*=6.0 Hz, 4H, CH$_2$-CH$_2$-CH$_3$), 0.95 (t, *J*=7.0 Hz, 6H, CH$_2$-CH$_3$). IR (ATR) 2937, 1578, 1499, 1451, 1390, 1323, 1213, 1273, 1213, 1051, 902, 739 cm^{-1}. MS (ESI) m/z: 547[M]$^+$. UV abs λ$_{max}$ = 796 nm.

3-Benzyl-2-[(E)-2-[(3E)-3-{2-[(2Z)-3-benzyl-2,3-dihydro-1,3-benzothiazol-2-ylidene]ethylidene}-2-chlorocyclohex-1-en-1-yl]ethenyl]-1,3-benzothiazol-3-ium bromide (5e).
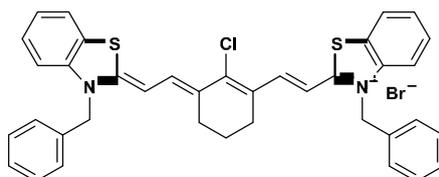
5e was synthesised as for **4g** using **2k** (2.56 g, 8.00 mmol) and anhydrous sodium acetate (0.66 g, 8.00 mmol) in EtOH (30.0 mL) and was added **VH1** (1.44 g, 4.00 mmol) to give the crude product which was purified by silica gel column chromatography (solvent; chloroform:methanol=7:3) to obtain cyanine dye **5e** (1.50 g, 54%) as a green solid; m.p. 254-256 °C: ^{1}H NMR (d$_6$-DMSO, 400 MHz) δ 7.94 (d, *J*=7.0 Hz, 2H, Ar-H), 7.74 (d, *J*=13.0 Hz, 2H, CH$_{alkene}$), 7.62 (d, *J*=8.0 Hz, 2H, Ar-H), 7.44 (t, *J*=7.0 Hz, 2H, Ar-H), 7.33 (d, *J*=6.0 Hz, 4H, Ar-H), 7.27-7.13 (m, 8H, Ar-H), 6.52 (d, *J*=13.0 Hz, 2H, CH$_{alkene}$), 5.70 (br s, 4H, N-CH$_2$-Ph), 3.12 (brs, 2H, CH$_2$), 2.57 (brs, 2H, CH$_2$), 1.67 (br s, 2H, CH$_2$). IR (ATR) 1543, 1506, 1363, 1225, 1099, 896, 784, 668, 597 cm^{-1}. MS (ESI) m/z: 615 [M]$^+$. HRMS(ESI): Calcd for C$_{38}$H$_{32}$ClN$_2$S$_2$ [M]$^+$615.1690, found 615.1682. UV abs λ$_{max}$ = 804 nm.

2-[(E)-2-[(3E)-2-Chloro-3-{2-[(2Z)-3-(3-sulfonatopropyl)-2,3-dihydro-1,3-benzothiazol-2-ylidene]ethylidene}cyclohex-1-en-1-yl]ethenyl]-3-(3-sulfonatopropyl)-1,3-benzothiazol-3-ium (5f).
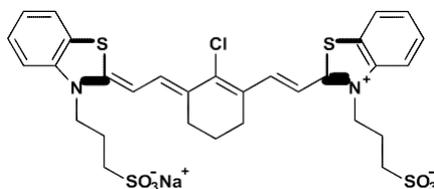
5f was synthesised as for **4g** using **2l** (0.66 g, 2.00 mmol) and anhydrous sodium acetate (0.16 g, 2.00 mmol) in EtOH (30.0 mL) and was added **VH1** (0.36 g, 1.00 mmol) to give the crude product which was purified by silica gel column chromatography (solvent; dichloromethane:methanol=9:1) to obtain cyanine dye **5f** (0.10 g, 15%) as a green solid; m.p. 240-242 °C: ^{1}H NMR (d$_6$-DMSO, 400 MHz) δ 7.88 (d, *J*=13.0 Hz, 2H, C$\underline{\text{H}}$*alkene*), 7.69-7.60 (m, 4H, Ar-$\underline{\text{H}}$), 7.43 (t, *J*=7.0 Hz, 2H, Ar-$\underline{\text{H}}$), 7.25 (t, *J*=7.0 Hz, 2H, Ar-$\underline{\text{H}}$), 6.56 (d, *J*=13.0 Hz, 2H, C$\underline{\text{H}}$*alkene*), 4.51 (t, *J*=7.0 Hz, 4H, N-C$\underline{\text{H}}_2$-CH$_2$), 2.55-2.45 (m, 8H, (C$\underline{\text{H}}_2$)$_4$-SO$_3$), 1.97 (t, *J*=6.0 Hz, 4H, C$\underline{\text{H}}_2$-CH$_2$), 1.76-1.70 (m, 2H, CH$_2$-C$\underline{\text{H}}_2$-CH$_2$). IR (ATR) 3050, 1527, 1499, 1454, 1324, 1208, 983 cm^{-1}. MS (ESI) m/z: 679 [M+2H]$^+$. UV abs λ$_{max}$ = 775 nm.

2-[(E)-2-[(3E)-2-Chloro-3-{2-[(2Z)-3-(4-sulfonatobutyl)-2,3-dihydro-1,3-benzothiazol-2-ylidene]ethylidene}cyclohex-1-en-1-yl]ethenyl]-3-(4-sulfonatobutyl)-1,3-benzothiazol-3-ium (5g).
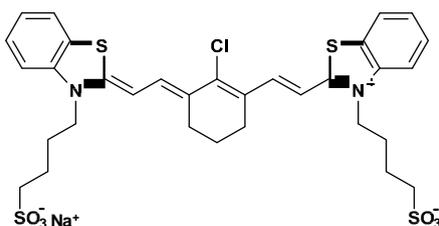

5g was synthesised as for **4g** using **2m** (0.58 g, 2.00 mmol) and anhydrous sodium acetate (0.16 g, 2.00 mmol) in EtOH (60.0 mL) and was added **VH1** (0.36 g, 1.00 mmol) to give the crude product which was purified by silica gel column chromatography (solvent; chloroform:methanol=9:1) to obtain cyanine dye **5g** (0.30 g, 42%) as a green solid; m.p. 247-249 °C: ^{1}H NMR (d$_6$-DMSO, 400 MHz) δ 7.98 (d, *J*=13.0 Hz, 2H, C$\underline{\text{H}}$*alkene*), 7.83-7.68 (m, 4H, Ar-$\underline{\text{H}}$), 7.58-7.56 (m, 2H, Ar-$\underline{\text{H}}$), 7.54-7.49 (m, 2H, Ar-$\underline{\text{H}}$), 6.57 (d, *J*=13.0 Hz, 2H,

CH$_{alkene}$), 4.46 (t, *J*=7.0 Hz, 4H, N-C$\underline{H}_2$-CH$_2$), 3.34 (br s, 1H, C$\underline{H}_2$), 2.70-2.65 (m, 4H, C$\underline{H}_2$-CH$_2$), 2.09 (br s, 1H, C$\underline{H}_2$), 1.76-1.50 (m, 12H, (C$\underline{H}_2$)$_6$-SO$_3$). IR (ATR) 3393, 1651, 1499, 1392, 1324, 1276, 1217, 1127, 1011, 852, 796, 743, 564 cm^{-1}. MS (ESI) m/z: 707 [M+2H]$^+$. UV abs λ_{max} = 800 nm.

2-[(E)-2-[(3E)-2-Chloro-3-{2-[(2E)-1,1,3-trimethyl-1H,2H,3H-benzo[e]indol-2-ylidene]ethylidene}cyclohex-1-en-1-yl]ethenyl]-1,1,3-trimethyl-1H-benzo[e]indol-3-ium iodide (6a).
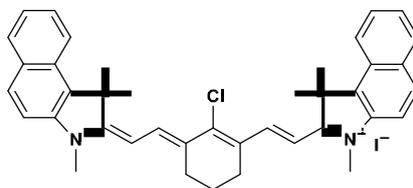
6a was synthesised as for **4g** using **3a** (1.40 g, 4.00 mmol) and anhydrous sodium acetate (0.33 g, 4.00 mmol) in EtOH (30.0 mL) and was added **VH1** (0.72 g, 2.00 mmol) to give the crude product which was purified by silica gel column chromatography (solvent; chloroform : methanol=8:2) to obtain cyanine dye **6a** (0.41 g, 29%) as a green solid; m.p. 212-214 °C: ^{1}H NMR (d$_6$-DMSO, 300 MHz) δ 8.38 (d, *J*=15.0 Hz, 2H, C$\underline{H}_{alkene}$), 8.31 (d, *J*=9.0 Hz, 2H, Ar-$\underline{H}$), 8.12-8.05 (m, 4H, Ar-$\underline{H}$), 7.81 (d, *J*=9.0 Hz, 2H, Ar-$\underline{H}$), 7.69 (t, *J*=9.0 Hz, 2H, Ar-$\underline{H}$), 7.52 (t, *J*=6.0 Hz, 2H, Ar-$\underline{H}$), 6.37 (d, *J*=15.0 Hz, 2H, C$\underline{H}_{alkene}$), 3.82 (s, 6H, N-C$\underline{H}_3$), 2.78 (t, *J*=6.0 Hz, 4H, CH$_2$-C$\underline{H}_2$), 1.95 (s, 12H, C-C$\underline{H}_3$), 1.91-1.86 (m, 2H, CH$_2$-C$\underline{H}_2$-CH$_2$). IR (ATR) 2927, 1544, 1429, 1339, 1152, 997, 799 cm^{-1}. MS (ESI) m/z: 583 [M]$^+$. UV abs λ_{max} = 813 nm.

2-[(E)-2-[(3E)-2-Chloro-3-{2-[(2E)-3-ethyl-1,1-dimethyl-1H,2H,3H-benzo[e]indol-2-ylidene]ethylidene}cyclohex-1-en-1-yl]ethenyl]-3-ethyl-1,1-dimethyl-1H-benzo[e]indol-3-ium iodide (6b).
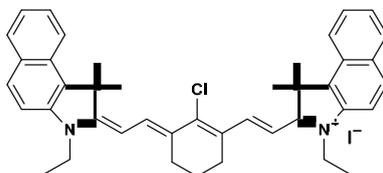
6b was synthesised as for **4g** using **3b** (1.46 g, 4.00 mmol) and anhydrous sodium acetate (0.33 g, 4.00 mmol) in EtOH (30.0 mL) and was added **VH1** (0.72 g, 2.00 mmol) to give the crude product which was purified by silica gel column chromatography (solvent; chloroform:methanol=8:2) to obtain cyanine dye **6b** (0.85 g, 58%) as a green solid; m.p. 199-201 °C: ^{1}H NMR (d$_6$-DMSO, 300 MHz) δ 8.40 (d, J=14.0 Hz, 2H, C$\underline{H}_{alkene}$), 8.33 (d, J=9.0 Hz, 2H, Ar-$\underline{H}$), 8.13-8.06 (m, 4H, Ar-$\underline{H}$), 7.81 (d, J=9.0 Hz, 2H, Ar-$\underline{H}$), 7.69 (t, J=9.0 Hz, 2H, Ar-$\underline{H}$), 7.55 (t, J=6.0 Hz, 2H, Ar-$\underline{H}$), 6.40 (d, J=14.0 Hz, 2H, C$\underline{H}_{alkene}$), 4.43 (q, J=6.0 Hz, 4H, N-C$\underline{H}_2$-CH$_3$), 2.79 (t, J=6.0 Hz, 4H, C$\underline{H}_2$-CH$_2$), 1.95 (s, 12H, C-C$\underline{H}_3$), 1.91-1.87 (m, 2H, CH$_2$-C$\underline{H}_2$-CH$_2$), 1.39 (t, J=6.0 Hz, 6H, CH$_2$-C$\underline{H}_3$). IR (ATR) 2923, 1501, 1345, 1225, 1153, 1082, 999, 898, 797, 708 cm^{-1}. MS (ESI) m/z: 611 [M]$^+$. UV abs λ_{max} = 815 nm.

2-[(E)-2-[(3E)-2-Chloro-3-{2-[(2E)-1,1-dimethyl-3-propyl-1H,2H,3H-benzo[e]indol-2-ylidene]ethylidene}cyclohex-1-en-1-yl]ethenyl]-1,1-dimethyl-3-propyl-1H-benzo[e]indol-3-ium iodide (6c).
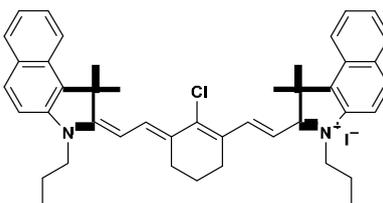
6c was synthesised as for **4g** using **3c** (1.52 g, 4.00 mmol) and anhydrous sodium acetate (0.33 g, 4.00 mmol) in EtOH (30.0 mL) and was added **VH1** (0.72 g, 2.00 mmol) to give the crude product which was purified by silica gel column chromatography (solvent; chloroform : methanol=8:2) to obtain cyanine dye **6c** (1.10 g, 72%) as a green solid; m.p. 198-200 °C: ^{1}H NMR (d$_6$-DMSO, 300 MHz) δ 8.40 (d, J=14.0 Hz, 2H, C$\underline{H}_{alkene}$), 8.33 (d, J=9.0 Hz, 2H, Ar-$\underline{H}$), 8.12-8.06 (m, J=9.0 Hz, 4H, Ar-$\underline{H}$), 7.83 (d, J=9.0 Hz, 2H, Ar-$\underline{H}$), 7.69 (t, J=9.0 Hz, 2H,

Ar-<u>H</u>), 7.55 (t, *J*=6.0 Hz, 2H, Ar-<u>H</u>), 6.42 (d, *J*=14.0 Hz, 2H, C<u>H</u>*alkene*), 4.36 (t, *J*=6.0 Hz, 4H, N-C<u>H</u>$_2$-CH$_2$), 2.78 (sex, *J*=6.0 Hz, 4H, CH$_2$-C<u>H</u>$_2$-CH$_3$), 1.96 (s, 12H, C-C<u>H</u>$_3$), 1.91-1.80 (m, 6H, (C<u>H</u>$_2$)$_3$), 1.02 (t, *J*=6.0 Hz, 6H, CH$_2$-C<u>H</u>$_3$). IR (ATR) 2922, 1543, 1384, 1266, 1050, 998, 875, 784 cm^{-1}. MS (ESI) m/z: 639[M]$^+$. UV abs λ_{max} = 818 nm.

Synthesis of 3-butyl-2-[(E)-2-[(3E)-3-{2-[(2E)-3-butyl-1,1-dimethyl-1H,2H,3H-benzo[e]indol-2-ylidene]ethylidene}-2-chlorocyclohex-1-en-1-yl]ethenyl]-1,1-dimethyl-1H-benzo[e]indol-3-ium iodide (6d).
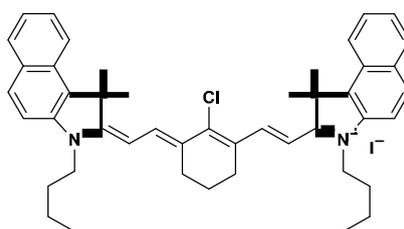
6d was synthesised as for **4g** using **3d** (1.58 g, 4.00 mmol) and anhydrous sodium acetate (0.33 g, 4.00 mmol) in EtOH (30 mL) and was added **VH1** (0.72 g, 2.00 mmol) to give the crude product which was purified by silica gel column chromatography (eluent solvent; chloroform:methanol=8:2) to obtain cyanine dye **6d** (0.72 g, 45%) as a green solid; m.p. 167-169 °C: ^{1}H NMR (d$_6$-DMSO, 300 MHz) δ 8.39 (d, *J*=14.0 Hz, 2H, C<u>H</u>*alkene*), 8.32 (d, *J*=9.0 Hz, 2H, Ar-<u>H</u>), 8.12-8.06 (m, 4H, Ar-<u>H</u>), 7.81 (d, *J*=9.0 Hz, 2H, Ar-<u>H</u>), 7.69 (t, *J*=9.0 Hz, 2H, Ar-<u>H</u>), 7.56 (t, *J*=6.0 Hz, 2H, Ar-<u>H</u>), 6.40 (d, *J*=14.0 Hz, 2H, C<u>H</u>*alkene*), 4.39 (t, *J*=6.0 Hz, 4H, N-C<u>H</u>$_2$-CH$_2$), 2.77 (t, *J*=6.0 Hz, 4H, C<u>H</u>$_2$-CH$_2$), 1.95 (s, 12H, C-C<u>H</u>$_3$), 1.89 (br s, 2H, C<u>H</u>$_2$-CH$_2$), 1.80-1.74 (m, 4H, CH$_2$-C<u>H</u>$_2$), 1.46-1.40 (m, 4H, CH$_2$-C<u>H</u>$_2$-CH$_3$), 0.98 (t, *J*=9.0 Hz, 6H, CH$_2$-C<u>H</u>$_3$). IR (ATR) 2920, 1543, 1385, 1226, 1040, 998, 712 cm^{-1}. MS (ESI) m/z: 669 [M]$^+$. UV abs λ_{max} = 818 nm.

Synthesis of 3-benzyl-2-[(E)-2-[(3E)-3-{2-[(2E)-3-benzyl-1,1-dimethyl-1H,2H,3H-benzo[e]indol-2-ylidene]ethylidene}-2-chlorocyclohex-1-en-1-yl]ethenyl]-1,1-dimethyl-1H-benzo[e]indol-3-ium bromide (6e).
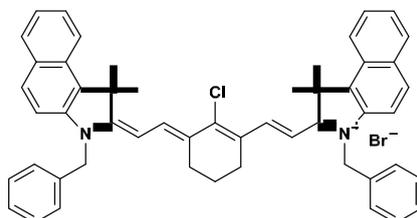

6e was synthesised as for **4g** using **3e** (1.52 g, 4.00 mmol) and anhydrous sodium acetate (0.33 g, 4.00 mmol) in EtOH (30.0 mL) and was added **VH1** (0.72 g, 2.00 mmol) to give the crude product which was purified by silica gel column chromatography (solvent; chloroform:methanol=8:2) to obtain cyanine dye **6e** (0.32 g, 20%) as a green solid; m.p. 215-217 °C: ^{1}H NMR (d$_6$-DMSO, 300 MHz) δ 8.37-8.32 (m, 4H, Ar-$\underline{H}$), 8.09-8.05 (m, 4H, Ar-$\underline{H}$), 7.75 (d, *J*=9.0 Hz, 2H, Ar-$\underline{H}$), 7.69 (d, *J*=9.0 Hz, 2H, Ar-$\underline{H}$), 7.57 (t, *J*=15.0 Hz, 2H, C$\underline{H}_{alkene}$), 7.40-7.31 (m, 10H, Ar-$\underline{H}$), 6.47 (d, *J*=15.0 Hz, 2H, C$\underline{H}_{alkene}$), 5.59 (br s, 4H, N-C$\underline{H}_2$-Ph), 2.61 (t, *J*=9.0 Hz, 4H, C$\underline{H}_2$-CH$_2$), 2.01 (s, 12H, C-C$\underline{H}_3$), 1.89-1.74 (m, 2H, CH$_2$-C$\underline{H}_2$-CH$_2$). IR (ATR) 2932, 1623, 1431, 1347, 1227, 1081, 997, 806. 706 cm^{-1}. MS (ESI) m/z: 735.26[M+]. HRMS(ESI): Calcd for C$_{52}$H$_{45}$ClN$_2$ [M]$^+$ 735.3482, found 735.3484. UV abs λ$_{max}$ = 822 nm.

2-[(E)-2-[(3E)-2-Chloro-3-{2-[(2E)-1,1-dimethyl-3-(3-sulfonatopropyl)-1H,2H,3H-benzo[e]indol-2-ylidene]ethylidene}cyclohex-1-en-1-yl]ethenyl]-1,1-dimethyl-3-(3-sulfonatopropyl)-1H-benzo[e]indol-3-ium (6f).
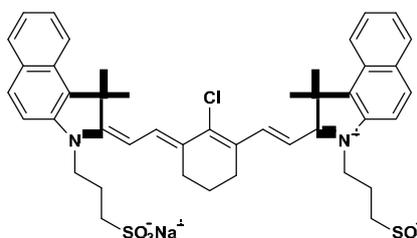
6f was synthesised as for **4g** using **3f** (1.32 g, 4.00 mmol) and anhydrous sodium acetate (0.33 g, 4.00 mmol) in EtOH (30.0 mL) and was added **VH1** (0.72 g, 2.00 mmol) to give the

crude product which was purified by silica gel column chromatography (solvent; chloroform : methanol=7:3) to obtain cyanine dye **6f** (1.12 g, 70%) as a green solid; m.p. 235-237 °C: ^{1}H NMR (d$_6$-DMSO, 300 MHz) δ 8.39 (d, *J*=14.0 Hz, 2H, C<u>H</u>$_{alkene}$), 8.31 (d, *J*=9.0 Hz, 2H, Ar-<u>H</u>), 8.10-8.04 (m, 4H, Ar-<u>H</u>), 7.88 (d, *J*=9.0 Hz, 2H, Ar-<u>H</u>), 7.68 (t, *J*=9.0 Hz, 2H, Ar-<u>H</u>), 7.54 (t, *J*=6.0 Hz, 2H, Ar-<u>H</u>), 6.59 (d, *J*=14.0 Hz, 2H, C<u>H</u>$_{alkene}$), 4.54 (t, *J*=6.0 Hz, 4H, N-C<u>H</u>$_2$-CH$_2$), 2.81 (t, *J*=6.0 Hz, 4H, CH$_2$-C<u>H</u>$_2$-SO$_3$), 2.65 (quin, *J*=6.0 Hz, 4H, CH$_2$-C<u>H</u>$_2$-CH$_2$), 2.12-1.99 (m, 2H, CH$_2$-C<u>H</u>$_2$-CH$_2$), 1.95 (s, 12H, C-C<u>H</u>$_3$), 1.89 (t, *J*=6.0 Hz, 4H, C<u>H</u>$_2$-CH$_2$). IR (ATR) 2931, 1626, 1389, 1271, 1096, 1003, 921, 818, 710 cm^{-1}. MS (ESI) m/z: 799 [M]$^+$. UV abs λ$_{max}$ = 820 nm.

2-[(E)-2-[(3E)-2-Chloro-3-{2-[(2E)-1,1-dimethyl-3-(4-sulfonatobutyl)-1H,2H,3H-benzo[e]indol-2-ylidene]ethylidene}cyclohex-1-en-1-yl]ethenyl]-1,1-dimethyl-3-(4-sulfonatobutyl)-1H-benzo[e]indol-3-ium (6g).
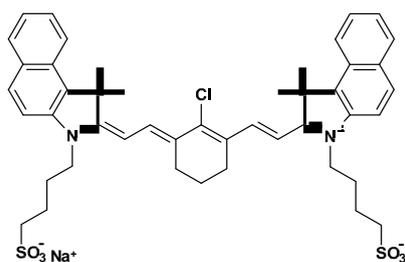
6g was synthesised as for **4g** using **3g** (1.38 g, 4.00 mmol) and anhydrous sodium acetate (0.33 g, 4.00 mmol) in EtOH (30.0 mL) and was added **VH1** (0.72 g, 2.00 mmol) to give the crude product which was purified by silica gel column chromatography (solvent; chloroform:methanol=7:3) to obtain cyanine dye **6g** (1.30 g, 79%) as a green solid; m.p. 232-234 °C: ^{1}H NMR (d$_6$-DMSO, 300 MHz) δ 8.38 (d, *J*=14.0 Hz, 2H, C<u>H</u>$_{alkene}$), 8.31 (d, *J*=9.0 Hz, 2H, Ar-<u>H</u>), 8.05-8.00 (m, 4H, Ar-<u>H</u>), 7.83 (d, *J*=9.0 Hz, 2H, Ar-<u>H</u>), 7.68 (t, *J*=9.0 Hz, 2H, Ar-<u>H</u>), 7.54 (t, *J*=9.0 Hz, 2H, Ar-<u>H</u>), 6.44 (d, *J*=14.0 Hz, 2H, C<u>H</u>$_{alkene}$), 4.38 (t, *J*=9.0 Hz, 4H, N-C<u>H</u>$_2$-CH$_2$), 2.79 (t, *J*=6.0 Hz, 4H, CH$_2$-C<u>H</u>$_2$-SO$_3$), 2.54-2.49 (m, 6H, (C<u>H</u>$_2$)$_4$), 1.94 (s, 12H, C-C<u>H</u>$_3$), 1.89-1.76 (m, 8H, (C<u>H</u>$_2$)$_4$-CH$_2$-SO$_3$). IR (ATR) 2929, 1544, 1388, 1347, 1227, 1035, 880 cm^{-1}. MS (ESI) m/z: 827 [M]$^+$. UV abs λ$_{max}$ = 820 nm.

1,3,3-Trimethyl-2-[(E)-2-[(3E)-2-(phenylamino)-3-{2-[(2E)-1,3,3-trimethyl- 2,3-dihydro-1H-indol-2-ylidene]ethylidene}cyclohex-1-en-1-yl]ethenyl]-3H-indol-1-ium iodide (7a)

was synthesised according to a reported procedure [261].
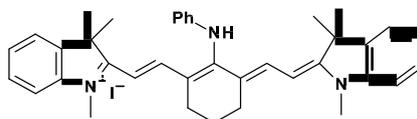
Aniline (0.09 g, 1.00 mmol) was added by syringe to **4a** (0.06 g, 0.10 mmol) dissolved in anhydrous DMF (10.0 mL) under nitrogen. The reaction mixture was stirred at 85 $^{\circ}$C overnight under nitrogen. The solvent was removed under reduced pressure, the crude product was purified by column chromatography on silica gel (dichloromethane:methanol = 9:1) and treated with 2-propanol to afford a dark green solid **7a** (20 mg, 30%); m.p. 213-215°C: ^{1}H NMR (d$_6$-DMSO, 250 MHz) δ 8.22 (br s, 1H, Ar-N<u>H</u>), 7.93 (d, *J*=14.0 Hz, 2H, C<u>H</u>$_{alkene}$), 7.49 (d, *J*=6.0 Hz, 2H, Ar-<u>H</u>), 7.30-7.21 (m, 9H, Ar-<u>H</u>), 6.90 (d, *J*=6.0 Hz, 2H, Ar-<u>H</u>), 6.05 (d, *J*=14.0 Hz, 2H, C<u>H</u>$_{alkene}$), 3.65 (s, 6H, N-C<u>H</u>$_3$), 2.62 (t, *J*=6.0 Hz, 4H, C<u>H</u>$_2$-CH$_2$), 1.85-1.79 (m, 2H, CH$_2$-C<u>H</u>$_2$-CH$_2$), 1.03 (s, 12H, C-C<u>H</u>$_3$). IR (ATR) 2928, 1555, 1484, 1436, 1349, 1308, 1206, 1149, 915, 786 cm^{-1}. MS (ESI) m/z: 540 [M]$^{+}$. UV abs λ$_{max}$ = 734 nm.

1-Ethyl-2-[(E)-2-[(3E)-3-{2-[(2E)-1-ethyl-3,3-dimethyl-2,3-dihydro-1H-indol-2-ylidene]ethylidene}-2-(phenylamino)cyclohex-1-en-1-yl]ethenyl]-3,3-dimethyl-3H-indol-1-ium iodide (7b).
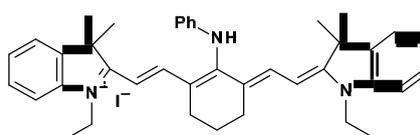
7b was synthesised as for **7a** using **4b** (0.06 g, 0.10 mmol), aniline (0.09 g, 1.00 mmol), and anhydrous DMF (10.0 mL). The solvent was removed under reduced pressure, the crude product was purified by column chromatography on silica gel (dichloromethane:methanol = 9:1) to afford a shiny dark blue solid **7b** (24 mg, 35%); m.p. 217-219 °C: ^{1}H NMR (CDCl$_3$, 400 MHz) δ 9.05 (br s, 1H, Ar-N<u>H</u>), 8.16 (d, *J*=14.0 Hz, 2H, C<u>H</u>$_{alkene}$), 7.41-7.35 (m, 5H, Ar-<u>H</u>), 7.22 (t, *J*=8.0 Hz, 4H, Ar-<u>H</u>), 7.09 (t, *J*=7.0 Hz, 2H, Ar-<u>H</u>), 6.92 (d, *J*=8.0 Hz, 2H, Ar-<u>H</u>), 6.80 (t, *J*=7.0 Hz, 2H, Ar-<u>H</u>), 5.79 (d, *J*=14.0 Hz, 2H, C<u>H</u>$_{alkene}$), 3.56 (q, *J*=9.0 Hz, 4H, N-C<u>H</u>$_2$-CH$_3$), 2.57 (t, *J*=6.0 Hz, 4H, C<u>H</u>$_2$-CH$_2$), 1.92-1.84 (m, *J*=6.0 Hz, 2H, CH$_2$-C<u>H</u>$_2$-CH$_2$),

1.72 (t, *J*=6.0 Hz, 6H, CH$_2$-C$\underline{H}_3$), 1.36 (s, 12H, C-C$\underline{H}_3$). IR (ATR) 2922, 1560, 1484, 1436, 1342, 1318, 1206, 1129, 905, 783 cm^{-1}. MS (ESI) m/z: 540 [M]$^+$. UV abs λ_{max} = 734 nm.

2-[(E)-2-[(3E)-3-{2-[(2E)-3,3-Dimethyl-1-propyl-2,3-dihydro-1H-indol-2-ylidene]ethylidene}-2-(phenylamino)cyclohex-1-en-1-yl]ethenyl]-3,3-dimethyl-1-propyl-3H-indol-1-ium iodide (7c).
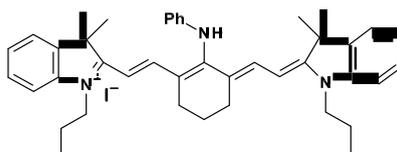
7c was synthesised as for **7a** using **4c** (0.07 g, 0.10 mmol), aniline (0.09 g, 1.00 mmol), and anhydrous DMF (10.0 mL). The solvent was removed under reduced pressure, the crude product was purified by column chromatography on silica gel (dichloromethane : methanol = 9:1) to afford a shiny dark blue solid **7c** (31 mg, 43%); m.p. 215-217 °C: ^{1}H NMR (CDCl$_3$, 400 MHz) δ 9.02 (br s, 1H, Ar-N$\underline{H}$), 8.14 (d, *J*=14.0 Hz, 2H, C$\underline{H}_{alkene}$), 7.45-7.38 (m, 3H, Ar-$\underline{H}$), 7.18-7.12 (m, 5H, Ar-$\underline{H}$), 7.09 (t, *J*=7.0 Hz, 2H, Ar-$\underline{H}$), 6.90 (d, *J*=8.0 Hz, 2H, Ar-$\underline{H}$), 6.78 (t, *J*=7.0 Hz, 1H, Ar-$\underline{H}$), 5.79 (d, *J*=14.0 Hz, 2H, C$\underline{H}_{alkene}$), 3.88 (t, *J*=7.0 Hz, 4H, N-C$\underline{H}_2$-CH$_2$), 2.56 (t, *J*=6.0 Hz, 4H, C$\underline{H}_2$-CH$_2$), 1.93 (quin, *J*=6.0 Hz, 2H, CH$_2$-C$\underline{H}_2$-CH$_2$), 1.83-1.76 (m, 4H, C$\underline{H}_2$-CH$_2$), 1.38 (s, 12H, C-C$\underline{H}_3$), 1.01 (t, *J*=7.0 Hz, 6H, CH$_2$-C$\underline{H}_3$). IR (ATR) 2920, 1549, 1431, 1344, 1232, 1151, 944, 787 cm^{-1}. MS (ESI) m/z: 596 [M]$^+$. UV abs λ_{max} = 746 nm.

1-Benzyl-2-[(E)-2-[(3E)-3-{2-[(2E)-1-benzyl-3,3-dimethyl-2,3-dihydro-1H-indol-2-ylidene]ethylidene}-2-(phenylamino)cyclohex-1-en-1-yl]ethenyl]-3,3-dimethyl-3H-indol-1-ium bromide (7d).
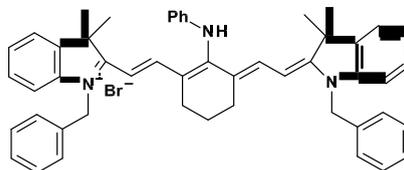
7d was synthesised as for **7a** using **4e** (0.07 g, 0.10 mmol), aniline (0.09 g, 1.00 mmol), and anhydrous DMF (10.0 mL). The solvent was removed under reduced pressure, the crude product was purified by column chromatography on silica gel (chloroform:methanol =9:1) to afford a dark shinny blue solid **7d** (13 mg, 17%); m.p. 210-212 °C: ^{1}H NMR (d$_6$-DMSO, 400 MHz) δ 8.87 (br s, 1H, Ar-N<u>H</u>), 7.95 (d, *J*=14.0 Hz, 2H, C<u>H</u>*alkene*), 7.48 (d, *J*=7.0 Hz, 2H, Ar-<u>H</u>), 7.33-7.32 (m, 4H, Ar-<u>H</u>), 7.31-7.28 (m, 6H, Ar-<u>H</u>), 7.22-7.19 (m, 6H, Ar-<u>H</u>), 7.14 (t, *J*=7.0 Hz, 2H, Ar-<u>H</u>), 6.95 (d, *J*=7.0 Hz, 2H, Ar-<u>H</u>), 6.78 (t, *J*=7.0 Hz, 1H, Ar-<u>H</u>), 6.07 (d, *J*=14.0 Hz, 2H, C<u>H</u>*alkene*), 5.36 (s, 4H, N-C<u>H</u>$_2$-Ph), 2.43 (t, *J*=5.0 Hz, 4H, C<u>H</u>$_2$-CH$_2$), 1.73 (quin, *J*=6.0 Hz, 2H, CH$_2$-C<u>H</u>$_2$-CH$_2$), 1.33 (s, 12H, C-C<u>H</u>$_3$). IR (ATR) 2921, 1504, 1436, 1361, 1224, 1005, 897, 787 cm^{-1}. MS (ESI) m/z: 692 [M]$^+$. HRMS(ESI): Calcd for C$_{50}$H$_{50}$N$_3$ [M]$^+$ 692.3978, found 692.3980. UV abs λ$_{max}$ = 738 nm.

2-[(E)-2-[(3E)-3-{2-[(2E)-3,3-Dimethyl-1-(3-sulfonatopropyl)-2,3-dihydro-1H-indol-2-ylidene]ethylidene}-2-(phenylamino)cyclohex-1-en-1-yl]ethenyl]-3,3-dimethyl-1-(3-sulfonatopropyl)-3H-indol-1-ium (7e).
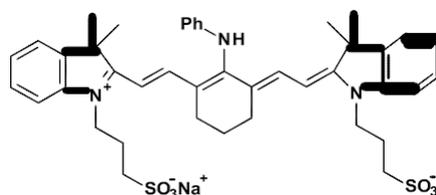
7e was synthesised as for **7a** using **4f** (0.07 g, 0.10 mmol), aniline (0.09 g, 1.00 mmol), and anhydrous DMF (10.0 mL). The solvent was removed under reduced pressure, the crude product was purified by column chromatography on silica gel (chloroform:methanol 8:2) to afford a dark green solid **7e** (25 mg, 33%); m.p. 222-224 °C: ^{1}H NMR (d$_6$-DMSO, 400 MHz)

δ 8.62 (br s, 1H, Ar-N<u>H</u>), 7.92 (d, *J*=14.0 Hz, 2H, C<u>H</u>*alkene*), 7.36 (d, *J*=7.0 Hz, 2H, Ar-<u>H</u>), 7.29-7.18 (m, 4H, Ar-<u>H</u>), 7.15 (t, *J*=8.0 Hz, 2H, Ar-<u>H</u>), 7.06 (t, *J*=7.0 Hz, 2H, Ar-<u>H</u>), 6.87 (d, *J*=8.0 Hz, 2H, Ar-<u>H</u>), 6.64 (t, *J*=7.0 Hz, 1H, Ar-<u>H</u>), 6.16 (d, *J*=14.0 Hz, 2H, C<u>H</u>*alkene*), 4.16 (t, *J*=7.0 Hz, 4H, N-C<u>H</u>$_2$-CH$_2$), 2.58 (t, *J*=6.0 Hz, 4H, C<u>H</u>$_2$-CH$_2$-SO$_3$), 2.47 (t, *J*=7.0 Hz, 4H, C<u>H</u>$_2$-CH$_2$), 1.91 (quin, *J*=7.0 Hz, 4H, CH$_2$-C<u>H</u>$_2$-CH$_2$), 1.78 (quin, *J*=6.0 Hz, 2H, CH$_2$-C<u>H</u>$_2$-CH$_2$), 1.17 (s, 12H, C-C<u>H</u>$_3$). IR (ATR) 2925, 1553, 1506, 1436, 1349, 1246, 1216, 1098, 903, 743 cm^{-1}. MS (ESI) m/z: 566 [M+2H]$^+$. UV abs λ$_{max}$ = 745 nm.

2-[(E)-2-[(3E)-3-{2-[(2E)-3,3-Dimethyl-1-(4-sulfonatobutyl)-2,3-dihydro-1H-indol-2-ylidene]ethylidene}-2-(phenylamino)cyclohex-1-en-1-yl]ethenyl]-3,3-dimethyl-1-(4-sulfonatobutyl)-3H-indol-1-ium (7f).
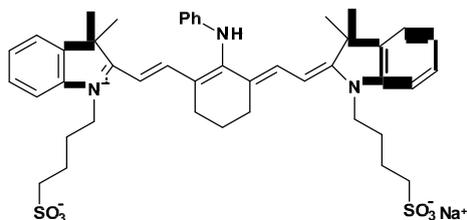
7f was synthesised as for **7a** using **4g** (0.07 g, 0.10 mmol), aniline (0.09 g, 1.00 mmol), and anhydrous DMF (10.0 mL). The solvent was removed under reduced pressure, the crude product was purified by column chromatography on silica gel (chloroform:methanol = 8:2) to afford a dark green solid **7f** (31 mg, 40%); m.p. 179-181 °C: ^{1}H NMR (d$_6$-DMSO, 400 MHz) δ 8.65 (br s, 1H, Ar-N<u>H</u>), 7.98 (d, *J*=14.0 Hz, 2H, C<u>H</u>*alkene*), 7.43 (d, *J*=7.0 Hz, 2H, Ar-<u>H</u>), 7.33-7.28 (m, 4H, Ar-<u>H</u>), 7.22 (t, *J*=8.0 Hz, 2H, Ar-<u>H</u>), 7.13-6.99 (m, 2H, Ar-<u>H</u>), 6.93 (d, *J*=7.0 Hz, 2H, Ar-<u>H</u>), 6.71 (d, *J*=7.0 Hz, 1H, Ar-<u>H</u>), 6.10 (d, *J*=14.0 Hz, 2H, C<u>H</u>*alkene*), 4.05 (t, 4H, *J*=7.0 Hz, N-C<u>H</u>$_2$-CH$_2$), 2.63 (t, *J*=6.0 Hz, 4H, CH$_2$-C<u>H</u>$_2$-SO$_3$), 2.47 (t, *J*=7.0 Hz, 4H, C<u>H</u>$_2$-CH$_2$), 1.89 (br s, 2H, CH$_2$-C<u>H</u>$_2$-CH$_2$), 1.71-1.63 (m, 8H, (C<u>H</u>$_2$)$_4$-CH$_2$-SO$_3$), 1.28 (s, 12H, C-C<u>H</u>$_3$). IR (ATR) 2928, 1508, 1437, 1366, 1097, 1101, 908, 790 cm^{-1}. MS (ESI) m/z: 784 [M+2H]$^+$. UV abs λ$_{max}$ = 745 nm.

1,1,3-Trimethyl-2-[(E)-2-[(3E)-2-(phenylamino)-3-{2-[(2E)-1,1,3-trimethyl-1H,2H,3H-benzo[e]indol-2-ylidene]ethylidene}cyclohex-1-en-1-yl]ethenyl]-1H-benzo[e]indol-3-ium iodide (8a).
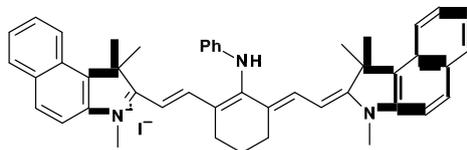
8a was synthesised as for **7a** using **6a** (0.07 g, 0.10 mmol), aniline (0.09 g, 1.00 mmol), and anhydrous DMF (10.0 mL). The solvent was removed under reduced pressure, the crude product was purified by column chromatography on silica gel (dichloromethane:methanol = 9:1) to afford a shiny dark blue solid **8a** (34 mg, 44%); m.p. 188-190 °C: ^{1}H NMR (d$_6$-DMSO, 300 MHz) δ 8.76 (br s, 1H, N$\underline{H}$), 8.37 (t, *J*=9.0 Hz, 2H, Ar-$\underline{H}$), 8.16 (d, *J*=9.0 Hz, 2H, Ar-$\underline{H}$), 7.77-7.67 (m, 4H, Ar-$\underline{H}$), 7.66-7.63 (m, 5H, Ar-$\underline{H}$), 7.46 (t, *J*=9.0 Hz, 2H, Ar-$\underline{H}$), 7.32 (t, *J*=9.0 Hz, 1H, Ar-$\underline{H}$), 7.25 (t, *J*=9.0 Hz, 2H, Ar-$\underline{H}$), 6.59 (d, *J*=12.0 Hz, 2H, C$\underline{H}_{alkene}$), 5.42 (d, *J*=12.0 Hz, 2H, C$\underline{H}_{alkene}$), 2.83-2.66 (m, 2H, CH$_2$-C$\underline{H}_2$-CH$_2$), 2.28 (t, *J*=6.0 Hz, 4H, CH$_2$-C$\underline{H}_2$), 1.90 (s, 6H, N-C$\underline{H}_3$), 1.20 (s, 12H, C-C$\underline{H}_3$). IR (ATR) 2992, 1515, 1441, 1350, 1228, 1011, 929, 747 cm^{-1}. MS (ESI) m/z: 638 [M]$^+$. HRMS(ESI): Calcd for C$_{46}$H$_{46}$N$_3$ [M]$^+$ 638.3530, found 638.3529. UV abs λ$_{max}$ = 780 nm.

3-Ethyl-2-[(E)-2-[(3E)-3-{2-[(2E)-3-ethyl-1,1-dimethyl-1H,2H,3H-benzo[e]indol-2-ylidene]ethylidene}-2-(phenylamino)cyclohex-1-en-1-yl]ethenyl]-1,1-dimethyl-1H-benzo[e]indol-3-ium iodide (8b).
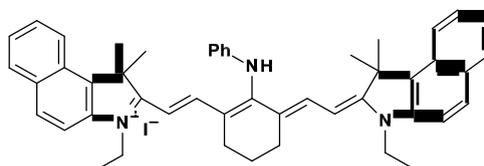
8b was synthesised as for **7a** using **6b** (0.07 g, 0.10 mmol), aniline (0.09 g, 1.00 mmol), and anhydrous DMF (10.0 mL). The solvent was removed under reduced pressure, the crude product was purified by column chromatography on silica gel (dichloromethane:methanol = 9:1) to afford a shiny dark blue solid **8b** (27 mg, 34%); m.p. 188-190 °C: ^{1}H NMR (d$_6$-

DMSO, 300 MHz) δ 8.74 (br s, 1H, N$\underline{H}$), 8.14-8.01 (m, 8H, Ar-$\underline{H}$), 7.67 (d, *J*=9.0 Hz, 2H, Ar-$\underline{H}$), 7.60 (t, *J*=9.0 Hz, 2H, Ar-$\underline{H}$), 7.47 (t, *J*=9.0 Hz, 2H, Ar-$\underline{H}$), 7.31 (d, *J*=15.0 Hz, 2H, C$\underline{H}_{alkene}$), 7.03 (d, *J*=9.0 Hz, 2H, Ar-$\underline{H}$), 6.79 (t, *J*=6.0 Hz, 1H, Ar-$\underline{H}$), 6.14 (d, *J*= 15.0 Hz, 2H, C$\underline{H}_{alkene}$), 4.25 (q, *J*=6.0 Hz, 4H, N-C$\underline{H}_2$-CH$_3$), 2.70 (t, *J*=6.0 Hz, 4H, CH$_2$-C$\underline{H}_2$), 1.96-1.87 (m, 2H, CH$_2$-C$\underline{H}_2$-CH$_2$), 1.62 (s, 12H, C-C$\underline{H}_3$), 1.32 (t, *J*=9.0 Hz, 6H, CH$_2$-C$\underline{H}_3$). IR (ATR) 2921, 1546, 1430, 1346, 1226, 1001, 901, cm^{-1}. MS (ESI) m/z: 668 [M]$^+$. HRMS(ESI): Calcd for C$_{48}$H$_{50}$N$_3$[M]$^+$ 668.3999, found 668.3993. UV abs λ$_{max}$ = 776 nm.

2-[(E)-2-[(3E)-3-{2-[(2E)-1,1-Dimethyl-3-propyl-1H,2H,3H-benzo[e]indol-2-ylidene]ethylidene}-2-(phenylamino)cyclohex-1-en-1-yl]ethenyl]-1,1-dimethyl-3-propyl-1H-benzo[e]indol-3-iumiodide (8c).
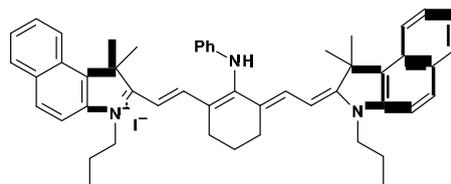
**8c** was synthesised as for **7a** using **6c** (0.08 g, 0.10 mmol), aniline (0.09 g, 1.00 mmol), and anhydrous DMF (10.0 mL). The solvent was removed under reduced pressure, the crude product was purified by column chromatography on silica gel (dichloromethane:methanol = 9:1) to afford a shiny dark blue solid **8c** (31 mg, 38%); m.p. 188-190 °C: ^{1}H NMR (d$_6$-DMSO, 300 MHz) δ 8.76 (br s, 1H, N$\underline{H}$), 8.13-8.07 (m, 4H, Ar-$\underline{H}$), 8.02-7.98 (m, 4H, Ar-$\underline{H}$), 7.68 (d, *J*=9.0 Hz, 2H, Ar-$\underline{H}$), 7.57 (t, *J*=9.0 Hz, 2H, Ar-$\underline{H}$), 7.46 (t, *J*=9.0 Hz, 2H, Ar-$\underline{H}$), 7.31 (d, *J*=15.0 Hz, 2H, C$\underline{H}_{alkene}$), 7.03 (d, *J*=9.0 Hz, 2H, Ar-$\underline{H}$), 6.78 (t, *J*=6.0 Hz, 1H, Ar-$\underline{H}$), 6.14 (d, *J*= 15.0 Hz, 2H, C$\underline{H}_{alkene}$), 4.20 (t, *J*=9.0 Hz, 4H, N-C$\underline{H}_2$-CH$_2$), 2.68 (t, *J*=6.0 Hz, 4H, CH$_2$-C$\underline{H}_2$), 1.92-180 (m, 2H, CH$_2$-C$\underline{H}_2$-CH$_2$), 1.78-1.61 (m, 4H, N-CH$_2$-C$\underline{H}_2$-CH$_3$), 0.97 (s, 12H, C-C$\underline{H}_3$), 0.97 (t, *J*=9.0 Hz, 6H, CH$_2$-C$\underline{H}_3$). IR (ATR) 2922, 1547, 1430, 1342, 1225, 1001, 897, 711 cm^{-1}. MS (ESI) m/z: 696 [M]$^+$. HRMS(FAB): Calcd for C$_{50}$H$_{54}$N$_3$[M]$^+$ 696.4312, found 696.4304. UV abs λ$_{max}$ = 778 nm.

3-Benzyl-2-[(E)-2-[(3E)-3-{2-[(2E)-3-benzyl-1,1-dimethyl-1H,2H,3H-benzo[e]indol-2-ylidene]ethylidene}-2-(phenylamino)cyclohex-1-en-1-yl]ethenyl]-1,1-dimethyl-1H-benzo[e]indol-3-ium bromide (8d).
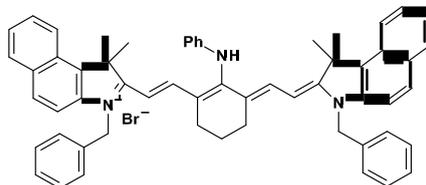
8d was synthesised as for **7a** using **6e** (0.06 g, 0.10 mmol), aniline (0.09 g, 1.00 mmol), and anhydrous DMF (10.0 mL). The solvent was removed under reduced pressure, the crude product was purified by column chromatography on silica gel (dichloromethane:methanol = 9:1) to afford a shiny dark blue solid **8d** (31 mg, 38%); m.p. 214-216 °C: ^{1}H NMR (d$_6$-DMSO, 300 MHz) δ 8.93 (brs, 1H, N$\underline{H}$), 8.32 (s, 1H, Ar-$\underline{H}$), 8.16 (d, *J*=9.0 Hz, 2H, Ar-$\underline{H}$), 8.08 (d, *J*=15.0 Hz, 2H, C$\underline{H}$$_{alkene}$), 7.99-7.90 (m, 4H, Ar-$\underline{H}$), 7.62-7.33 (m, 4H, Ar-$\underline{H}$), 7.46 (t, *J*=9.0 Hz, 2H, Ar-$\underline{H}$), 7.31-7.23 (m, 11H, Ar-$\underline{H}$), 7.03 (d, *J*=9.0 Hz, 2H, Ar-$\underline{H}$), 6.83 (t, *J*=6.0 Hz, 1H, Ar-$\underline{H}$), 6.11 (d, *J*= 15.0 Hz, 2H, C$\underline{H}$$_{alkene}$), 5.50 (br s, 4H, N-C$\underline{H}$$_2$-Ph), 2.64-2.56 (m, 4H, CH$_2$-C$\underline{H}$$_2$), 1.78 (quin, *J*=6.0 Hz, 2H, CH$_2$-C$\underline{H}$$_2$-CH$_2$), 1.65 (s, 12H, C-C$\underline{H}$$_3$). IR (ATR) 2924, 1592, 1433, 1345, 1271, 1093, 886, 664 cm^{-1}. MS (ESI) m/z: 792 [M]$^+$. HRMS(FAB): Calcd for C$_{58}$H$_{54}$N$_3$[M]$^+$ 792.4312, found 792.4307. UV abs λ$_{max}$ = 769 nm.

2-[(E)-2-[(3E)-3-{2-[(2E)-1,1-Dimethyl-3-(4-sulfonatobutyl)-1H,2H,3H-benzo[e]indol-2-ylidene]ethylidene}-2-(phenylamino)cyclohex-1-en-1-yl]ethenyl]-1,1-dimethyl-3-(4-sulfonatobutyl)-1H-benzo[e]indol-3-ium (8e).
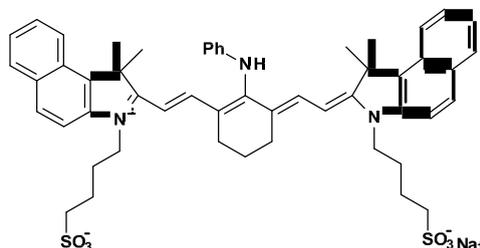
8e was synthesised as for **7a** using **6g** (0.08 g, 0.10 mmol), aniline (0.09 g, 1.00 mmol), and anhydrous DMF (10.0 mL). The solvent was removed under reduced pressure, the crude product was purified by column chromatography on silica gel (dichloromethane:methanol = 9:1) to afford a green solid **8e** (35 mg, 40%); m.p. 230-232 °C: ^{1}H NMR (d$_6$-DMSO, 300 MHz) δ 8.75 (brs, 1H, N$\underline{H}$), 8.12-8.08 (m, 4H, Ar-$\underline{H}$), 8.00 (d, *J*=6.0 Hz, 4H, Ar-$\underline{H}$), 7.69 (d, *J*=9.0 Hz, 2H, Ar-$\underline{H}$), 7.58 (t, *J*=15.0 Hz, 2H, C$\underline{H}$*$_{alkene}$*), 7.45 (t, *J*=9.0 Hz, 2H, Ar-$\underline{H}$), 7.30 (t, *J*=6.0 Hz, 2H, Ar-$\underline{H}$), 7.03 (d, *J*=9.0 Hz, 2H, Ar-$\underline{H}$), 6.77 (t, *J*=6.0 Hz, 1H, Ar-$\underline{H}$), 6.16 (d, *J*=15.0 Hz, 2H, C$\underline{H}$*$_{alkene}$*), 4.19 (t, *J*=6.0 Hz, 4H, N-C$\underline{H}_2$-CH$_2$), 2.73 (t, *J*=6.0 Hz, 4H, CH$_2$-C$\underline{H}_2$-SO$_3$), 2.48-2.35 (m, 4H, C$\underline{H}_2$-CH$_2$), 1.93-187 (m, 2H, CH$_2$-C$\underline{H}_2$-CH$_2$), 1.76-1.65 (m, 8H, C$\underline{H}_2$-(CH$_2$)$_4$-SO$_3$), 1.60 (s, 12H, C-C$\underline{H}_3$). IR (ATR) 2928, 1594, 1433, 1349, 1227, 1004, 886, 714 cm^{-1}. MS (ESI) m/z: 884 [M]$^+$. UV abs λ$_{max}$ = 779 nm.

***N*-(2,4-Dinitrophenyl) pyridinium chloride (PY1)** was synthesised according to a reported procedure [262].
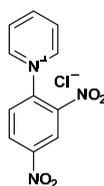
Pyridine (3.00 mL, 37.9 mmol) was dissolved in acetone (17.0 mL) and stirred, while 2,4-dinitrochlorobenzene (7.67 g, 37.9 mmol) was added to the reaction mixture. The mixture was heated under reflux overnight and then cooled to room temperature. The precipitate

produced was filtered under suction and washed with *n*-hexane to obtain **PY1** (8.10 g, 76%) as a pale yellow powder; m.p. 197-199 °C, literature m.p. 197-200 °C [262]: ^{1}H NMR (d₆-DMSO, 250 MHz) δ 9.43 (d, *J*=6.0 Hz, 2H, Ar-<u>H</u>), 9.21 (s, 1H, Ar-<u>H</u>), 8.95 (t, *J*=7.0 Hz, 2H, Ar-<u>H</u>), 8.50-8.41 (m, 3H, Ar-<u>H</u>). ^{13}C NMR (d₆-DMSO, 68.2 MHz) δ 149.1, 148.9, 146.1, 143.1, 138.8, 132.0, 130.3, 128.1, 121.4. IR (ATR) 2971, 1540, 1474, 1341, 1266, 1154, 943, 855, 739 cm^{-1}. MS (ESI) m/z: 246 [M]$^+$.

N-(2,4-Dinitrophenyl)-3-methylpyridinium chloride (PY2).
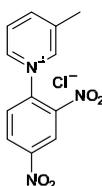
PY2 was synthesised as for **PY1** using 3-picoline (2.00 mL, 21.0 mmol) and 2,4-dinitrochlorobenzene (4.00 g, 19.7 mmol) to give the product **PY2** (4.00 g, 69%) as a pale purple powder; m.p. 206-208 °C, literature m.p. 206-207 °C [263] : ^{1}H NMR (d₆-DMSO, 250 MHz) δ 9.44 (s, 1H, Ar-<u>H</u>), 9.35 (d, *J*=6.0 Hz, 1H, Ar-<u>H</u>), 9.12 (d, *J*=3.0 Hz, 1H, Ar-<u>H</u>), 9.01-8.97 (m, 1H, Ar-<u>H</u>), 8.83 (d, *J*=8.0 Hz, 1H, Ar-<u>H</u>), 8.49 (d, *J*=8.0 Hz, 1H, Ar-<u>H</u>), 8.38-8.33 (m, 1H, Ar-<u>H</u>), 2.59 (s, 3H, C<u>H</u>₃). ^{13}C NMR (d₆-DMSO, 62.8 MHz) δ 149.6, 145.9, 143.9, 143.5, 139.3, 139.2, 132.5, 130.8, 127.8, 122.0, 41.0. IR (ATR) 2959, 1570, 1455, 1356, 1274, 1134, 952, 867, 726 cm^{-1}. MS (ESI) m/z: 260 [M]$^+$.

N-(2,4-Dinitrophenyl)-4-phenylpyridinium chloride (PY5).
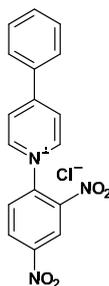
PY5 was synthesised as for **PY1** using 4-phenylpyridrine (2.74 g, 17.7 mmol) and 2,4-dinitrochlorobenzene (3.57 g, 17.7 mmol) to give the product **PY5** (5.12 g, 81%) as a pale yellow powder; m.p. 185-187 °C, literature m.p. 186-187 °C [264]: ^{1}H NMR (d$_6$-DMSO, 400 MHz) δ 9.43 (d, *J*=7.0 Hz, 2H, Ar-H), 9.08 (s, *J*=6.0 Hz, 1H, Ar-H), 8.95-8.92 (m, 1H, Ar-H), 8.82 (d, *J*=7.0 Hz, 2H, Ar-H), 8.45 (d, *J*=8.0 Hz, 1H, Ar-H), 8.23-8.20 (m, 2H, Ar-H), 7.71-7.64 (m, 3H, Ar-H). IR (ATR) 2960, 1557, 1462, 1367, 1258, 1151, 949, 850, 754 cm^{-1}. MS (ESI) m/z: 322 [M]$^+$.

3-Bromo-1-(2,4-dinitrophenyl) pyridinium chloride (PY3).
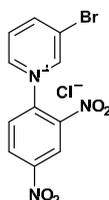
PY3 was synthesised as for **PY1** using 3-bromopyridrine (2.00 mL, 21.0 mmol) and 2,4-dinitrochlorobenzene (4.00 g, 19.7 mmol) to give the product **PY3** (5.60 g, 79%) as a yellow solid; m.p. 143-145 °C: ^{1}H NMR (d$_6$-DMSO, 300 MHz) δ 8.88 (d, *J*=3.0 Hz, 1H, Ar-H), 8.66 (s, 1H, Ar-H), 8.54 (d, *J*=6.0 Hz, 1H, Ar-H), 8.52-8.49 (m, 1H, Ar-H), 8.06-7.99 (m, 2H, Ar-H), 7.38-7.34 (m, 1H, Ar-H). ^{13}C NMR (d$_6$-DMSO, 75.4 MHz) δ 150.7, 148.5, 147.8, 146.7, 139.2, 132.2, 128.4, 127.8, 126.0, 121.2, 120.9. IR (ATR) 2949, 1570, 1485, 1355, 1271, 1162, 965, 873, 767 cm^{-1}. MS (ESI) m/z: 325 [M]$^+$.

3-Chloro-1-(2,4-dinitrophenyl) pyridinium chloride (PY4).
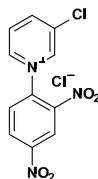
PY4 was synthesised as for **PY1** using 3-chloropyridrine (2.00 mL, 21.0 mmol) and 2,4-dinitrochlorobenzene (4.00 g, 19.7 mmol) to give the product **PY4** (4.93 g, 79%) as a yellow solid; m.p. 146-148 °C: ^{1}H NMR (d$_6$-DMSO, 300 MHz) δ 8.92 (d, J=3.0 Hz, 1H, Ar-$\underline{H}$), 8.59 (s, 1H, Ar-$\underline{H}$), 8.55-8.52 (m, 2H, Ar-$\underline{H}$), 7.92-7,89 (m, 2H, Ar-$\underline{H}$), 7.48-7.43 (m, 1H, Ar-$\underline{H}$). ^{13}C NMR (d$_6$-DMSO, 75.4 MHz) δ 148.5, 148.1, 147.7, 146.6, 136.3, 133.5, 132.2, 131.6, 128.3, 125.3, 121.4. IR (ATR) 2988, 1523, 1469, 1256, 1124, 968, 852, 748 cm^{-1}. MS (ESI) m/z: 280 [M]$^+$.

1,3,3-Trimethyl-2-[(1E,3E,5E)-7-[(2E)-1,3,3-trimethyl-2,3-dihydro-1H-indol-;2-ylidene]hepta-1,3,5-trien-1-yl]-3H-indol-1-ium iodide (9a).
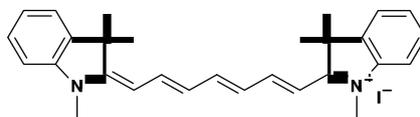
To a solution of *N*-(2,4-dinitrophenyl) pyridinium chloride (0.22 g, 0.80 mmol) in EtOH (10.0 mL) was added **1a** (0.60 g, 2.00 mmol). The reaction mixture was stirred for 5 mins, and then followed by the addition of sodium acetate (0.41 g, 5.00 mmol). The reaction was stirred at room temperature overnight and 20.0 mL *n*-hexane added. The precipitate produced was filtered under suction and washed with *n*-hexane. The crude product was purified by silica gel column chromatography (solvent; chloroform:methanol = 9:1) to obtain cyanine dye **9a** (0.12 g, 28%) as a green solid; m.p. 178-180 °C: ^{1}H NMR (d$_6$-DMSO, 400 MHz) δ 7.89 (t, J=13.0 Hz, 2H, C$\underline{H}_{alkene}$), 7.79 (t, J=13.0 Hz, 1H, C$\underline{H}_{alkene}$), 7.58 (d, J=7.0 Hz, 2H, Ar-$\underline{H}$), 7.41-7.35 (m, 4H, Ar-$\underline{H}$), 7.24 (t, J=6.0 Hz, 2H, Ar-$\underline{H}$), 6.51 (t, J=13.0 Hz, 2H, C$\underline{H}_{alkene}$), 6.32 (d, J=13.0 Hz, 2H, C$\underline{H}_{alkene}$), 3.62 (s, 6H, N-C$\underline{H}_3$), 1.63 (s, 12H, C-C$\underline{H}_3$). IR (ATR) 2924, 1597, 1438, 1384, 1308, 1141, 987, 887, 740 cm^{-1}. MS (ESI) m/z: 409 [M]$^+$. UV abs λ_{max} = 740 nm.

1-Ethyl-2-[(1E,3E,5E)-7-[(2E)-1-ethyl-3,3-dimethyl-2,3-dihydro-1H-indol-2-ylidene]hepta-1,3,5-trien-1-yl]-3,3-dimethyl-3H-indol-1-ium iodide (9b).
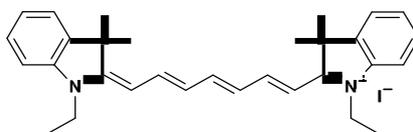
9b was synthesised as for **9a** using **PY1** (0.22 g, 0.80 mmol) and anhydrous sodium acetate (0.41 g, 5.00 mmol) in EtOH (10.0 mL) with **1b** (0.58 g, 2.00 mmol) to give the crude product which was purified by silica gel column chromatography (solvent; chloroform: methanol=9:1) to obtain cyanine dye **9b** (0.21 g, 47%) as a shiny green solid; m.p. 188-190 °C: ^{1}H NMR (d$_6$-DMSO, 400 MHz) δ 7.91 (t, *J*=13.0 Hz, 2H, C$\underline{H}_{alkene}$), 7.79 (t, *J*=13.0 Hz, 1H, C$\underline{H}_{alkene}$), 7.59 (d, *J*=7.0 Hz, 2H, Ar-$\underline{H}$), 7.42-7.36 (m, 4H, Ar-$\underline{H}$), 7.24 (t, *J*=6.0 Hz, 2H, Ar-$\underline{H}$), 6.56 (t, *J*=13.0 Hz, 2H, C$\underline{H}_{alkene}$), 6.38 (d, *J*=13.0 Hz, 2H, C$\underline{H}_{alkene}$), 4.14 (q, *J*=6.0 Hz, 4H, N-C$\underline{H}_2$-CH$_3$), 1.62 (s, 12H, C-C$\underline{H}_3$), 1.34 (t, *J*=7.0 Hz, 6H, CH$_2$-C$\underline{H}_3$). IR (ATR) 2962, 1595, 1509, 1394, 1192, 1089, 882, 739 cm^{-1}. MS (ESI) m/z: 437 [M]$^+$. UV abs λ$_{max}$ = 742 nm.

2-[(1E,3E,5E)-7-[(2E)-3,3-Dimethyl-1-propyl-2,3-dihydro-1H-indol-2-ylidene]hepta-1,3,5-trien-1-yl]-3,3-dimethyl-1-propyl-3H-indol-1-ium iodide (9c).
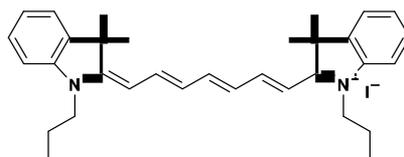
9c was synthesised as for **9a** using **PY1** (0.22 g, 0.80 mmol) and anhydrous sodium acetate (0.41 g, 5.00 mmol) in EtOH (10.0 mL) with **1c** (0.66 g, 2.00 mmol) to give the crude product which was purified by silica gel column chromatography (solvent; chloroform: methanol=9:1) to obtain cyanine dye **9c** (0.31 g, 66%) as a shiny green solid; m.p. 166-168 °C: ^{1}H NMR (d$_6$-DMSO, 400 MHz) δ 7.91 (t, *J*=13.0 Hz, 2H, C$\underline{H}_{alkene}$), 7.75 (d, *J*=14.0 Hz, 1H, C$\underline{H}_{alkene}$), 7.59 (d, *J*=7.0 Hz, 2H, Ar-$\underline{H}$), 7.39-7.38 (m, 4H, Ar-H), 7.24-7.20 (m, 2H, Ar-$\underline{H}$), 6.57 (d, *J*=13.0 Hz, 2H, C$\underline{H}_{alkene}$), 6.40 (t, *J*=14.0 Hz, 2H, C$\underline{H}_{alkene}$), 4.06 (t, *J*=7.0 Hz, 4H, N-C$\underline{H}_2$-CH$_2$), 1.74 (quin, *J*=7.0 Hz, 4H, CH$_2$-C$\underline{H}_2$-CH$_3$), 1.63 (s, 12H, C-C$\underline{H}_3$), 0.97 (t, *J*=7.0

Hz, 6H, CH$_2$-C$\underline{H}_3$). IR (ATR) 2957, 1601, 1508, 1397, 1312, 1191, 1144, 960, 877, 783 cm^{-1}. MS (ESI) m/z: 465 [M]$^+$. UV abs λ_{max} = 746 nm.

1-Butyl-2-[(1E,3E,5E)-7-[(2E)-1-butyl-3,3-dimethyl-2,3-dihydro-1H-indol-2-ylidene]hepta-1,3,5-trien-1-yl]-3,3-dimethyl-3H-indol-1-ium iodide (9d).
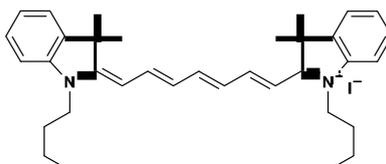
9d was synthesised as for **9a** using **PY1** (0.22 g, 0.80 mmol) and anhydrous sodium acetate (0.41 g, 5.00 mmol) in EtOH (10.0 mL) with **1d** (0.69 g, 2.00 mmol) to give the crude product which was purified by silica gel column chromatography (solvent; chloroform: methanol=9:1) to obtain cyanine dye **9d** (0.15 g, 31%) as a green solid; m.p. 169-171 °C: ^{1}H NMR (d$_6$-DMSO, 300 MHz) δ 7.92 (t, *J*=13.0 Hz, 2H, C$\underline{H}_{alkene}$), 7.80 (d, *J*=13.0 Hz, 1H, C$\underline{H}_{alkene}$), 7.60 (d, *J*=6.0 Hz, 2H, Ar-$\underline{H}$), 7.39-7.35 (m, 4H, Ar-H), 7.25-7.20 (m, 2H, Ar-$\underline{H}$), 6.58 (t, *J*=13.0 Hz, 2H, C$\underline{H}_{alkene}$), 6.40 (d, *J*=13.0 Hz, 2H, C$\underline{H}_{alkene}$), 4.10 (t, *J*=9.0 Hz, 4H, N-C$\underline{H}_2$-CH$_2$), 1.69 (quin, *J*=9.0 Hz, 4H, CH$_2$-C$\underline{H}_2$-CH$_2$), 1.63 (s, 12H, C-CH$_3$), 1.43 (sex, *J*=9.0 Hz, 4H, CH$_2$-C$\underline{H}_2$-CH$_3$), 0.95 (t, *J*=6.0 Hz, 6H, CH$_2$-C$\underline{H}_3$). IR (ATR) 2920, 1595, 1508, 1401, 1316, 1217, 1144, 985, 893, 783 cm^{-1}. MS (ESI) m/z: 493 [M]$^+$. UV abs λ_{max} = 746 nm.

1-Benzyl-2-[(1E,3E,5E)-7-[(2E)-1-benzyl-3,3-dimethyl-2,3-dihydro-1H-indol-2-ylidene]hepta-1,3,5-trien-1-yl]-3,3-dimethyl-3H-indol-1-ium bromide (9e).
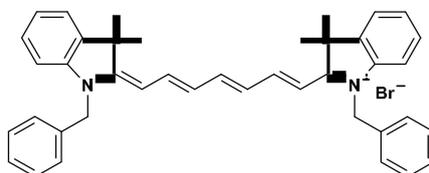
9e was synthesised as for **9a** using **PY1** (0.22 g, 0.80 mmol) and anhydrous sodium acetate (0.41 g, 5.00 mmol) in EtOH (10.0 mL) with **1k** (0.66 g, 2.00 mmol) to give the crude product which was purified by silica gel column chromatography (solvent; chloroform:

methanol=9:1) to obtain cyanine dye **9e** (0.11 g, 21%) as a shiny purple solid; m.p. 170-172 °C: ^{1}H NMR (d$_6$-DMSO, 400 MHz) δ 8.34 (t, *J*=13.0 Hz, 2H, C$\underline{H}_{alkene}$), 7.61 (d, *J*=7.0 Hz, 2H, Ar-$\underline{H}$), 7.32-7.25 (m, 8H, Ar-$\underline{H}$), 7.23-6.99 (m, 10H, Ar-$\underline{H}$), 6.90 (d, *J*=9.0 Hz, 1H, Ar-$\underline{H}$), 6.40 (d, *J*=13.0 Hz, 2H, C$\underline{H}_{alkene}$), 5.34 (s, 4H, Ph-C$\underline{H}_2$), 1.67 (s, 12H, C-C$\underline{H}_3$). IR (ATR) 2971, 1598, 1507, 1397, 1060, 983, 893, 738 cm^{-1}. MS (ESI) m/z: 561 [M]$^+$. UV abs λ$_{max}$ = 748 nm.

2-[(1E,3E,5E)-7-[(2E)-3,3-Dimethyl-1-(3-sulfonatopropyl)-2,3-dihydro-1H-indol-2-ylidene]hepta-1,3,5-trien-1-yl]-3,3-dimethyl-1-(3-sulfonatopropyl)-3H-indol-1-ium (9f).
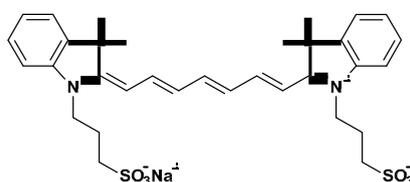
9f was synthesised as for **9a** using **PY1** (0.22 g, 0.80 mmol) and anhydrous sodium acetate (0.41 g, 5.00 mmol) in EtOH (10.0 mL) with **1l** (0.56 g, 2.00 mmol) to give the crude product which was purified by silica gel column chromatography (solvent; chloroform: methanol=7:3) to obtain cyanine dye **9f** (0.30 g, 60%) as a green solid; m.p. 220-222 °C: ^{1}H NMR (d$_6$-DMSO, 400 MHz) δ 8.26 (t, *J*=13.0 Hz, 2H, C$\underline{H}_{alkene}$), 7.51-7.42 (m, 2H, Ar-$\underline{H}$), 7.39 (t, *J*=7.0 Hz, 2H, Ar-$\underline{H}$), 7.27-7.18 (t, *J*=7.0 Hz, 3H, Ar-$\underline{H}$), 7.11 (t, *J*=7.0 Hz, 2H, Ar-$\underline{H}$), 6.44 (t, *J*=13.0 Hz, 2H, C$\underline{H}_{alkene}$), 6.29 (d, *J*=13.0 Hz, 2H, C$\underline{H}_{alkene}$), 4.12-3.87 (m, 4H, N-C$\underline{H}_2$), 2.46-2.32 (m, 4H, C$\underline{H}_2$-SO$_3$), 1.85-1.72 (m, 4H, C$\underline{H}_2$-CH$_2$-SO$_3$), 1.56 (s, 12H, C-C$\underline{H}_3$). IR (ATR) 2975, 2361, 1600, 1451, 1381, 1336, 1033, 924, 749 cm^{-1}. MS (ESI) m/z: 623 [M+2H]$^+$. UV abs λ$_{max}$ = 747 nm.

2-[(1E,3E,5E)-7-[(2E)-3,3-Dimethyl-1-(4-sulfonatobutyl)-2,3-dihydro-1H-indol-2-ylidene]hepta-1,3,5-trien-1-yl]-3,3-dimethyl-1-(4-sulfonatobutyl)-3H-indol-1-ium (9g).
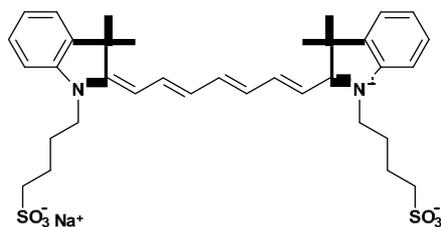
9g was synthesised as for **9a** using **PY1** (0.22 g, 0.80 mmol) and anhydrous sodium acetate (0.41 g, 5.00 mmol) in EtOH (10.0 mL) with **1m** (0.59 g, 2.00 mmol) to give the crude product which was purified by silica gel column chromatography (solvent; chloroform: methanol=7:3) to obtain cyanine dye **9g** (0.38 g, 73%) as a green solid; m.p. 221-223 °C: ^{1}H NMR (d$_6$-DMSO, 400 MHz) δ 7.90 (t, *J*=13.0 Hz, 2H, C$\underline{H}$$_{alkene}$), 7.80-7.44 (m, 1H, Ar-$\underline{H}$), 7.57 (d, *J*=7.0 Hz, 2H, Ar-$\underline{H}$), 7.41-7.35 (m, 4H, Ar-H), 7.23 (t, *J*=8.0 Hz, 2H, Ar-$\underline{H}$), 6.58 (t, *J*=13.0 Hz, 2H, C$\underline{H}$$_{alkene}$), 6.44 (d, *J*=13.0 Hz, 2H, C$\underline{H}$$_{alkene}$), 4.06 (t, *J*=7.0 Hz, 4H, N-C$\underline{H}$$_2$-CH$_2$), 2.47 (t, *J*=7.0 Hz, 4H, C$\underline{H}$$_2$-CH$_2$-SO$_3$), 1.74-1.66 (m, 8H, (C$\underline{H}$$_2$)$_4$-CH$_2$-SO$_3$) 1.62 (s, 12H, C-C$\underline{H}$$_3$). IR (ATR) 2924, 1597, 1509, 1317, 1158, 966, 741 cm^{-1}. MS (ESI) m/z: 653 [M+2H]$^+$. UV abs λ$_{max}$ = 747 nm.

3-Methyl-2-[(1E,3E,5E)-7-[(2Z)-3-methyl-2,3-dihydro-1,3-benzothiazol-2-ylidene]hepta-1,3,5-trien-1-yl]-1,3-benzothiazol-3-ium iodide (10a).

10a was synthesised as for **9a** using **PY1** (0.22 g, 0.80 mmol) and anhydrous sodium acetate (0.41 g, 5.00 mmol) in EtOH (10.0 mL) with **2a** (0.58 g, 2.00 mmol) to give the crude product which was purified by silica gel column chromatography (solvent; chloroform: methanol=9:1) to obtain cyanine dye **10a** (0.32 g, 78%) as a green solid; m.p. 210-212 °C: ^{1}H NMR (d$_6$-DMSO, 400 MHz) δ 7.95 (d, *J*=7.0 Hz, 2H, Ar-$\underline{H}$), 7.67 (d, *J*=8.0 Hz, 2H, Ar-$\underline{H}$), 7.53 (t, *J*=7.0 Hz, 2H, Ar-$\underline{H}$), 7.43-7.35 (m, 5H, Ar-H), 6.54 (d, *J*=13.0 Hz, 2H, C$\underline{H}$$_{alkene}$),
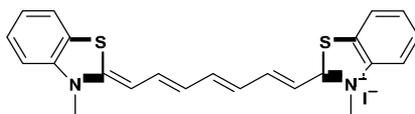
6.48 (t, *J*=13.0 Hz, 2H, C$\underline{H}_{alkene}$), 3.77 (s, 6H, N-C$\underline{H}_3$). IR (ATR) 1543, 1518, 1356, 1232, 1081, 887, 764, 615 cm^{-1}. MS (ESI) m/z: 389 [M]$^+$. UV abs λ_{max} = 756 nm.

3-Ethyl-2-[(1E,3E,5E)-7-[(2Z)-3-ethyl-2,3-dihydro-1,3-benzothiazol-2-ylidene]hepta-1,3,5-trien-1-yl]-1,3-benzothiazol-3-ium iodide (10b).
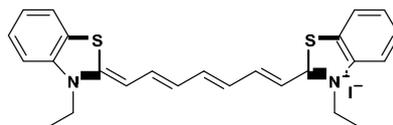
10b was synthesised as for **9a** using **PY1** (0.22 g, 0.80 mmol) and anhydrous sodium acetate (0.41 g, 5.00 mmol) in EtOH (10.0 mL) with **2b** (0.61 g, 2.00 mmol) to give the crude product which was purified by silica gel column chromatography (solvent; chloroform: methanol=9:1) to obtain cyanine dye **10b** (0.20 g, 46%) as a green solid; m.p. 216-218 °C: ^{1}H NMR (d$_6$-DMSO, 400 MHz) δ 7.95 (d, *J*=7.0 Hz, 2H, Ar-$\underline{H}$), 7.68 (d, *J*=6.0 Hz, 2H, Ar-$\underline{H}$), 7.54 (t, *J*=6.0 Hz, 2H, Ar-$\underline{H}$), 7.43-7.32 (m, 5H, Ar-H), 6.58 (d, *J*=13.0 Hz, 2H, C$\underline{H}_{alkene}$), 6.45 (t, *J*=13.0 Hz, 2H, C$\underline{H}_{alkene}$), 4.36 (q, *J*=6.0 Hz, 4H, N-C$\underline{H}_2$-CH$_3$), 1.30 (t, *J*=7.0 Hz, 6H, CH$_2$-C$\underline{H}_3$). IR (ATR) 2971, 1579, 1507, 1396, 1059, 983, 830, 738 cm^{-1}. MS (ESI) m/z: 417 [M]$^+$. UV abs λ_{max} = 759 nm.

3-Propyl-2-[(1E,3E,5E)-7-[(2Z)-3-propyl-2,3-dihydro-1,3-benzothiazol-2-ylidene]hepta-1,3,5-trien-1-yl]-1,3-benzothiazol-3-ium iodide (10c).
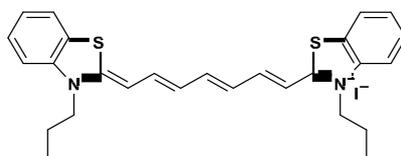
10c was synthesised as for **10a** using **PY1** (0.22 g, 0.80 mmol) and anhydrous sodium acetate (0.41 g, 5.00 mmol) in EtOH (10.0 mL) with **2c** (0.64 g, 2.00 mmol) to give the crude product which was purified by silica gel column chromatography (solvent; chloroform: methanol=9:1) to obtain cyanine dye **10c** (0.30 g, 66%) as a green solid; m.p. 193-195 °C: ^{1}H NMR (d$_6$-DMSO, 400 MHz) δ 7.95 (d, *J*=7.0 Hz, 2H, Ar-$\underline{H}$), 7.71 (d, *J*=8.0 Hz, 2H, Ar-$\underline{H}$),

7.53 (d, *J*=7.0 Hz, 2H, Ar-<u>H</u>), 7.44 (d, *J*=13.0 Hz, 2H, C<u>H</u>*alkene*), 7.37-733 (m, 3H, Ar-<u>H</u>), 6.60 (d, *J*=13.0 Hz, 2H, C<u>H</u>*alkene*), 6.40 (t, *J*=13.0 Hz, 2H, C<u>H</u>*alkene*), 4.27 (t, *J*=7.0 Hz, 4H, N-C<u>H</u>$_2$-CH$_2$), 1.75 (quin, *J*=7.0 Hz, 4H, CH$_2$-C<u>H</u>$_2$-CH$_3$), 0.97 (t, *J*=7.0 Hz, 6H, CH$_2$-C<u>H</u>$_3$). IR (ATR) 2960, 1579, 1500, 1393, 1324, 970, 805, 743 cm^{-1}. MS (ESI) m/z: 445 [M]$^+$. HRMS(FAB): Calcd for C$_{27}$H$_{29}$N$_2$S$_2$ [M]$^+$ 445.1766, found 445.1758. UV abs λ_{max} = 761 nm.

3-Butyl-2-[(1E,3E,5E)-7-[(2Z)-3-butyl-2,3-dihydro-1,3-benzothiazol-2-ylidene]hepta-1,3,5-trien-1-yl]-1,3-benzothiazol-3-ium iodide (10d).
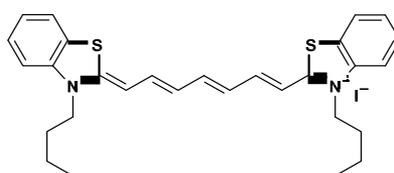
10d was synthesised as for **9a** using **PY1** (0.22 g, 0.80 mmol) and anhydrous sodium acetate (0.41 g, 5.00 mmol) in EtOH (10.0 mL) with **2d** (0.67 g, 2.00 mmol) to give the crude product which was purified by silica gel column chromatography (solvent; chloroform: methanol=9:1) to obtain cyanine dye **10d** (0.21 g, 44%) as a green solid; m.p. 176-178 °C: ^{1}H NMR (d$_6$-DMSO, 300 MHz) δ 7.98 (d, *J*=9.0 Hz, 2H, Ar-<u>H</u>), 7.71 (d, *J*=9.0 Hz, 2H, Ar-<u>H</u>), 7.57 (t, *J*=12.0 Hz, 2H, C<u>H</u>*alkene*), 7.47-7.35 (m, 5H, Ar-<u>H</u>), 6.60 (d, *J*=12.0 Hz, 2H, C<u>H</u>*alkene*), 6.49 (t, *J*=12.0 Hz, 2H, C<u>H</u>*alkene*), 4.33 (t, *J*=6.0 Hz, 4H, N-C<u>H</u>$_2$-CH$_2$), 1.71 (quin, *J*=6.0 Hz, 4H, CH$_2$-C<u>H</u>$_2$-CH$_3$), 1.47-1.37 (m, 4H, CH$_2$-C<u>H</u>$_2$-CH$_3$), 0.95 (t, *J*=6.0 Hz, 6H, CH$_2$-C<u>H</u>$_3$). IR (ATR) 2951, 1501, 1451, 1391, 1320, 1051, 918, 821, 737 cm^{-1}. MS (ESI) m/z: 473 [M]$^+$. UV abs λ_{max} = 761 nm.

3-Benzyl-2-[(1E,3E,5E)-7-[(2Z)-3-benzyl-2,3-dihydro-1,3-benzothiazol-2-ylidene]hepta-1,3,5-trien-1-yl]-1,3-benzothiazol-3-ium bromide (10e).
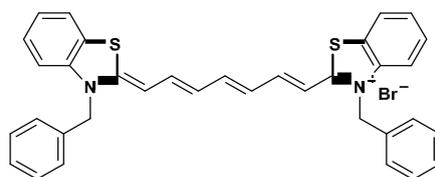
10e was synthesised as for **9a** using **PY1** (0.22 g, 0.80 mmol) and anhydrous sodium acetate (0.41 g, 5.00 mmol) in EtOH (10.0 mL) with **2k** (0.64 g, 2.00 mmol) to give the crude product which was purified by silica gel column chromatography (solvent; chloroform: methanol=8:2) to obtain cyanine dye **10e** (0.30 g, 60%) as a green solid; m.p. 209-211 °C: ^{1}H NMR (d$_6$-DMSO, 400 MHz) δ 8.02 (d, *J*=7.0 Hz, 2H, Ar-H), 7.65 (d, *J*=8.0 Hz, 2H, Ar-H), 7.52-7.36 (m, 11H, Ar-H), 7.33 (t, *J*=8.0 Hz, 2H, Ar-H), 7.26 (d, *J*=7.0 Hz, 4H, Ar-H), 6.64 (d, *J*=13.0 Hz, 2H, CH$_{alkene}$), 6.31 (t, *J*=13.0 Hz, 2H, CH$_{alkene}$), 5.64 (br s, 4H, Ph-CH$_2$). IR (ATR) 2979, 1582, 1504, 1459, 1328, 1114, 994, 814, 732 cm^{-1}. MS (ESI) m/z: 541 [M]$^+$. HRMS(ESI): Calcd for C$_{35}$H$_{29}$N$_2$S$_2$ [M]$^+$. 541.1766, found 541.1756. UV abs λ_{max} = 765 nm.

3-(3-Sulfonatopropyl)-2-[(1E,3E,5E)-7-[(2Z)-3-(3-sulfonatopropyl)-2,3-dihydro-1,3-benzothiazol-2-ylidene]hepta-1,3,5-trien-1-yl]-1,3-benzothiazol-3-ium (10f).
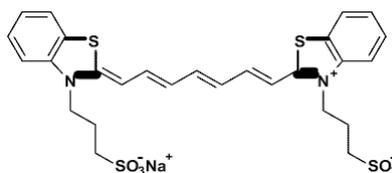
10f was synthesised as for **9a** using **PY1** (0.22 g, 0.80 mmol) and anhydrous sodium acetate (0.41 g, 5.00 mmol) in EtOH (10.0 mL) with **2l** (0.54 g, 2.00 mmol) to give the crude product which was purified by silica gel column chromatography (solvent; chloroform: methanol=7:3) to obtain cyanine dye **10f** (0.22 g, 46%) as a green solid; m.p. 225-227 °C: ^{1}H NMR (d$_6$-DMSO, 400 MHz) δ 7.95 (d, *J*=7.0 Hz, 2H, Ar-H), 7.79 (d, *J*=8.0 Hz, 2H, Ar-H), 7.55 (t, *J*=8.0 Hz, 2H, Ar-H), 7.44-7.34 (m, 5H, Ar-H), 6.69 (d, *J*=13.0 Hz, 2H, CH$_{alkene}$), 6.44 (t, *J*=13.0 Hz, 2H, CH$_{alkene}$), 4.48 (t, *J*=8.0 Hz, 4H, N-CH$_2$-CH$_2$), 2.58 (t, *J*=7.0 Hz, 4H, CH$_2$-CH$_2$-SO$_3$), 2.03 (quin, *J*=8.0 Hz, 4H, CH$_2$ CH$_2$-CH$_2$). IR (ATR) 3398, 2361, 1581, 1504,

1405, 1329, 1091, 993, 749 cm^{-1}. MS (ESI) m/z: 603 [M+2H]$^+$. HRMS(ESI): Calcd for C$_{27}$H$_{27}$N$_2$O$_6$S$_4$ [M+2H]$^+$. 603.0757, found 603.0742. UV abs λ_{max} = 762 nm.

3-(4-Sulfonatobutyl)-2-[(1E,3E,5E)-7-[(2Z)-3-(4-sulfonatobutyl)-2,3-dihydro-1,3-benzothiazol-2-ylidene]hepta-1,3,5-trien-1-yl]-1,3-benzothiazol-3-ium (10g).
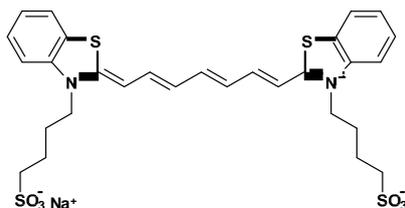

10g was synthesised as for **9a** using **PY1** (0.22 g, 0.80 mmol) and anhydrous sodium acetate (0.41 g, 5.00 mmol) in EtOH (10.0 mL) with **2m** (0.57 g, 2.00 mmol) to give the crude product which was purified by silica gel column chromatography (solvent; chloroform: methanol=7:3) to obtain cyanine dye **10g** (0.23 g, 47%) as a green solid; m.p. 228-230 °C: ^{1}H NMR (d$_6$-DMSO, 400 MHz) δ 7.94 (d, *J*=8.0 Hz, 2H, Ar-<u>H</u>), 7.78 (d, *J*=8.0 Hz, 2H, Ar-<u>H</u>), 7.53 (t, *J*=8.0 Hz, 2H, Ar-<u>H</u>), 7.43-7.33 (m, 5H, Ar-H), 6.68 (d, *J*=13.0 Hz, 2H, C<u>H</u>*alkene*), 6.42 (d, *J*=13.0 Hz, 2H, C<u>H</u>*alkene*), 4.06-3.87 (m, 4H, N-C<u>H</u>$_2$-CH$_2$), 2.56 (t, *J*=8.0 Hz 4H, CH$_2$-C<u>H</u>$_2$-SO$_3$), 2.41-2.06 (m, 4H, N-CH$_2$-C<u>H</u>$_2$), 1.91-1.65 (m, 4H, C<u>H</u>$_2$-CH$_2$-SO$_3$-). IR (ATR) 3405, 2361, 1683, 1505, 1400, 1328, 1074, 978, 742 cm^{-1}. MS (ESI) m/z: 631 [M+2H]$^+$. UV abs λ_{max} = 762 nm.

1,1,3-Trimethyl-2-[(1E,3E,5E)-7-[(2E)-1,1,3-trimethyl-1H,2H,3H-benzo[e]indol-2-ylidene]hepta-1,3,5-trien-1-yl]-1H-benzo[e]indol-3-ium iodide (11a).
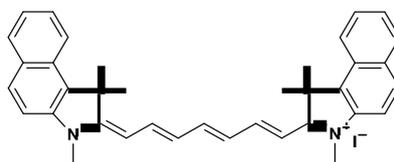
11a was synthesised as for **9a** using **PY1** (0.22 g, 0.80 mmol) and anhydrous sodium acetate (0.41 g, 5.00 mmol) in EtOH (10.0 mL) with **3a** (0.70 g, 2.00 mmol) to give the crude product which was purified by silica gel column chromatography (solvent; chloroform:

methanol=9:1) to obtain cyanine dye **11a** (0.19 g, 37%) as a green solid; m.p. 176-178 °C: ^{1}H NMR (d$_6$-DMSO, 300 MHz) δ 8.27 (d, *J*=9.0 Hz, 2H Ar-<u>H</u>), 8.09-8.02 (m, 5H, Ar-<u>H</u>), 7.98 (t, *J*=13.0 Hz, 1H, C<u>H</u>*alkene*), 7.83 (t, *J*=13.0 Hz, 1H, C<u>H</u>*alkene*), 7.74 (d, *J*=9.0 Hz, 2H, Ar-<u>H</u>), 7.67 (t, *J*=6.0 Hz, 2H, Ar-<u>H</u>), 7.52 (t, *J*=6.0 Hz, 2H, Ar-<u>H</u>), 6.61 (t, *J*=13.0 Hz, 2H, C<u>H</u>*alkene*), 6.44 (d, *J*=14.0 Hz, 2H, C<u>H</u>*alkene*), 3.70 (br s, 6H, N-C<u>H</u>$_2$), 1.91 (s, 12H, C-C<u>H</u>$_3$). IR (ATR) 2925, 1626, 1508, 1390, 1322, 1055, 916, 817, 716 cm^{-1}. MS (ESI) m/z: 509 [M]$^+$. UV abs λ$_{max}$ = 778 nm.

3-Ethyl-2-[(1E,3E,5E)-7-[(2E)-3-ethyl-1,1-dimethyl-1H,2H,3H-benzo[e]indol-2-ylidene]hepta-1,3,5-trien-1-yl]-1,1-dimethyl-1H-benzo[e]indol-3-ium iodide (11b).
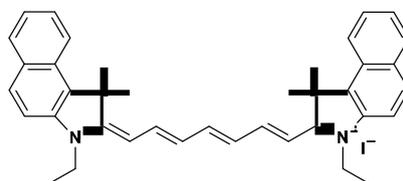
11b was synthesised as for **9a** using **PY1** (0.22 g, 0.80 mmol) and anhydrous sodium acetate (0.41 g, 5.00 mmol) in EtOH (10.0 mL) with **3b** (0.73 g, 2.00 mmol) to give the crude product which was purified by silica gel column chromatography (solvent; chloroform: methanol=9:1) to obtain cyanine dye **11b** (0.10 g, 19%) as a green solid; m.p. 198-200 °C: ^{1}H NMR (d$_6$-DMSO, 300 MHz) δ 8.27 (d, *J*=9.0 Hz, 2H Ar-<u>H</u>), 8.09-8.03 (m, 5H, Ar-<u>H</u>), 7.99 (t, *J*=13.0 Hz, 1H, C<u>H</u>*alkene*), 7.85 (t, *J*=13.0 Hz, 2H, C<u>H</u>*alkene*), 7.74 (d, *J*=9.0 Hz, 2H, Ar-<u>H</u>), 7.68 (t, *J*=6.0 Hz, 2H, Ar-<u>H</u>), 7.52 (t, *J*=7.0 Hz, 2H, Ar-<u>H</u>), 6.63 (t, *J*=13.0 Hz, 2H, C<u>H</u>*alkene*), 6.46 (d, *J*=14.0 Hz, 2H, C<u>H</u>*alkene*), 4.29 (q, *J*=6.0 Hz, 4H, N-C<u>H</u>$_2$-CH$_3$), 1.91 (s, 12H, C-C<u>H</u>$_3$), 1.35 (t, *J*=6.0 Hz, 6H, CH$_2$-C<u>H</u>$_3$). IR (ATR) 2969, 1620, 1507, 1471, 1396, 1192, 1082, 952, 859, 706 cm^{-1}. MS (ESI) m/z: 537 [M]$^+$. UV abs λ$_{max}$ = 781 nm.

2-[(1E,3E,5E)-7-[(2E)-1,1-Dimethyl-3-propyl-1H,2H,3H-benzo[e]indol-2-ylidene]hepta-1,3,5-trien-1-yl]-1,1-dimethyl-3-propyl-1H-benzo[e]indol-3-ium iodide (11c).
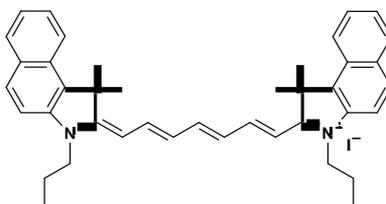
11c was synthesised as for **9a** using **PY1** (0.22 g, 0.80 mmol) and anhydrous sodium acetate (0.41 g, 5.00 mmol) in EtOH (10.0 mL) with **3c** (0.76 g, 2.00 mmol) to give the crude product which was purified by silica gel column chromatography (solvent; chloroform: methanol=9:1) to obtain cyanine dye **11c** (0.11 g, 20%) as a green solid; m.p. 195-197 °C: ^{1}H NMR (d$_6$-DMSO, 300 MHz) δ 8.27 (d, *J*=8.0 Hz, 2H Ar-H), 8.08-8.03 (m, 5H, Ar-H), 7.80 (t, *J*=13.0 Hz, 2H, CH$_{alkene}$), 7.75 (t, *J*=13.0 Hz, 2H, Ar-H), 7.67 (t, *J*=8.0 Hz, 2H, Ar-H), 7.52 (t, *J*=8.0 Hz, 2H, Ar-H), 6.59 (t, *J*=13.0 Hz, 2H, CH$_{alkene}$), 6.48 (d, *J*=14.0 Hz, 2H, CH$_{alkene}$), 4.21 (t, *J*=9.0 Hz, 4H, N-CH$_2$-CH$_2$), 1.91 (s, 12H, C-CH$_3$), 1.82 (sex, *J*=6.0 Hz, 4H, N-CH$_2$-CH$_2$-CH$_3$), 1.01 (t, *J*=6.0 Hz, 6H, CH$_2$-CH$_3$). IR (ATR) 2922, 1600, 1504, 1467, 1346, 1191, 1052, 915, 871, 711 cm^{-1}. MS (ESI) m/z: 565.31 [M]$^+$. UV abs λ$_{max}$ = 782 nm.

3-Butyl-2-[(1E,3E,5E)-7-[(2E)-3-butyl-1,1-dimethyl-1H,2H,3H-benzo[e]indol-2-ylidene]hepta-1,3,5-trien-1-yl]-1,1-dimethyl-1H-benzo[e]indol-3-ium iodide (11d).
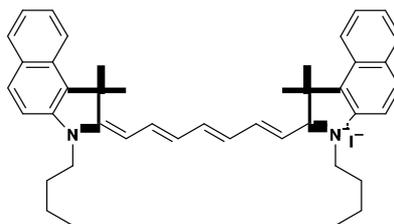
11d was synthesised as for **9a** using **PY1** (0.22 g, 0.80 mmol) and anhydrous sodium acetate (0.41 g, 5.00 mmol) in EtOH (10.0 mL) with **3d** (0.63 g, 2.00 mmol) to give the crude product which was purified by silica gel column chromatography (solvent; chloroform: methanol=9:1) to obtain cyanine dye **11d** (0.16 g, 28%) as a green solid; m.p. 196-198 °C: ^{1}H NMR (d$_6$-DMSO, 300 MHz) δ 8.27 (d, *J*=9.0 Hz, 2H Ar-H), 8.08-8.03 (m, 5H, Ar-H), 7.99

195

(t, *J*=12.0 Hz, 2H, C<u>H</u>*alkene*), 7.74 (d, *J*=9.0 Hz, 2H, Ar-<u>H</u>), 7.67 (t, *J*=13.0 Hz, 2H, C<u>H</u>*alkene*), 7.52 (t, *J*=8.0 Hz, 2H, Ar-<u>H</u>), 6.63 (t, *J*=13.0 Hz, 2H, C<u>H</u>*alkene*), 6.46 (d, *J*=14.0 Hz, 2H, C<u>H</u>*alkene*), 4.23 (t, *J*=6.0 Hz, 4H, N-C<u>H</u>$_2$-CH$_2$), 1.91 (s, 12H, C-C<u>H</u>$_3$), 1.77 (quin, *J*=6.0 Hz, 4H, N-CH$_2$-C<u>H</u>$_2$-CH$_2$), 1.47 (sex, *J*=9.0 Hz, 4H, N-CH$_2$-C<u>H</u>$_2$-CH$_3$), 0.97 (t, *J*=9.0 Hz, 6H, CH$_2$-C<u>H</u>$_3$). IR (ATR) 2924, 1601, 1504, 1400, 1346, 1181, 1053, 881, 713 cm^{-1}. MS (ESI) m/z: 593[M]$^+$. UV abs λ_{max} = 783 nm.

3-Benzyl-2-[(1E,3E,5E)-7-[(2E)-3-benzyl-1,1-dimethyl-1H,2H,3H-benzo[e]indol-2-ylidene]hepta-1,3,5-trien-1-yl]-1,1-dimethyl-1H-benzo[e]indol-3-ium bromide (11e).
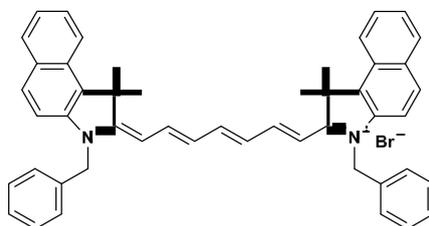

11e was synthesised as for **9a** using **PY1** (0.22 g, 0.80 mmol) and anhydrous sodium acetate (0.41 g, 5.00 mmol) in EtOH (10.0 mL) with **3e** (0.76 g, 2.00 mmol) to give the crude product which was purified by silica gel column chromatography (eluent solvent; chloroform: methanol=9:1) to obtain cyanine dye **11e** (0.10 g, 17%) as a light green solid; m.p. 157-159 °C: ^{1}H NMR (d$_6$-DMSO, 300 MHz) δ 8.63 (d, *J*=8.0 Hz, 2H, Ar-<u>H</u>), 8.04-7.98 (m, 6H, Ar-<u>H</u>), 7.69-7.60 (m, 4H, Ar-<u>H</u>), 7.54 (t, *J*=12.0 Hz, 2H, C<u>H</u>*alkene*), 7.41-7.33 (m, 4H, Ar-<u>H</u>), 7.31-7.27 (m, 6H, Ar-<u>H</u>), 6.65 (d, *J*=12.0 Hz, 1H, C<u>H</u>*alkene*), 6.53 (t, *J*=12.0 Hz, 4H, C<u>H</u>*alkene*), 5.54 (s, 4H, N-CH$_2$-Ph), 1.98 (s, 12H, C-C<u>H</u>$_3$). IR (ATR) 2923, 1601, 1501, 1462, 1393, 1346, 1051, 991, 876, 716 cm^{-1}. MS (ESI) m/z: 661 [M]$^+$. UV abs λ_{max} = 786 nm.

2-[(1E,3E,5E)-7-[(2E)-1,1-Dimethyl-3-(3-sulfonatopropyl)-1H,2H,3H-benzo[e]indol-2-ylidene]hepta-1,3,5-trien-1-yl]-1,1-dimethyl-3-(3-sulfonatopropyl)-1H-benzo[e]indol-3-ium (11f).
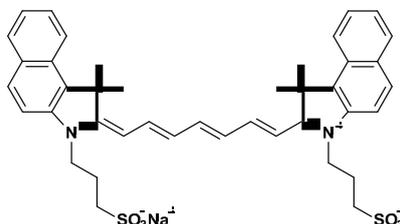
11f was synthesised as for **9a** using **PY1** (0.22 g, 0.80 mmol) and anhydrous sodium acetate (0.41 g, 5.00 mmol) in EtOH (10.0 mL) with **3f** (0.66 g, 2.00 mmol) to give the crude product which was purified by silica gel column chromatography (solvent; chloroform: methanol=8:2) to obtain cyanine dye **11f** (0.18 g, 32%) as a green solid; m.p. 240-242 °C: ^{1}H NMR (d$_6$-DMSO, 300 MHz) δ 8.26 (d, *J*=9.0 Hz, 2H Ar-H), 8.03-8.01 (m, 6H, Ar-H), 7.83 (d, *J*=9.0 Hz, 3H, Ar-H), 7.67 (t, *J*=12.0 Hz, 2H, CH$_{alkene}$), 7.52 (t, *J*=8.0 Hz, 2H, Ar-H), 6.60 (t, *J*=12.0 Hz, 4H, CH$_{alkene}$), 4.39 (t, *J*=6.0 Hz, 4H, N-CH$_2$-CH$_2$), 2.66 (t, *J*=9.0 Hz, 4H, CH$_2$-CH$_2$-SO$_3$), 2.08 (quin, *J*=6.0 Hz, 4H, N-CH$_2$-CH$_2$-CH$_2$), 1.91 (s, 12H, C-CH$_3$). IR (ATR) 2286, 1504, 1471, 1355, 1073, 913, 806, 716 cm^{-1}. MS (ESI) m/z: 723 [M+2H]$^+$. UV abs λ$_{max}$ = 784 nm.

2-[(1E,3E,5E)-7-[(2E)-1,1-Dimethyl-3-(4-sulfonatobutyl)-1H,2H,3H-benzo[e]indol-2-ylidene]hepta-1,3,5-trien-1-yl]-1,1-dimethyl-3-(4-sulfonatobutyl)-1H-benzo[e]indol-3-ium (11g).
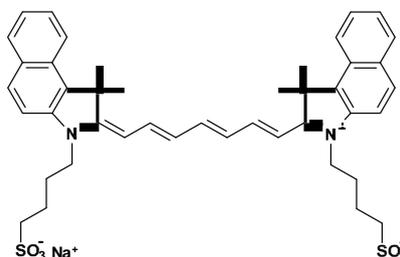
11g was synthesised as for **9a** using **PY1** (0.22 g, 0.80 mmol) and anhydrous sodium acetate (0.41 g, 5.00 mmol) in EtOH (10.0 mL) with **3g** (0.69 g, 2.00 mmol) to give the crude

product which was purified by silica gel column chromatography (solvent; chloroform: methanol=8:2) to obtain cyanine dye **11g** (0.17 g, 28%) as a green solid; m.p. 247-249 °C: ^{1}H NMR (d$_6$-DMSO, 300 MHz) δ 8.26 (t, *J*=9.0 Hz, 2H Ar-<u>H</u>), 8.06-7.88 (m, 6H, Ar-<u>H</u>), 7.71 (d, *J*=8.0 Hz, 3H, Ar-<u>H</u>), 7.76 (t, *J*=8.0 Hz, 2H, Ar-<u>H</u>), 7.45 (t, *J*=8.0 Hz, 2H, Ar-<u>H</u>), 6.63 (d, *J*=13.0 Hz, 2H, C<u>H</u>*alkene*), 6.51 (t, *J*=13.0 Hz, 2H, C<u>H</u>*alkene*), 4.20 (t, *J*=6.0 Hz, 4H, N-C<u>H</u>$_2$-CH$_2$), 2.55 (quin, *J*=6.0 Hz, 4H, N-CH$_2$-C<u>H</u>$_2$-CH$_2$), 1.91 (s, 12H, C-C<u>H</u>$_3$), 1.83 (br s, 8H, SO$_3$-(C<u>H</u>$_2$)$_4$-CH$_2$). IR (ATR) 2927, 1620, 1405, 1352, 1042, 997, 881, 715 cm^{-1}. MS (ESI) m/z: 753 [M+2H]$^+$. UV abs λ$_{max}$ = 784 nm.

1,1,3-Trimethyl-2-[(1E,3E,5E)-5-methyl-7-[(2E)-1,1,3-trimethyl-1H,2H,3H-benzo[e]indol-2-ylidene]hepta-1,3,5-trien-1-yl]-1H-benzo[e]indol-3-ium iodide (OA188).
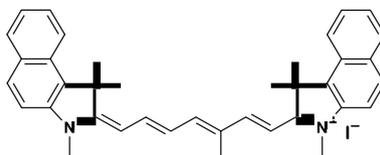
OA188 was synthesised as for **9a** using **PY2** (0.24 g, 0.80 mmol) and anhydrous sodium acetate (0.41 g, 5.00 mmol) in EtOH (10.0 mL) with **3a** (0.70 g, 2.00 mmol) to give the crude product which was purified by silica gel column chromatography (solvent; chloroform: methanol=9:1) to obtain cyanine dye **OA188** (0.11 g, 21%) as a green solid; m.p. 206-208 °C: ^{1}H NMR (d$_6$-DMSO, 300 MHz) δ 8.27 (d, *J*=9.0 Hz, 2H, Ar-<u>H</u>), 8.09 (t, *J*=9.0 Hz, 5H, Ar-<u>H</u>), 7.91 (d, *J*=15.0 Hz, 1H, C<u>H</u>*alkene*), 7.80-7.70 (m, 3H, Ar-H), 7.68 (t, *J*=15.0 Hz, 2H, C<u>H</u>*alkene*), 7.52 (t, *J*=8.0 Hz, 2H, Ar-<u>H</u>), 6.74 (t, *J*=15.0 Hz, 1H, C<u>H</u>*alkene*), 6.46 (d, *J*=15.0 Hz, 1H, C<u>H</u>*alkene*), 6.23 (d, *J*=15.0 Hz, 1H, C<u>H</u>*alkene*), 3.75 (s, 3H, N-C<u>H</u>$_3$), 3.71 (s, 3H, N-C<u>H</u>$_3$), 2.06 (s, 3H, C-C<u>H</u>$_3$), 1.93 (s, 6H, C-C<u>H</u>$_3$), 1.92 (s, 6H, C-C<u>H</u>$_3$). IR (ATR) 2919, 1598, 1512, 1435, 1387, 1217, 1151, 982 cm^{-1}. MS (ESI) m/z: 523 [M]$^+$. HRMS(ESI): Calcd for C$_{38}$H$_{39}$N$_2$ [M]$^+$. 523.3107, found 523.3101. UV abs λ$_{max}$ = 759 nm.

1 1,3,3-Trimethyl-2-[(1E,3Z,5E)-4-phenyl-7-[(2E)-1,3,3-trimethyl-2,3-dihydro-1H-indol-2-ylidene]hepta-1,3,5-trien-1-yl]-3H-indol-1-ium iodide (21).
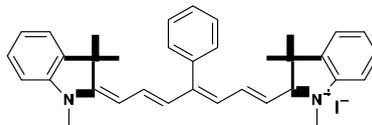
21 was synthesised as for **9a** using **PY5** (0.30 g, 0.80 mmol) and anhydrous sodium acetate (0.41 g, 5.00 mmol) in EtOH (10.0 mL) with **1a** (0.63 g, 2.00 mmol) to give the crude product which was purified by silica gel column chromatography (solvent; chloroform: methanol=9:1) to obtain cyanine dye **21** (0.10 g, 21%) as a green solid; m.p. 145-147 °C: ^{1}H NMR (d$_6$-DMSO, 300 MHz) δ 7.63-7.52 (m, 3H, Ar-$\underline{H}$), 7.47 (d, *J*=7.0 Hz, 2H, Ar-$\underline{H}$), 7.36-7.27 (m, 8H, Ar-$\underline{H}$), 7.20 (t, *J*=7.0 Hz, 2H, Ar-$\underline{H}$), 6.75 (d, *J*=14.0 Hz, 2H, C$\underline{H}_{alkene}$), 6.40 (d, *J*=14.0 Hz, 2H, C$\underline{H}_{alkene}$), 3.50 (s, 6H, N-CH$_3$), 1.25 (s, 12H, C-C$\underline{H}_3$). IR (ATR) 3333, 2291, 1585, 1507, 1439, 1325, 1262, 1141, 907, 741 cm^{-1}. MS (ESI) m/z: 485 [M]$^+$. UV abs λ$_{max}$ = 750 nm.

2-[(1E,3E,5Z)-5-Bromo-7-[(2E)-1,3,3-trimethyl-2,3-dihydro-1H-indol-2-ylidene]hepta-1,3,5-trien-1-yl]-1,3,3-trimethyl-3H-indol-1-ium iodide (19).
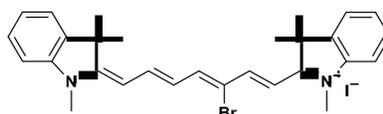

19 was synthesised as for **9a** using **PY3** (0.30 g, 0.80 mmol) and anhydrous sodium acetate (0.41 g, 5.00 mmol) in EtOH (10.0 mL) with **1a** (0.60 g, 2.00 mmol) to give the crude product which was purified by silica gel column chromatography (eluent solvent; chloroform: methanol=9:1) to obtain cyanine dye **19** (0.12 g, 24%) as a shiny green solid; m.p. 209-211 °C: ^{1}H NMR (d$_6$-DMSO, 300 MHz) δ 8.12-8.04 (m, 2H, Ar-$\underline{H}$), 7.96 (d, *J*=12.0 Hz, 1H, C$\underline{H}_{alkene}$), 7.70 (d, *J*=6.0 Hz, 1H, Ar-$\underline{H}$), 7.58-7.55 (m, 2H, Ar-$\underline{H}$), 7.51 (t, *J*=12.0 Hz, 1H, C$\underline{H}_{alkene}$), 7.39-7.33 (m, 3H, Ar-$\underline{H}$), 7.23 (t, *J*=12.0 Hz, 1H, C$\underline{H}_{alkene}$), 6.79-6.68 (m, 2H, Ar-$\underline{H}$), 6.08 (d, *J*=12.0 Hz, 1H, C$\underline{H}_{alkene}$), 3.75 (s, 3H, N-C$\underline{H}_3$), 3.56 (s, 3H, N-C$\underline{H}_3$), 1.67 (s, 6H, C-C$\underline{H}_3$), 1.64 (s, 6H, C-C$\underline{H}_3$). IR (ATR) 2918, 1590, 1400, 1354, 1270, 980, 740 cm^{-1}. MS

(ESI) m/z: 487 [M]$^+$. HRMS(ESI): Calcd for C$_{29}$H$_{32}$BrN$_2$[M]$^+$ 487.1743, found 487.1742. UV abs λ_{max} = 732 nm.

2-[(1E,3E,5Z)-5-Chloro-7-[(2Z)-3-methyl-2,3-dihydro-1,3-benzothiazol-2-ylidene]hepta-1,3,5-trien-1-yl]-3-methyl-1,3-benzothiazol-3-ium iodide (20).
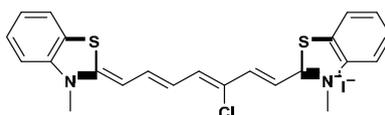
20 was synthesised as for **9a** using **PY4** (0.25 g, 0.80 mmol) and anhydrous sodium acetate (0.41 g, 5.00 mmol) in EtOH (10.0 mL) with **2a** (0.58 g, 2.00 mmol) to give the crude product which was purified by silica gel column chromatography (solvent; chloroform: methanol=9:1) to obtain cyanine dye **20** (0.16 g, 36%) as a green solid; m.p. 196-198 °C: ^{1}H NMR (d$_6$-DMSO, 300 MHz) δ 8.10 (d, *J*=7.0 Hz, 1H, Ar-<u>H</u>), 7.91 (d, *J*=7.0 Hz, 1H, Ar-<u>H</u>), 7.86 (d, *J*=8.0 Hz, 1H, Ar-<u>H</u>), 7.68-7.55 (m, 4H, Ar-<u>H</u>), 7.50 (t, *J*=8.0 Hz, 2H, Ar-<u>H</u>), 7.41 (d, *J*=13.0 Hz, 1H, C<u>H</u>*alkene*), 7.32 (t, *J*=7.0 Hz, 1H, Ar-<u>H</u>), 6.97 (d, *J*=13.0 Hz, 1H, C<u>H</u>*alkene*), 6.63 (d, *J*=13.0 Hz, 1H, C<u>H</u>*alkene*), 6.18 (d, *J*=13.0 Hz, 1H, C<u>H</u>*alkene*), 3.93 (s, 3H, N-C<u>H</u>$_3$), 3.73 (s, 3H, N-C<u>H</u>$_3$). IR (ATR) 3396, 2357, 1579, 1439, 1371, 1267, 1194, 999, 813 cm^{-1}. MS (ESI) m/z: 423 [M]$^+$. HRMS(ESI): Calcd for C$_{23}$H$_{20}$BrN$_2$S$_2$[M]$^+$ 423.0751, found 423.0748. UV abs λ_{max} = 752 nm.

2-[(1E,3E,5E)-7-[(2E)-3,3-Dimethyl-1-(4-sulfonatobutyl)-2,3-dihydro-1H-indol-2-ylidene]-5-methylhepta-1,3,5-trien-1-yl]-3,3-dimethyl-1-(4-sulfonatobutyl)-3H-indol-1-ium (12).
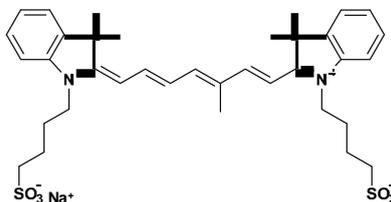
12 was synthesised as for **9a** using **PY2** (0.23 g, 0.80 mmol) and anhydrous sodium acetate (0.41 g, 5.00 mmol) in EtOH (10.0 mL) with **1m** (0.59 g, 2.00 mmol) to give the crude product which was purified by silica gel column chromatography (solvent; chloroform: methanol=7:3) to obtain cyanine dye **12** (0.10 g, 19%) as a shiny purple solid; m.p. 160-162 °C: ^{1}H NMR (d$_6$-DMSO, 400 MHz) δ 7.88 (t, *J*=13.0 Hz, 1H, C$\underline{H}_{alkene}$), 7.71-7.65 (m, 2H, Ar-$\underline{H}$), 7.51 (d, *J*=7.0 Hz, 2H, Ar-$\underline{H}$), 7.34-7.28 (m, 4H, Ar-$\underline{H}$), 7.16 (t, *J*=7.0 Hz, 2H, Ar-$\underline{H}$), 6.64 (t, *J*=13.0 Hz, 1H, C$\underline{H}_{alkene}$), 6.43 (d, *J*=14.0 Hz, 1H, C$\underline{H}_{alkene}$), 6.16 (d, *J*=14.0 Hz, 1H, C$\underline{H}_{alkene}$), 4.07 (t, *J*=7.0 Hz, 2H, N-C$\underline{H}_2$-CH$_2$), 3.99 (t, *J*=7.0 Hz, 2H, N-C$\underline{H}_2$-CH$_2$), 2.43-2.40 (m, 4H, C$\underline{H}_2$-SO$_3$), 1.95 (s, 3H, C-C$\underline{H}_3$), 1.75-1.66 (m, 8H, C$\underline{H}_2$), 1.18 (br s, 12H, (C$\underline{H}_3$)$_4$). IR (ATR) 2928, 1585, 1511, 1404, 1318, 974, 744 cm^{-1}. MS (ESI) m/z: 665 [M+2H]$^+$. HRMS(ESI): Calcd for C$_{36}$H$_{45}$N$_2$O$_6$S$_2$.[M+2H]$^+$ 665.2725, found 665.2710. UV abs λ$_{max}$ = 784 nm.

2-[(1E,3E,5Z)-5-Bromo-7-[(2E)-3,3-dimethyl-1-(4-sulfonatobutyl)-2,3-dihydro-1H-indol-2-ylidene]hepta-1,3,5-trien-1-yl]-3,3-dimethyl-1-(4-sulfonatobutyl)-3H-indol-1-ium (13).
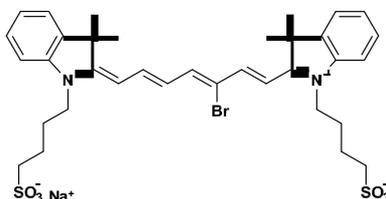
13 was synthesised as for **9a** using **PY3** (0.28 g, 0.80 mmol) and anhydrous sodium acetate (0.41 g, 5.00 mmol) in EtOH (10.0 mL) with **1m** (0.59 g, 2.00 mmol) to give the crude product which was purified by silica gel column chromatography (solvent; chloroform:

methanol=7:3) to obtain cyanine dye **13** (0.11 g, 19%) as a green solid; m.p. 231-233 °C: ^{1}H NMR (d$_6$-DMSO, 400 MHz) δ 8.14-8.03 (m, 2H, Ar-<u>H</u>), 7.96 (d, *J*=15.0 Hz, 1H, C<u>H</u>$_{alkene}$), 7.69 (d, *J*=6.0 Hz, 1H, Ar-<u>H</u>), 7.63 (d, *J*=6.0 Hz, 1H, Ar-<u>H</u>), 7.57 (d, *J*=6.0 Hz, 1H, Ar-<u>H</u>), 7.50 (t, *J*=9.0 Hz, 1H, Ar-<u>H</u>), 7.39-7.33 (m, 3H, Ar-<u>H</u>), 7.22 (t, *J*=9.0 Hz, 1H, Ar-<u>H</u>), 6.92 (d, *J*=15.0 Hz, 1H, C<u>H</u>$_{alkene}$), 6.81 (t, *J*=15.0 Hz, 1H, C<u>H</u>$_{alkene}$), 6.13 (d, *J*=15.0 Hz, 1H, C<u>H</u>$_{alkene}$), 4.27 (t, *J*=6.0 Hz, 2H, N-C<u>H</u>$_2$-CH$_2$), 4.07 (t, *J*=6.0 Hz, 2H, N-C<u>H</u>$_2$-CH$_2$), 1.78-1.69 (m, 12H, C<u>H</u>$_2$-SO$_3$), 1.67 (s, 6H, C-C<u>H</u>$_3$), 1.63 (s, 6H, C-C<u>H</u>$_3$). IR (ATR) 2925, 1588, 1405, 1366, 1289, 977, 746 cm^{-1}. MS (ESI) m/z: 731 [M+2H]$^+$. HRMS(ESI): Calcd for C$_{35}$H$_{44}$BrN$_2$O$_6$S$_2$.[M+2H]$^+$ 731.1819, found 731.1813. UV abs λ$_{max}$ = 753 nm.

2-[(1E,3E,5Z)-5-chloro-7-[(2E)-3,3-dimethyl-1-(4-sulfobutyl)-2,3-dihydro-1H-indol-2-ylidene]hepta-1,3,5-trien-1-yl]-3,3-dimethyl-1-(4-sulfinatobutyl)-3H-indol-1-ium (14).
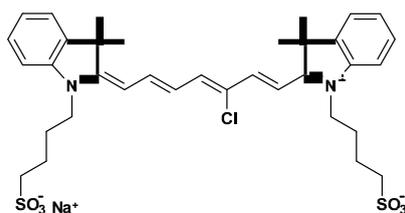
14 was synthesised as for **9a** using **PY4** (0.25 g, 0.80 mmol) and anhydrous sodium acetate (0.41 g, 5.00 mmol) in EtOH (10.0 mL) with **1m** (0.59 g, 2.00 mmol) to give the crude product which was purified by silica gel column chromatography (solvent; chloroform: methanol=7:3) to obtain cyanine dye **14** (0.10 g, 18%) as a green solid; m.p. 233-235 °C: ^{1}H NMR (d$_6$-DMSO, 300 MHz) δ 8.13 (d, *J*=12.0 Hz, 1H, C<u>H</u>$_{alkene}$), 8.04 (d, *J*=12.0 Hz, 1H, C<u>H</u>$_{alkene}$), 7.62 (d, *J*=9.0 Hz, 1H, Ar-<u>H</u>), 7.56 (d, *J*=9.0 Hz, 1H, Ar-<u>H</u>), 7.48 (t, *J*=15.0 Hz, 1H, C<u>H</u>$_{alkene}$), 7.40-7.30 (m, 3H, Ar-<u>H</u>), 7.20-7.15 (m, 1H, Ar-<u>H</u>), 6.90 (d, *J*=15.0 Hz, 1H, C<u>H</u>$_{alkene}$), 6.81 (t, *J*=12.0 Hz, 1H, C<u>H</u>$_{alkene}$), 6.12 (d, *J*=12.0 Hz, 1H, C<u>H</u>$_{alkene}$), 4.25 (t, *J*=6.0 Hz, 2H, N-C<u>H</u>$_2$-CH$_2$), 4.07 (t, *J*=6.0 Hz, 2H, N-C<u>H</u>$_2$-CH$_2$), 1.79-1.71 (m, 12H, C<u>H</u>$_2$-SO$_3$), 1.65 (s, 6H, C-C<u>H</u>$_3$), 1.62 (s, 6H, C-C<u>H</u>$_3$). IR (ATR) 2921, 1511, 1405, 1366, 1290, 980, 746 cm^{-1}. MS (ESI) m/z: 687 [M+2H]$^+$. HRMS(ESI): Calcd for C$_{35}$H$_{44}$ClN$_2$O$_6$S$_2$.[M+2H]$^+$ 687.2324, found 687.2318. UV abs λ$_{max}$ = 774 nm.

2-[(1E,3Z,5E)-7-[(2E)-3,3-dimethyl-1-(4-sulfonatobutyl)-2,3-dihydro-1H-indol-2-ylidene]-4-phenylhepta-1,3,5-trien-1-yl]-3,3-dimethyl-1-(4-sulfonatobutyl)-3H-indol-1-ium (15).
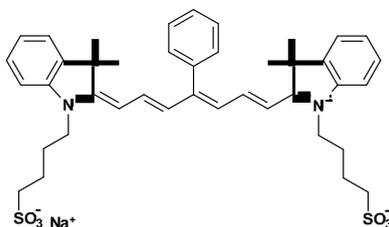
15 was synthesised as for **9a** using **PY5** (0.30 g, 0.80 mmol) and anhydrous sodium acetate (0.41 g, 5.00 mmol) in EtOH (10.0 mL) with **1m** (0.59 g, 2.00 mmol) to give the crude product which was purified by silica gel column chromatography (solvent; chloroform: methanol=7:3) to obtain cyanine dye **15** (0.12 g, 20%) as a green solid; m.p. 259-261 °C: ^{1}H NMR (d$_6$-DMSO, 300 MHz) δ 7.65-7.59 (m, 3H, Ar-$\underline{H}$), 7.49 (d, *J*=9.0 Hz, 2H, Ar-$\underline{H}$), 7.40-7.33 (m, 6H, Ar-$\underline{H}$), 7.27 (d, *J*=8.0 Hz, 2H, Ar-$\underline{H}$), 7.20 (t, *J*=12.0 Hz, 2H, C$\underline{H}$$_{alkene}$), 6.78 (d, *J*=12.0 Hz, 2H, C$\underline{H}$$_{alkene}$), 6.53 (d, *J*=12.0 Hz, 2H, C$\underline{H}$$_{alkene}$), 4.07 (t, *J*=9.0 Hz, 4H, N-C$\underline{H}$$_2$-CH$_2$), 2.46 (br s, 4H, C$\underline{H}$$_2$-SO$_3$), 1.76-1.69 (m, 8H, C$\underline{H}$$_2$), 1.24 (s, 12H, C-C$\underline{H}$$_3$). IR (ATR) 2968, 1561, 1445, 1368, 1209, 1006, 756 cm^{-1}. MS (ESI) m/z: 729 [M+2H]$^+$. HRMS(ESI): Calcd for C$_{41}$H$_{49}$N$_2$O$_6$S$_2$.[M+2H]$^+$ 729.3027, found 729.3023. UV abs λ$_{max}$ = 758 nm.

2-[(1E,3E,5Z)-5-bromo-7-[(2Z)-3-(3-sulfonatopropyl)-2,3-dihydro-1,3-benzothiazol-2-ylidene]hepta-1,3,5-trien-1-yl]-3-(3-sulfonatopropyl)-1,3-benzothiazol-3-ium (16).


16 was synthesised as for **9a** using **PY3** (0.28 g, 0.80 mmol) and anhydrous sodium acetate (0.41 g, 5.00 mmol) in EtOH (10.0 mL) with **2l** (0.54 g, 2.00 mmol) to give the crude product which was purified by silica gel column chromatography (solvent; chloroform: methanol=7:3) to obtain cyanine dye **16** (0.10 g, 18%) as a green solid; m.p. 232-234 °C: ^{1}H NMR (d$_6$-DMSO, 300 MHz) δ 8.13 (d, *J*=9.0 Hz, 1H, Ar-$\underline{H}$), 8.02 (d, *J*=9.0 Hz, 1H, Ar-$\underline{H}$),

7.93 (d, *J*=9.0 Hz, 1H, Ar-H̲), 7.78 (d, *J*=9.0 Hz, 1H, Ar-H̲), 7.70-7.65 (m, 3H, Ar-H̲), 7.55-7.51 (m, 3H, Ar-H̲), 7.35 (t, *J*=15.0 Hz, 1H, CH̲*alkene*), 7.15 (d, *J*=12.0 Hz, 1H, CH̲*alkene*), 6.63 (t, *J*=12.0 Hz, 1H, CH̲*alkene*), 6.29 (d, *J*=12.0 Hz, 1H, CH̲*alkene*), 4.67 (t, *J*=9.0 Hz, 2H, N-CH̲$_2$-CH$_2$), 4.47 (t, *J*=9.0 Hz, 2H, N-CH̲$_2$-CH$_2$), 2.63 (t, *J*=9.0 Hz, 4H, CH$_2$-CH̲$_2$-SO$_3$), 2.09 (quin, *J*=9.0 Hz, 4H, CH̲$_2$-CH$_2$-SO$_3$). IR (ATR) 2966, 1458, 1402, 1327, 1270, 810, 746 cm^{-1}. MS (ESI) m/z: 682 [M+2H]$^+$. HRMS(ESI): Not successful. UV abs λ$_{max}$ = 753 nm.

2-[(1E,3E,5Z)-5-chloro-7-[(2Z)-3-(3-sulfonatopropyl)-2,3-dihydro-1,3-benzothiazol-2-ylidene]hepta-1,3,5-trien-1-yl]-3-(3-sulfonatopropyl)-1,3-benzothiazol-3-ium (17).

17 was synthesised as for **9a** using **PY4** (0.25 g, 0.80 mmol) and anhydrous sodium acetate (0.41 g, 5.00 mmol) in EtOH (10.0 mL) with **2l** (0.54 g, 2.00 mmol) to give the crude product which was purified by silica gel column chromatography (solvent; chloroform: methanol=7:3) to obtain cyanine dye **17** (0.11 g, 22%) as a green solid; m.p. 242-244 °C: ^{1}H NMR (d$_6$-DMSO, 300 MHz) δ 8.11 (d, *J*=6.0 Hz, 1H, Ar-H̲), 8.00 (d, *J*=9.0 Hz, 1H, Ar-H̲), 7.91 (d, *J*=6.0 Hz, 1H, Ar-H̲), 7.76 (d, *J*=9.0 Hz, 1H, Ar-H̲), 7.66-7.60 (m, 3H, Ar-H̲), 7.51-7.46 (m, 2H, Ar-H̲), 7.43 (d, *J*=15.0 Hz, 1H, CH̲*alkene*), 7.34 (t, *J*=15.0 Hz, 1H, CH̲*alkene*), 7.13 (d, *J*=15.0 Hz, 1H, CH̲*alkene*), 6.63 (t, *J*=15.0 Hz, 1H, CH̲*alkene*), 6.32 (d, *J*=15.0 Hz, 1H, CH̲*alkene*), 4.65 (t, *J*=6.0 Hz, 2H, N-CH̲$_2$-CH$_2$), 4.47 (t, *J*=6.0 Hz, 2H, N-CH̲$_2$-CH$_2$), 2.63-2.55 (m, 4H, CH$_2$-CH̲$_2$-SO$_3$), 2.08 (quin, *J*=9.0 Hz, 4H, CH$_2$-CH̲$_2$-CH$_2$-SO$_3$). IR (ATR) 2939, 1578, 1401, 1269, 811, 741 cm^{-1}. MS (ESI) m/z: 637 [M+2H]$^+$. HRMS(ESI): Calcd for C$_{27}$H$_{28}$ClN$_2$O$_6$S$_4$ [M+2H]$^+$ 637.0367, found 637.0346. UV abs λ$_{max}$ = 758 nm.

2-[(1E,3E,5E)-5-methyl-7-[(2Z)-3-(3-sulfonatopropyl)-2,3-dihydro-1,3-benzothiazol-2-ylidene]hepta-1,3,5-trien-1-yl]-3-(3-sulfonatopropyl)-1,3-benzothiazol-3-ium (18).

18 was synthesised as for **9a** using **PY2** (0.23 g, 0.80 mmol) and anhydrous sodium acetate (0.41 g, 5.00 mmol) in EtOH (10.0 mL) with **2m** (0.54 g, 2.00 mmol) to give the crude product which was purified by silica gel column chromatography (solvent; chloroform: methanol=7:3) to obtain cyanine dye **18** (0.10 g, 20%) as a green solid; m.p. 245-247 °C: ^{1}H NMR (d$_6$-DMSO, 300 MHz) δ 7.96 (d, *J*=6.0 Hz, 2H, Ar-H̲), 7.80 (d, *J*=9.0 Hz, 2H, Ar-H̲), 7.56 (t, *J*=9.0 Hz, 2H, Ar-H̲), 7.44-7.28 (m, 5H, Ar-H̲), 6.75 (d, *J*=15.0 Hz, 1H, CH̲$_{alkene}$), 6.67 (t, *J*=15.0 Hz, 1H, CH̲$_{alkene}$), 6.55 (t, *J*=15.0 Hz, 1H, CH̲$_{alkene}$), 4.60 (t, *J*=9.0 Hz, 2H, N-CH̲$_2$-CH$_2$), 4.49 (t, *J*=9.0 Hz, 2H, N-CH̲$_2$-CH$_2$), 2.59 (s, 3H, CH̲$_3$), 2.02 (br s, 8H, CH̲$_2$-SO$_3$), IR (ATR) 2925, 1506, 1400, 1329, 1273, 868, 741 cm^{-1}. MS(ESI) m/z: 617 [M+2H]$^+$. HRMS(ESI): Calcd for C$_{28}$H$_{31}$N$_2$O$_6$S$_4$.[M+2H]$^+$ 617.0896, found 617.0889. UV abs λ$_{max}$ = 784 nm.

2-Methyl-3-(prop-2-yn-1-yl)-1,3-benzothiazol-3-ium bromide (2n).

2n was synthesised as for **1a** using 2-methylbenzothiazole (15.0 mL, 100 mmol) and propargyl bromide (4.00 mL, 34.0 mmol) to give the product **2n** (0.84 g, 9%) as a grey solid; m.p. 201-204 °C: ^{1}H NMR (d$_6$-DMSO, 300 MHz) δ 8.55 (d, *J*=8.0 Hz, 1H, Ar-H̲), 8.40 (d, *J*=8.0 Hz, 1H, Ar-H̲), 7.96 (t, *J*=7.0 Hz, 1H, Ar-H̲), 7.85 (t, *J*=8.0 Hz, 1H, Ar-H̲), 5.80 (s, 2H, N-CH̲$_2$), 3.87 (s, 1H, CH̲), 3.29 (s, 3H, C-CH̲$_3$). ^{13}C NMR (d$_6$-DMSO, 75.4 MHz) δ 178.9, 140.7, 130.0, 129.4, 128.7, 125.4, 117.1, 79.5, 79.4, 75.1, 17.7. IR (ATR) 2946, 1578, 1513, 1434, 1329, 1195, 1091, 804, 756, 629 cm^{-1}. MS (ESI) m/z: 188 [M]$^+$.

3-(Prop-2-yn-1-yl)-2-[(1E,3E,5E)-7-[(2Z)-3-(prop-2-yn-1-yl)-2,3-dihydro-1,3-benzothiazol-2-ylidene]hepta-1,3,5-trien-1-yl]-1,3-benzothiazol-3-ium bromide (22).

22 was synthesised as for **9a** using **PY1** (0.22 g, 0.80 mmol) and anhydrous sodium acetate (0.41 g, 5.00 mmol) in EtOH (10.0 mL) with **2n1** (0.54 g, 2.00 mmol) to give the crude product which was purified by silica gel column chromatography (eluent solvent; chloroform: methanol=9:1) to obtain cyanine dye (**22**, 0.20 g, 48%) as a green solid; m.p. 168-170 °C: ^{1}H NMR (d$_6$-DMSO, 300 MHz) δ 8.00 (d, *J*=6.0 Hz, 2H, Ar-H̲), 7.74 (d, *J*=6.0 Hz, 2H, Ar-H̲), 7.59-7.43 (m, 3H, Ar-H̲), 7.42-7.37 (m, 4H, Ar-H), 6.67 (d, *J*=12.0 Hz, 2H, CH̲$_{alkene}$), 6.54 (t, *J*=12.0 Hz, 2H, CH̲$_{alkene}$), 5.28 (s, 4H, N-CH̲$_2$), 3.60 (s, 2H, CH̲). IR (ATR) 2982, 1613, 1504, 1397, 1324, 1063, 990, 803, 737 cm^{-1}. MS (ESI) m/z: 436.98 [M]$^{+}$. HRMS(ESI): Calcd for C$_{27}$H$_{21}$N$_2$S$_2$ [M]$^{+}$ 437.1140, found 437.1131. UV abs λ$_{max}$ = 758 nm.

2-[(E)-2-[(3E)-2-Chloro-3-{2-[(2Z)-3-(prop-2-yn-1-yl)-2,3-dihydro-1,3-benzothiazol-2-ylidene]ethylidene}cyclohex-1-en-1-yl]ethenyl]-3-(prop-2-yn-1-yl)-1,3-benzothiazol-3-ium bromide (23).

**23** was synthesised as for **4a** using **2n** (2.16 g, 8.00 mmol) and anhydrous sodium acetate (0.66 g, 8.00 mmol) in EtOH (40.0 mL) and was added **VH1** (1.44 g, 4.00 mmol) to give the crude product which was purified by silica gel column chromatography (solvent; chloroform : methanol=8:2) to obtain cyanine dye **23** (1.11 g, 47%) as a green solid; m.p. 191-193 °C: ^{1}H NMR (d$_6$-DMSO, 300 MHz) δ 7.95 (d, *J*=7.0 Hz, 2H, Ar-H̲), 7.78-771 (m, 4H, Ar-H̲), 7.55 (t, *J*=8.0 Hz, 2H, Ar-H̲), 7.32 (t, *J*=8.0 Hz, 2H, Ar-H̲), 6.59 (d, *J*=14.0 Hz, 2H, CH̲$_{alkene}$), 5.38 (s, 4H, N-CH̲$_2$), 3.61 (s, 2H, CH̲), 2.50 (t, *J*=3.0 Hz, 4H, CH̲$_2$-CH$_2$), 1.98-1.88 (m, 2H, CH$_2$-CH̲$_2$-CH$_2$). IR (ATR) 3283, 1659, 1580, 1498, 1382, 1321, 1092, 991, 851, 738 cm^{-1}. MS

(ESI) m/z: 510 [M]$^+$. HRMS(ESI): Calcd for $C_{30}H_{24}ClN_2S_2$ [M]$^+$ 511.1063, found 511.1054. UV abs λ_{max} = 800 nm.

2-[(1E,3E,5E)-5-Methyl-7-[(2Z)-3-(prop-2-yn-1-yl)-2,3-dihydro-1,3-benzothiazol-2-ylidene]hepta-1,3,5-trien-1-yl]-3-(prop-2-yn-1-yl)-1,3-benzothiazol-3-ium bromide (24).


24 was synthesised as for **9a** using **PY2** (0.24 g, 0.80 mmol) and anhydrous sodium acetate (0.41 g, 5.00 mmol) in EtOH (10.0 mL) with **2n** (0.54 g, 2.00 mmol) to give the crude product which was purified by silica gel column chromatography (solvent; chloroform: methanol=9:1) to obtain cyanine dye **24** (0.11 g, 26%) as a dark green solid; m.p. 171-173 °C: ^{1}H NMR (d$_6$-DMSO, 300 MHz) δ 8.00 (d, *J*=6.0 Hz, 2H, Ar-<u>H</u>), 7.74 (d, *J*=6.0 Hz, 2H, Ar-<u>H</u>), 7.59 (t, *J*=15.0 Hz, 2H, C<u>H</u>*alkene*), 7.50-7.32 (m, 5H, Ar-H), 6.72 (d, *J*=15.0 Hz, 1H, C<u>H</u>*alkene*), 6.61 (t, *J*=15.0 Hz, 2H, C<u>H</u>*alkene*), 5.39 (s, 2H, N-C<u>H</u>$_2$), 5.27 (s, 2H, N-C<u>H</u>$_2$), 3.60 (s, 2H, C<u>H</u>), 2.02 (s, 3H, C-C<u>H</u>$_3$). IR (ATR) 3177, 1574, 1506, 1402, 1269, 1124, 1010, 801, 737 cm^{-1}. MS (ESI) m/z: 450 [M]$^+$. HRMS(ESI): Calcd for $C_{28}H_{23}N_2S_2$ [M]$^+$ 451.1297, found 451.1294. UV abs λ_{max} = 759 nm.

3-[(1-Benzyl-1H-1,2,3-triazol-4-yl)methyl]-2-[(1E,3E,5E)-7-[(2Z)-3-[(1-benzyl-1H-1,2,3-triazol-4-yl)methyl]-2,3-dihydro-1,3-benzothiazol-2-ylidene]hepta-1,3,5-trien-1-yl]-1,3-benzothiazol-3-ium bromide (25).

22 (0.17 g, 0.34 mmol), benzylazide (0.09 g, 0.68 mmol), copper(II)sulfhate (0.03 g, 0.16 mmol) and sodium ascorbate (0.13 g, 0.68 mmol) were dissolved in a 75% acetone/water solution (20.0 mL) and stirred at room temperature overnight. The reaction was stopped and the crude product was purified by silica gel column chromatography (solvent; chloroform: methanol = 8:2) to afford the desired cyanine dye azide conjugate **25** (70 mg, 26%) as a green solid; m.p. 158-160 °C: ^{1}H NMR (d$_6$-DMSO, 300 MHz) δ 8.34 (s, 2H, N-C$\underline{H}$$_{alkene}$), 7.97 (d, J=6.0 Hz, 2H, Ar-$\underline{H}$), 7.84 (d, J=6.0 Hz, 2H, Ar-$\underline{H}$), 7.54 (t, J=9.0 Hz, 2H, Ar-$\underline{H}$), 7.49-7.26 (m, 15H, Ar-$\underline{H}$), 6.79 (d, J=15.0 Hz, 2H, C$\underline{H}$$_{alkene}$), 6.48 (t, J=15.0 Hz, 2H, C$\underline{H}$$_{alkene}$), 5.63 (s, 4H, N-C$\underline{H}$$_2$), 5.59 (s, 4H, N-C$\underline{H}$$_2$-Ph). IR (ATR) 3389, 2286, 1503, 1455, 1322, 1068, 982, 806, 717 cm^{-1}. MS (ESI) m/z: 703 [M]$^+$. HRMS (ESI): Calcd for C$_{41}$H$_{35}$N$_8$S$_2$ [M]$^+$ 703.2420, found 703.2414. UV abs λ$_{max}$ = 764 nm.
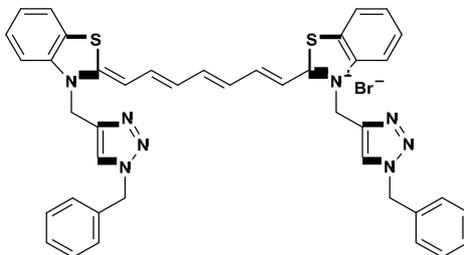
3-[(1-Benzyl-1H-1,2,3-triazol-4-yl)methyl]-2-[(E)-2-[(3E)-3-{2-[(2Z)-3-[(1-benzyl-1H-1,2,3-triazol-4-yl)methyl]-2,3-dihydro-1,3-benzothiazol-2-ylidene]ethylidene}-2-chlorocyclohex-1-en-1-yl]ethenyl]-1,3-benzothiazol-3-ium bromide (26).
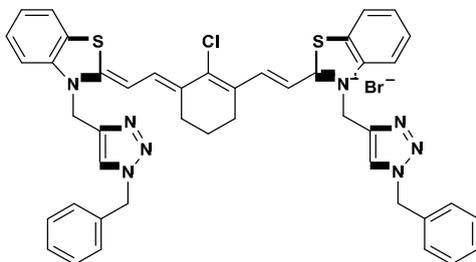
26 was synthesised as for **25** using **23** (0.201 g, 0.34 mmol), benzylazide (0.09 g, 0.68 mmol), copper(II)sulfate (0.03 g, 0.16 mmol) and sodium ascorbate (0.13 g, 0.68 mmol) to give the crude product which was purified by silica gel column chromatography (solvent; chloroform: methanol = 8:2) to afford the desired cyanine dye azide conjugate **26** (89 mg, 31%) as a green solid; m.p. 214-216 °C: ^{1}H NMR (d$_6$-DMSO, 300 MHz) δ 8.34 (s, 2H, N-C$\underline{H}_{alkene}$), 7.98 (d, J=6.0 Hz, 2H, Ar-$\underline{H}$), 7.91 (d, J=9.0 Hz, 2H, Ar-$\underline{H}$), 7.82 (d, J=15.0 Hz, 2H, C$\underline{H}_{alkene}$), 7.59 (t, J=8.0 Hz, 2H, Ar-$\underline{H}$), 7.42-7.27 (m, 13H, Ar-$\underline{H}$), 6.76 (d, J=15.0 Hz, 2H, C$\underline{H}_{alkene}$), 5.77 (s, 4H, N-C$\underline{H}_2$), 5.60 (s, 4H, N-C$\underline{H}_2$-Ph), 2.60-2.55 (m, 4H, C$\underline{H}_2$-CH$_2$), 1.80-1.75 (m, 2H, CH$_2$-C$\underline{H}_2$-CH$_2$). IR (ATR) 2182, 1499, 1390, 1278, 1104, 998, 848, 714 cm^{-1}. MS (ESI) m/z: 777 [M]$^+$. HRMS(FAB): Calcd for C$_{44}$H$_{38}$ClN$_8$S$_2$ [M+] 777.2343, found 777.2342. UV abs λ$_{max}$ = 804 nm.

3-[(1-benzyl-1H-1,2,3-triazol-4-yl)methyl]-2-[(1E,3E,5E)-7-[(2Z)-3-[(1-benzyl-1H-1,2,3-triazol-4-yl)methyl]-2,3-dihydro-1,3-benzothiazol-2-ylidene]-5-methylhepta-1,3,5-trien-1-yl]-1,3-benzothiazol-3-ium bromide (27).
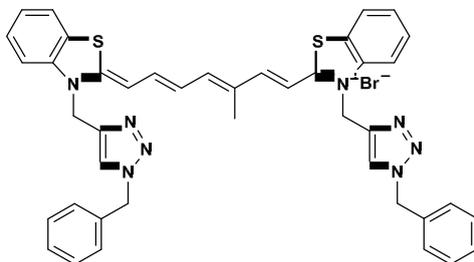
27 was synthesised as for **25** using **24** (0.18 g, 0.34 mmol), benzylazide (0.09 g, 0.68 mmol), copper(ll)sulphate (0.03 g, 0.16 mmol) and sodium ascorbate (0.13 g, 0.68 mmol) to give the crude product which was purified by silica gel column chromatography (eluent solvent; chloroform: methanol = 8:2) to produce the desired cyanine dye azide conjugate **27** (64 mg, 24%) as a dark green solid; m.p. 175-177 °C: ^{1}H NMR (d_6-DMSO, 300 MHz) δ 8.37 (d, *J*=6.0 Hz, 2H, N-C$\underline{H}_{alkene}$), 7.98 (d, *J*=6.0 Hz, 2H, Ar-$\underline{H}$), 7.87 (d, *J*=8.0 Hz, 2H, Ar-$\underline{H}$), 7.39 (t, *J*=9.0 Hz, 2H, Ar-$\underline{H}$), 7.35-7.27 (m, 15H, Ar-$\underline{H}$), 6.84 (d, *J*=12.0 Hz, 1H, C$\underline{H}_{alkene}$), 6.66 (d, *J*=12.0 Hz, 1H, C$\underline{H}_{alkene}$), 6.56 (d, *J*=12.0 Hz, 1H, C$\underline{H}_{alkene}$), 5.73 (s, 2H, N-C$\underline{H}_2$), 5.64 (s, 2H, N-C$\underline{H}_2$), 5.60 (s, 4H,-C$\underline{H}_2$-Ph), 1.96 (s, 3H, C-CH$_3$). IR (ATR) 3276, 2285, 1512, 1330, 1123, 1010, 807, 722 cm^{-1}. MS (ESI) m/z: 717.11 [M]$^+$. HRMS (FAB): Calcd for C$_{42}$H$_{37}$N$_8$S$_2$ [M]$^+$ 717.2577, found 777.2591. UV abs λmax = 770 nm.

References

1. E.A. te Velde, Th. Veerman, V. Subramaniam, Th. Ruers, *EJSO.*, 2010, **36**, 6.

2. R. Blasberg, *Clin Cancer Res*., 2007, **13**, 3444.

3. S.J. Campbell , A. Gaulton , J. Marshall , D. Bichko , S. Martin , C. Brouwer , L. Harland , Visualising the drug land scape. *Drug Discov. Today* 2010, 15, 315.

4. R. Weissleder, B.D. Ross, A. Rehemtulla, *Molecular Imaging. Shelton, CT, USA: PMPH USA, Ltd*., 2010. p.1

5. J.L. Kovar, M.A. Simpson, A. Schutz-Geschwender, *Anal Biochem*., 2007, **367**, 1.

6. R. Jianghong, D-A. Anca, Y. Hequan, *Biotechnol*., 2007, **18**, 17.

7. Q. Wu, F.A. Merchant, K.R. Castleman, Eds., *Microscope Image Processing*, Academic Press, New York, NY, USA, 2008.

8. A.P. de Silva, H.Q.N. Gunaratne, T. Gunnlaugsson, A.J.M. Huxley, C.P. McCoy, J.T. Rademacher, T.E. Rice, *Chem. Rev*., 1997, **97**, 1515.

9. E.M. Nolan, S.J. Lippard, *Chem. Rev*., 2008, **108**, 3443.

10. E.L. Que, D.W. Domaille, C.J. Chang, *Chem. Rev*., 2008, **108**, 1517.

11. D.T. Quang, J.S. Kim*, Chem. Rev*., 2010, **110**, 6280.

12. S.W. Thomas, G.D. Joly, T.M. Swager, *Chem. Rev*., 2007, **107**, 1339.

13. J.T. Alander, I. Kaartinen, A. Laakso, T. Patila, T. Spillmann, V.V. Tuchin, M. Venermo, P. Valisuo, *Int. Journ. Biomed. Imaging* 2012, 1.

14. J. Du, M. Hu, J. Fan, X. Peng, *Chem. Soc. Rev*., 2012, **41**, 4511.

15. D.D. Nolting, J.C. Gore, W. Pham, *Curr. Org. Synth*., 2011, **8**, 521.

16. J.O. Escobedo, O. Rusin, S. Lim, R.M. Strongin*, Curr. Opin. Chem. Biol*., 2010, **14**, 64.

17. C. Tung, Y. Lin, W. Moon, R. Weissleder, *Chem. Bio. Chem*, 2002, **3**, 784.

18. B. Ballou, L.A. Ernst, A.S. Waggoner, *Curr Med Chem*., 2005, **12**, 795.

19. R. Weissleder, V. Ntziachristos, *Nat. Med*., 2003, **9**, 123.

20. R. Raghavachari, Marcel Dekker, *Near-Infrared Applications in Biotechnology,* 1st ed. New York, 2001.

21. V. Ntziachristos, A.G. Yodh, M. Schnall, B. Chance, *Proc. Natl. Acad. Sci. USA* 2000, **97**, 2767.

22. W.T. Che, U. Mahmood, R. Weissleder, C.H. Tung, *Arthritis Res Ther.*, 2005, **7**, 310.

23. R. Jianghong, A. Dragulescu-Andrasi, Y. Hequan, *Current Opinion in Biotechnology* 2007, **18**, 17.

24. M. Wainwright, *Photosensitisers in Biomedicine*. 1st ed. 2009 Liverpool: Wiley-Blackwell. **298**.

25. The Molecular Probes Handbook: *A guide to fluorescent probes and labelling technologies, Eleventh Edition* 2010. p. 69

26. P. Ehrlich, 'Contributions to the Atiologie and histology pleuritischer exudates', (charite'-Annals, 1882), in abysmally (ed.), vol. **1**, p. 29.

27. K. Licha, C. Olbrich, *Adv. Drug Deliv. Rev.*, 2005, **57**, 1087.

28. M.Wainwright, *Dyes and Pigments* 2008, **76**, 582.

29. R.B. Mujumdar, L.A. Ernst, S.R. Mujumdar, A.S. Waggoner, *Cytometry* 1989, **10**, 11.

30. R.B. Mujumdar, L.A. Ernst, S.R. Mujumdar, *Bioconjug Chem.*, 1993, **4**, 105.

31. M. Amaresh, B.K. Rajani, P.K. Behera, B. K. Mishra, G.B. Behera*, Chem. Rev.*, 2000, **100**, 1973.

32. C. Reichardt, *J Phys Org Chem.*, 1995, **8**, 761.

33. W.M. Leevy, S.T. Gammon, H. Jiang, J.R. Johnson, D.J. Maxwell, E.N. Jackson, M. Marquez, B.D. Smith, *J. Am. Chem. Soc.*, 2006, **128**, 16476.

34. R.C. Benson, H.A Kues, *J.Chem.Eng.Data* 1977, **22**, 379.

35. C.H.G. Williams, *Trans. R. Soc. Edinburg* 1856, **21**, 377.

36. M. Sameiro, *Chem. Rev.*, 2009, **109**, 190.

37. G. Patonay, J. Salon, J. Sowell, L. Strekowski, *Molecules* 200, **9**, 40.

38. K. Venkataraman, *The Chemistry of Synthetic Dyes*; Academic Press, INC. 1952, **2**, 1146.

39. H. Maged, P. Vaishali, O.A. Owens, A. Ritu, *Bio and Med. Chem. Lett.*, 2012, **22**, 1242.

40. M. Mojzych, M. Henary, *Topics in Heterocyclic*; Strekowski, Ed.; Springer: Berlin, 2008; **14**, Verlag, Heidelberg.

41. F.M. Hamer, *The Chemistry of Heterocyclic Compounds*; Weissberger, A., Ed.;Interscience: New York, NY, 1964; p 18.

42. M. Mojzyc, M. Henary, *Synthesis of Cyanine Dyes, Heterocyclic Polymethine Dyes,* 2008, Springer-VerlagBerlin Heidelberg.

43. L.J.E. Hofer, R.J. Grabenstetter, E.O. Wiig, *J. Am. Chem. Soc*., 1950, **72**, 203.

44. E. Delaey, F. VanLaar, D. DeVos, A. Kamuhabwa, P. Jacobs, P. De Witte, *J. Photochem and Photobio*., 2000, **55**, 27.

45. J. Griffiths, *Colour and Constitution of Organic Molecules*, Academic Press, London 1976.

46. J. Fabian, H. Hartmann, *Light Absorption of Organic Colorants*, Springer-Verlag, Berlin 1980.

47. M. Matsuoka, *Chemistry of Functional Dyes, eds*. Z. Yoshida and T. Kitao, Tokyo, Japan, 1989, p.9.

48. T.G. Deligeorgiev, D.A. Zaneva, H.E. Katerionopoulos, V.N. Kolev, *Dyes and Pigments* 1999, **41**, 49.

49. Z.H. Peng, L. Qun, X.H. Zhou, S. Caroll, S.J. Geise, B.X. Peng, R. Dommisse, R. Carleer, *J. Mater. Chem.*, 1996, **6**, 559.

50. Z.H. Peng, H.J. Geise, X.F. Zhou, B.X. Peng, R. Carleer, R. Dommisse, *Liebigs Ann Recueil*, 1997, p.27.

51. U. De Rossi, J. Moll, M. Spieles, G. Bach, S. Daehne, *J. Pract. Chem*., 1995, **337**, 203.

52. M.E. Jung, W.J. Kim, *Bioorg. Med. Chem*., 2006, **14**, 92.

53. R.M. El-Shishtawey, P. Almeida, *Tetrahedron* 2006, **62**, 7793.

54. H. Mitekura, T. No, K. Suzuki, K. Satake, M. Kimura, *Dyes and Pigment* 2002, **54**, 113.

55. S.R. Mujumdar, R.B. Mujumdar, C.M. Grant, A.S. Waggoner, *Bioconjugate Chem*., 1996, **7**, 356.

56. B. Chipon, G. Clave, C. Bouteiller, M. Massonneau, P. Renard, A. Romieua, *Tetrahedron Letters* 2006, **47**, 8279.

57. S. Achilefu, R.B. Dorshow, J.E. Bugaj, R. Rajagopalan, *Invest Radiol*., 2000, **35**, 479.

58. K. Kelly, H. Alencar, M. Funovics, U. Mahmood, R. Weissleder, *Cancer Res*., 2004, **64**, 6247.

59. X. Gao, Y. Cui, R.M. Leveson, L.W. Chung, S. Nie, *Nat Biotechnol*., 2004, **22**, 969.

60. S.M. Makin, I.I. Boiko, O.A. Shavrygina, *Zh Org Khim*., 1977, **13**, 1189.

61. M. Lipowska, G. Patonay, L. Strekowski, *Heterocyl. Commun.*, 1995, **1**, 427.

62. L. Strekowski, M. Lipowska, G. Patonay, *J Org Chem.,* 1992, **57**, 4578.

63. J.O. Tocho, R. Duchowicz, L. Scaffardi, G. M. Blimes, R. Dipaolo, M. Murphy, *Trends Phys. Chem*., 1992, **3**, 31.

64. K. Saito, H. Yokoyama, *Thin Solid Films* 1994, **234**, 526.

65. R. Kietzmann, A. Ehret, M. Spitler, F. Willig, *J. Am. Chem. Soc.*, 1993, **115**, 1930.

66. B. Trosken, F. Willig, K.Schwarzburg, A. Ehret, M.Spitler, *J. Phys. Chem.*, 1995, **99**, 562.

67. M.T. Spitler, A. Ehret, R. Kietzmann, F. Willig, *J. Phys. Chem.*, 1997, **101**, 2552.

68. J.M. Lanzafame, A.A. Muenter, D.V. Brumbaugh, *Chem. Phys.*, 1996, **210**, 79.

69. J.M. Lanzafame, L. Min, R. J. D. Miller, A.A. Muenter, B.A. Parkinson, *Mol. Cryst. Liq. Cryst.*, 1991, **194**, 287.

70. D.M. bius, *Adv. Mater.*, 1995, **7**, 437.

71. T. Tani, *Photographic Sensitivity*; Oxford University Press: New York, 1995; Chapter **5**, p.111.

72. J. Arden, G. Deltau, V. Huth, U. Kringel, D. Peros, K.H. Drexhage, *J. Lumin.*, 1991, **48**, 352.

73. C. Chen, B. Zhou, D. Lu, G. Xu, *J. Photogr. Sci.*, 1995, **43**, 134.

74. C. Chen, X. Qi, B. Zhou, *J. Photochem. Photobiol. A* 1997, **109**, 155.

75. T.P. Causagrove, S.Yang, W.S. Struve, *J. Phys. Chem.*, 1988, **92**, 6121.

76. W.F. Beck, K. Sauer, *J. Phys. Chem.*, 1992, **96**, 4658.

77. K. Kemnitz, N. Nakashima, K. Yoshihara, H. Matsunami, *J. Phys. Chem.*, 1989, **93**, 6704.

78. R. Eichberger, F. Willig, *Chem. Phys.*, 1990, **141**, 159.

79. M. Kawakami, K. Koya, T. Ukai, N. Tatsuta, A. Ikegawa, K. Ogawa, T. Shishidi, L.B. Chen, *J. Med. Chem.*, 1998, **41**,130.

80. M.Z. Hossain, L.A. Ernst, J.L. Nagy, *Neurosci. Lett.*, 1996, **184,** 183.

81. J.O. Escobedo, O. Rusin, S. Lim, R.M. Strongin, *Curr. Opin. Chem. Biol.*, 2010, **14**, 64.

82. D. T. Quang, J. S. Kim, *Chem. Rev.*, 2010, **110**, 6280.

83. H. Kobayashi, M. Ogawa, R. Alford, P.L. Choyke, Y. Urano, *Chem. Rev.*, 2010, **110**, 2620.

84. X. Chen, X. Tian, I. Shin, J. Yoon, *Chem. Soc. Rev.*, 2011, **40**, 4783.

85. H.N. Kim, W.X. Ren, J.S. Kim, J.Yoon, *Chem. Soc. Rev.*, 2012, **41**, 3210.

86. M. Dutta, D. Das, *Trends Anal. Chem.*, 2012, **32**, 113.

87. A. Hagfeldt, M. Gratzel, *Acc. Chem. Res.*, 2000, **33**, 269.

88. K. Sayama, K. Hara, N. Mori, M. Matsuki, S. Suga, S. Sugihara, H. Arakawa, *Chem. Commun.*, 2000, 1173.

89. K. Hara, M. Kurashige, S. Ito, A. Shinpo, S. Suga, K. Sayama, H. Arakawa, *Chem. Commun.*, 2003, 252.

90. K. Hara, K. Sayama, Y. Ohga, A. Shinpo, S. Suga, H. Arakawa, *Chem. Commun.*, 2001, 569.

91. M. Matsuia, Y. Hashimotoa, K. Funabikia, J. Jinb, T. Yoshidac, H. Minourac, *Synthetic Metals* 2005, **148**, 147.

92. K. Hara, T. Sato, R. Katoh, A. Furube, Y. Ohga, A. Shinpo, S. Suga, K. Sayama, H. Sugihara, H. Arakawa, *J. Phys. Chem.* B 2003, **107**, 597.

93. W. Wenjun, G. Fuling, L. Jing, H. Jinxiang, H. Jianli, *Synthetic Metals* 2010, **160**, 1008.

94. R. Laia, P. Mar, M. Serguei, V. Francisco, A. Julian, *Sensors and Actuators* B 2006. **114**, 705.

95. M. Serguei, E. Cristina, A. Julian, *Tetrahedron Letters* 2001, **42**, 6129.

96. O. Ostroverkhova, W.E. Moerner*, Chem. Rev.*, 2004, **104**, 3267.

97. F. Wurthner, R. Wortmann, K. Meerholz, *Chem. Phys. Chem.*, 2002, **3**, 17.

98. D.R. Kanis, M.A. Ratner, T.J. Marks, *Chem. Rev.*, 1994, **94**, 195.

99. L.R. Dalton, A.W. Harper, R. Ghosen, W.H. Steier, M. Ziari, H. Fetterman, Y. Shi, R.V. Mustacich, A.K-Y. Jen, K.J. Shea, *Chem. Mater.*, 1995, **7**, 1060.

100. http://www.science20.com/mei/nonlinear optics

101. G.U. Bublitz, R. Ortiz, C. Runser, A. Fort, M. Barzoukas, S.R. Marder, S.G. Boxer, *J. Am. Chem. Soc.*, 1997, **119**, 2311.

102. F. Pan, M.S. Wong, V. Gramlich, C. Bosshard, P. Gunther, *J. Am. Chem. Soc.*, 1996, **118**, 6315.

103. K. Tsuboi, K. Seki, Y.Ouchi, K. Fujita, K. Kajikawa, *Jpn. J. Appl. Phys.*, 2003, **42**, 607.

104. T.J. Dougherty, *Photochem Photobiol.*, 1987, **45**, 879.

105. D.E. Dolmans, D. Fukumura, R.K. Jain, *Nat Rev Cancer* 2003, **3**, 380.

106. D. Kessel, *Adv Drug Delivery Rev.*, 2004, **56**, 7.

107. M. Krieg, R.W. Redmond, *Photochem Photobiol.*, 1993, **7**, 472.

108. R.K. Pandey, L.N. Goswami, Y. Chen, A. Gryshuk, J.R. Missert, A. Oseroff, T.J. Dougherty*, Laser. Surg. Med.*, 2006, **38**, 445.

109. C. Gomer*, J. Photochem. Photobiol.*, 1991, **54**, 1093.

110. A. Harriman, L.C. Shoute, P. Neta, *J. Phys. Chem.*, 1991, **95**, 2415.

111. G. Salma, M. Mordar, *Science* 1976, **191**, 485.

112. B. Frank, U. Schneider, *Photochem. Photobiol.*, 1992, **56**, 271.

113. A.C. Benniston, K.S. Gulliya, A. Harriman, *J. Chem. Soc. Faraday Trans.*, 1997, **93**, 2491.

114. R. Bonnett, A. Harriman, A.N. Kozyrev, *J. Chem. Soc. Faraday Trans.*, 1992, **88**, 763.

115. F. Welder, B. Paul, H. Nakazumi, S. Yagi, C.L. Colyer, *J. Chromatogr. B* 2003,**793**, 93.

116. G. Patonay, J. Salon, J. Sowell, L. Strekowski, *Molecules* 2004, **9**, 40.

117. T. Fukushima, N. Usui, T. Santa, K. Imai, *J. Pharm. Biomed. Anal.*, 2003, **30**, 1655.

118. A. Garman, *Non-radioactive labelling: a practical introduction.* Academic, San Diego. 1997.

119. R.J. Williams, M. Lipowska, G. Patonay, L. Strekowski, *Anal. Chem.*, 1993, **65**, 601.

120. C.P. Parungo, S. Ohnishi, A.M. De Grand, R.G. Laurence, E.G. Soltesz, Y.L. Colson, P.M. Kang, T. Mihaljevic, L.H. Cohn, J.V. Fragioni, *Ann. Surg. Oncol.*, 2004, **11**, 1085.

121. A. Nakayama, F. Del Monte, R.J. Hajjar, J.V. Frangioni, *Mol. Imaging.*, 2002, **1**, 365.

122. J.E. Bugaj, S. Achilefu, R.B. Dorshow, R. Rajgopalan, *J. Biomed. Opt.*, 2001, **6**, 122.

123. S. Achilefu, Y. Ye, W.P. Li, C.J. Anderson, J. Kao, G.V. Nikiforovich, *J. Am. Chem. Soc.*, 2003, **125**, 7766.

124. K. Licha, C. Hessenius, A. Becker, P. Henklein, M. Bauer, S. Wisniewski, B. Wiedenmann, W. Semmler, *Bioconjugate Chem.*, 2001, **12***, 44.

125. K. Glunde, C. Li, T.R. Greenwood, Z.M. Bhujwalla, *Org. Lett.*, 2006, **8**, 3623.

126. M. Akira, K-K. Shinae, Y. Ryo, H.Isao, K. Tatsuya, O. Eiichi, H. Masahiro, K. Shunsaku, *Biomaterials* 2009, **30**, 5156.

127. L. Tiancheng, W. Lisa, H. Mark, C. Joseph, B. Clifford, *Bioorg. Med. Chem. Lett.*, 2010, **20**, 7124.

128. N.K. Devaraj, R. Weissleder, *Molecular Imaging. Shelton, CT, USA: PMPH USA,Ltd.*, 2010. p. 471.

129. K.B. Sharpless, H.C. Kolb, M.G. Finn, *Angew. Chem. Int. Ed.*, 2001, **40**, 2004.

130. K.B. Sharpless, H.C. Kolb, M.G. Finn, *drug discoverytoday* 2003, **8**, 1128.

131. M.G. Finn, H.C. Kolb, K.B. Sharpless, *Kagaku Kogyo* 2007, **60**, 976.

132. R. Huisgen, *1,3-dipolar cycloaddition chemistry. New York: Wiley*;1984

133. T.R. Chan, R. Hilgraf, K.B. Sharpless, V.V. Fokin, *Org Lett.*, 2004, **6**, 2853.

134. A.H. El-Sagheer, T. Brown, *Chem. Soc. Rev.*, 2010, **39**, 1388.

135. N.K. Devaraj, R.A. Decreau, W. Ebina, *J. Am. Chem. Soc.*, 2006, **110**, 15955.

136. V.V. Rostovtsev, L.G. Green, V.V. Fokin, K.B. Sharpless, *Angew. Chem. Int. Ed.* 2002, **41**, 2596.

137. S. Berndl, N. Herzig, P. Kele, D. Lachmann, X.H. Li, O.S. Wolfbeis, H.A. Wagenknecht, *Bioconjugate Chem.*, 2009, **20**, 558.

138. T.L. Hsu, S.R. Hanson, K. Kishikawa, *Proc Natl Acad Sci USA* 2007. **104**, 2614.

139. M. Sawa, T.L. Hsu, T. Itoh, *Proc Natl Acad Sci USA* 2006, **103**, 12371.

140. A. Deiters, T.A, Cropp, M. Mukherji, *J. Am. Chem. Soc.*, 2003, **125**, 11782.

141. J.V. Frangioni, *Curr. Opin. Chem. Biol.*, 2003, **7**, 626.

142. W.M. Leevy, S.T. Gammon, H. Jiang, J.R. Johnson, D.J. Maxwell, E.N. Jackson, M. Marquez, D. Piwnica-Worms, B.D. Smith, *J. Am. Chem. Soc.*, 2006, **128**, 16476.

143. R. Weissleder, C.H. Tung, U. Mahmood, J.A. Bogdanov, *Nat. Biotechnol.*, 1999, **17**, 375.

144. W. Cai, D.W. Shin, K. Chen, O. Gheysens, Q. Cao, S.X. Wang, S.S. Gambhir, X. Chen, *Nano Lett.*, 2006, **6**, 669.

145. L.Q. Wang, X.J. Peng, W.B. Zhang, F.Yin, J.N. Cui, X.Q. Gao, *Chin. Chem. Lett.*, 2005, **16**, 341.

146. E. Arunkumar, C.C. Forbes, B.C. Noll, B.D. Smith, *J. Am. Chem. Soc.*, 2005, **127,** 3288.

147. P.P. Ghoroghchian, P.R. Frail, P.R. Susumu, T.H. Park, S.P. Wu, H.T. Uyeda, D.A. Hammer, M.J. Therien, *J. Am. Chem. Soc.*, 2005, **127**, 15388.

148. K.C. Smith, *Basic photochemistry*. http://www.photobiology.info/Photochem.html

149. J.J. Fox, L.G. Brooker, D.W. Heseltine, *Mayo. Clin.*, 1957, **32**, 478.

150. J.J. Fox, E.H. Wood, *Mayo. Clin.*, 1957, **32**, 541.

151. J. Caesar, S. Sheldon, L. Chianduss, *Clin. Sci.*, 1961, **21**, 43.

152. M. Choi, K. Choi, S.W. Ryu, J. Lee, C. Choi, *Journ. Biomed. Opt.*, 2011.**16**, 4.

153. E.M. Sevick-Muraca, J.P. Houston, M. Gurfinkel, *Curr. Opin. Chem. Bio.*, 2002. **6**, 642.

154. K. Kogur, E. Choromokos, *J. Appl. Physio.*, 1969, **26**,154.

155. R.W. Flower, *Investigative Ophthalmology* 1973, **12**, 881.

156. Y. Tajima, M. Murakami, K. Yamazaki, T. Kato, M. Kusano, *The Open Surgical Oncology Journal* 2010, **2**, 65.

157. Y. Ogasawara, H. Ikeda, M. Takahashi, K. Kawaski, H. Doihara, *World J Surg*., 2008, **32**, 1924.

158. G.E. Cohn, R. Domanik, *Biomedical photonics handbook. Vo-Dinh T (ed)*, CRC Press, Boca Raton, 2002.

159. M. Hope-Ross, L.A. Yaannuzzi, E.S. Gragoudas, D.R. Guyer, J.S. Slakter, J.A. Sorenson, *Opthalmology* 1994, **101**, 529.

160. L. Yuhui, W. Ralph, T. Ching-Hsuan, *Bioconjugate Chem*., 2002, **13**, 605.

161. K. Jan, W. Andreas, K. Licha, *Basic Res Cardiol*., 2008, **103**, 144.

162. J.R. Lakowicz, *Principles of Fluorescent Spectroscopy*. Springer US, 1.

163. R. Weissleder, B.D. Ross, A. Rehemtulla, *Molecular Imaging: Principles and practice. Shelton, CT, USA: PMPH USA, Ltd*., 2010. p.4

164. M. Yanagida, *Geno.Bio*., 2003, **3**, 3.

165. J.L. Nitiss, *Biomedical and life sciences 2007*. DOI:10.1007/978-1-4020-5963-63. 75-.

166. A. Barberis, T. Gunde, C. Berset, S. Audetat, U. Luthi, *Drug discovery today technologies* 2005, **2**, 187.

167. A. Trabocchi, I. Stefanini, M. Morvillo, L. Ciofi, D. Cavalieri, A. Guarna, *Org. Biomol. Chem*., 2010, **8**, 5552.

168. Johanna Hoog, EMBL Heidelberg, *European Molecular Biology Laboratory.* http://www.eurekalert.org/multimedia/pub/3409.php?from=91643.

169. C-H. Tung, Y. Lin, R. Weissleder, *Bioconjugate Chem.*, 2002, **13**, 605.

170. X. Cheng, X. Peng, A. Cui, B. Wang, L. Wang, R. Zhang, *J. Photochem. Photobiol*., 2006, **181**, 79.

171. T. Hirata, H. Kogiso, K. Morimoto, S. Miyamoto, H. Taue, S. Sano, N. Muguruma, S. Ito, Y. Nagao, *Bio. Med. Chem*., 1998, **6**, 2179.

172. W. Aibin, D. Liping, *Turk J Chem*., 2011, **25**, 475.

173. A. Samuel, L. Hyeran, B.Y. Mikhail, H. Maged, S. Lucjan, *J Photochem and Photobio A:Chem*., 2008, **200**, 438.

174. B.W. Henderson, T.J. Dougherty, *Photochem Photobiol* 1992, **55**, 145.

175. G. Chapman, M. Henary, G. Patonay, *Anal. Chem. Insights* 2011, **6**, 29.

176. B.D.Autreaux, M.B. Toledano, *Nat. Rev. Mol. Cell. Biol.*, 2007, **8**, 813.

177. M. Valko, D. Leibfritz, J. Moncol, M. T. D.Cronin, M. Mazur, J. Telser, *Int. J. Biochem. Cell Biol.*, 2007, **39**, 44.

178. C.C. Winterbourn, *Nat. Chem. Biol.* 2008, **4**, 278.

179. Tetsuo Nagano, D. Oushiki, H. Kojima, T. Terai, M. Arita, K. Hanaoka, Y. Urano, *J. Am. Chem. Soc.*, 2010, **132**, 279.

180. T. Nagano, H. Takakusa, K. Kikuchi, Y. Urano, H. Kojima, *Chem. Eur. J.*, 2003, **9**, 1479.

181. H. Keli, Y. Fabiao, L. Peng, L. Guangyue, Z. Guangjiu, C. Tianshu, *J. Am. Chem. Soc.*, 2011, **133**, 11030.

182. G. Ferrer-Sueta, R. Radi, *Chem. Biol.*, 2009, **4**, 161.

183. J.T. Rotruck, A.L. Pope, H.E. Ganther, A.B. Swanson, D.G. Hafeman, W.G. Hoekstra, *Science* 1973, **179**, 588.

184. L. Flohe, D. Dolphin, R. Poulson, O. Avramovic, *In Glutathione: Chemical, Biochemical, and MedicalAspects*; 1st Eds; Wiley: New York, 1989.

185. B. Tang, F. Yu, P. Li, L. Tong, X. Duan, T. Xie, X. Wang, *J. Am. Chem. Soc.*, 2009, **131**, 3016.

186. C.W. Nogueira, G. Zeni, J.B. Rocha, *Chem. Rev.*, 2004, **104**, 6255.

187. Y. Xiaojian, S. Chunmeng, T. Rong, Q. Weiping, Z.E. Haiyen, W. Ruoxiang, Z. Guodong, C. Jianjun, Y.W. Vincent, C. Tianmin, H. Maged, S. Lucjan, C.W. Chung, *Clin Cancer Res.*, 2010, **16**, 2833.

189. C. Bertolino, G. Caputol, C. Barolo, G. Viscardi, S. Coluccial, *J. Fluoresce.*, 2006, **16**, 221.

190. E. Delaey, F. van Laar, D. De Vos, A. Kamuhabwa, P. Jacobs, P. de Witte, *J Photochem Photobiol B.*, 2000, **55**, 27.

191. R.B. Kim, *Eur J Clin Invest* 2003, **33**, 1.

192. X. Tan, S. Luo, D. Wang, Y. Su, T. Cheng, C. Shi, *Biomaterials* 2012, **33**, 2230.

193. H. Maged, P. Vaishali, O.A. Eric, A. Ritu, *Bio and Med Chem Lett.*, 2012, **22**, 1242.

194. H.K. Han, D.M. Oh, G.L. Amidon, *Pharm. Res.*, 1998, **15**, 1382.

195. A.C. Guyton, *Textbook of Medical Physiology*. 8th ed. 1991, Philadelphia: W.B. Saunders.

196. E.L. Hill, *BSc Chemistry Project report*, University of Central Lancashire, 2010.

197. C. Encinas, S. Miltsov, E. Otazo, L. Rivera, M. Puyol, J. Alonso, *Dyes Pigments* 2006, **71**, 28.

198. A.S. Galvez, P. Hunt, M.A. Robb, M. Olivucci, T. Vreven, H.B. Schlegel, *J. Am. Chem Soc.*, 2000, **122**, 2911.

199. J.H. Flanagan, S.H. Khan, S. Menchen, S.A. Soper, R.P. Hammer, *Bioconjugate Chem.,* 1997, **8**, 751.

200. X. Peng, D.R. Draney, *LabPlus International* 2004.

201. G. Patonay, M.D. Antoine, *Anal. Chem.*, 1991, **63**, 321.

202. A.S. Waggoner, L.A. Ernst, R.B. Mujumdar, *U.S. Patent* 1993, **5**, 268.

203. X. Peng, F. Song, E. Lu, Y. Wang, W. Zhou, J. Fan, Y. Gao, *J. Am. Chem. Soc.*, 2005, **127**, 4170.

204. C. A. Bertolino, G. Caputo, C. Barolo, G. Viscardi, S. Coluccia, *J. Fluoresc.*, 2006, **16**, 221.

205. M.Khati, *J Clin Pathol.*, 2010, **63***,* 480.

206. B.P.Joshi, T.D. Wang, *Cancers* 2010, **2***,* 1251.

207. C. Li, T.R. Greenwood, K. Glunde, *Neoplasia* 2008, **10***,* 389.

208. H. Xiaoxiao, W. Kemin, C. Zhen, *Wiley Interdiscip Rev Nanomed Nanobiotechnol.*, 2010, **2**, 349.

209. N. Kosaka, M. Mitsunaga, M.R. Longmire, P.L. Choyke, H. Kobayashi, *Int J Cancer* 2011, **167**, 1.

210. E.N. Marvell, G. Caple, I. Shahidi*, J. Am. Chem. Soc.*, 1970, **92**, 5646.

211. C. Pavlik , N.C. Biswal, F.C. Gaenzler, M.D. Morton, L.T. Kuhn, K.P. Claffey, Q. Zhu, M.B. Smith, *Dyes and Pigments* 2011, **89**, 9.

212. M. Taariq, P. Alexis, L. Sylvain, *J. Org. Chem.*, 2010, **75**, 204.

213. J. Pernak, J. Rogoza, *Arkivoc* 2000, **1**, 889.

214. L. Atmaca, A. Onen, Y. Yagci, *Eur. Polym. J*., 2001, **37**, 677.

215. J. Pernak, J. Kalewska, H. Ksycinska, J. Cybulski, *Eur. J. Med. Chem.*, 2001, **36**, 899.

216. E. F. V. Scriven, *Chem. Soc. Rev*., 1983, **12**, 129.

217. W. Konig*, J. Prakt. Chem.*, 1904, **69**, 105.

218. T. Zincke, *Liebigs Ann. Chem.*, 1903, **330**, 361.

219. T. Zincke, W. Wurker, *Liebigs Ann. Chem.*, 1905, **338**, 107.

220. A.M. Kearney, C.D. Vanderwal, *Angew. Chem. Int. Ed.*, 2006, **45**, 7803.

221. L. J. Jack, *Name Reactions, 4th expanded ed.* 2009, p. 596.

222. Q. Li, J. Tan, B. Peng, *Molecules* 1997, **2**, 91.

223. P. Kele, X. Li, M. Link, K. Nagy, A. Herner, K. Lorincz, S. Benid O.S. Wolfbeis*, Org. Biomol. Chem.*, 2009, **7**, 3486.

224. C.W. Tornoe, C. Christensen, M. Meldal, *J. Org. Chem.*, 2002, **67**, 3057.

225. V.V. Rostovtsev, L.G. Green, V.V. Fokin, K.B. Sharpless, *Angew. Chem. Int. Ed.*, 2002, **41**, 2596.

226. M. Cooper, A.Ebner, M. Briggs, M. Burrows, N. Gardner, R. Richardson, *J. Fluoresc*., 2004, **14**, 145.

227. W.R. Henderson, J.A. Guenette, P.B. Dominelli, D.E. Griesdale, J.S. Querido, R. Boushel, A.W. Sheel, *Respir Physiol Neurobiol*., 2012, **31***, 302.

228. N. Kosaka, M. Mitsunaga, M.R. Longmire, P.L. Choyke, H. Kobayashi, *Int J Cancer* 2011, **167**, 1.

229. R. Jianghong, D. Anca, Y. Hequan, *Current Opinion in Biotechnology* 2007, **18**, 17.

230. M. Hope-Ross, L.A.Yaannuzzi, E.S Gragoudas, D.R. Guyer, J.S. Slakter, J.A. Sorenson, *Opthalmology* 1994, **101**, 529.

231. L. Yuhui, W. Ralph, T. Ching-Hsuan, *Bioconjugate Chem*., 2002, **13**, 605.

232. A. Fernandez-Fernandez, R. Manchanda, T. Lei, D.A. Carvajal, Y. Tang, S.Z. Kazmi, A.J. McGoron, *Mol. Imaging* 2012, **11**, 99.

233. J.V. Sukhatankar, K.S Korgaonkar, *Int. J. Cancer* 1966. **1**, 297.

234. F.S. Southwick, H.S. Carr, G.A. Carden, R.M. Alisa, H.S. Rosenkranz, *J Bacteriol*., 1972, **1**, 439.

235. S. Moreno, A. Klar, P. Nurse, *Enzymol*., 1991, **194**, 795.

236. P. Chen, J. Li, Z. Qian, D. Zheng, T. Okasaki, M. Hayami, *Dyes Pigm*ents, 1998, **37**, 213.

237. S. Lepaja, H. Strub, D.J. Lougnot, *Z Naturforsch* 1982, **38**, 56.

238. T.R. Gemmill, R.B. Trimble, *Biochimica et Biophysica Acta* 1999, **1426**, 227.

239. M. Cooper, A. Ebner, M. Briggs, M. Burrows, N. Gardner, R. Richardson, R. West, *J. Fluoresc*., 2004, **14**, 145.

240. J.H. Flanagan, C.V. Owens, S.E. Romero, E. Waddell, S.H. Kahn, R.P. Hammer, S.A. Soper, *Anal. Chem*., 1998, **70**, 2676.

241. R. Gollapudy, S. Ajmani, S.A. Kulkarni *Bioorg. Med. Chem*., 2004, **12**, 2937.

242. S.A. Soper, Q.L. Mattingly, *J. Am. Chem. Soc.*, 1994, **116**, 3744.

243. U. Yuichiro, J. Jiney, L. Aurore, B. Kevin, P.B. Cesar, A. Pavel, *J. Am. Chem.* Soc., 2011, **133**, 51.

244. M. Natali, S. Giordani, *Org. Bio. Chem.*, 2012, **10**, 1162.

245. A.C. Pardal, S.S. Ramos, P.F. Santos, L.V. Reis, P. Almeida, *Molecules* 2002, **7**, 320 .

246. J. Shin, S-Y. Park, S.R. Shin, K. Jun, H.S. Youn, K-L. An, Y.A. Son, *Revue Roumaine de Chimie* 2010, **55**, 621.

247. D. Oushiki, T. Terai, M. Arita, , K. Hanaoka, Y. Urano, T. Nagano, H. Kojima, *J. Am. Chem. Soc.*, 2010, **132**, 2795.

248. D.E. Lynch, A.N.Kirkham, M. Z.H.Chowdhury, E.S. Wane, J. Heptinstall, *Dyes and Pigments* 2012, **94**, 393.

249. J.R. Carreon, K.M. Stewart, K.P. Mahon, S. Shin, S. O. Kelley, *Bio. Med. Chem. Lett.*, 2007, **17**, 5182 .

250. R. Buffa, P. Zahradnik, P. Foltinova, *Het. Comm.*, 2001, **7**, 331.

251. A.C. Pardal, S.S. Ramos, P.F. Santos, L.V. Reis, P. Almeida, *Molecules* 2002, **7**, 320.

252. W. Brooker. *J. Am. Chem. Soc.*, 1935, **57**, 2485.

253. Y.L. Slominskii. *J. Org. Chem.*, *USSR* (*English Translation*) 1978, **14**, 2046.

254. S.P. Gromov, E.N. Ushakov, O.A Fedorova, V.A. Soldatenkova, M.V. Alfimov, *Russian Chemical Bulletin* 1997, **46**, 1143.

255. M.T. Kennedy. Patent: US2008/75777 A1; 2008.

256. D. Zhang, J. Su, X. Ma, H. Tian, *Tetrahedron* 2008, **64**, 8515.

257. T. Hirata, H. Kogiso, K. Morimoto, S. Miyamoto, H. Taue, *Bio. Org. Med. Chem.*, 1998, **6**, 2179.

258. M.V. Kvach, V.V. Shmanai, A.V. Ustinov, I.A. Stepanova, A.D. Malakhov, M.V. Skorobogatyi, V.A. Korshun, *Eur. J. Org. Chem.*, 2008, **12**, 2107.

259. N. Yukinori, S. Toshifumi, K. Kozo, U. Toshiyuki, *Dyes and Pigments* 2007, **73**, 344.

260. S.A. Hilderbrand, K.A. Kelly, R. Weissleder, C.H. Tung, *Bioconjugate Chem.*, 2005, **16**, 1275.

261. M. Mojzych, A. Raszkiewicz, L. Strekowski, *Heterocyclic Comm.*, 2009, **15**, 123.

262. N.O. Mahmoodia, M. Mamaghania, A. Ghanadzadeha, M. Arvanda, M. Fesangharia, *J. Phys. Org. Chem.*, 2010, **23**, 266.

263. D. Gnecco, J. Juarez, A. Galindo, C. Marazano, R.G. Enriquez, *Syn. Comm.*, 1999, **29**, 281.

264. S.E. Steinhardt, J.S. Silverston, C.D. Vanderwal, *J. Am. Chem. Soc.*, 2008, **130**, 7560 .

265. R.B. Smith, O.A. Okoh, *UK. Patent application No*. **1201641.6**

266. O.A. Okoh, R.H. Bisby, C.L. Lawrence, C.E. Rolph, R.B. Smith, *J. Sulf. Chem.*, 2013, http://dx.doi.org/10.1080/17415993.2013.778258.

267. M.J Kosch, S. Makinen, F.Sigernes, O.Harang, Experiment. In: Proceedings of the 30th Annual European Meeting on Atmospheric Studies by Optical Methods. 2003.

268. Log*P* values were obtained from http://www.molinspiration.com.

Appendix

Taylor & Francis
Taylor & Francis Group

Promising near-infrared non-targeted probes: benzothiazole heptamethine cyanine dyes

Okoh Adeyi Okoh,[a] Roger H. Bisby,[b] Clare L. Lawrence,[c] Carole E. Rolph[c] and Robert B. Smith[a]*

[a] *Centre for Material Sciences, University of Central Lancashire, Preston PR1 2HE, UK;* [b] *School of Environment and Life Sciences, University of Salford, Salford M5 4WT, UK;* [c] *School of Pharmacy and Biomedical Sciences, University of Central Lancashire, Preston PR1 2HE, UK*

A series of benzothiazole heptamethine cyanine dyes have been synthesized and their photophysical properties evaluated in relation to their structural features. These have been compared against two classical probes of this type: Indocyanine Green (IGC) and New Indocyanine Green (IR-820). Growth inhibitory studies were also performed using a eukaryotic, unicellular organism, fission yeast *Schizosaccharomyces pombe*. Herein we highlight some potentially interesting candidates with improved fluorescence quantum yields when compared with ICG and IR-820.
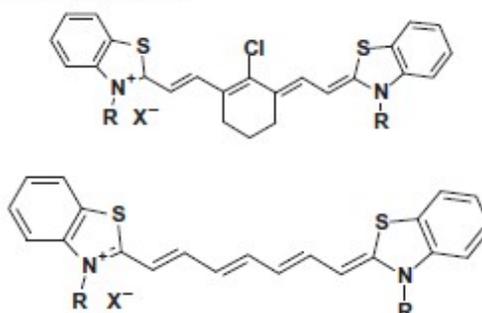
Keywords: benzothiazole; cyanine dyes; fluorescence; growth inhibition; near infrared

1. Introduction

The detection, imaging and quantification of biomolecules using fluorescent probes is an area of increasing interest and importance (*1–4*). With dyes that fluoresce in the visible region, autofluorescence of a sample matrix may interfere (*5*) The use of near-infrared (NIR) probes (700–1000 nm) has generated a vast array of interest, as these can be efficiently used to visualize and investigate *in-vivo* molecular targets as most tissues generate little NIR fluorescence (*6*). Other useful characteristics of probes operating in NIR region are that they often have low phototoxicity,

---

*Corresponding author. Email: rbsmith@uclan.ac.uk

2 *O.A. Okoh* et al.

advantageous for cell and tissue imaging (*7*) and deeper light penetration in tissues is achieved in the NIR.

Two classical NIR probes are Indocyanine Green (IGC) and New Indocyanine Green (IR-820). ICG is commercially available and approved by the United States Food and Drug Administration for use in clinical applications, in particular, evaluating blood flow (*8–11*) and clearance (*11–13*). It also has the potential as a tool for fluorescence-guided management and treatment of cancer (*14, 15*). One of the main drawbacks of ICG is its low fluorescence quantum yield (*16–18*). IR-820 is structurally related to ICG except with the incorporation of a rigid cyclohexane moiety providing improved *in vitro* and *in vivo* stability. However, it is documented that IR-820 has a notably lower quantum yield than ICG (*19*).

The literature reports that benzothiazole heptamethine cyanine dyes featuring two benzothiazole rings linked by a polymethine chain possess the greatest potential for use in visualization of cellular changes occurring *in vivo* due to their excellent biocompatibility (*20*). Patonay and Antoine (*21*) have previously reported that heptamethine cyanine dyes bearing sulfur atoms within their heterocyclic ring system bind preferentially to human serum albumin binding sites and furthermore, the sulfur atom on the heterocyclic ring system could enhance the specificity of the dye molecule. Waggoner and coworkers (*22, 23*) have also reported that the presence of sulfonate groups on the aromatic rings of the dyes helps to increase aqueous solubility and thereby reduces aggregation.

Motivated by this, we report the synthesis and photophysical properties of a series of structurally related non-targeting NIR benzothiazole heptamethine cyanine dyes. These contain either a chain that is partially rigidified by the inclusion of a central cyclic ring (compounds 3a–g) or the simple heptamethine conjugated chain (compounds 5a–g). Our intention is to compare the photophysical (absorption and fluorescence spectra, fluorescence quantum yields and Stokes shifts) and biological properties of the dyes bearing a sulfur moiety (3 and 5a–g) against those of the
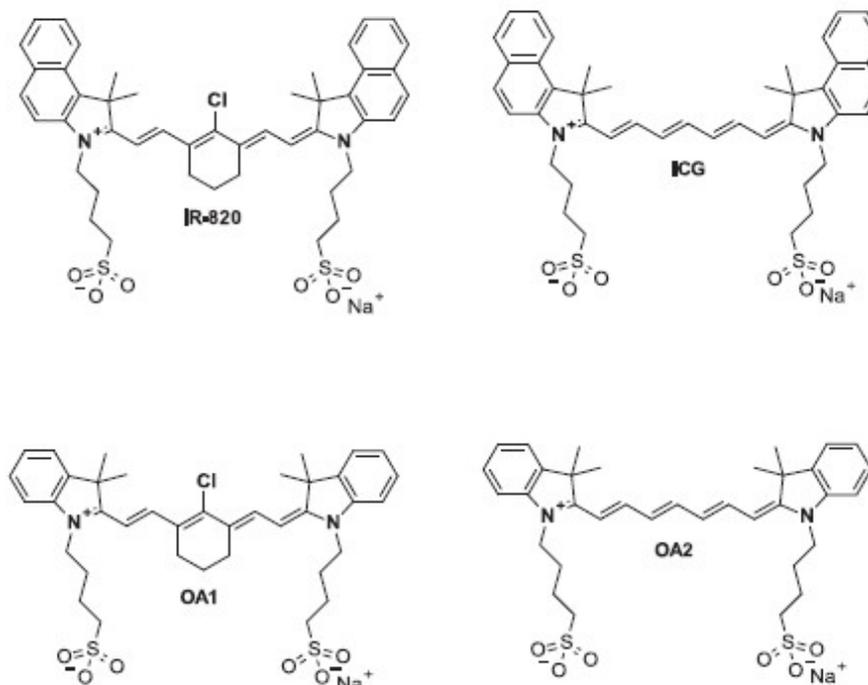
Figure 1.   The structures of IR-820, ICG, **OA1** and **OA2**.

standard fluorophores ICG and IR-820. As shown in Figure 1, the established ICG (linear chain) and IR-820 (rigidified chain) dyes have terminal dimethyl-indolyl groups with an additional fused benzene ring. Two further analogs of IR-820 and ICG (**OA1** and **OA2**, respectively) have thus been synthesized, which lack the additional fused ring (also shown in Figure 1). This allows the direct evaluation of the effects of replacement of the dimethyl-indolyl group by the benzothiazole ring on spectroscopic and biological properties.

The impact of this research is timely, highlighting the development of cost-effective molecular probes with enhanced photophysical and toxicity characteristics when compared against the current clinical standard ICG and IR820. The synthesis of the linear heptamethine dyes (**5a–g**) is in itself significant. This *in situ* cascade reaction is a modification of the Zincke reaction and provides an elegant approach to the linear dyes which can be tailored to develop more structurally sophisticated cyanine dyes.

2. Results and discussion

2.1. *Synthesis*

Synthesis of both the linear and rigid cyanine dyes (**3a–g** and **5a–g**) was straightforward and required no harsh or unusual synthetic methodology. The starting benzothiazolium salts were prepared by the alkylation of benzothiazole in either toluene or acetonitrile using the corresponding alkyl halides or sulfones to afford the benzothiazolium salts (**1a–g**) (Scheme 1). The iminium salt (**2**) was prepared by Vilsmeier–Haack formylation of cyclohexanone (**26**) (Scheme 1). The rigid cyanine dyes (**3a–g**) and linear cyanine dyes (**5a–g**) were prepared using an aldol-like condensation of the benzothiazolium salts and the iminium salt, in the presence of sodium acetate as the base. The reaction mixture was heated under reflux in ethanol overnight (**24**) to produce the crude dyes (**3a–g**) (Scheme 2). The linear cyanine dyes (**5a–g**) were produced using a standard method to produce the 5-anilino-*N*-phenyl-2,4-pentadienylideniminium chloride (**25**) followed by the *in situ* addition of **1a–g** in the presence of sodium acetate as the base (Scheme 3). The reaction mixture was stirred in ethanol overnight to produce the crude dyes (**5a–g**) (**26**). All the crude dyes were purified by column chromatography using silica gel to obtain the pure compounds (**3a–g** and **5a–g**). It should be noted that the N-alkylations for dyes **3a–g** are the same as **5a–g**; these groups are shown in Scheme 1 under R.
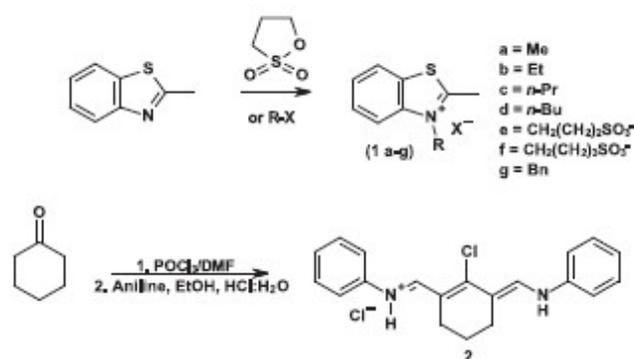
Scheme 1.   The synthetic route to the alkylated salts (**1 a–g**) and the Vilsmeier–Haack iminium salt (**2**).

4 *O.A. Okoh et al.*
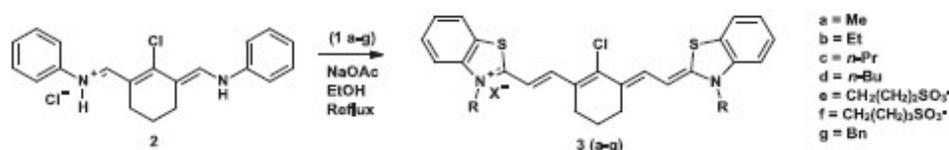
Scheme 2.   The synthetic route to the rigid benzothiazole heptamethine cyanine dyes (**3a–g**).
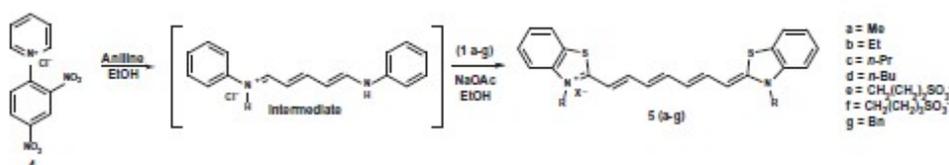
Scheme 3.   The synthetic route to the rigid benzothiazole heptamethine cyanine dyes (**5a–g**).

2.2.   *Photophysical properties*

The photophysical properties of the benzothiazole heptamethine cyanine dyes used in this study are summarized in Tables 1 and 2. Stock solutions of dyes were prepared in methanol. The absorption and fluorescence spectra of each of the dyes were measured sequentially to reduce photobleaching and solubility issues. The fluorescence quantum yields of the dyes were calculated using the relative method, *i.e.* integrated fluorescence peak area versus fraction of light absorbed at the excitation wavelength were plotted for both the standards and cyanine dyes (27). It is well noted that rigidification of the polymethine chain is an established approach for improving the chemical and photostability of NIR dyes (28).

Table 1.   Photophysical and growth inhibition data for rigid benzothiazole heptamethine cyanine dyes (**3a–g**), IR-820 and **OA1** in MeOH. Quantum yields ±10%, λ_{max} ± 1 nm.

3 (a–g)

Compounds		Fluorescence studies				Growth inhibition studies	
Code	R	Absorption λ_{max} (nm)	Fluorescence emission (nm)	Fluorescence quantum yield (Φ)	Stokes shift (nm)	Minimum growth inhibition (µM)	Log P
3a	Me	796	812	0.087	16	0.66[a]	3.923
3b	Et	796	812	0.087	16	0.63[a]	4.675
3c	n-Pr	797	814	0.091	17	0.60[a]	5.68
3d	n-Bu	796	813	0.093	17	0.05[a]	6.799
3e	$CH_2(CH_2)_2SO_3^-$	798	815	0.066	17	18.43[b]	−2.424
3f	$CH_2(CH_2)_3SO_3^-$	800	817	0.082	17	17.71[b]	−1.883
3g	Bn	804	820	0.093	16	1.01[b]	9.176
IR-820	Commercial dye	820	840	0.032	20	11.78[b]	1.441
OA1	$CH_2(CH_2)_3SO_3^-$	782	802	0.085	20	17.2[b]	−0.877

Notes: [a]No visible yeast growth observed at this concentration of dye.
[b]Highest possible concentration tested, visible yeast growth observed.

Table 2. Photophysical and growth inhibition data for linear benzothiazole heptamethine cyanine dyes (**5a–g**) ICG and **OA2** in MeOH. Quantum yields $\pm 10\%$, $\lambda_{max} \pm 1$ nm.

Compounds		Fluorescence studies				Growth inhibition studies	
Code	R	Absorption λ_{max} (nm)	Fluorescence λ_{max} (nm)	Fluorescence quantum yield (Φ)	Stokes shift (nm)	Minimum growth inhibition (μM)	Log P
5a	Me	756	783	0.165	27	1.21[b]	2.805
5b	Et	759	785	0.161	26	0.57[a]	3.557
5c	*n*-Pr	761	786	0.176	25	0.54[a]	4.562
5d	*n*-Bu	761	787	0.181	26	0.06[a]	5.681
5e	$CH_2(CH_2)_2SO_3^-$	762	789	0.146	27	16.58[b]	−1.733
5f	$CH_2(CH_2)_3SO_3^-$	762	789	0.166	27	15.85[b]	−1.192
5g	Bn	765	791	0.229	26	4.62[b]	5.776
ICG	Commercial dye	785	814	0.072	29	12.92[b]	1.591
OA2	$CH(CH_2)_3SO_3^-$	747	775	0.13	28	15.36[b]	−0.728

Notes: [a]No visible yeast growth observed at this concentration of dye.
[b]Highest possible concentration tested, visible yeast growth observed.

2.2.1. *Absorption and fluorescence spectra*

This study focused on the structural diversity of the NIR dyes and the results obtained from this experiment show that the rigid benzothiazole heptamethine cyanine dyes (**3a–g**) exhibited absorption spectra maxima at longer wavelengths than the linear dyes (**5a–g**), with all absorbing in the NIR region between 747 and 820 nm. Tables 1 and 2 demonstrate that rigidification shifts the absorption and fluorescence maxima approximately 30–40 nm to the red when comparing **3a** (796 and 812 nm, respectively) with **5a** (756 and 783 nm).

This increase is not unusual and can also be seen when comparing ICG (785 and 814 nm) with IR-820 (820 and 840 nm). It is also interesting to note that the replacement of a 3,3-dimethylindolenine ring with a benzathiazole also shifts the absorption and fluorescence maxima deeper into the red as shown by comparing **OA1** (782 and 802 nm) with **3f** (800 and 817 nm) and **OA2** (747 and 775 nm) with **5f** (762 and 789 nm). Indeed, this comparison is seen throughout both series in Tables 1 and 2.

The similarities in the absorbance wavelength of the dyes could be attributed to the fact that the *N*-donor and *N*-acceptor substituting groups are too far away from the chromophore and as such have very little influence on the spectroscopic properties of the dyes.

2.2.2. *Fluorescent quantum yields*

An interesting observation is that the rigid benzothiazole heptamethine cyanine dyes (**3a–g**) demonstrated an approximate three-fold increase in quantum yield when compared with IR-820 but showed comparable quantum yields when compared with **OA1**. The linear benzothiazole heptamethine dyes (**5a–g**) show a two-fold increase in quantum yield when compared with ICG as well as an approximate 1.5-fold increase when compared with **OA2**. We also note that rigidification of the polymethine chain reduces the quantum yields for fluorescence by approximately 50%, as shown by comparing **5a** ($\Phi = 0.165$) with **3a** ($\Phi = 0.087$). This reduction in quantum yield is also seen when comparing ICG ($\Phi = 0.072$) with IR-820 ($\Phi = 0.032$) and when comparing **OA1** ($\Phi = 0.085$) with **OA2** ($\Phi = 0.13$). The lower quantum yield in methanol for IR820

6 *O.A. Okoh* et al.

relative to that for ICG is also consistent with the shorter fluorescence lifetime of 250 ps for IR820 compared with 510 ps for ICG (*29*). It is interesting to note that the introduction of a *N*-benzyl group to the non-restricted linear polymethine chain increases the quantum yields for fluorescence by comparing **5g** ($\Phi = 0.229$) with **3g** ($\Phi = 0.093$).

Due to these interesting quantum yields, the benzothiazole heptamethine cyanine dyes (**3a–g** and **5a–g**) show potential for clinical applications when compared with the clinical standard ICG.

2.2.3. *Stokes shifts*

We note the Stokes shifts for the rigid dyes **3a–g** show comparable shifts (16–20 nm) when compared against IR-820 and **OA1**. This is also the case for the unrestricted dyes **5a–g** (25–29 nm) upon comparison with ICG and **OA2**.

2.3. *Growth inhibitory screening*

Apart from the photophysical characteristics of the dyes, the solubility and growth inhibitory properties are important characteristics which determine the practical use of these fluorophores (**3a–g** and **5a–g**) in living cells. The effects of the newly synthesized dyes on cell growth were compared with ICG, IR-820, **OA1** and **OA2**. Dimethyl sulfoxide (DMSO), ICG, IR820, **OA1** and **OA2** were used as controls throughout the screening process.

Comparative growth inhibitory studies were performed using *Schizosaccharomyces pombe*, an eukaryotic microorganism previously used as an important and valuable screening tool for the identification of toxicity (*30, 31*). This is important should these dyes show potential for clinical applications. Using *S. pombe* as a model for mammalian cells is advantageous as many cellular processes are highly conserved between the two (*30, 31*). Cell permeability and growth inhibition can be tested simultaneously and *S. pombe* strains are low in cost, easy to prepare and the results obtained are highly reproducible (*30*).

The growth inhibitory screening procedure involved the inoculation of *S. pombe* wild-type cells (NJ2 *h⁻ ura4-D18 leu1-32 ade6-M210 his7-366*) (*32*) into yeast extract broth (YE), as previously reported (*33*). The culture was then incubated overnight at 30°C with shaking at 200 rpm. Stock solutions of the dyes were prepared in 20% DMSO in YE. DMSO and YE were used as controls for the experiment. 3×10^4 yeast cells were transferred into the wells of a 96-well plate. A 1:2 serial dilution of the dyes was then performed. The well plates were visually inspected for growth after 24 h of incubation at 30°C. Growth was indicated by full or partial appearance of yeast on the bottom of the wells. The minimum growth inhibitory concentration of the dyes was estimated to be the concentration of the compound in the well before yeast growth was first seen. The experiment was repeated three times to ensure reproducibility of the results.

For a number of dyes, no growth was observed at the lowest concentration tested. These are included in Tables 1 and 2, where the lowest concentration tested is indicated. In addition, a number of dyes had limited solubility; the values within the tables indicate the highest possible concentration tested. Wells containing 10% DMSO and only YE showed 100% yeast growth. The results in Tables 1 and 2 show that most of the dyes which exhibited no growth inhibitory effects were the dyes bearing the sulfonic acid group (**3e–f** and **5e–f**) on their *N*-donor and *N*-acceptor systems. Most of the dyes that exhibited growth inhibition were the dyes bearing the alkyl or benzyl group at their *N*-donor and *N*-acceptor system (**3a–d, f** and **5a–d, f**). We therefore suggest that the growth inhibitory effect of these dyes could be attributed to the nature of substituent on the *N*-donor and *N*-acceptor system and using a virtual method, the log *P* (the base 10 logarithm was used throughout) values were obtained (log *P* values were obtained from http://www.molinspiration.com) and these are shown in Tables 1 and 2. The presence of the

sulfonic acid group on the dyes tends to increase their solubility and reduce their growth inhibitory characteristics, possibly through suppressing membrane permeability and cellular uptake. The dyes bearing the sulfonic groups are structurally very similar to ICG, IR820, **OA1** and **OA2**. The presence of the alkyl group tends to reduce the solubility and increase the growth inhibitory characteristic of the dyes due to their lipophilic nature. Our findings also indicated that the linear benzothiazole heptamethine cyanine dyes (**5a–g**) were more soluble and more bio-assimilable than the rigid benzothiazole heptamethine cyanine dyes (**3a–g**).

3. Conclusions

In summary, a series of benzothiazole heptamethine cyanine dyes have been synthesized and their photophysical properties have been evaluated by placing emphasis on their structural diversity and nature of the substituent on the *N*-donor and *N*-acceptor system. It is clear to see that both series of benzothiazole dyes (**3a–g** and **5a–g**) show notably improved fluorescence quantum yield in comparison to ICG, IR820, **OA1** and **OA2**. It is also clear to see that each of the dyes show increased bathochromic shift when compared against **OA1** and **OA2**. However, the fused benzyl rings on ICG and IR-820 lead to an increased bathochromic shift by approximately 20 nm into red. The growth inhibitory characteristics of the dyes were also affected by the nature of substituent on the *N*-donor and *N*-acceptor system. It is noted that compounds **3e–f** and **5e–f** showed low growth inhibitory effects and are comparable to ICG, IR820, **OA1** and **OA2**. To conclude, the benzothiazole heptamethine cyanine dyes reported herein show huge potential as new fluorescent probes.

4. Experimental

4.1. *General information*

^{1}H and ^{13}C NMR spectra were measured on either a Bruker DPX 250 MHz, 300 MHz or a Bruker Avance 400 MHz spectrometer with tetramethylsilane (TMS) as an internal standard for ^{1}H NMR and deuteriochloroform (CDCl$_3$, 77.23 ppm) and deuteriodimethylsulfoxide (d_6-DMSO, 39.52 ppm) for ^{13}C NMR unless otherwise stated. All chemical shifts are quoted in δ (ppm) and coupling constants in Hertz (Hz) using the high-frequency positive convention. The abbreviations used for the multiplicity of the NMR signals are: s = singlet, d = doublet, t = triplet, q = quartet, quin = quintet, sex = sextet, m = multiplet, dd = doublet of doublet, td = triplet of doublets, dm = doublet of multiplets, brs = broad singlet, etc. Low- and high-resolution mass spectra were obtained using electrospray ionization mass spectrometry on a hybrid linear ion trap-Fourier transform mass spectrometer. The ultraviolet absorptions were recorded on a WPA Lightwave II UV/Visible spectrophotometer. IR spectra were recorded on a Specac ATR with a He/Ne-633 nm laser. Thin layer chromatography was carried out on Machery-Nagel polygram Sil/G/UV$_{254}$ pre-coated plates. Melting point (Mp) analysis was carried out in capillary tubes using the Griffin Mp apparatus. All chemicals, solvents and silica gel were obtained from Sigma Aldrich and used without further purification.

4.2. *Photophysical information*

Fluorescence quantum yields (Φ) were measured using a fluorimeter based on an Innovative Photonic Solutions 785 nm diode laser, operating with a power output of 8 mW, an Andor Shamrock

SR-303i spectrograph and an Andor iDus CCD detector (model DU420A-BR-DD). Fluorescence was detected at right angles without any filters. The spectral response of the system was corrected following the method outlined by Kosch *et al.* (*34*). Absorbance values (*A*) of solutions at 785 nm were measured using a Perkin Elmer Lambda 25 spectrophotometer. Corrected fluorescence spectra for a series of solutions of increasing concentration were rescaled in energy and the integrated intensity was plotted versus $1-10^{-A}$, with *A* (785 nm) ≤ 0.1. The quantum yields were obtained from the relative slopes of such plots compared with that from solutions of ICG in DMSO, for which a quantum yield of $\Phi = 0.13$ has been reported (*35*). For determinations in different solvents, the refractive index (n^2) correction was applied.

4.3.   Synthesis

*Below is the general synthetic procedure for salts **1a–g**. Full spectroscopic data are given for all compounds.*

4.3.1.   *2-Methyl-3-(methyl)-benzothiazolium iodide (**1a**)*

To a solution of 2-methylbenzothiazole (0.94 g, 6.30 mmol) in toluene (50.0 ml) was added iodomethane (10.5 ml, 168 mmol) and with constant stirring, the solution was refluxed for 18 h. Upon cooling, the precipitate produced was filtered under pressure, washed with *n*-hexane and dried *in vacuo* to yield **1a** (1.57 g, 87%) as a white solid. ^{1}H NMR (d_6-DMSO, 250 MHz) δ 8.52 (d, *J* = 8.0 Hz, 1H, Ar-<u>H</u>), 8.35 (d, *J* = 9.0 Hz, 1H, Ar-<u>H</u>), 7.95 (t, *J* = 7.0 Hz, 1H, Ar-<u>H</u>), 7.81 (t, *J* = 9.0 Hz, 1H, Ar-<u>H</u>), 4.23 (s, 3H, N-C<u>H</u>$_3$), 3.11 (s, 3H, C-C<u>H</u>$_3$). ^{13}C NMR (d_6-DMSO, 62.8 MHz) δ 179.2, 141.2, 129.8, 129.2, 123.4, 118.5, 83.2, 19.1. IR (ATR) 2965 (CH), 1548 (C=N), 1441, 1336, 1210, 1131, 1011, 764, 717, 579 cm^{-1}. MS (ESI) m/z: 164 [M+]. Mp 227–231°C, Literature Mp 225-226 °C (*36*).

4.3.2.   *2-Methyl-3-(ethyl)-benzothiazolium iodide (**1b**)*

Yield: **1b** (0.78 g, 41%) as a white solid. ^{1}H NMR (d_6-DMSO, 250 MHz) δ 8.49 (d, *J* = 7.0 Hz, 1H, Ar-<u>H</u>), 8.40 (d, *J* = 7.0 Hz, 1H, Ar-<u>H</u>), 7.83 (t, *J* = 8.0 Hz, 1H, Ar-<u>H</u>), 7.79 (t, *J* = 7.0 Hz, 1H, Ar-<u>H</u>), 4.75 (q, *J* = 7.0 Hz, 2H, N-C<u>H</u>$_2$), 3.19 (s, 3H, N-C-C<u>H</u>$_3$), 1.45 (t, *J* = 9.0 Hz, 3H, C-C<u>H</u>$_3$). ^{13}C NMR (d_6-DMSO, 62.8 MHz) δ 176.8, 140.4, 129.1, 128.1, 124.7, 116.6, 44.7, 16.7, 13.2. IR (ATR) 2912 (CH), 1613 (C=N), 1513, 1445, 1329, 1270, 1203, 1100, 777, 713, 670 c^{m-1}. MS (ESI) m/z: 178 [M+]. Mp 196–200°C, Literature Mp 198-199°C (*37*).

4.3.3.   *2-Methyl-3-(propyl)-benzothiazolium iodide (**1c**)*

Yield: **1c** (1.62 g, 81%) as a white solid. ^{1}H NMR (d_6-DMSO, 400 MHz) δ 8.51 (d, *J* = 6.0 Hz, 1H, Ar-<u>H</u>), 8.42 (d, *J* = 6.0 Hz, 1H, Ar-<u>H</u>), 7.93 (t, *J* = 9.0 Hz, 1H, Ar-<u>H</u>), 7.84 (t, *J* = 6.0 Hz, 1H, Ar-<u>H</u>), 4.74 (t, *J* = 9.0 Hz, 2H, N-C<u>H</u>$_2$-CH$_2$), 3.25 (s, 3H, N-C-C<u>H</u>$_3$), 1.93 (q, *J* = 6.0 Hz, 2H, CH$_2$-C<u>H</u>$_2$), 1.05 (t, *J* = 6.0 Hz, 3H, CH$_2$-C<u>H</u>$_3$). IR (ATR) 2919 (CH), 1607 (C=N), 1518, 1449 cm^{-1}. MS (ESI) *m/z*: 192.21 [M+]. Mp 199–203°C.

4.3.4.   *2-Methyl-3-(butyl)-benzothiazolium iodide (**1d**)*

Yield: **1d** (3.65 g, 33%) as a cream solid. ^{1}H NMR (d_6-DMSO, 300 MHz) δ 8.48 (d, *J* = 6.0 Hz, 1H, Ar-<u>H</u>), 8.37 (d, *J* = 6.0 Hz, 1H, Ar-<u>H</u>), 7.92 (t, *J* = 6.0 Hz, 1H, Ar-<u>H</u>), 7.83 (t, *J* = 6.0 Hz,

1H, Ar-$\underline{H}$), 4.74 (t, $J = 6.0$ Hz, 2H, N-C$\underline{H_2}$-CH$_2$), 3.23 (s, 3H, N-C-C$\underline{H_3}$), 1.86–1.71 (m, 2H, N-CH$_2$-C$\underline{H_2}$-CH$_2$), 1.49-1.31 (m, 2H, N-CH$_2$-CH$_2$-C$\underline{H_2}$), 0.96 (t, $J = 9.0$ Hz, 3H, CH$_2$-C$\underline{H_3}$). ^{13}C NMR (75.4 MHz, CDCl$_3$): δ 177.5, 141.3, 129.5, 128.5, 125.1, 117.3, 49.5, 30.2, 19.7, 17.4, 14.0. IR (ATR) 2951(CH), 1577 (C=N), 1439, 1378, 1280, 948, 764 cm^{-1}. MS (ESI) *m/z*: 206.09 [M+]. Mp 189–193°C, Literature Mp 186–187°C (*38*).

4.3.5. *2-Methyl-3-(4-sulfopropyl)-benzothiazolium (1e)*

Yield: **1e** (15.3 g, 91%) as a white solid. ^{1}H NMR (d_6-DMSO, 250 MHz) δ 8.23–7.80 (m, 2H, Ar-$\underline{H}$), 7.28 (t, $J = 7.0$ Hz, 1H, Ar-$\underline{H}$), 7.67 (t, $J = 7.0$ Hz, 1H, Ar-$\underline{H}$), 4.72 (t, $J = 7.0$ Hz, 2H, N-C$\underline{H_2}$), 3.08 (s, 3H, N-C-C$\underline{H_3}$), 3.02 (t, $J = 7.0$ Hz, 2H, SO$_3$-C$\underline{H_2}$), 2.28–2.20 (m, 2H, CH$_2$-C$\underline{H_2}$-CH$_2$). IR (ATR) 2917 (CH), 1511 (C=N), 1413, 1353, 1263, 1032, 756, 663 cm^{-1}. MS (ESI) *m/z*: 272.20 [M+]. Mp 258–262°C, Literature Mp 276–278°C (*39*).

4.3.6. *2-Methyl-3-(4-sulfobutyl)-benzothiazolium (1f)*

Yield: **1f** (9.29 g, 52%) as a white solid. ^{1}H NMR (D$_2$O, 400 MHz) δ 8.06 (d, $J = 8.0$ Hz, 1H, Ar-$\underline{H}$), 8.02 (d, $J = 8.0$ Hz, 1H, Ar-$\underline{H}$), 7.76 (t, $J = 6.0$ Hz, 1H, Ar-$\underline{H}$), 7.66 (t, $J = 7.0$ Hz, 1H, Ar-$\underline{H}$), 4.65 (t, $J = 8.0$ Hz, 2H, N-C$\underline{H_2}$), 3.06 (s, 3H, N-C-C$\underline{H_3}$), 2.87 (t, $J = 7.0$ Hz, 2H, SO$_3$-C$\underline{H_2}$), 2.01–1.96 (m, 2H, N-CH$_2$-C$\underline{H_2}$-CH$_2$), 1.83–1.78 (m, 2H, CH$_2$-C$\underline{H_2}$-CH$_2$-SO$_3$). ^{13}C NMR (D$_2$O, 62.8 MHz) δ 175.9, 140.9, 129.6, 128.9, 128.4, 123.6, 116.4, 50.0, 48.9, 26.3, 21.4, 16.2. IR (ATR) 2947 (CH), 1523 (C=N), 1443, 1343, 1283, 1175, 1032, 796, 777, 714, 683 cm^{-1}. MS (ESI) *m/z*: 286 [M+]. Mp 258–262°C, Literature Mp 294°C (*40*).

4.3.7. *2-Methyl-3-(2-benzyl)-benzothiazolium bromide (1g)*

Yield: **1g** (0.13 g, 7%) as a pink solid. ^{1}H NMR (d_6-DMSO, 250 MHz) δ 8.47 (d, $J = 7.0$ Hz, 1H, Ar-$\underline{H}$), 8.12 (d, $J = 7.0$ Hz, 1H, Ar-$\underline{H}$), 7.45-7.40 (m, 2H, Ar-$\underline{H}$), 7.32–7.11 (m, 5H, Ar-$\underline{H}$), 6.12 (s, 2H, C$\underline{H_2}$-Ph), 3.21 (s, 3H, C-C$\underline{H_3}$). ^{13}C NMR (d_6-DMSO, 62.8 MHz) δ ppm 186.4, 178.4, 140.9, 132.7, 129.5, 129.2, 128.1, 126.9, 124.8, 117.0, 51.8, 17.2. IR (ATR) 2938 (CH), 1578 (C=N), 1455, 1339, 1021, 808, 748, 577 cm^{-1}. MS (ESI) *m/z*: 249 [M+]. Mp 94–98°C, Literature Mp 93°C (*41*).

4.3.8. *N-[5-Anilino-3-chloro-2,4-(propane-1,3-diyl)-2,4-pentadiene]-anilinium chloride (2)*

At 0°C, phosphorus oxychloride (11.0 ml, 120 mmol) was added dropwise from a pressure-equalizing funnel to anhydrous DMF (13.0 ml, 170 mmol) with stirring. After 30 min, cyclo-hexanone (5.50 ml, 53.0 mmol) was added and the mixture was heated under reflux for 1 h. The reaction was cooled to 20°C and with stirring, a mixture of aniline/EtOH [1:1 (v/v), 180 ml] was added dropwise to the reaction mixture. The reaction was continued for 30 min at 20°C with vig-orous stirring, and then the deep purple mixture was poured into H$_2$O/HCl [10:1 (v/v), 110 ml]. Crystals were allowed to form for 2 h in an ice bath. The reaction was filtered, washed with cold H$_2$O and Et$_2$O, and then dried *in vacuo* to yield **2** (14.8 g, 97%) as a dark purple solid. ^{1}H NMR (d_6-DMSO, 250 MHz) δ 11.2 (s, 2H, NH), 8.55 (d, $J = 14.0$ Hz, 2H, C$\underline{H}_{alkene}$), 7.68 (d, $J = 5.0$ Hz 4H, Ar-$\underline{H}$), 7.44 (t, $J = 7.0$ Hz 4H, Ar-$\underline{H}$), 3.03 (t, $J = 6.0$ Hz, 4H, CH$_2$-C$\underline{H_2}$), 2.05–1.98 (m, 2H, C$\underline{H_2}$-CH$_2$). IR (ATR) 1609 (C=N), 1562, 1457, 1267, 1179, 752, 683, 565 cm^{-1}. MS (ESI) *m/z*: 323.22 [M+]. Mp 226–231°C.

Below is the general synthetic procedure for rigid cyanine dyes **3a–g** and **OA1**. Full spectroscopic data are given for all compounds along with chromatography details where required.

10   *O.A. Okoh* et al.

4.3.9.   *2-[(E)-2-[(3E)-2-Chloro-3-{2-[(2Z)-3-methyl-2,3-dihydro-1,3-benzothiazol-2-ylidene] ethylidene}cyclohex-1-en-1-yl]ethenyl]-3-methyl-1,3-benzothiazol-3-ium iodide (3a)*

To a solution of **1a** (0.29 g, 1.0 mmol) in EtOH (20.0 ml) was added anhydrous sodium acetate (0.08 g, 1.00 mmol) and **2** (0.18 g, 0.50 mmol). With constant stirring, the reaction was heated under reflux for 3.5 h. Upon cooling, green crystals precipitated from the reaction mixture. These were washed with *n*-hexane and dried *in vacuo* to yield the cyanine dye **3a** (0.30 g, 51%) as green crystals. ^{1}H NMR (d_6-DMSO, 400 MHz) δ 7.95 (d, $J = 7.0$ Hz, 2H, Ar-<u>H</u>), 7.70 (d, $J = 13.0$ Hz, 2H, C<u>H</u>$_{alkene}$), 7.70 (d, $J = 8.0$ Hz, 2H, Ar-<u>H</u>), 7.52–7.48 (m, 2H, Ar-<u>H</u>), 7.34 (t, $J = 8.0$ Hz, 2H, Ar-<u>H</u>), 6.47 (d, $J = 13.0$ Hz, 2H, C<u>H</u>$_{alkene}$), 3.85 (s, 6H, N-C<u>H</u>$_3$), 2.66 (t, $J = 6.0$ Hz, 4H, C<u>H</u>$_2$-CH$_2$), 1.08–1.03 (m, 2H, CH$_2$-C<u>H</u>$_2$-CH$_2$). IR (ATR) 2936 (CH), 1652 (C=N), 1506, 1423, 1384, 905, 849, 563 cm^{-1}. MS (ESI) *m/z*: 463 [M+]. UV$_{abs}$ λ$_{max}$ = 796 nm. Mp 255–260°C.

4.3.10.   *2-[(E)-2-[(3E)-2-Chloro-3-{2-[(2Z)-3-ethyl-2,3-dihydro-1,3-benzothiazol-2-ylidene] ethylidene}cyclohex-1-en-1-yl]ethenyl]-3-ethyl-1,3-benzothiazol-3-ium iodide (3b)*

Yield: cyanine dye **3b** (0.37 g, 60%) as a green solid. ^{1}H NMR (d_6-DMSO, 400 MHz) δ 8.01 (d, $J = 14.0$ Hz, 2H, C<u>H</u>$_{alkene}$), 7.66 (d, $J = 7.0$ Hz, 2H, Ar-<u>H</u>), 7.46–7.38 (m, 4H, Ar-<u>H</u>), 7.30–7.25 (m, 2H, Ar-<u>H</u>), 6.35 (d, $J = 14.0$ Hz, 2H, C<u>H</u>$_{alkene}$), 4.28 (t, $J = 7.0$ Hz, 4H, N-C<u>H</u>$_2$-CH$_2$), 2.63–2.59 (m, 4H, C<u>H</u>$_2$-CH$_2$), 2.51–2.48 (m, 2H, CH$_2$-C<u>H</u>$_2$-CH$_2$), 1.51 (t, $J = 7.0$ Hz, 6H, C<u>H</u>$_3$-CH$_2$). IR (ATR) 2957 (CH), 1552 (C=N), 1509, 1478, 1397, 1282, 1249, 1208, 1034, 913, 828, 742, 579 cm^{-1}. MS (ESI) *m/z*: 491 [M+]. UV$_{abs}$ λ$_{max}$ = 796 nm. Mp 246–250°C, Literature Mp 248–249°C (*39*).

4.3.11.   *2-[(E)-2-[(3E)-2-Chloro-3-{2-[(2Z)-3-propyl-2,3-dihydro-1,3-benzothiazol-2-ylidene] ethylidene}cyclohex-1-en-1-yl]ethenyl]-3-propyl-1,3-benzothiazol-3-ium iodide (3c)*

Purified by flash chromatography (eluent, chloroform:methanol = 8:2). Yielded the cyanine dye **3c** (0.81 g, 31%) as a green solid. ^{1}H NMR (d_6-DMSO, 400 MHz) δ 7.82 (d, $J = 8.0$ Hz, 2H, Ar-<u>H</u>), 7.63 (d, $J = 13.0$ Hz, 4H, C<u>H</u>$_{alkene}$), 7.39 (t, $J = 7.0$ Hz, 2H, Ar-<u>H</u>), 7.20 (t, $J = 7.0$ Hz, 2H, Ar-<u>H</u>), 6.38 (d, $J = 13.0$ Hz, 2H, C<u>H</u>$_{alkene}$), 4.25 (t, $J = 6.0$ Hz, 4H, N-C<u>H</u>$_2$-CH$_2$), 2.51–2.47 (m, 4H, C<u>H</u>$_2$-CH$_2$), 1.63–1.57 (m, 6H, C<u>H</u>$_2$), 0.85 (t, $J = 7.0$ Hz, 6H, CH$_2$-C<u>H</u>$_3$). IR (ATR) 2950 (CH), 1528 (C=N), 1496, 1387, 1274, 1216, 1055, 983, 844, 740 cm^{-1}. MS (ESI) *m/z*: 519.15 [M+]. UV$_{abs}$ λ$_{max}$ = 797 nm. Mp 245–249°C.

4.3.12.   *3-Butyl-2-[(E)-2-[(3E)-3-{2-[(2Z)-3-butyl-2,3-dihydro-1,3-benzothiazol-2-ylidene] ethylidene}-2-chlorocyclohex-1-en-1-yl]ethenyl]-1,3-benzothiazol-3-ium iodide (3d)*

Purified by flash chromatography (eluent, chloroform:methanol = 8:2). Yielded the cyanine dye **3d** (0.38 g, 19%) as a green solid. ^{1}H NMR (d_6-DMSO, 400 MHz) δ 7.99 (d, $J = 6.0$ Hz, 2H, Ar-<u>H</u>), 7.83 (d, $J = 15.0$ Hz, 2H, C<u>H</u>$_{alkene}$), 7.77 (d, $J = 6.0$ Hz, 2H, Ar-<u>H</u>), 7.59 (t, $J = 6.0$ Hz, 2H, Ar-<u>H</u>), 7.43 (t, $J = 9.0$ Hz, 2H, Ar-<u>H</u>), 6.52 (d, $J = 12.0$ Hz, 2H, C<u>H</u>$_{alkene}$), 4.47 (t, $J = 6.0$ Hz, 4H, N-C<u>H</u>$_2$), 2.67–2.60 (m, 4H, C<u>H</u>$_2$-CH$_2$), 1.84-1.80 (m, 2H, CH$_2$-C<u>H</u>$_2$), 1.74 (t, $J = 9.0$ Hz, 4H, C<u>H</u>$_2$-CH$_2$), 1.44 (q, $J = 6.0$ Hz, 4H, C<u>H</u>$_2$-CH$_3$), 0.95 (t, $J = 7.0$ Hz, 6H, C<u>H</u>$_3$-CH$_2$). IR (ATR) 2937 (CH), 1578 (C=N), 1499, 1451, 1390, 1323, 1213, 1273, 1213, 1051, 902, 739 cm^{-1}. MS (ESI) *m/z*: 547.18 [M+]. UV$_{abs}$ λ$_{max}$ = 796 nm. Mp 212–216°C.

4.3.13. 2-[(E)-2-[(3E)-2-Chloro-3-{2-[(2Z)-3-(3-sulfonatopropyl)-2,3-dihydro-1,3-benzothiazol-2-ylidene]ethylidene}cyclohex-1-en-1-yl]ethenyl]-3-(3-sulfonatopropyl)-1,3-benzothiazol-3-ium (3e)

Purified by flash chromatography (eluent, dichloromethane:methanol = 9 : 1). Yielded the cyanine dye 3e (0.10 g, 9%) as a green solid. ^{1}H NMR (d_6-DMSO, 400 MHz) δ 7.88 (d, $J = 13.0$ Hz, 2H, CH$_{alkene}$), 7.69–7.60 (m, 4H, Ar-H), 7.43 (t, $J = 7.0$ Hz, 2H, Ar-H), 7.25 (t, $J = 7.0$ Hz, 2H, Ar-H), 6.56 (d, $J = 13.0$ Hz, 2H, CH$_{alkene}$), 4.51 (t, $J = 7.0$ Hz, 4H, N-CH$_2$-CH$_2$), 2.55–2.45 (m, 8H, SO$_3$-CH$_2$), 1.97 (t, $J = 6.0$ Hz, 4H, CH$_2$-CH$_2$), 1.76-1.70 (m, 2H, CH$_2$-CH$_2$). IR (ATR) 3050 (CH), 1527 (C=N), 1499, 1454, 1324, 1208, 983 cm^{-1}. MS (ESI) m/z: 679.07 [M+]. UV$_{abs}$ $\lambda_{max} = 775$ nm. Mp 240–244°C.

4.3.14. 2-[(E)-2-[(3E)-2-Chloro-3-{2-[(2Z)-3-(4-sulfonatobutyl)-2,3-dihydro-1,3-benzothiazol-2-ylidene]ethylidene}cyclohex-1-en-1-yl]ethenyl]-3-(4-sulfonatobutyl)-1,3-benzothiazol-3-ium (3f)

Purified by flash chromatography (eluent, chloroform:methanol = 9:1). Yielded the cyanine dye 3f (0.30 g, 49%) as a green solid. ^{1}H NMR (d_6-DMSO, 400 MHz) δ 7.98 (d, $J = 13.0$ Hz, 2H, CH$_{alkene}$), 7.83–7.68 (m, 4H, Ar-H), 7.58–7.56 (m, 2H, Ar-H), 7.54–7.49 (m, 2H, Ar-H), 6.57 (d, $J = 13.0$ Hz, 2H, CH$_{alkene}$), 4.46 (t, $J = 7.0$ Hz, 4H, N-CH$_2$-CH$_2$), 3.34 (s, 1H, CH$_2$), 2.70–2.65 (m, 4H, CH$_2$-CH$_2$), 2.09 (s, 1H, CH$_2$), 1.76–1.50 (m, 12H, SO$_3$-CH$_2$). IR (ATR) 3393 (CH), 1651 (C=N), 1499, 1392, 1324, 1276, 1217, 1127, 1011, 852, 796, 743, 564 cm^{-1}. MS (ESI) m/z: 707 [M+]. UV$_{abs}$ $\lambda_{max} = 800$ nm. Mp 247–251°C.

4.3.15. 3-Benzyl-2-[(E)-2-[(3E)-3-{2-[(2Z)-3-benzyl-2,3-dihydro-1,3-benzothiazol-2-ylidene]ethylidene}-2-chlorocyclohex-1-en-1-yl]ethenyl]-1,3-benzothiazol-3-ium bromide (3g)

Purified by flash chromatography (eluent, chloroform:methanol = 9:1). Yielded the cyanine dye 3g (1.50 g, 27%) as a green solid. ^{1}H NMR (d_6-DMSO, 400 MHz) δ 7.94 (d, $J = 7.0$ Hz, 2H, Ar-H), 7.74 (d, $J = 13.0$ Hz, 2H, CH$_{alkene}$), 7.62 (d, $J = 8.0$ Hz, 2H, Ar-H), 7.44 (t, $J = 7.0$ Hz, 2H, Ar-H), 7.33 (d, $J = 6.0$ Hz, 4H, Ar-H), 7.27–7.13 (m, 8H, Ar-H), 6.52 (d, $J = 13.0$ Hz, 2H, CH$_{alkene}$), 5.70 (s, 4H, N-H-Ph), 3.12 (s, 2H, CH$_2$), 2.57 (s, 2H, CH$_2$), 1.67 (s, 2H, CH$_2$). IR (ATR) 1543 (C=N), 1506, 1363, 1225, 1099, 896, 784, 668, 597 cm^{-1}. MS (ESI) m/z: 615.06 [M+]. HRMS (FAB): Calculated for C$_{38}$H$_{32}$ClN$_2$S$_2$ [M+] 615.1689, found 615.1682. UV$_{abs}$ $\lambda_{max} = 804$ nm. Mp 254–258°C.

4.3.16. 2-[(E)-2-[(3E)-2-Chloro-3-{2-[(2E)-3,3-dimethyl-1-(4-sulfonatobutyl)-2,3-dihydro-1H-indol-2-ylidene]ethylidene}cyclohex-1-en-1-yl]ethenyl]-3,3-dimethyl-1-(4-sulfonatobutyl)-3H-indol-1-ium (OA1)

Purified by flash chromatography (eluent, chloroform:methanol = 7:3). Yielded the cyanine dye OA1 (1.01 g, 46%) as a shiny purple solid. ^{1}H NMR (d_6-DMSO, 400 MHz) δ 8.21 (d, $J = 14.0$ Hz, 2H, CH$_{alkene}$), 7.67 (d, $J = 7.0$ Hz, 2H, Ar-H), 7.39–7.31 (m, 4H, Ar-H), 7.12–7.06 (m, 2H, Ar-H), 6.31 (d, $J = 14.0$ Hz, 2H, CH$_{alkene}$), 4.89 (t, $J = 5.0$ Hz, 4H, N-CH$_2$-CH$_2$), 3.01–2.96 (m, 4H, CH$_2$-CH$_2$), 2.68–2.60 (m, 4H, CH$_2$-CH$_2$), 1.70–1.61 (m, 8H, CH$_2$-CH$_2$-CH$_2$-SO$_3^-$), 1.50 (s, 12H, C-CH$_3$), 1.30–1.09 (m, 2H, CH$_2$-CH$_2$). IR (ATR) 2921 (CH), 1541 (C=N), 1240, 1004, 889, 707, 565 cm^{-1}. MS (ESI) m/z: 727 [M+]. UV$_{abs}$ $\lambda_{max} = 770$ nm. Mp 253–257°C.

12   *O.A. Okoh* et al.

4.3.17.   *N-(2,4-Dinitrophenyl) pyridinium chloride (4)*

Pydrine (3.00 ml, 37.9 mmol) was dissolved in acetone (17.0 ml) and stirred, while 2,4-dinitrochlorobenzene (7.67 g, 37.9 mmol) was added to the reaction mixture. The mixture was heated under reflux overnight and cooled to room temperature. The precipitate produced was filtered under suction and washed with *n*-hexane to obtain *N*-(2,4-dinitrophenyl) pyridinium chloride (**4**, 8.10 g, 97%) as a pale yellow powder. ^{1}H NMR (d_6-DMSO, 250 MHz) δ 9.43 (d, $J = 6.0$ Hz, 2H, Ar-H), 9.21 (s, 1H, Ar-H), 8.95 (t, $J = 7.0$ Hz, 2H, Ar-H), 8.50-8.41 (m, 3H, Ar-H). ^{13}C NMR (d_6-DMSO, 68.2 MHz) δ 149.1, 148.9, 146.1, 143.1, 138.8, 132.0, 130.3, 128.1, 121.4. IR (ATR) 2971 (CH), 1540 (C=N), 1474, 1341, 1266, 1154, 943, 855, 739 cm^{-1}. MS (ESI) *m/z*: 186.24 [M+]. Mp 197–201°C.

Below is the general synthetic procedure for linear cyanine dyes 5a–g. Full spectroscopic data are given for all compounds along with chromatography details where required.

4.3.18.   *3-Methyl-2-[(1E,3E,5E)-7-[(2Z)-3-methyl-2,3-dihydro-1,3-benzothiazol-2-ylidene] hepta-1,3,5-trien-1-yl]-1,3-benzothiazol-3-ium iodide (5a)*

To a solution of *N*-(2,4-dinitrophenyl) pyridinium chloride (0.22 g, 0.80 mmol) in EtOH (10.0 ml) was added 5a (0.58 g, 2.00 mmol) and aniline (0.19 g, 2.00 mmol). The reaction mixture was stirred for 5 min, and then followed by the addition of sodium acetate (0.41 g, 5 mmol). The reaction was stirred at room temperature overnight and 20.0 ml *n*-hexane added. The precipitate produced was filtered under suction and washed with *n*-hexane. The crude product was purified by silica gel column chromatography (eluent solvent, chloroform:methanol = 9:1) to obtain cyanine dye 5a (0.32 g, 78%) as a green solid. ^{1}H NMR (d_6-DMSO, 400 MHz) δ 7.95 (d, $J = 7.0$ Hz, 2H, Ar-H), 7.67 (d, $J = 8.0$ Hz, 2H, Ar-H), 7.53 (t, $J = 7.0$ Hz, 2H, Ar-H), 7.43-7.35 (m, 5H, Ar-H), 6.54 (d, $J = 13.0$ Hz, 2H, C$\underline{H}_{alkene}$), 6.48 (t, $J = 12.0$ Hz, 2H, C$\underline{H}_{alkene}$), 3.77 (s, 6H, N-C$\underline{H}_3$). IR (ATR) 1543 (C=N), 1518, 1356, 1232, 1081, 887, 764, 615 cm^{-1}. MS (ESI) *m/z*: 389.07 [M+]. UV$_{abs}$ $\lambda_{max} = 756$ nm. Mp 210–214°C.

4.3.19.   *3-Ethyl-2-[(1E,3E,5E)-7-[(2Z)-3-ethyl-2,3-dihydro-1,3-benzothiazol-2-ylidene]hepta-1,3,5-trien-1-yl]-1,3-benzothiazol-3-ium iodide (5b)*

Purified by flash chromatography (eluent, chloroform:methanol = 9:1). Yielded the cyanine dye 5b (0.20 g, 46%) as a green solid. ^{1}H NMR (d_6-DMSO, 400 MHz) δ 7.95 (d, $J = 7.0$ Hz, 2H, Ar-H), 7.68 (d, $J = 6.0$ Hz, 2H, Ar-H), 7.54 (t, $J = 6.0$ Hz, 2H, Ar-H), 7.43–7.32 (m, 5H, Ar-H), 6.58 (d, $J = 13.0$ Hz, 2H, C$\underline{H}_{alkene}$), 6.45 (t, $J = 13.0$ Hz, 2H, C$\underline{H}_{alkene}$), 4.36 (q, $J = 6.0$ Hz, 4H, N-C$\underline{H}_2$-CH$_3$), 1.30 (t, $J = 7.0$ Hz, 6H, C$\underline{H}_3$-CH$_2$). IR (ATR) 2971 (CH), 1579 (C=N), 1507, 1396, 1059, 983, 830, 738 cm^{-1}. MS (ESI) *m/z*: 417.07 [M+]. UV$_{abs}$ $\lambda_{max} = 759$ nm. Mp 216–221°C.

4.3.20.   *3-Propyl-2-[(1E,3E,5E)-7-[(2Z)-3-propyl-2,3-dihydro-1,3-benzothiazol-2-ylidene] hepta-1,3,5-trien-1-yl]-1,3-benzothiazol-3-ium iodide (5c)*

Purified by flash chromatography (eluent, chloroform:methanol = 9:1). Yielded the cyanine dye 5c (0.30 g, 66%) as a shiny green solid. ^{1}H NMR (d_6-DMSO, 400 MHz) δ 7.95 (d, $J = 7.0$ Hz, 2H, Ar-H), 7.71 (d, $J = 8.0$ Hz, 2H, Ar-H), 7.53 (d, $J = 7.0$ Hz, 2H, Ar-H), 7.44 (d, $J = 13.0$ Hz, 2H, C$\underline{H}_{alkene}$), 7.37 (d, $J = 8.0$ Hz, 2H, Ar-H), 6.60 (d, $J = 12.0$ Hz, 2H, C$\underline{H}_{alkene}$), 6.40 (t, $J = 13.0$ Hz, 2H, C$\underline{H}_{alkene}$), 4.27 (t, $J = 7.0$ Hz, 4H, N-C$\underline{H}_2$-CH$_2$), 1.75 (q, $J = 7.0$ Hz, 4H, C$\underline{H}_2$-CH$_3$), 0.97 (t, $J = 7.0$ Hz, 6H, CH$_2$-C$\underline{H}_3$). IR (ATR) 2960 (CH), 1579 (C=N), 1500, 1393, 1324,

970, 805, 743 cm^{-1}. MS (ESI) *m/z*: 445.12 [M+]. HRMS (FAB): Calculated for C$_{27}$H$_{29}$N$_2$S$_2$I [M+] 445.1766, found 445.1758. UV$_{abs}$ λ_{max} = 761 nm. Mp 193–197°C.

4.3.21. *3-Butyl-2-[(1E,3E,5E)-7-[(2Z)-3-butyl-2,3-dihydro-1,3-benzothiazol-2-ylidene]hepta-1,3,5-trien-1-yl]-1,3-benzothiazol-3-ium iodide (5d)*

Purified by flash chromatography (eluent, chloroform:methanol = 9:1). Yielded the cyanine dye **5d** (0.21 g, 44%) as a shiny purple green solid. ^{1}H NMR (*d*$_6$-DMSO, 300 MHz) δ 7.98 (d, *J* = 9.0 Hz, 2H, Ar-H̲), 7.71 (d, *J* = 9.0 Hz, 2H, Ar-H̲), 7.57 (t, *J* = 12.0 Hz, 2H, CH̲$_{alkene}$), 7.47–7.35 (m, 5H, Ar-H̲), 6.60 (d, *J* = 12.0 Hz, 2H, CH̲$_{alkene}$), 6.49 (d, *J* = 12.0 Hz, 2H, CH̲$_{alkene}$), 4.33 (t, *J* = 6.0 Hz, 4H, N-CH̲$_2$-CH$_2$), 1.71 (quin, *J* = 6.0 Hz, 4H, CH$_2$-CH̲$_2$-CH$_2$), 1.47–1.37 (m, 4H, CH$_2$-CH̲$_2$-CH$_3$), 0.95 (t, *J* = 6.0 Hz, 6H, CH$_2$-CH̲$_3$). ^{13}C NMR (*d*$_6$-DMSO, 75.4 MHz) δ ppm 196.4, 170.8, 141.9, 128.5, 125.7, 125.3, 123.4, 113.7, 79.6, 60.2, 49.0, 29.9, 21.2, 19.8, 14.5, 14.1. IR (ATR) 2951 (CH), 1501 (C=N), 1451, 1391, 1320, 1051, 918, 821, 737 cm^{-1}. MS (ESI) *m/z*: 473.14 [M+]. UV$_{abs}$ λ_{max} = 761 nm. Mp 176–180°C.

4.3.22. *3-(3-Sulfonatopropyl)-2-[(1E,3E,5E)-7-[(2Z)-3-(3-sulfonatopropyl)-2,3-dihydro-1,3-benzothiazol-2-ylidene]hepta-1,3,5-trien-1-yl]-1,3-benzothiazol-3-ium (5e)*

Purified by flash chromatography (eluent, chloroform:methanol = 7:3). Yielded the cyanine dye **5e** (0.22 g, 47%) as a green solid. ^{1}H NMR (*d*$_6$-DMSO, 400 MHz) δ 7.95 (d, *J* = 7.0 Hz, 2H, Ar-H̲), 7.79 (d, *J* = 8.0 Hz, 2H, Ar-H̲), 7.55 (t, *J* = 8.0 Hz, 2H, Ar-H̲), 7.44–7.34 (m, 5H, Ar-H), 6.69 (d, *J* = 13.0 Hz, 2H, CH̲$_{alkene}$), 6.44 (t, *J* = 12.0 Hz, 2H, CH̲$_{alkene}$), 4.48 (t, *J* = 8.0 Hz, 4H, N-CH̲$_2$-CH$_2$), 2.58 (t, *J* = 7.0 Hz, 4H, SO$_3$-CH̲$_2$-CH$_2$), 2.03 (quin, *J* = 8.0 Hz, 4H, CH$_2$-CH̲$_2$-CH$_2$). IR (ATR) 3398, 2361 (CH), 1581 (C=N), 1504, 1405, 1329, 1091, 993, 749 cm^{-1}. MS (ESI) *m/z*: 603.07 [M+]. HRMS(FAB): Calculated for C$_{27}$H$_{27}$N$_2$O$_6$S$_4$ [M+] 603.0757, found 603.0742. UV$_{abs}$ λ_{max} = 762 nm. Mp 225–229°C.

4.3.23. *3-(4-Sulfonatobutyl)-2-[(1E,3E,5E)-7-[(2Z)-3-(4-sulfonatobutyl)-2,3-dihydro-1,3-benzothiazol-2-ylidene]hepta-1,3,5-trien-1-yl]-1,3-benzothiazol-3-ium (5f)*

Purified by flash chromatography (eluent, chloroform:methanol = 7:3). Yielded the cyanine dye **5f** (0.23 g, 43%) as a dark green solid. ^{1}H NMR (*d*$_6$-DMSO, 400 MHz) δ 7.94 (d, *J* = 8.0 Hz, 2H, Ar-H̲), 7.78 (d, *J* = 8.0 Hz, 2H, Ar-H̲), 7.53 (t, *J* = 8.0 Hz, 2H, Ar-H̲), 7.43-7.33 (m, 5H, Ar-H), 6.68 (d, *J* = 13.0 Hz, 2H, CH̲$_{alkene}$), 6.42 (d, *J* = 13.0 Hz, 2H, CH̲$_{alkene}$), 4.06–3.87 (m, 4H, N-CH̲$_2$-CH$_2$), 2.56 (t, *J* = 8.0 Hz 4H, SO$_3$-CH̲$_2$-CH$_2$), 2.41–2.06 (m, 4H, CH$_2$-CH̲$_2$), 1.91–1.65 (m, 4H, CH̲$_2$-CH$_2$). IR (ATR) 3405, 2361 (CH), 1683 (C=N), 1505, 1400, 1328, 1074, 978, 742 cm^{-1}. MS (ESI) *m/z*: 631.84 [M+]. UV$_{abs}$ λ_{max} = 762 nm. Mp 228–232°C.

4.3.24. *3-Benzyl-2-[(1E,3E,5E)-7-[(2Z)-3-benzyl-2,3-dihydro-1,3-benzothiazol-2-ylidene]hepta-1,3,5-trien-1-yl]-1,3-benzothiazol-3-ium bromide (5g)*

Purified by flash chromatography (eluent, chloroform:methanol = 8:2). Yielded the cyanine dye **5g** (0.300 g, 60%) as a green solid. ^{1}H NMR (*d*$_6$-DMSO, 400 MHz) δ 8.02 (d, *J* = 7.0 Hz, 2H, Ar-H̲), 7.65 (d, *J* = 8.0 Hz, 2H, Ar-H̲), 7.52–7.36 (m, 11H, Ar-H̲), 7.33 (t, *J* = 8.0 Hz, 2H, Ar-H̲), 7.26 (d, *J* = 7.0 Hz, 4H, Ar-H̲), 6.64 (d, *J* = 13.0 Hz, 2H, CH̲$_{alkene}$), 6.31 (t, *J* = 12.0 Hz, 2H, CH̲$_{alkene}$), 5.64 (s, 4H, Ph-CH̲$_2$). IR (ATR) 2979 (CH), 1582 (C=N), 1504, 1459, 1328, 1114, 994, 814, 732 cm^{-1}. MS (ESI) *m/z*: 541.03 [M+]. HRMS (FAB): Calculated for C$_{35}$H$_{29}$N$_2$S$_2$.Br [M+] 541.1766, found 541.1756. UV$_{abs}$ λ_{max} = 765 nm. Mp 209–213°C.

14 *O.A. Okoh* et al.

4.3.25. *2-[(1E,3E,5E)-7-[(2E)-3,3-Dimethyl-1-(4-sulfonatobutyl)-2,3-dihydro-1H-indol-2-ylidene]hepta-1,3,5-trien-1-yl]-3,3-dimethyl-1-(4-sulfonatobutyl)-3H-indol-1-ium (OA2)*

Purified by flash chromatography (eluent, chloroform:methanol = 7:3). Yielded the cyanine dye **OA2** (0.380 g, 73%) as a green solid. ^{1}H NMR (d_6-DMSO, 400 MHz) δ 7.90 (t, $J = 13.0$ Hz, 2H, CH$_{\text{alkene}}$), 7.74 (s, 1H, Ar-H), 7.57 (d, $J = 7.0$ z, 2H, Ar-H), 7.41–7.35 (m, 4H, Ar-H), 7.23 (t, $J = 8.0$ Hz, 2H, Ar-H), 6.58 (t, $J = 12.0$ Hz, 2H, CH$_{\text{alkene}}$), 6.44 (d, $J = 14.0$ Hz, 2H, CH$_{\text{alkene}}$), 4.06 (t, $J = 7.0$ Hz, 4H, N-CH$_2$-CH$_2$), 2.47 (t, $J = 7.0$ Hz, 4H, SO$_3$-CH$_2$-CH$_2$), 1.74–1.68 (m, 8H, CH$_2$-CH$_2$), 1.62 (s, 12H, C-CH$_3$). IR (ATR) 2924 (CH), 1597 (C=N), 1509, 1317, 1158, 966, 741 cm^{-1}. MS (ESI) m/z: 653.29 [M+]. Mp 221–225°C.

Acknowledgements

References

(1) Cibiel, A.; Pestourie, C.; Ducongé, F. *Biochimie* **2012**, *94*, 1595–606.
(2) Escobedo, J.O.; Rusin, O.; Lim, S.; Strongin, R.M. *Curr. Opin. Chem. Biol.* **2010**, *14*, 64–70.
(3) Yin, J.; He, X.; Jia, X.; Wang, K.; Xu, F. *Analyst* [Online early access] **2013**. DOI:10.1039/C3AN00029J
(4) Tatikolov, A. *J. Photochem. Photobiol. C: Photochem. Rev.* **2012**, *13*, 55–90.
(5) Yuan, L.; Lin, W.; Zheng, K.; He, L.; Huang, W. *Chem. Soc. Rev.* **2013**, *42*, 622–661.
(6) Rao, J.; Dragulescu-Andrasi, A.; Yao, H. *Curr. Opin. Biotechnol.* **2007**, *18*, 17–25.
(7) Wainwright, M. *Color. Technol.* **2010**, *126*, 115–126.
(8) Henderson, W.R.; Guenette, J.A.; Dominelli, P.B.; Griesdale, D.E.; Querido J.S.; Boushel, R.; Sheel. A.W. *Respir. Physiol. Neurobiol.* **2012**, *181*, 302–307
(9) Yoneya, S.; Saito, T.; Komatsu, Y.; Koyama, I.; Takahashi, K.; Duvoll-Young, J. *Invest. Ophthalmol. Vis. Sci.* **1998**, *39*, 1286–1290.
(10) Saito, T.; Komatsu, Y.; Mori, S.; Deguchi, T.; Koyama, I.; Yoneya, S. *Nihon. Ganka. Gakkai. Zasshi.* **1996**, *8*, 617–623.
(11) Raabe, A.; Beck, J.; Gerlach, R.; Zimmermann, M.; Seifert, V. *Neurosurgery* **2003**, *52*, 132–139.
(12) Dashti, R.; Laakso, A.; Niemelä, M.; Porras, M.; Celik, O.; Navratil, O.; Romani, R.; Hernesniemi, J. *Acta Neurochir. Suppl.* **2010**, *107*, 107–109.
(13) Gupta, S.; Chawla, Y.; Kaur, J.; Saxena, R.; Duseja, A.; Dhiman, R.K.; Choudhary, N.S. *Trop. Gastroenterol.* **2012**, *33*, 129–134.
(14) Schneider, P.D. *Surg. Clin. North Am.* **2004**, *84*, 355–373.
(15) Kosaka, N.; Mitsunaga, M.; Longmire, M.R.; Choyke, P.L.; Kobayashi, H. *Int. J. Cancer.* **2011**, *167*, 1–7.
(16) Jianghong, R.; Anca, D.; Hequan, Y. *Curr. Opin. Biotechnol.* **2007**, *18*, 17–25.
(17) Hope-Ross, M.; Yaannuzzi, L.A.; Gragoudas, E.S.; Guyer, D.R.; Slakter, J.S.; Sorenson, J.A. *Opthalmology* **1994**, *101*, 529–533.
(18) Yuhui, L.; Ralph, W.; Ching-Hsuan, T. *Bioconjugate Chem.* **2002**, *13*, 605–610.
(19) Fernandez-Fernandez, A.; Manchanda, R.; Lei, T.; Carvajal, D.A.; Tang, Y.; Kazmi, S.Z.; McGoron, A.J. *Mol. Imaging* **2012**, *11*, 99–113.
(20) Peng, X.; Draney, D.R. *LabPlus Int.* **2004**, *18*, 8.
(21) Patonay, G.; Antoine, M.D. *Anal. Chem.* **1991**, *63*, 321–327.
(22) Waggoner, A.S.; Ernst, L.A.; Mujumdar, R.B. U.S. Patent, **1993**, *5*, 268–486.
(23) Gruber, H.J.; Hahn, C.D.; Kada, G.; Riener, C.K.; Harms, G.S.; Ahrer, W.; Dax, T.G.; Knaus, H.G. *Bioconjug. Chem.* **2000**, *11*, 696–704.
(24) Flanagan, J.H. Jr; Khan, S.H.; Menchen, S.; Soper, S.A.; Hammer, R.P. *Bioconjug. Chem.* **1997**, *8*, 751–756.
(25) Marvell, E.N.; Caple, G.; Shahidi, I. *J. Am. Chem. Soc.* **1970**, *92*, 5641–5645.
(26) Smith, R.B.; Okoh, O.A. Centre for Material Science, University of Central Lancashire, UK. Patent Application No. 1201641.6, 2012.
(27) Chapman, G.; Henary, M.; Patonay, G. *Anal. Chem. Insight.* **2011**, *6*, 29–36.
(28) Cooper, M.; Ebner, A.; Briggs, M.; Burrows, M.; Gardner, N.; Richardson, R. *J. Fluoresc.* **2004**, *14*, 145–150.
(29) Lee, H.; Berezin, M.Y; Henary, M.; Strekowski, L.; Achilefu, S. *J. Photochem. Photobiol. A Chem.* **2008**, *15*, 438–444.
(30) Barberis, A.; Gunde, T.; Berset, C.; Audetat, S.; Luthi, U. *Drug Discovery Today: Technol.* **2005**, *2*, 187–192
(31) Nitiss, J.L. *Yeast as a Tool in Cancer Research;* Springer: Dordrecht, The Netherlands, 2007.

(32) Lawrence, C.L.; Maekawa, H.; Worthington J.L.; Reiter, W.; Wilkinson, C.R; Jones, N. *J. Biol. Chem.* **2007**, *282*, 5160–5170.
(33) Moreno, S.; Klar, A.; Nurse, P. *Method Enzymol.* **1991**, *194*, 795–823.
(34) Kosch, MJ.; Mäkinen, S.; Sigernes, F.; Harang, O. In *Experiment*, Proceedings of the 30th Annual European Meeting on Atmospheric Studies by Optical Methods; University Center on Svalbard: Longyearbyen, Norway, 2003, 1900-01-01.
(35) Benson, R.C.; Kues, H.A. *J. Chem. Eng. Data* **1977**, *22*, 379–383.
(36) Buffa, R.; Zahradnik, P.; Foltinova, P. *Heterocycl. Commun.* **2001**, *7*, 331–336.
(37) Pardal, A.C.; Ramos, S.S.; Santos, P.F.; Reis, L.V.; Almeida, P. *Molecules* **2002**, *7*, 320–330.
(38) Brooker, L.; White, F. *J. Am. Chem. Soc.* **1935**, *57*, 2480–2488.
(39) Gromov, S.P.; Ushakov, E.N.; Fedorova, O.A.; Soldatenkova, V.A.; Alfimov, M.V. *Russ. Chem. Bull.* **1997**, *46*, 1143–1148.
(40) Kennedy, M.T. Patent US 2008/75777 A1, 2008.
(41) Slominskii, Y.L. *J. Org. Chem. USSR (English Translation)* **1978**, *14*, 2046–2051.

239

Preliminary communication

N-Alkylated 2,3,3-trimethylindolenines and 2-methylbenzothiazoles. Potential lead compounds in the fight against *Saccharomyces cerevisiae* infections

Andrew R. Tyler [a], Adeyi Okoh Okoh [b], Clare L. Lawrence [c], Vicky C. Jones [c], Colin Moffatt [b], Robert B. Smith [b,*]

[a] *Chemistry, School of Forensic and Investigative Sciences, University of Central Lancashire, Preston PR1 2HE, UK*
[b] *Centre for Material Sciences, School of Forensic and Investigative Sciences, University of Central Lancashire, Preston PR1 2HE, UK*
[c] *School of Pharmacy and Biomedical Sciences, University of Central Lancashire, Preston PR1 2HE, UK*

ARTICLE INFO

ABSTRACT

The synthesis of a variety of N-alkylated 2,3,3-trimethylindolenines and 2-methylbenzothiazoles is reported herein. Their potential as antifungal agents is evaluated by preliminary screening against *Saccharomyces cerevisiae* (*S. cerevisiae*), *Schizosaccharomyces pombe* (*S. pombe*), and *Candida albicans* (*C. albicans*). Statistical analyses illustrate a strong relationship between chain length and growth inhibition for *S. cerevisiae* and *S. pombe* ($p < 0.0001$ in every case).

Of particular interest is the activity of both sets of compounds against *S. cerevisiae*, as this is emerging as an opportunistic pathogen, especially in immunosuppressed and immunocompromised patients. Bioassays were set up to compare the efficacy of our range of N-alkylated compounds against classic antifungal agents; Amphotericin B and Thiabendazole.

© 2013 Elsevier Masson SAS. All rights reserved.

1. Introduction

The rise in number of immunocompromised patients (either through infections, nutritional irregularities or medical treatment) has led to an increase in opportunistic fungal infections [1]. This in turn, is forcing health care professionals to seek more aggressive forms of chemotherapeutic treatments, which inevitably leads to fungal infections with greater resistance to current therapies. Although systemic antifungal agents have been available since the 1950s, the end of the last century saw the development of a new generation of antifungal agent; the triazoles; which revolutionised clinical mycology. Itraconazole **1** and Fluconazole **2** (Fig. 1) were two such triazoles, licensed by the Food and Drug Administration (FDA) for topical use [2]. The dawn of the new millennium brought the new echinocandin antifungals, such as Micafungin **3**, as shown in Fig. 2. These drugs inhibit cell wall synthesis, in particular the synthesis of

(1,3)-β-ᴅ-glucan; their structure being based on natural lipopeptide products [3]. The shift towards natural products is not particularly surprising; these appear to be more acceptable to both the pharmaceutical industry and patients from a toxicity viewpoint. Indeed many natural products which are being derived from plants, are being identified as antifungal agents[4]. Benzothiazoles are one such type of compound, whose core molecular structure can be found in a large number of natural products [5]. The benzathiazoles exhibit great pharmaceutical importance due to their potent biological activities, these include anti-bacterial [6], anti-ulcer [7], anti-cancer [8], anti-inflammatory [9] and anti-viral [10] to mention a few.

Inspired by the aforementioned medicinal activity of the benzothiazoles, we have set out to create two small libraries of structurally similar N-alkylated molecules: 2,3,3-trimethylindolenine (**1a–m**) and 2-methylbenzothiazole (**2a–m**). Each of these subclasses has a step-wise increase in linear alkyl chain length (C1–C10). The resulting derivatives show varying degrees of lipophilicity, as judged by their log P (base 10 logarithm of the partition coefficient) values (shown in Tables 1 and 2, respectively). It's widely accepted that an increase in the length of the carbon

* Corresponding author. Tel.: +44 (0)1772 894384; fax: +44 (0)1772 894981.
*E-mail address:* rbsmith@uclan.ac.uk (R.B. Smith).
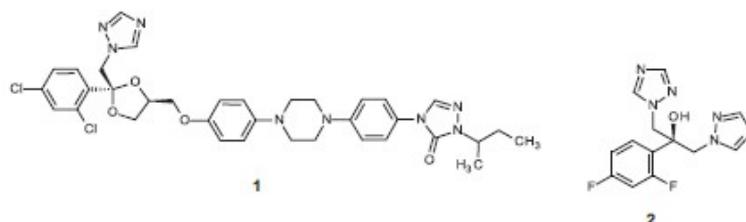
Fig. 1. Two licensed triazole antifungals, Itraconazole **1** and Fluconazole **2**.

chain, goes hand in hand with an increase in pharmacological activity (this is usual from C1–C10), due to an increase in lipid membrane penetration. However, above C10 a decrease in activity is usually seen and this is attributed to poor transport through aqueous media [10]. Our intention was to examine the growth inhibition of three yeast strains up to a linear chain length of C10 and assess any potential antifungal activity observed.

The compounds were tested against three different yeast species; *Schizosaccharomyces pombe* (*S. pombe*), a fission yeast; *Saccharomyces cerevisiae* (*S. cerevisiae*), a budding yeast and *Candida albicans* (*C. albicans*) a diploid fungus known for opportunistic oral and genital infections in humans [11]. Both *S. pombe* and *S. cerevisiae* yeast species are used extensively in eukaryotic microbiological research and demonstrate close homology to a number of pathogenic fungi. For example, *S. cerevisiae* is closely related to *C. albicans*, which, as mentioned above, is a widespread commensal and important pathogen of humans. Similarly, *S. pombe* is closely related to *Pneumocystis jiroveci*, a yeast-like fungus which commonly causes pneumonia in immunocompromised patients [12]. *S. cerevisiae* is of particular importance, emerging as an opportunistic pathogen, especially in immunosuppressed and immunocompromised patients, and has been associated with fungemia, endocarditis, peritonitis, meningitis, ventriculitis, and with polymicrobial fatal pneumonia in HIV/AIDS patients [13–19]. These yeast species can serve as excellent models to learn more about pathogenic fungi, in particular with regard to regulatory features and drug therapy, because they share many characteristics with their pathogenic relatives [20–22].

2. Results and discussion

2.1. Chemistry

The synthesis of both sets of salts was straightforward and required no harsh or unusual synthetic methodologies, as shown in
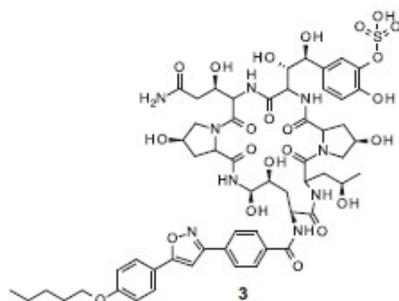

Fig. 2. Micafungin **3**, an echinocandin natural product antifungal.

Scheme 1. The salts of 2,3,3-trimethylindolenine and 2-methylbenzothiazole were prepared by alkylation with the corresponding alkyl/benzyl halides or sultones to afford the compounds in excellent to poor yield as shown in Tables 1 and 2. Compounds **1a–d**, **k–m** and **2a–m** precipitated from the reaction mixture and were isolated by filtration under reduced pressure. What is noticeable is the increased hygroscopic nature of the indolenium bromide salts with increased chain length (C5–C10). To counteract this problem, a counter ion exchange based on the Finkelstein reaction was performed to yield the iodide salts which are not as hygroscopic as the bromides; thus easier to handle and work with from a biological viewpoint. The synthesis of four 2,3,3-trimethylindolenine salts (**1a**, **e**, **k** and **l**) are shown in the experimental section below for clarity. The synthesis of the full set of compounds (**1a–m** and **2a–m**) is also shown in the Supporting information.

2.2. Antifungal activity

The synthesised compounds were tested *in vitro* to determine growth inhibitory activity. Minimum inhibitory concentration (MIC) values were determined in sets, by comparison with 2,3,3-trimethylindolenine (**1n**) and 2-methylbenzathiazole (**2n**) (purchased from Alfa Aesar), under the same conditions noted in

Table 1
The antifungal data for compounds **1a–n**.

Number	R	% Yield	Log P	MIC (µg/mL) Sc	Sp	Ca
1a	CH$_3$	58	−0.691	500	500	1000
1b	CH$_2$CH$_3$	86	−0.315	500	500	1000
1c	CH$_2$CH$_2$CH$_3$	85	0.188	250	250	1000
1d	CH$_2$(CH$_2$)$_2$CH$_3$	67	0.747	250	250	1000
1e	CH$_2$(CH$_2$)$_3$CH$_3$	38 (99)	1.252	250	125	1000
1f	CH$_2$(CH$_2$)$_4$CH$_3$	22 (99)	1.758	125	125	1000
1g	CH$_2$(CH$_2$)$_5$CH$_3$	19 (86)	2.263	125	62.5	1000
1h	CH$_2$(CH$_2$)$_6$CH$_3$	11 (40)	2.768	62.5	62.5	1000
1i	CH$_2$(CH$_2$)$_7$CH$_3$	20 (27)	3.273	31.3	31.3	1000
1j	CH$_2$(CH$_2$)$_8$CH$_3$	53 (99)	3.778	15.6	15.6	500
1k	CH$_2$C$_6$H$_5$	77	0.904	1000	1000	1000
1l	CH$_2$CH$_2$CH$_2$SO$_3^-$	58	−4.33	1000	1000	1000
1m	CH$_2$CH$_2$CH$_2$CH$_2$SO$_3^-$	50	−4.114	1000	1000	1000
1n	NA	–	3.286	1000	250	500

Minimal Inhibitory Growth Concentration (MIC) of synthesised compounds tested in *S. cerevisiae*, *S. pombe*, and *C. albicans*. Cells were inoculated at a concentration of 3×10^4/mL. Culture media tested were in yeast extract broth (YE) for *S. pombe* and complex growth media (YPD) for *S. cerevisiae* and *C. albicans*. Growth of yeast was determined visually after 24 h incubation at 30 °C. The MIC of the compounds was determined to be the well before yeast growth was first seen. The experiment was repeated twice. Sc — (*S. cerevisiae*), Sp — (*S. pombe*) and Ca — (*C. albicans*). Yielded brackets highlight yield for iodo counter ion exchange. X⁻ Indicates either a bromide or iodide counter ion.

Table 2
The antifungal data for compounds **2a–n**.

Number	R	% Yield	Log P	MIC (µg/mL) Sc	Sp	Ca
2a	CH₃	87	−1.077	500	500	1000
2b	CH₂CH₃	41	−0.701	500	250	1000
2c	CH₂CH₂CH₃	44	−0.199	250	250	1000
2d	CH₂(CH₂)₂CH₃	51	0.36	250	250	1000
2e	CH₂(CH₂)₃CH₃	11	1.252	62.5	250	1000
2f	CH₂(CH₂)₄CH₃	7	1.371	62.5	250	1000
2g	CH₂(CH₂)₅CH₃	10	1.876	31.3	125	1000
2h	CH₂(CH₂)₆CH₃	15	2.381	15.6	62.5	1000
2i	CH₂(CH₂)₇CH₃	9	2.887	7.8	31.3	500
2j	CH₂(CH₂)₈CH₃	6	3.392	3.9	7.8	250
2k	CH₂C₆H₅	90	0.517	1000	1000	1000
2l	CH₂CH₂CH₂SO₃	50	−4.576	1000	1000	1000
2m	CH₂CH₂CH₂CH₂SO₃	7	−4.411	1000	1000	1000
2n	N/A	–	2.085	1000	250	1000

Minimal Inhibitory Growth Concentration (MIC) of synthesised compounds tested in *S. cerevisiae*, *S. pombe*, and *C. albicans*. Cells were inoculated at a concentration of 3×10^4/mL. Culture media tested were in yeast extract broth (YE) for *S. pombe* and complex growth media (YPD) for *S. cerevisiae* and *C. albicans*. Growth of yeast was determined visually after 24 h incubation at 30 °C. The MIC of the compounds was determined to be the well before yeast growth was first seen. The experiment was repeated twice. Sc — (*S. cerevisiae*), Sp — (*S. pombe*) and Ca — (*C. albicans*). X⁻ Indicates either a bromide or iodide counter ion.

Tables 1 and 2. It is important to note that the yeast cell surfaces carry a negative charge [23] and thus a good interaction between the yeast cell surface should be observed with the quaternary *N*-alkylated compounds (**1a–m** and **2a–m**).

We chose to vary one physiochemical property (log *P*) to examine how this affected growth inhibition (log 1/*C*), due to the medicinal target i.e. yeast cell wall. Using a virtual method, the log *P* (the base 10 logarithm was used throughout) values were obtained [24]. Neither sets of compounds inhibited the growth of *C. albicans*, so this species was removed from subsequent analyses.

From analysing the MIC values in Tables 1 and 2, the assumption can be made that the 2,3,3-trimethylindolenine salts (**1a–h**) showed a poor growth inhibition relationship against both the *S. cerevisiae* and *S. pombe* yeast strains. However, compounds **1i–j** with an *N*-alkylated chain length > C9, are shown to be the most potent of the set. The lowest MIC value was recorded against both the aforementioned stains at 15.6 µg/mL for compound **1j**. In comparison the 2-methylbenzathiazole salts (**2a–j**) showed varying degrees of growth inhibition. Against *S. cerevisiae*, compound **2a–f** showed poor growth inhibition. Conversely, compounds **2g–j** with *N*-alkylated chain length > C7, gave the lowest MIC values for growth inhibition, with the compound **2j** displaying most potency at 3.9 µg/mL. However, upon comparison with the *S. pombe* yeast strain, a different result is observed. Compounds **2a–h** are deemed

to be the least potent with the highest MIC values, yet compounds **2i–j** with *N*-alkylated chain length > C9 show the lowest MIC values, again with compound **2j** displaying most potency at 7.8 µg/mL.

It is also noted that the sulfonic acid salts of both the 2,3,3-trimethylindolenine and the 2-methylbenzothiazole (**1l–m** and **2l–m**) showed no antifungal activity, it is assumed that the presence of the sulfonic acid groups tends to increase their solubility and reduces their growth inhibitory characteristics, possibly through suppressing membrane permeability and cellular uptake. It is also noted that the benzyl substituent showed no activity against any of the three fungi types and again this could possibly be due to the molecule having little membrane permeability due to the sp² hybridised ring system. It is interesting to note that the starting material 2,3,3-trimethylindolenine (**1n**) showed slight growth inhibition of *S. pombe* and *C. albicans* with MIC's of 250 µg/mL and 500 µg/mL respectively. The 2-methylbenzathiazole (**2n**) also showed growth inhibition of *S. pombe* again at 250 µg/mL but showed no growth inhibition against *S. cerevisiae* or *C. albicans*. This indicates that varying the alkyl chain length has a very positive impact on growth inhibition.

2.2.1. Control bioassays

Two bioassays with Amphotericin B **4** and Thiabendazole **5** (Fig. 4) were set up to compare the efficacy of our range of *N*-alkylated compounds against classic antifungal agents. The rationale behind the choice of these antifungals was as follows. Amphotericin B is an extremely potent antifungal and targets the membrane sterol of fungal cell membranes, this choice of antifungal agent is crucial as it provides a similar mode of action in comparison to our compounds. Thiabendazole inhibits nucleic acid metabolism and protein synthesis and has a similar core structure when compared against our compounds. However, the Thiabendazole has previously shown poor activity against *C. albicans* [25] and *S. cerevisiae*, which may be explained by poor aqueous solubility [26]. Amphotericin B showed high potency against all three species of yeast at 0.49 µg/mL, which is in line with published data [25]. Thiabendazole, showed poor results against *S. cerevisiae* and *C. albicans* species at 1000 µg/mL, however against *S. pombe* species the MIC was 31.25 µg/mL. We thus conclude that the longer chain *N*-alkylated 2,3,3-trimethylindolenines and 2-methylbenzothiazoles (**1i–j** and **2g–j**) at concentrations <35 µg/mL show a comparable efficacy profile with the known antifungals used in the treatment of fungal infections. This suggests further investigation into these compounds would be beneficial for the treatment of fungal infections. The bioassays were set-up in line with experimental procedure highlighted in Section 4.2.

2.3. Statistical analysis

The intention was to analyse the relationship between increasing chain length and growth inhibition by ordinary least squares
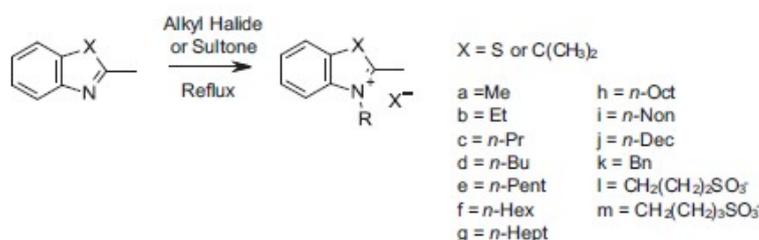
Scheme 1. The synthetic strategy to making the 2,3,3-trimethylindolenine (**1a–m**) and 2-methylbenzothiazole (**2a–m**) salts.

225
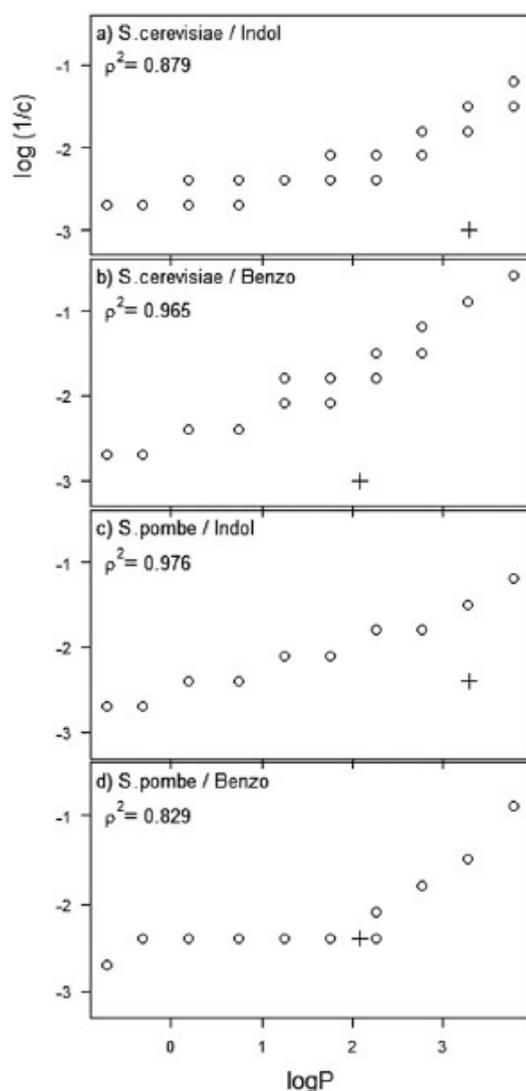
Fig. 3. Relationship between (base 10 logarithms of) the inverse of minimum concentration for growth inhibition and the partition coefficient for the fungal species *S. pombe* and *S. cerevisiae* and alkylated molecule type. Two replicates were used, and points overlap where only one appears at each log *P* value. 2,3,3-Trimethylindolenine (Indol) (**1a–j**) and 2-methylbenzothiazole (Benzo) (**2a–j**) values for each replicate are marked by a plus symbol. The square of Spearman's rho (see text for explanation) on each plot quantifies the strength of the relationship.

regression, since, with the limited range of log *P* values, a straight line relationship was expected. However, the relationship was not sufficiently linear to use this method, as a slight upward curve — made more noticeable in a plot of residuals against fitted values (not shown) — is evident (Fig. 3a–d). Furthermore, since the dependent variable was restricted by the small numbers of serial dilution concentrations, consistent with experimental protocol, residual values from the model were very unlikely to be normally

distributed. For these reasons linear regression was deemed inappropriate, and a correlation was used. This is unfortunate as it means the relationship between the variables could not be quantified as a straight line equation. As the log $(1/C)$ variable was not normally distributed in three out of four cases, a non-parametric method was required. Spearman's rank correlation coefficient is simply Pearson's Product–Moment correlation on ranks rather than original values. Its statistic ρ ('Spearman's rho') is thus related to r^2, the coefficient of determination, so values of ρ^2 are given in Fig. 3 to facilitate comparison with studies which report this quantity.

A strong relationship is clear in all four plots of Fig. 3, with that for *S. pombe* and 2-methylbenzothiazole (Fig. 3d) the weakest ($\rho = 0.910$, $t = 9.34$, $n = 20$, $p < 0.0001$); increasing the alkyl chain length increases growth inhibition.

3. Conclusion

The quaternary *N*-alkylated derivatives of both 2,3,3-trimethylindolenine and 2-methylbenzothiazole salts show varying degrees of antifungal activity with the longer chain substituents being more potent against *S. cerevisiae* and *S. pombe*. We propose that the growth inhibition can be attributed to the charged *N*-alkylated compounds with the increasing linear chain lengths. We postulate that these compounds are attracted to the negatively charged yeast membrane, with the longer lipophilic chains being absorbed into and subsequently distorting the lipid bilayer. Compounds **1i–j** and **2g–j**, all show MIC values of <35 μg/mL and are thus deemed from this study to be the most potent towards *S. cerevisiae* and *S. pombe*. Together with further compounds, which are being generated with higher degrees of lipophilicity these compounds will be taken forward for mammalian screening. This preliminary study has also highlighted that none of the synthesised compounds (**1a–m** and **2a–m**) has shown any real activity towards *C. albicans*. This response may be the result of *C. albicans*' ability to adapt to the antifungal stress and develop drug tolerance. As a diploid fungus, *C. albicans* contains a large number of drug exclusion mechanisms with varying substrate specificities enabling it to obtain tolerance to many novel antifungals, a resistance not seen with the haploid yeast species, *S. cerevisiae* and *S. pombe* [27,28]. The results highlighted above imply that longer *N*-alkylated (*i.e.* >C7) 2,3,3-trimethylindolenines and 2-methylbenzothiazole salts show potential for selective targeting towards *S. cerevisiae* infections which are a major problem in health care.

4. Experimental section

4.1. General procedure

^{1}H and ^{13}C NMR spectra were measured on either a Bruker DPX 250 MHz, Bruker Avance-III 300 MHz or a Bruker Avance 400 MHz spectrometer at ambient temperature with tetramethylsilane (TMS) as internal standard for ^{1}H NMR and deuteriochloroform (CDCl$_3$, δ_C 77.23 ppm) and deuteriodimethylsulfoxide (d_6-DMSO, δ_C 39.51 ppm) for ^{13}C NMR unless otherwise stated. All chemical shifts are quoted in δ (ppm) and coupling constants in Hertz (Hz) using the high frequency positive convention. The abbreviations used for the multiplicity of the NMR signals are: s = singlet, d = doublet, t = triplet, q = quartet, quin = quintet, sex = sextet, m = multiplet, dd = doublet of doublet, td = triplet of doublets, dm = doublet of multiplets, br s = broad singlet, etc. Mass spectra were recorded on a Thermo Scientific Trace LC Ultra DSQ II using Electron Ionisation (LCMS-EI). Infrared spectra were recorded on a Specac ATR with a He Ne −633 nm laser. Thin Layer Chromatography (TLC) was carried out on Machery–Nagel polygramSil/G/UV$_{254}$ pre-coated plates. Melting point (Mp) analysis was carried out using the Griffin

226   A.R. Tyler et al. / European Journal of Medicinal Chemistry 64 (2013) 222–227
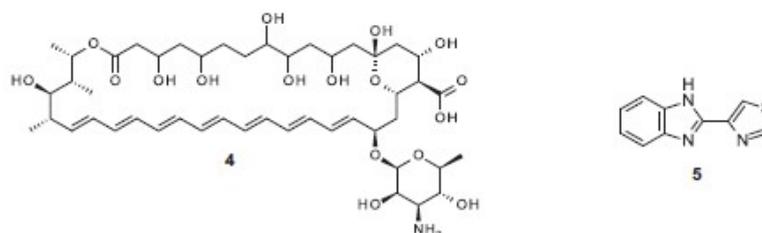

Fig. 4. The structures of Amphotericin B **4** and Thiabendazole **5**.

melting point apparatus. All chemicals were purchased from Sigma–Aldrich or Alfa Aesar and used without purification.

4.1.1. 1,2,3,3-Tetramethyl-3H-indol-1-ium iodide (**1a**)

2,3,3-Trimethylindolenine (63.0 mmol) was dissolved in iodomethane (168 mmol) and with constant stirring, the solution was refluxed for 24 h. The precipitate produced was filtered under suction, washed with n-hexane and dried in vacuo to yield the product (58%) as a pink solid.

^{1}H NMR (d_6-DMSO, 300 MHz): δ 7.90 (t, J = 6.0 Hz, 1H, Ar–H), 7.82 (t, J = 6.0 Hz, 1H, Ar–H), 7.66–7.61 (m, 2H, Ar–H), 3.96 (s, 3H, N–C$\underline{H}_3$), 2.75 (s, 3H, C–C$\underline{H}_3$), 1.52 (s, 6H, C–(C$\underline{H}_3$)$_2$). ^{13}C NMR (d_6-DMSO, 75.4 MHz): δ 196.45, 142.56, 142.05, 129.77, 129.28, 123.76, 115.57, 100.00, 54.38, 22.14, 14.51. IR (ATR, cm^{-1}): 2968.4, 1628.9, 1455.1, 1392.7, 1357.8, 774.4. MS (ESI) m/z: 174.09 [M$^+$]. Melting point = 255–257 °C.

4.1.2. 1-Pentyl-2,3,3-trimethyl-3H-indol-1-ium iodide (**1e**)

2,3,3-Trimethylindolenine (15.0 mmol) was dissolved in acetonitrile (10.0 mL), followed by the addition of 1-bromopentane (20.0 mmol). With constant stirring, the solution was refluxed for 24 h to produce a brown solution. The solution was concentrated under reduced pressure to yield brown oil, which was purified by column chromatography to yield the product as a bromide salt (38%) which was hygroscopic. The bromide salt (1.00 mmol) was dissolved in acetone (10.0 mL) and heated under reflux with sodium iodide (1.00 mmol) for 24 h. The white solid produced (KBr) was filtered and the solution was evaporated under reduced pressure yielding the iodide salt (99%) as a purple solid.

^{1}H NMR (d_6-DMSO, 300 MHz): δ 7.97 (t, J = 6.0 Hz, 1H, Ar–H), 7.84 (t, J = 6.0 Hz, 1H, Ar–H), 7.64–7.61 (m, 2H, Ar–H), 4.44 (t, J = 9.0 Hz, 2H, N–C$\underline{H}_2$), 2.83 (s, 3H, C–C$\underline{H}_3$), 1.82 (sex, J = 9.0 Hz, 2H, CH$_2$–C$\underline{H}_2$–CH$_3$), 1.53 (s, 6H, C–(C$\underline{H}_3$)$_2$), 1.38–1.31 (m, 4H, C–C$\underline{H}_2$), 0.88 (t, J = 6.0 Hz, 3H, CH$_2$–C$\underline{H}_3$). ^{13}C NMR (d_6-DMSO, 75.4 MHz): δ 196.65, 142.22, 141.34, 129.83, 129.40, 124.20, 105.20, 54.70, 28.42, 27.47, 26.85, 22.61, 22.18, 15.91, 10.33. IR (ATR, cm^{-1}): 3412.6, 3213.4, 1605.1. MS (ESI) m/z: 230.20 [M$^+$]. Melting point = 139–140 °C.

4.1.3. 1-Benzyl-2,3,3-trimethyl-3H-indol-1-ium bromide (**1k**)

Benzyl bromide (6.80 mmol) dissolved in acetonitrile (20.0 mL) was heated with constant stirring until a state of reflux was established. 2,3,3-Trimethylindolenine (6.30 mmol) dissolved in acetonitrile (20.0 mL) was added dropwise to the reaction mixture from a dropping funnel. Once all the reactants had been added the reaction was continued for 48 h. The precipitate produced was filtered under suction, washed with n-hexane and dried in vacuo to yield the product (77%) as a red hygroscopic solid.

^{1}H NMR (d_6-DMSO, 250 MHz): δ 7.89 (d, J = 7.0 Hz, 1H, Ar–$\underline{H}$), 7.84 (d, J = 7.0 Hz, 1H, Ar–$\underline{H}$), 7.67–7.59 (m, 2H, Ar–$\underline{H}$), 7.45–7.38 (m, 5H, Ar–H), 5.87 (s, 2H, N–CH$_2$), 3.59 (s, 3H, N–C–C$\underline{H}_3$), 1.55 (s, 6H C–(CH$_3$)$_2$). ^{13}C NMR (d_6-DMSO, 75.4 MHz): δ 198.7, 142.5, 141.6,

132.7, 130.1, 129.5, 129.3, 128.1, 124.2, 116.5, 55.1, 51.2, 15.1, 9.81. IR (ATR, cm^{-1}): 2969, 1603, 1454, 931, 741, 701, 567. MS (ESI) m/z: 250.33 [M$^+$]. Melting point = 226–230 °C.

4.1.4. 2,3,3-Trimethyl-1-(3-sulfonatopropyl)-3H-indol-1-ium (**1l**)

To a solution of 2,3,3-trimethylindolenine (62.3 mmol) in toluene (50.0 mL) was added 1,3-propanesultone (93.5 mmol) and with constant stirring, the solution was refluxed for 24 h. The precipitate produced was filtered under suction, washed with toluene and dried in vacuo to yield the product (58%) as a white solid.

^{1}H NMR (d_6-DMSO, 300 MHz): δ 7.43 (d, J = 9.0 Hz, 2H, Ar–H), 7.88 (t, J = 9.0 Hz, 1H, Ar–H), 7.78 (t, J = 9.0 Hz, 2H, Ar–H) 4.91 (t, J = 9.0 Hz, 2H, N–CH$_2$) 3.54 (s, 6H, C–(C$\underline{H}_3$)$_2$), 2.65 (t, J = 6.0 Hz, 2H, CH$_2$–CH$_2$) 2.16 (quin, J = 6.0 Hz, 2H, CH$_2$–C$\underline{H}_2$–C$\underline{H}_2$) 2.08 (s, 3H, C–C$\underline{H}_3$). ^{13}C NMR (d_6-DMSO, 75.4 MHz) δ 207.08, 177.75, 177.72, 141.35, 129.61, 128.51, 125.01, 117.31, 47.80, 47.78, 31.17, 24.72, 17.21 IR (ATR, cm^{-1}): 2904.9, 1634.1, 1455.5, 1326.4, 1161.7, 1028.6, 781.9. MS (ESI) m/z: 282.32 [M$^+$] Melting point = 265–268 °C.

4.2. Determination of antifungal activity

The growth inhibitory activity of the compounds (**1a–n** and **2a–n**) were determined by screening S. pombe, S. cerevisiae and C. albicans using the following method:

Yeast species were inoculated into relevant media; S. pombe (NJ2 h⁻ ura4-D18 leu1-32 ade6-M210 his7-366) [29] into yeast extract broth (YE) [30], and S. cerevisiae (strain BY4741a, a derivative of S288C), (MATahis31 leu20 met150 ura30) [31] and C. albicans (strain SC5314) [32] into complex media (YPD) [33]. The culture was then incubated for 12 h at 30 °C with shaking at 200 rpm. Stock solutions of the compounds were prepared in 20% (v/v) DMSO and culture media. DMSO and culture media were all used as controls for the experiment. 3×10^4 yeast cells were transferred into the wells of a 96-well plate. A 1:2 serial dilution of the compounds was then performed. The wells were inspected visually for growth of yeast after 24 h of incubation at 30 °C. Growth was indicated by full or partial white appearance of yeast on the bottom of the wells. The MIC values of the compounds were determined to be the well before yeast growth was first seen. The experiment was repeated two times to ensure reproducibility of the results.

Acknowledgements

244

Chemistry (Lancaster and District Section) for providing the funds to present this work at YoungChem 2013 in Gdansk, Poland.

Appendix A. Supplementary data

Supplementary data related to this article can be found at http://dx.doi.org/10.1016/j.ejmech.2013.03.031.

References

[1] A. Wong-Beringer, J. Kriengkauykiat, Systemic antifungal therapy: new opinions, new challenges, Pharmacotherapy 23 (2003) 1441–1462.
[2] L. Ostrosky-Zeichner, A. Casadevall, J.N. Galgiani, F.C. Odds, J.H. Rex, An insight into the antifungal pipeline: selected new molecules and beyond, Nat. Rev. Drug Discov. 9 (2010) 719–727.
[3] D.W. Denning, Echinocandins: a new class of antifungal, J. Antimicrob. Chemother. 49 (2002) 889–891.
[4] T. Arif, T.K. Mandal, R. Dabur, Opportunity, Challenge and Scope of Natural Products in Medicinal Chemistry, Research Signpost, Kerala, 2011, pp. 283–311.
[5] V. Bellavia, M. Natangelo, R. Fanelli, D. Rotilio, Analysis of benzothiazole in italian wines using headspace solid-phase microextraction and gas chromatography–mass spectrometry, J. Agric. Food Chem. 48 (2000) 1239–1242.
[6] C. Franchini, M. Muraglia, F. Corbo, M.A. Florio, A. Di Mola, A. Rosato, R. Matucci, M. Nesi, F. van Bambeke, C. Vitali, Synthesis and biological evaluation of 2-mercapto-1,3-benzothiazole derivatives with potential antimicrobial activity, Arch. Pharm. 342 (2009) 605–613.
[7] Y. Katsura, Y. Inoue, S. Nishino, M. Tomoi, H. Takasugi, Chem. Pharm. Bull. 40 (7) (1992) 1818–1822.
[8] C.G. Mortimer, G. Wells, J.P. Crochard, E.L. Stone, T.D. Bradshaw, M.F.G. Stevens, A.D. Westwell, Antitumor benzothiazoles. 26.1 2-(3,4-Dimethoxyphenyl)-5-fluorobenzothiazole (GW 610, NSC 721648), a simple fluorinated 2-arylbenzothiazole, shows potent and selective inhibitory activity against lung, colon, and breast cancer cell lines, J. Med. Chem. 49 (2006) 179–185.
[9] C.H. Suresh, J. Venkateshwara Rao, K.N. Jayaveera, Anti inflammatory activity of 3-(2-hydrazino benzothiazoles)-substituted indole-2-one, Int. J. Pharm. Sci. Res. 1 (2011) 30–34.
[10] T. Akhtar, S. Hameed, N.A. Al-Masoudi, R. Loddo, P. La Colla, In vitro antitumor and antiviral activities of new benzothiazole and 1,3,4-oxadiazole-2-thione derivatives, Acta Pharm. 58 (2008) 135–149.
[11] R.B. Silverman, The Organic Chemistry of Drug Design and Drug Action, Elsevier Academic Press, San Diego, 2002.
[12] A.J. Brown, Fungal pathogens – the devil is in the detail, Microbiol. Today 29 (2002) 120–122.
[13] J.B. Anderson, C. Sirjusingh, A.B. Parsons, C. Boone, C. Wickens, L.E. Cowen, L.M. Kohn, Mode of Selection and experimental evolution of antifungal drug resistance in Saccharomyces cerevisiae, Genetics 163 (2003) 1287–1298.
[14] M. Marcet-Houben, T. Gabaldón, The tree versus the forest: the fungal tree of life and the topological diversity within the yeast phylome, PLoS One 4 (2009) 4357.
[15] N. Skovgaard, New trends in emerging pathogens, Int. J. Food Microbiol. 120 (2007) 217–224.
[16] J. Zupan, P. Raspor, Invasive growth of Saccharomyces cerevisiae depends on environmental triggers: a quantitative model, Yeast 27 (2010) 217–228.
[17] A. Enache-Angoulvant, C. Hennequin, Invasive Saccharomyces infection: a comprehensive review, Clin. Infect. Dis. 41 (2005) 1559–1568.
[18] N. Tani, M. Rahnasto-Rilla, C. Wittekindt, K.A. Salminen, A. Ritvanen, R. Ollakka, J. Koskiranta, H. Raunio, R.O. Juvonen, Antifungal activities of novel non-azole molecules against S. cerevisiae and C. albicans, Eur. J. Med. Chem. 47 (2012) 270–277.
[19] P. Muñoz, E. Bouza, M. Cuenca-Estrella, J.M. Eiros, M.J. Pérez, M. Sánchez-Somolino, C. Rincón, J. Hortal, T. Peláez, Saccharomyces cerevisiae fungemia: an emerging infectious disease, Clin. Infect. Dis. 40 (2005) 1625–1634.
[20] K.C. Hazen, New and emerging yeast pathogens, Clin. Microbiol. Rev. 8 (1995) 462–478.
[21] D. Auerbach, A. Arnoldo, B. Bogdan, M. Fetchko, I. Stagljar, Drug discovery using yeast as a model system: a functional genomic and proteomic view, Curr. Proteomics 2 (2005) 1–13.
[22] B. Qaddouri, A. Guaadaoui, A. Bellirou, A. Hamal, A. Melhaoui, G.W. Brown, M. Bellaoui, The budding yeast "Saccharomyces cerevisiae" as a drug discovery tool to identify plant-derived natural products with anti-proliferative properties, J. Evidence-Based Complement. Altern. Med. 1 (2011) 1–5.
[23] S.M. Tazhibaeva, K.B. Musabekov, A.B. Orazymbetova, A.A. Zhubanova, Surface properties of yeast cells, Colloid J. 65 (2003) 122–124.
[24] Log P values were obtained from http://www.molinspiration.com.
[25] P.B. Fai, A. Grant, A rapid resazurin bioassay for assessing the toxicity of fungicides, Chemosphere 74 (2009) 1165–1170.
[26] M. Devereux, M. McCann, D.O. Shea, R. Kelly, D. Egan, C. Deegan, K. Kavanagh, V. McKee, G. Finn, Synthesis, antimicrobial activity and chemotherapeutic potential of inorganic derivatives of 2-(4'-thiazolyl)benzimidazole[thiabendazole]: X-ray crystal structures of [Cu(TBZH)2Cl]Cl·H$_2$O·EtOH and TBZH$_2$NO$_3$ (TBZH = thiabendazole), J. Inorg. Biochem. 98 (2004) 1023–1031.
[27] G.D. Wright, The antibiotic resistome: the nexus of chemical and genetic diversity, Nat. Rev. Microbiol. 5 (2007) 175–186.
[28] J.B. Anderson, Evolution of antifungal-drug resistance: mechanisms and pathogen fitness, Nat. Rev. Microbiol. 3 (2005) 547–556.
[29] C.L. Lawrence, H. Maekawa, J.L. Worthington, W. Reiter, C.R. Wilkinson, N. Jones, Regulation of Schizosaccharomyces pombe Atf1 protein levels by Sty1-mediated phosphorylation and heterodimerization with Pcr1, J. Biol. Chem. 282 (2007) 5160–5170.
[30] S. Moreno, A. Klar, P. Nurse, Molecular genetic analysis of fission yeast Schizosaccharomyces pombe, Methods Enzymol. 194 (1991) 795–823.
[31] C.B. Brachmann, A. Davis, G.J. Cost, E. Caputo, J. Li, P. Hieter, J.D. Boeke, Designer deletion strains derived from Saccharomyces cerevisiae S288C: a useful set of strains and plasmids for PCR-mediated gene disruption and other applications, Yeast 14 (1998) 115–132.
[32] A.M. Gillum, E.Y. Tsay, D.R. Kirsch, Isolation of the Candida albicans gene for orotidine-5'-phosphate decarboxylase by complementation of S. cerevisiae ura3 and E. coli pyrF mutations, Mol. Gen. Genet. 198 (1984) 179–182.
[33] D.A. Treco, V. Lundblad, Preparation of yeast media, Curr. Protoc. Mol. Biol. 23 (2001) 1–13, http://dx.doi.org/10.1002/0471142727.mb1301s23. John Wiley and Sons, Inc., Kansas City.

INTELLECTUAL
PROPERTY OFFICE

Concept House
Cardiff Road
South Wales
NP10 8QQ
United Kingdom

Telephone +44 (0) 1633 814000
Minicom +44 (0) 8459 222250

DX 722540/41 Cleppa Park 3

Website www.ipo.gov.uk

Electronic Filing Receipt

Harrison Goddard Foote
4th Floor, Merchant Exchange
17-19 Whitworth Street West
Manchester
United Kingdom
M1 5WG

Your Ref: P137328GB

31 January 2012

PATENT APPLICATION NUMBER 1201641.6

We have received your request for grant of a patent and recorded its details as follows:

Filing date(*)	31 January 2012
Earliest priority date (if any)	
Applicant(s) / contact point	University of Central Lancashire
Application fee paid	Yes
Description (number of pages or reference)	46
Certified copy of referenced application	Not applicable
If description not filed	Not applicable
Claims (number of pages)	7
Drawings (number of pages)	None
Abstract (number of pages)	1
Statement of inventorship (Form 7)	No, file by 31 May 2013
Request for search (Form 9A)	Yes
Request for examination (Form 10)	None
Priority Documents	None
Other Attachments Received	PDAS Registration Form PDASRegistration.pdf
	Fee Sheet FeeSheet.pdf

	Validation Log	ValidLog.pdf
Signed by	CN=M. Holmes 25129,O=Harrison Goddard Foote,C=GB	
Submitted by	D. Coutts 13463	
Timestamp of Receipt	31 January 2012, 15:49:44 (GMT)	
Digest of Submission	30:8B:87:6C:74:CF:6D:86:BF:B5:3C:4A:55:55:B A:93:D0:04:6F:C3	
Received	/Intellectual Property Office, Newport/	

Please quote the application number in the heading whenever you contact us about this application.

As requested your application as filed will be lodged in the Priority Document Access Service (PDAS) at WIPO. For further information relating to PDAS please see our website http://www.ipo.gov.uk/p-apply-online-pdas.htm or contact our e-filing section on 01633 814870.

If you have any queries about the accuracy of this receipt, please phone Christine Davis on +44 (0) 1633 814570. For all other queries, please phone our Central Enquiry Unit on 08459 500 505 if you are calling from the UK, or +44 (0) 1633 813930 if you are calling from outside the UK. Or e-mail enquiries@ipo.gov.uk

This date is provisional. We may have to change it if we find during preliminary examination that the application does not satisfy section 15(1) of the Patents Act 1977 or if we re-date the application to the date when we get any later filed documents.